U.S. DEPARTMENT OF COMMERCE
National Technical Information Service

PB-258 071

Fluidized Vortex Incineration of Waste

Southern Methodist Univ, Dallas, Texas

Prepared for

Industrial Environmental Research Lab, Research Triangle Park, N C

Aug 76

324

TECHNICAL REPORT DATA
(Please read Instructions on the reverse before completing)

1. REPORT NO. EPA-600/2-76-225	2.	3. RECIPIENT'S ACCESSION NO.
4. TITLE AND SUBTITLE FLUIDIZED VORTEX INCINERATION OF WASTE		5. REPORT DATE August 1976 6. PERFORMING ORGANIZATION CODE
7. AUTHOR(S) Jack P. Holman and Richard A. Razgaitis		8. PERFORMING ORGANIZATION REPORT NO.
9. PERFORMING ORGANIZATION NAME AND ADDRESS Southern Methodist University Civil and Mechanical Engineering Department Dallas, Texas 75275		10. PROGRAM ELEMENT NO. 1AB013; ROAP 21AQQ 11. CONTRACT/GRANT NO. Grant R801078
12. SPONSORING AGENCY NAME AND ADDRESS EPA, Office of Research and Development Industrial Environmental Research Laboratory Research Triangle Park, NC 27711		13. TYPE OF REPORT AND PERIOD COVERED Final; 5/70-8/74 14. SPONSORING AGENCY CODE EPA-ORD

15. SUPPLEMENTARY NOTES Project officer for this report is J.D. Kilgroe, Mail Drop 61, Ext 2851.

16. ABSTRACT
The report gives results of an experimental investigation of an incineration concept utilizing fluidized wastes in a confined vortex flow with simultaneous heat recovery. The incinerator consisted of a vortex combustion chamber and a cooled vertical furnace column 5 feet long and half a foot in diameter. (No transition section was used.) The vortex incinerator was operated using propane, sawdust/propane, and sawdust. The principal experiments were performed using propane at air/fuel ratios and total mass flow rates (in lbs per hour) in three combinations: 15 and 125, 20 and 220, and 20 and 280. Radial temperature profiles and heat transfer to the wall of the vortex tube were measured as a function of air/fuel ratio, vertical position, total gas flow rate, and inlet/outlet configurations. Tube entrance temperature profiles demonstrated a peak of approximately 1800 F at a radius ratio of 0.5; at the tube exit, the maximum temperature shifted to the centerline and decreased to less than 1000 F. Total energy recovery rates varied from 84,000 to 152,000 Btu/hr and energy recovery efficiencies varied from 54 to 70%. Maximum energy fluxes experienced were on the order of 37,000 Btu/hr-sq ft. A helicoidal flow-model correlation was developed which was about 4 times that predicted for the Colburn j-Factor using the Reynolds analogy for fluid friction for turbulent flow past a flat plate.

17. KEY WORDS AND DOCUMENT ANALYSIS

a. DESCRIPTORS		b. IDENTIFIERS/OPEN ENDED TERMS	c. COSATI Field/Group
Air Pollution	Sawdust	Air Pollution Control	13B 11L
Fluidizing		Stationary Sources	07A, 13H
Waste Disposal		Fluidized Vortex Incinerator	15E
Incinerators			
Heat Recovery		Fluidized Wastes	13M, 13A
Propane			07C

18. DISTRIBUTION STATEMENT Unlimited	19. SECURITY CLASS *(This Report)* Unclassified	21. NO. OF PAGES 339
	20. SECURITY CLASS *(This page)* Unclassified	22. PRICE 10.00 - 3.00

EPA Form 2220-1 (9-73)

PRICES SUBJECT TO CHANGE

PB 258 071

REPRODUCED BY
NATIONAL TECHNICAL
INFORMATION SERVICE
U. S. DEPARTMENT OF COMMERCE
SPRINGFIELD, VA. 22161

EPA-600/2-76-225
August 1976

FLUIDIZED VORTEX INCINERATION OF WASTE

by

Jack P. Holman and Richard A. Razgaitis

Southern Methodist University
Civil and Mechanical Engineering Department
Dallas, Texas 75275

Grant No. R801078
ROAP No. 21AQQ
Program Element No. 1AB013

EPA Project Officer: James D. Kilgroe

Industrial Environmental Research Laboratory
Office of Energy, Minerals, and Industry
Research Triangle Park, NC 27711

Prepared for

U.S. ENVIRONMENTAL PROTECTION AGENCY
Office of Research and Development
Washington, DC 20460

ia

ABSTRACT

An alternative concept of incineration utilizing fluidized wastes in a confined vortex flow with simultaneous heat recovery was experimentally investigated. The apparatus consisted of a vortex tube five-feet in length and 0.4800 feet in internal diameter which was cooled in five one-foot sections by water flowing through refrigeration tubing spirally wound and soldered to the exterior of the tube. The vortex was generated by means of two tangential air-inlets located at a radius of 0.638 feet from the centerline of the tube in a sandwich-like structure 0.312 feet high and 1.50 feet in diameter attached to the base of the vortex tube. No transition section was used.

The vortex incinerator was operated using propane/air, sawdust/propane/air, and sawdust/air. The principal data investigation was performed using propane/air at air fuel ratios and total mass flow rates (in units of pounds per hour) in three combinations: 15 and 125; 20 and 220; 20 and 280.

Radial temperature profiles and heat transfer to the wall of the vortex tube were measured as a function of air/fuel ratio, vertical position (in five discrete steps), total gas flow rate, and inlet-outlet configurations. The temperature profiles at the entrance to the tube demonstrated a peak of approximately 1800°F at a radius ratio of one-half; at the exit of the vortex tube the location of the maximum temperature had shifted to the centerline and the temperature had decreased to less than 1000°F. Total energy recovery rates varied from 84,000 to 152,000 Btu/hour depending upon propane flow rate and inlet-outlet configuration at recovery efficiencies (defined as the ratio of the heat recovered to

Preceding page blank

the maximum possible) of 54 to 70 percent. Maximum energy fluxes experienced were approximately on the order of 37,000 Btu/hour-square foot.

Application of the helicoidal flow-model, axial velocity independent of radius (slug flow) and tangential velocity linearly dependent upon radius (solid-body rotation), developed the following correlation: $St_x\ Pr^{2/3} = 0.117\ Re_x^{-0.241}$ for fluid properties evaluated at the film temperature. The characteristic length used in the definition of the Reynolds number was the equivalent flat-plate length of the surface of the vortex tube obtained by calculating the path length of the flow-helix in terms of axial position. The characteristic velocity used in both the Stanton and Reynolds numbers was the estimated velocity vector near the wall of the vortex tube based upon the assumption of perfect conversion of the injected angular momentum flux to a solid-body rotation profile.

This correlation is approximately four-times that predicted for the Colburn j-Factor using the Reynolds analogy for fluid friction for turbulent flow past a flat plate.

TABLE OF CONTENTS

Page

ABSTRACT iii

TABLE OF CONTENTS v

LIST OF TABLES viii

LIST OF ILLUSTRATIONS xi

Chapter

I. INTRODUCTION 1

Backround of Research Problem 1
  Three societal needs 1
  Resource and energy production potential of solid wastes 3
  Schemes for energy recovery from solid wastes 6
  Recent operating experience with waste heat recovery incinerators 10

Literature Survey of "Swirling Flows" 14
  Classification of subject field 14
  Outline of survey 16
  Literature common to vortex flows 26
  Literature survey of free vortex flows . . . 31
  Literature survey of confined vortex flows 43
  Literature survey of rotating flows 73
  Literature survey of curved flows 80

Scope, Significance, and Objective of Research Investigation 93

II. EXPERIMENTAL APPARATUS AND PROCEDURE 95

Experimental Apparatus 95
  Vortex chamber 95
  Furnace column/heat recovery system 100
  Separator 106
  Exhaust stack/sampling equipment 110
  Fluidizer 116

Air/propane supply system 119
Instrumentation and calibration 121

Procedure 122

III. RESULTS AND DISCUSSION 125

Independent Variables Investigated 125

Heat Recovery/Vortex Gas Temperature-Profile Data 129
Effect of exit configuration and condition . . 129
Effect of inlet configuration and condition. . 138

Discussion of Heat Recovery Data 143

Discussion of Vortex Gas Temperature-Profile Data 154

Wall Temperature Data 158

Orsat Data 160

Slagging Effects 161

Sawdust as Fuel/Stack Sampling Results 162

IV. DATA ANALYSIS AND ANALYTICAL INVESTIGATIONS . . . 165

Philosophy of Approach 165

Heat Recovery Efficiency 166

Energy Balance 172
Radiation loss 174
Free convection loss 178
Conduction loss 181
Total energy loss 183

Determination of Convective Heat Transfer Component 185
Conduction flux component 186
Radiation flux component 188
Convection flux component 199

Nusselt Number Correlation 201
Evaluation of convection conductance 201
Mean Nusselt number correlation 202
Length Nusselt number correlation 205

Stanton Number Correlation 208
Concept 208
Characterization of swirl intensity 210

Calculation of mean axial velocity 214
Calculation of inlet air velocity 216
Calculation of free-stream velocity 217
Equivalent flat plate length 218
Entry length effect upon convection conductance 219
Calculation of Colburn j-factor 220
Chemical reaction effect 222

APPENDICES

A. EQUIPMENT CALIBRATION 228

B. DATA REDUCTION PROCEDURE 238

C. CALCULATION OF AVERAGE TEMPERATURE 241

D. REYNOLDS NUMBER CALCULATIONS 247

E. ASSESSMENT OF RADIATION AND CONDUCTION ERROR 255

F. THERMOCHEMISTRY CALCULATIONS 263

G. CONFIGURATION FACTOR CALCULATIONS 270

H. NUSSELT NUMBER CALCULATIONS 278

I. STANTON NUMBER CALCULATIONS 282

J. LEAST-SQUARES CURVE-FIT CALCULATION 286

REFERENCES 289

LIST OF TABLES

Table		Page
1	Distinguishing Characteristics of the Three Types of Swirling Flows	17
2	Geometric Classification of Swirling Flows	18
3	Thermodynamic Classification of Swirling Flows . .	20
4	Summary of Principal Investigations of Swirl Tape Flow	88
5	Summary of Operating Conditions	126
6	Independent Variables Investigated	127
7	Configuration 1 Heat Recovery Data	131
8	Configuration 2 Heat Recovery Data	132
9	Configuration 3 Heat Recovery Data	133
10	Mean, Standard Deviation, and Standard Deviation of the Mean of the Heat Recovery Data	134
11	Configuration 1 Vortex Gas Temperature Profiles . .	135
12	Configuration 2 Vortex Gas Temperature Profiles . .	136
13	Configuration 3 Vortex Gas Temperature Profiles . .	137
14	Average Vortex Gas Temperatures	139
15	Inlet Configuration Effect Upon Heat Recovery . . .	141
16	Vortex Gas Temperatures for 3 Inlet Configurations	142
17	Furnace Column Wall Temperature vs. Furnace Column Height	159
18	Vortex Chamber/Copper Plate Temperatures	160
19	Orsat Data	161

Table Page

20 Radiation Loss from Vortex Chamber 176

21 Summary of Energy Losses from System 184

22 Energy Balance Table 184

23 Conduction Flux to Each Section 188

24 External Radiation Flux to Each Section 190

25 Internal Plate Radiation Flux to Each Section 192

26 External Radiation Flux Loss from Each Section 193

27 Radiation Flux from Copper Base Plate to Each Section 194

28 Calculation of Radiation Flux from Vortex Gas to Each Section 198

29 Calculation of Total Radiation Flux to Each Section 200

30 Convection Flux at Each Section 202

31 Evaluation of Convection Conductance 204

32 Gas Constant of Products 215

33 Mean Axial Velocity 216

34 Inlet Air Velocity 217

35 Swirl Parameter Calculation 218

A-1 Honeywell Recoder Calibration 229

C-1 Average Vortex Gas Temperature at Station 1 . . 242

C-2 Average Vortex Gas Temperature at Station 2 . . 243

C-3 Average Vortex Gas Temperature at Station 3 . . 244

C-4 Average Vortex Gas Temperature at Station 4 . . 245

C-5 Average Vortex Gas Temperature at Station 5 . . 246

D-1 Axial Reynolds Number Calculation for 3 Exit Configurations 249

Table		Page
D-2	Axial Reynolds Number Calculation for 3 Inlet Configurations	249
D-3	Exit Reynolds Number Calculation	251
D-4	Inlet Reynolds Number Calculation	251
D-5	Length Reynolds Number Calculation	253
D-6	Free-Stream Reynolds Number Calculation . . .	254
F-1	Molar Coefficients of the Theoretical Chemical Reaction Based Upon the Measured Air/Fuel Ratio.	264
F-2	Theoretical Enthalpy of Combustion at 77°F . .	265
F-3	Sensible Enthalpy of Reactants	267
F-4	Sensible Enthalpy of Products/ Net Enthalpy of Reaction	268
F-5	Net Enthalpy of Reaction at the Exit	269
G-1	Numerical Integration Results for Configuration Factor	274
G-2	Configuration Factor from Vortex Chamber to Each Furnace Column Section	274
H-1	Mean Nusselt Number Calculation	280
H-2	Length Nusselt Number Calculation	281
I-1	Calculation of Colburn j-Factor	283
I-2	Calculation of Modified Colburn j-Factor . . .	285

LIST OF ILLUSTRATIONS

Figure		Page
1	Chigier Swirl Generators	33
2	Two Fundamental Geometries	45
3	Swirl Generators	92
4	Overall Configuration of Vortex Incinerator	96
5	Vortex Combustion Chamber	98
6	Vortex Combustion Chamber and Furnace Column	101
7	Furnace Column Cooling Water Schematic	103
8	Furnace Column	104
9	Thermocouple Locations	107
10	Gas Temperature Measurement System	108
11	Separator	109
12	Collar	111
13	Separator (Exit Orifice Removed)	112
14	Exhaust Stack, Separator, and Furnace Column	114
15	"Staksamplr" Installation	115
16	Fluidizer Motor/Drive Shaft	118
17	Sawdust Mixture	120
18	Total Heat Recovery Rate vs. Axial Reynolds Number	145
19	Total Heat Recovered per Pound of Propane vs. Axial Reynolds Number	145
20	Total Heat Recovery Rate vs. Axial Reynolds Number	147

Figure		Page
21	Total Heat Recovered per Pound of Propane vs. Axial Reynolds Number	147
22	Total Heat Recovered per Pound of Propane vs. Exit Reynolds Number	148
23	Total Heat Recovered per Pound of Propane vs. Inlet Reynolds Number	148
24	Heat Flux Recovered vs. Length Reynolds Number	151
25	Heat Flux Recovered per Unit Flow Rate of Propane vs. Length Reynolds Number	153
26	Vortex Gas Temperature Profiles for Configuration 2	155
27	Vortex Gas Temperature Profiles for Condition 8	156
28	Absolute and Practical Efficiency vs. Axial Reynolds Number	168
29	Comparison of Incinerator Efficiency vs. Available Heat with Broido Curve	171
30	Conduction Heat Transfer Schematic	187
31	Mean Nusselt Number vs. Axial Reynolds Number	206
32	Length Nusselt Number vs. Length Reynolds Number	207
33	Colburn j-Factor vs. Free-Stream Reynolds Number	221
34	Modified Colburn j-Factor vs. Free-Stream Reynolds Number	225
35	Modified Colburn j-Factor vs. Free-Stream Reynolds Number	226
A-1	Daystrom Recorder Calibration	230
A-2	Air Rotameter No. 1 Calibration	235
A-3	Air Rotameter No. 2 Calibration	236
D-1	Absolute Viscosity of Flue Gas as 1 Atm. . . .	248

Figure Page

E-1 Comparison of Shielded and Un-Shielded Thermocouple Data 257

E-2 Aspirated Thermocouple 258

E-3 Comparison of Aspirated and Sheathed Thermocouple Data 259

G-1 Configuration Factor Geometry 271

G-2 Configuration Factor Equation 273

G-3 Internal Radiation Transfer Schematic 276

H-1 Thermal Conductivity of Flue Gas 279

CHAPTER I

INTRODUCTION

Background of Research Problem

Three Societal Needs

There are three fundamental societal needs which have drawn a great deal of attention in the last several years: the production and availability of energy, the ever-diminishing supply of inorganic resources, and the disposal of wastes. The process of satisfying these needs has created a relatively new problem area broadly referred to as pollution. Concern for the impact of these four problem areas has recently resulted in an incredible number of legislative acts and executive orders at all levels of government. In the last five years, the United States Congress alone has produced the National Environmental Policy Act of 1969, the Clean Air Act as Ammended in 1970, the Solid Waste Disposal Act of 1970, the National Materials Policy Act of 1970, the Water Resources Planning Act as Ammended in 1971, the Federal Water Pollution Control Act as Ammended in 1972, the Marine Protection, Research, and Sanctuaries Act of 1972, and the Noise Control Act of 1972 [1]*.

In the last several years the methods of waste disposal have been reexamined in light of the opportunities to recover inorganic resources and produce energy thus using the means to meet one of the aforementioned societal needs to mitigate the remaining two as well. The potential of energy from wastes, particulary solid wastes, was the fundamental motivation for this study.

---

* Numbers in brackets refer to References listed after the Appendices.

Energy Requirements

In the past 30 years, the United States has consumed more energy than all of mankind in all previous history [2]. We presently require one-third of the world's energy production and by 1980 our annual consumption for all uses will be on the order of 100 quadrillion Btu (i.e. 10^{17} Btu) [3] which is equivalent to 50 million barrels of oil per day (based upon a calorific value of 130,000 Btu per gallon). If all the proven reserves of the Alaskan North Slope Field (approximately 10 billion barrels) were dedicated to our nation's energy needs in 1980, we would run out in mid-July of that year.

Furthermore, as the sources of new energy become scarcer, they will naturally become more expensive. Typical estimates are for a doubling in unit cost in the next 10 years [4].

The Magnitude of Solid Waste

The solid waste production statistics for the United States are absolutely staggering. A 1968 estimate [5] of the total generation of solid waste put the figure at 7.12 trillion pounds annually (roughly 10 million tons per day or more than 90 pounds per person per day). Of this total 4.20 trillion pounds came from agricultural and animal wastes, 2.20 trillion pounds from mining and mineral processing wastes, and 720 billion pounds from residential, commercial, industrial, and institutional sources. Due to the lack of any complete measurements, the amount of solid wastes actually collected by U. S. municipalities is a topic of some debate. Cohen [6] gives this figure as 539 billion pounds per year, while Regan [7] and Stabenow [8] suggest 400 billion pounds, Niessen [9] 380 billion, and still another source [10] quotes 270 billion. A figure of 5 pounds per person per day is a commonly noted rule-of-thumb for municipally collected solid wastes. These figures are just for the United States, which comprises only 6% of the world's population.

As overwhelming as these figures are for current collection and disposal needs, they will be even larger in the future. Not only is the population steadily increasing, but it appears that we are becoming continuously more productive of solid wastes. The magnitude of the disposal problem is expected to more than double in the next 25 years [11].

Resource and Energy Production Potential of Solid Wastes

The usual terminology for solid waste (i.e. refuse, garbage, trash, and even the work "wastes" itself) implies a substance of little or no value. This could not be further from the truth. Not only does this "waste" possess significant heating value (on the order of 10 million Btu per ton [6]) but it is a veritable mine field of both ferrous and non-ferrous metals (including, for instance, 48 billion cans annually), glass (28 billion bottles annually), as well as a wide assortment of organic materials (100 million tires, 60 billion pounds of paper, and 8 billion pounds of plastic annually) [12]. It has been estimated that typical municipal waste with a moisture content of 25% contains inorganic materials worth between $2.35 and $7.20 per ton in addition to its organic materials whose worth (principally in terms of heating value) is between $3.40 and $11.40 per ton suggesting a total value of between $5.75 and $18.60 in each ton [12]. This means that the annual value of collected municipal wastes is between $1 billion and $3 billion based upon 400 billion pounds per year; yet, it currently costs about $1 billion to dispose of this material in addition to the $3.4 billion expended for collection [12].

Dr. Lesher of the National Center for Resource Recovery, Inc. (NCRR) has cited 1973 as the pivotal year in having swung the economic balance in favor of resource recovery [13]. He points out that the first large scale resource recovery system just began construction in 1974 (in New Orleans) and by 1976 the estimate is for 15 such systems under construction with a majority of U. S. cities practicing resource recovery by 1984. Russell Train, administrator of the Environmental Protection Agency, has stated: "It is significant that 7% of the iron, 8% of the aluminum, 20% of the tin, and 14% of the paper consumed annually could be met by materials recycled from solid waste generated in urban areas." [14]

The solid wastes of municipalities is also valuable in terms of its heating value. The energy content of urban refuse has been estimated at 4,000 Btu per pound by Stabenow [8] and 6,200 Btu per pound by Engdahl [15] with various other estimates between these figures [6, 7, 10]; these values are based upon the wastes as collected without either air or magnetic classification. Murray [11] estimates that when the

70% light fraction is separated its energy content is approximately 7,000 Btu per pound.

Stabenow [8], using 400 billion pounds of 4,000 Btu per pound wastes per year, points out that this has the energy equivalent of 687,000 barrels per day of 152,000 Btu per gallon oil which is the typical capacity of a 120,000 ton tanker. Other sources, [10], using annual production figures of 272 billion pounds of 5,3000 Btu per pound wastes, point out that this could be used to generate approximately 136 billion kilowatt-hours of electricity (about 11% of the annual U. S. total) which would otherwise require 100 billion pounds of coal or 10 billion gallons of oil. For just the New York City area alone, recent estimates [16] point out that the 22 billion pounds of wastes produced per year there could generate approximately 20% of the base electrical load of the same metropolitan area if it is efficiently incinerated with waste heat recovery. Typically, however, refuse incineration processes consume about 75 cents-worth or electrical energy per ton [17].

In addition to energy recovery from urban wastes there is even greater potential for conservation by utilising the wastes of animals and feedlots, agricultural crops, forest slash, as well as from industrial sources not collected by municipalities. Several years ago Engdahl [18] identified 17 industrial wastes suitable for incineration with heat recovery. Hescheles [19] has presented an even more extensive list of wastes from petroleum, pulp and paper, metal, chemical, food, and furniture industries. Recently data has become available for the heating value of this wide variety of potential "fuels" (see

[20], for instance).

A 1974 book published by the National Center for Resource Recovery entitled Resource Recovery from Municipal Solid Waste [21], contains a wealth of additional information regarding the possibilities of using one of our country's critical needs—the economic and nondeleterious disposal of its solid wastes—to contribute to the solution of the other two previously-mentioned needs (energy and inorganic resources).

Schemes for Energy Recovery
from Solid Wastes

The selection of the optimum method or methods for the utilization of the energy content of municipal solid wastes is an extremely complicated one. Although this study is directed toward the concept of incineration by means of vortex combustion with simultaneous waste heat recovery, it is useful to briefly consider recent proposals for other possible concepts.

Pyrolysis

One of the most novel energy recovery proposals is documented by Finney [12] wherein one barrel of synthetic fuel oil roughly equivalent to a No. 6 oil is produced from a single ton of raw, wet municipal garbage by means of a proprietary pyrolysis process of the Garrett Research and Development Company. A 200 ton per day facility using this process is currently being constructed for the city of San Diego from which each ton of waste will provide $1.40 of salvageable magnetic metals, $0.72 of high purity mixed-color glass cullet, and one barrel of synthetic crude which will be sold to the San Diego Gas and Electric Company as a boiler fuel for $2.32. This plant should begin operation in 1975. Garrett estimates that for metropolitan areas of population exceeding 800,000 (of which there are currently 49 such areas in the U. S.) this process can produce a profit without any charge for the waste collection service. Even for populations on the order of 200,000 they estimate that this process would only require about the same charge as that of the most inexpensive landfill operations (about $2.50 per ton).

Combustible gas can also be produced from a pyrolysis process using municipal wastes. Baille [22] has developed a process, using the wastes in the form of a fluidized bed, which is capable of producing 12,600 standard cubic feet (SCF) of 435 Btu per SCF gas per ton.

Digestion

The use of digestion to produce a combustible gas is a very old technique and it has found wide use in countries not known for their advanced technological societies (in Taiwan, for instance, it is claimed that 20 pigs provide the total energy needs for a family of 8 [23]). Recent improvements in the use of methane digestion have demonstrated that one ton of shredded municipal wastes can yield about 100 SCF of 975 Btu per SCF gas after four days of digestion [23].

Incineration

The combustion of solid wastes to provide warmth and for cooking requirements dates from antiquity. The advent of municipal incineration, where the dispersed wastes of a society are collected and burned in a central facility, is however, of comparatively recent origin. The first such incinerator appeared in 1874 in Nottingham, England (where it was called a "destructor") and by the 1920's they were commonly used to generate steam and produce power without the need of any auxiliary fuel [24]. In the United States, the first municipal incinerator is reported to have been built on Governor's Island in New York in 1885. In 1903, an experimental facility demonstrated that steam could be efficiently produced from the incineration of wastes and shortly thereafter a large number of full-scale plants were built (called "crematories") which used the community's waste to provide the community's energy. During the second decade of this century virtually all incinerators constructed were designed for the production of steam [24].

Starting in the 1930's an interesting change took place. While the Europeans continued the development of steam-from-wastes incinerators, the concept fell into disfavor in the United States. By 1966, this process had become the rule in Europe and the exception here and led Eberhardt [25] to say:

> American and European incineration starts from two different prerequisites. In America, volume reduction of the refuse is strived for, in Europe the aim is to completely burn out the refuse, to utilise the waste heat, and to minimize air pollution as far as possible through the use of expensive flue-gas cleaning equipment.

At the 1966 National Incinerator Conference two of the presented papers quantitatively outlined this contrast. Rogus [26] reported upon his visit to 13 modern incinerators in 7 countries with a detailed description of 3 of the facilities (Dusseldorf, Rotterdam, and Vienna); all 13 of these incinerators utilised the heat of combustion for the production of steam. Stephenson [27], on the other hand, presented data on 205 U. S. incinerators all constructed since 1945. Only 43 of these incinerators put the waste heat to any use at all and only 5 of these utilized the heat for the production of electric power (24 used it for building heat and/or hot water, 6 used it for sewage sludge drying, while the remaining 8 used it in a variety of other ways). This led Stephenson to conclude: "Waste-heat utilization can seldom be justified." [27]

The two principal advantages of incineration, which has led to its wide-spread use, are very efficient volume reduction (about 94% reduction for "slagging" incinerators [28] and 97.5% for "bonfire-ash" incinerators [29]) and simplicity of operation (although the advent of stringent air pollution restrictions has negated this latter advantage somewhat). The disadvantages are the cost of operation (roughly twice that of simple dumping) and the resultant air pollution. Surprisingly, odor does not seem to be a problem as long as the furnace temperature is above 1500°F (although in some cases it can be as low as 1000°F) [30]. Shredding of the wastes prior to incineration almost miraculously produces a homogeneous, grayish material which is esthetically inoffensive and virtually odorfree [31]. In addition, shredding greatly enhances the combustion efficiency of incinerators by permitting suspension-firing of the wastes rather then the conventional and less-efficient stoker-firing. Using waste heat boilers with incinerators also tends to diminish the air pollution problems. With no heat removal it is necessary to inject large quantities of excess air or water to sufficiently cool the flue gas temperature so that it may be treated by electrostatic precipitators. The presence of heat recovery coils eliminates this requirement and greatly diminishes (approximately by a factor of 5 [32]) the gas volume requiring clean-up. Also, municipal refuse is inherently low in sulfur content (the light fraction typically contains about 0.2% sulfur [11], which is about one-tenth that of coal [10]) and thus tends to aid the achievement of pollution control standards when burned in combination with conventional fuels.

A recent analysis of 11 methods utilizing energy from wastes, concluded that the best mode was the use of wastes as a supplemental boiler fuel [11]. The principal difficulty has been associated with the fouling and corrosion of the boiler and/or furnace wall surfaces, although recent work in this area has indicated that this can be minimized by a combination of increased boiler tube spacing, metal temperature control, furnace dew point control, and the prevention of a locally reducing atmosphere within the combustion chamber (see [7, 20, 33, 34], for instance). The use of waste in combination with other fuels also tends to minimize the corrosion/fouling problem.

There is a very large number of reference works available on the related subjects of incineration and air pollution. Several of these have been included in the list of References [35-43].

Recent Operating Experiences with Waste Heat Recovery Incinerators

In Appendix A of the recent NCRR publication already cited [21] a list of 33 resource recovery systems and their experiences is presented; some of these systems include heat recovery. Typical performance of 60-70% thermal efficiency and 1-3½ pounds of steam per pound of waste has been realized [44-47]; this means that each ton of waste could produce $1.50 to $5.00 of electrical energy based upon a 25% cycle efficiency and an electrical value of 10 mils per kilowatt-hour [45]. Although there continues to be interest in stoker-fired configurations (see [47] for work with "briquettes" and [2] for "cubettes") most of the effort appears to be directed toward suspension-firing configurations. A brief description of some of the more-recent, successful energy recovery schemes follows.

In France, the Issy-les-Moulineaux Plant located in southwest Paris has used refuse collected in Paris to generate 9,000 kilowatts of electrical energy [48] and has been in operation since 1965. Even the outlet steam from the generating turbine is sold to the Compagnie Parisienne de Chauffage Urbain for use in district heating while the residue remaining in the incinerator is sold for use in road construction. In 1969 another plant began operation (called the "Ivry" Plant) which has an annual capacity of 600,000 tons of refuse and is used to drive a 64,000 kilowatt generator [49]. In England a new refuse power facility has just been recently constructed that is used to produce 25,000 to 35,000 kilowatts of electrical energy [50].

In the United States the Union Electric Company's experiment with its Meramec Plant serving the city of St. Louis has recently received a great deal of attention. There a facility designed to use coal as the fuel has been supplemented (about 10% based upon heating value) with municipally collected wastes. In this manner the incineration of approximately 10 tons per hour of refuse aids in the operation of a 125,000 kolowatt boiler [51]. The refuse preparation consists of shredding to a 1½-inch particle size and magnetic separation prior to ingestion into a tangentially-fired furnace. Wisely [52] concludes on the basis of the St. Louis experience that, "almost all powerplant boilers designed to burn pulverized coal as fuel should be adaptable to permit the firing of refuse as supplementary fuel."

In Chicago, the Southwest Incinerator has been burning 1200 tons per day of refuse (nominally) and generating steam for sale to private customers on a contractual basis since 1962 [53]. The success of this plant led to the construction (completed in 1971) of the largest incinerator of its kind in the United States--the Chicago Northwest Incinerator [8]. This incinerator uses a water-wall configuration and is capable of handling 1600 tons per day of refuse. It will produce 250,000 pounds per hour of steam for sale to neighboring industries. With the addition of this incinerator, Chicago becomes the first major city in the United States that has the capability of incinerating all its municipal refuse [54].

In Maryland the Dickerson Plant has been designed to use coal and oil as the primary fuels in conjunction with municipal refuse and sewage sludge. The fuel nozzles are located in the eight windboxes (it has a divided rectangular-furnace configuration) with tangential firing producing a single flame envelope with apparently large recirculation zones and very efficient combustion [55]. The energy liberated is used to generate 1,700,000 kilowatts of electrical energy for the Washington, D. C. area.

In Nashville the energy from refuse will be used to provide steam and chilled water to 24 buildings initially (scheduled for completion in 1974) and eliminate 50% of the cities landfill requirements. Ultimately they expect to use three-fourths of the city's wastes and serve 38 buildings. [56]

In Menlo Park, California an unconventional energy recovery technique is being developed by the Combustion Power Company. The municipal wastes are burned in a fluidized bed configuration incinerator and then are used directly to drive a specially designed gas turbine obviating the need for steam entirely. [57]

Industries are also rapidly developing energy recovery facilities. The Spaulding Fibre Plant in New York replaced their coal-fired boilers with 5 heat-recovery incinerators one of which is designed to use 60 tons per day of 8,000 to 10,000 Btu per pound solid wastes (the other four incinerators are designed for fumes and liquid wastes) [58]. Mockridge [59] has reported upon package boilers that have been developed for industrial use that are capable of delivering 15,000 to 250,000 pounds of steam per hour (at 1000 pounds per square inch and 925°F). He points out how they can be used for energy recovery in the furniture industry where sawdust production rates can reach 7,000 pounds per hour.

This rapid development of energy recovery schemes has led many (e.g. [6]) to predict a parallel development to the use of pulverized coal which in its 40-year history has come to be the primary power generation fuel. It is interesting to speculate what might-have-been but for the forty-year hiatus of the energy-recovery philosophy in the United States.

Literature Survey of "Swirling Flows"

Classification of Subject-Field

Fluid-Dynamic Classification

Any survey of this subject must first of all cope with the problem of ill-defined terminology. This problem is especially acute because the subject of swirling or vortex flows has been studied from widely different perspectives (wing theory, cylconic separation, Ranque-Hilsch effect, tornado modeling, etc.). As a result, investigators have come from widely different backgrounds each with their own terminology and symbol-convention. In addition, there are subject-areas that appear to be entirely unrelated to the study of vortex flow but which are, in fact, pertinent; the study of flow past concave walls and in helical tubing would be two such examples.

The term "swirling flows" has been selected to represent that class of fluid flows with a significant global vorticity (defined as the curl of the velocity vector) which results in a significant interaction with the stream function. The term "global" is necessary since localized vorticity effects are present in virtually all fluid flows. The term "vortex flows" is reserved for configurations which result in a significant region of flow for which the product of tangential velocity and radius from the centerline is nearly constant (often termed a "circulation preserving" region in the literature although it actually is a region of zero circulation). Due to the effects of viscosity this condition can never hold true at either a physical boundary or the axis of such a flow. The term "rotating flows" is used for that category of swirling flows for which the global vorticity is generated by either externally or internally rotating boundaries. These flows are characterized by regions of constant fluid angular velocity (if the flow is permitted to become fully-developed) in contrast to constant circulation (i.e. circulation preserving). Rotating flows are further distinguishable in that they are generated by a rotating boundary in contrast to vortex flows which are generated "fluid-dynamically" by means of tangential injection or inlet vanes or even by the decay of fluid flowing initially in solid-body rotation. The third category of swirling flows is referred to here as "curved flows". These flows are distinguished by a stationary boundary causing a continual bending of the local velocity vector. They differ from vortex flows in that the vector turning process continues throughout the entire flow not just as the initial generation mechanism. The distinguishing characteristics of these three types of swirling flows are presented in Table 1.

Geometric Classification

Within each type of swirling flow there have been widely different geometrical configurations studied. Each different kind of physical boundary causes a unique flow pattern which is usually not similar to that obtained with a different configuration. A classification scheme for these different geometries is presented in Table 2.

Thermo-Dynamic Classification

A final classification requirement is necessary because the presence or absence of heat transfer in a swirling flow can be just as significant as the effect of its geometry or flow-type. There are two kinds (referred to here as "Classes") of heat transfer boundary conditions for a system: adiabatic or diabatic. Within each class it is also pertinent to specify whether the fluid is reacting or inert. In addition, there is a special condition that occurs in confined vortex flows wherein a non-isothermal flow is produced even for inert fluids flowing in an adiabatic system; this is as a result of an energy separation process, which is adiabatic, and is to be carefully distinguished from an energy transfer process, which is diabatic. Also it should be noted that class A2 and D2 flow fields are significantly more complex because of the presence of specie gradients and radiation effects. These two Classes of heat transfer conditions are defined in Table 3.

Outline of Survey

Survey Philosophy

Any serious attempt to survey the entire field of swirling flows would easily result in 5,000 citations for literature published in the past 25 years alone. It is clearly necessary to not only exclude certain aspects of swirling flows from the survey but also to be selective within those areas deemed most-pertinent.

Areas excluded from this survey would include geophysical flows of large time scales (i.e. oceanographic and atmospheric motions which are rotating flows), swirling flows generated by aircraft (these are free vortex flows), flows which are driven by bouyancy forces (such as the thermosiphon), flows of conducting fluids, boiling or condensing flows, astrophysical applications of vortex flow, and those flows which

TABLE 1

DISTINGUISHING CHARACTERISTICS OF THE THREE TYPES OF SWIRLING FLOWS

Type 1: Vortex Flow	(1) The tangential velocity varies with the inverse first power of the radius (circulation preserving) over a significant portion of the flow field. (2) There is a core of fluid rotating in solid body motion (constant angular velocity). (3) The tangential velocity decays with respect to length. (4) Boundaries, when present, serve only to retard the adjacent fluid layers through viscous action.
Type 2: Rotating Flow	(1) There is no region that can be characterized as being circulation preserving. (2) If the configuration permits the attainment of fully-developed flow, the tangential velocity will vary linearly with the radius (i.e. solid body rotation). (3) The tangential velocity will increase with respect to axial length until the flow is fully-developed and then will remain constant. (4) Boundaries are always present and act to generate the rotating motion through the action of viscosity (hence, the boundary velocity always exceeds the fluid velocity).
Type 3: Curved Flow	(1) The tangential velocity is not a simple function of radius anywhere in the flow field due to the superposition of complex secondary flows. (2) There is no decay in velocity components with respect to length of boundary. (3) The boundary, although not itself rotating, generates the rotating motion as a result of the fluid dynamic reaction to the continual rotation of the local velocity vector by the walls of the geometry.

TABLE 2

GEOMETRIC CLASSIFICATION OF SWIRLING FLOWS

Type 1: Vortex Flow
- A. Free Vortex Flow
  - 1. No Boundary Interaction
    - a. Origin of Flow is an Aircraft
    - b. Origin of Flow is Geophysically Generated
    - c. Origin of Flow is a Swirl Generator
  - 2. With a Boundary Interaction
    - a. Tornado, Hurricane, et. al. Modeling
    - b. Vortex Breakdown Phenomenon
- B. Confined Vortex Flow
  - 1. Fundamental Studies
    - a. Vortex Generator Studies
    - b. Vortex Tube Studies
  - 2. Practical Devices
    - a. Ranque-Hilsch Tube
    - b. Cyclone Separator
    - c. Fluidic Devices
    - d. Containment/Stabilization Configurations
    - e. Nozzles/Diffusers
    - f. Cyclonic Combustion Chamber
    - g. Tangentially-Fired Combustion Chamber

Type 2: Rotating Flow
- A. External Rotating Flow
  - 1. With an Otherwise Quiescent Fluid
  - 2. With an Imposed Free-Stream Velocity
- B. Internal Rotating Flow
  - 1. Simple Rotating Tube
  - 2. Tube with Centerline Inserts
    - a. Small Diameter Inner Tubes
    - b. Axi-Symmetric Bodies of Revolution
  - 3. Ducts with Vortex Generators on Internal Walls
    - a. Spiral Wire
    - b. Trips
  - 4. Annular Tube
  - 5. Shrouded Rotating and Corotating Disks
    - a. Without a Source Flow
    - b. With a Source Flow

Type 3: Curved Flow
- A. Boundary Layer Flow Past Concave/Convex Walls
- B. Flow Through Helically-Formed Tubes
- C. Flow Through Tubes with Axially-Mounted Swirl Generators
  - 1. Swirl Tape
  - 2. Helical Vane
  - 3. Spiral Brush
  - 4. Wire Coil

are investigated from the perspective of pure mathematics.

The survey will be selective in emphasizing Class D conditions (i.e. heat transfer) since that is the primary focus of this investigation. However, Class A flows will also be cited when the results appear to be relevant. The emphasis of the survey will be to give some indication of the earliest work, the most significant papers in the development of the particular flow-type, and the most recent results available.

The primary reason for the prolific publication record on the subject of swirling flows is that it remains very much an unsolved science. Even for the simplest thermodynamic class (i.e. Class A1) insuperable analytical difficulties arise for almost any problem of practical engineering interest. Even the usual analytical technique of fluid mechanics—boundary-layer analysis—becomes much more unmanageable. For a Class A1/confined vortex flow, for instance, instead of the usual viscous boundary layer we find instead a boundary layer "pair" wherein a second layer (usually called the "inertial" layer) arises purely as a result of the fluid rotation. For a Class D1 flow it is necessary to consider a thermal boundary layer in addition to the aforementioned two with even a fourth boundary layer for Class D2 flows (the mass specie concentration layer). In addition, data for most turbulent flows (i.e. those of practical interest) indicate that the exchange coefficients of the flow field are highly anisotropic and non-homogeneous. The net result is that the analytical solutions available in the literature are almost exclusively of the "bits and pieces" variety and are usually applicable only to very simplistic boundary conditions.

TABLE 3

THERMODYNAMIC CLASSIFICATION OF SWIRLING FLOWS

Class A: Adiabatic Systems		
	1. Isothermal Fluid	Approximately isothermal flow field with adiabatic boundaries.
	2. Exothermically Reacting Gas	Thermal energy is released by means of an exothermic reaction but this energy is not transmitted across the boundaries.
	3. Non-Isothermal, Non-Reacting Gas	A non-isothermal flow field which originates as a result of energy separation and not because of heat transfer or chemical reaction.
Class D: Diabatic Systems		
	1. Non-Reacting Fluid	Heat transfer is present at the boundaries as a result of a difference in thermal energy between the inert fluid and the walls.
	2. Exothermically Reacting Gas	The released thermal energy of chemical reaction is transported across the system boundaries.

In March 1974 issue of the *Journal of Fluids Engineering*, Dr. Joshua Swithenbank [60], a well-known professor and consultant in the area of combustion, commented on the limitations of our current knowledge of combustion processes. His remarks are appropriate in that they delimit what one can hope to expect in any literature search in the turbulent combustion area even without the presence of swirl:

> . . . It is widely thought they we understand the industrial combustion processes, and it is this myth which I wish to explode. . . .
>
> . . . we do not even know the turbulence level nor its distribution in any industrial combustor. We have no satisfactory theory which accounts for turbulent flame speeds in gaseous systems . . . our predictions of convective heat transfer to combustor walls are, to say the least, inaccurate, while the true effects of the unsteady gas temperatures on radiant heat transfer are a long way from comprehension.
>
> . . . burners incorporating particle separation could be designed using confined vortex flow, however there is no theoretical method of predicting these flow patterns nor any meaningful measurements in confined vortex systems since the presence of probes modifies the flow field.
>
> Many of the practical problems of turbulent flow are not even defined . . . the rate of growth, agglomeration, and burnout of soot is not understood, and in fact the rates of most pertinent reactions are not known within a factor of two. . . . we cannot fundamentally predict the combustion efficiency or even the limits of operation of any practical combustor. . . .

It is not surprising, then, that the most extensive survey of Class A2 or D2 flows provides principally empirical correlations for special geometries.

Basic Theory of Swirling Flows

Swirling flow has been a subject of scientific interest for at least four centuries. Da Vinci recorded a number of observations on vortices which are available in publications of his papers. Newton applied his considerable analytical prowess to rotating spheres of liquid in attempting to explain the oblateness of the earth. In the nineteenth century, Helmholtz, Kelvin, and Rayleigh (among others) achieved notoriety, in part, for their work on rotating flows. Helmholtz developed three famous theorems on the transmission of vorticity in fluids which are now known by his name. Rayleigh published a very famous work in 1917 [61] that is still widely quoted in regard to the stability criteria for a rotating fluid. In 1916 Proudman [62] predicted that a rotating fluid could maintain a two-dimensional column of fluid within a fluid; this phenomenon was demonstrated in the now famous experiment of Taylor [63] in 1921.

Perhaps the first analytical effort to determine heat transfer in a swirling flow was due to von Karman [64] who in 1921 developed one of the classic solutions of the Navier-Stokes Equations—that of a flow field induced by a rotating disk.

One of the earliest books available that provided an extensive treatment of the subject of swirling flows was Lamb's classic work [65]. He included a chapter on "vortex motion" as well as one on "rotating masses of liquids." Goldstein [66] also included this subject in his edited work. In more recent times, Truesdell [67] has published a widely cited work on the kinematics of vorticity, Batchellor [68] has treated rotating flows in addition to vorticity transport, and Owczarek [69] has discussed the effect of fluid rotation on the development of flow instabilities and transition from laminar to turbulent flow.

It appears that Greenspan [70] in 1968 published the first book that dealt solely with the topic of swirling flow. His work is concerned with the motion of an incompressible, viscous fluid rotating either in a container or an unbounded environment with geophysical flows as the primary application in mind. Like all the previously-mentioned books, his treatment is restricted to adiabatic, isothermal conditions (i.e. Clas A1). A very extensive bibliography of 312 citations is included in Professor Greenspan's book.

More recently (1971), Murthy [71] has written a monograph with the purpose of providing a survey of swirling flows from a theoretical viewpoint oriented primarily toward non-geophysical applications (he has included a bibliography of 220 references). Frequent reference will be made to this work. Murthy brings out many of the sources of difficulty in analyzing swirling flows some of which are summarized below:

(1) The use of a scalar eddy viscosity has had very limited success in correlating experimental data (Page 34).

(2) Although a boundary layer develops as for simple linear flows the casual and sustaining mechanism is much more sophisticated (Page 35).

(3) A large number of additional dimensionless parameters are necessary due to the fluid rotation but even these do not fully define the flow field; specifically, he writes: "It may be remarked here that the use of such dimensionless parameters as similarity parameters for confined vortex flows is beset with a great number of difficulties. Such difficulties arise because *changes in the geometrical configurations cannot simply be accounted for by changes in the geometrical non-dimensional parameters based upon characteristic lengths*. Rotating fluid flows, as stated in the introduction, involve curious wave motions, instabilities and transition (from laminar to turbulent state). The occurrence of such phenomena is not subject to simple scaling laws. Even in the absence of such processes, the influence of wall boundary layers presents considerable difficulties particularly in regions where the swirl is introduced into the flow. Lastly, apart from such uncertainties in the initial conditions, the exit conditions from a system are not in general subject to similarity considerations." (Page 38, italics mine)

(4) The analogy that can sometimes be invoked for linear flows between the transport of heat and vorticity is not possible when the flow has a component of tangential (i.e. circumferential) velocity (Page 185).

The quote given above (3) is especially significant because it indicates the difficulty in using the results available in the literature since the geometry is rarely ever similar let alone identical. This has led Dr. Erich Soehngen; whose work with vortex flows has spanned 3 decades, to recently comment, "Experimental vortex flows are like their maker, each is one-of-a-kind." [72]

Heat Transfer Aspects

Heat transfer augmentation is a subject of much current research as the need continues for higher heat flux densities in smaller volumes. Bergles in two recent surveys on the subject [73, 74] classifies swirling flow as one of about a dozen ways that higher heat transfer rates can be achieved. He identifies 5 kinds of Swirling Flow heat transfer configurations:

(1) coiled wires/spiral fins
(2) stationary propellers
(3) coiled (or helical) tubes
(4) inlet vortex generators
(5) swirl tapes

Of these five, the coiled wires/spiral fins are treated as surface roughness effects since they produce only a slight fluid rotation, the stationary propellers are dismissed as being ineffective, the inlet vortex generators are noted to be the subject of limited research (he gives only two citations for single-phase flows), and only the helical tubes and swirl tapes are surveyed in any depth. It should be noted that this latter category (helically-coiled tubes and swirl tapes) is characterised by a non-decaying swirl-level in contrast to the stationary propeller or inlet vortex generator configurations. All five of these swirl flow heat transfer augmentation concepts are for confined or internal geometrical configurations without rotating boundaries (i.e. Types 1A or 3 in Table 2).

Kreith [75] has reviewed the state of heat transfer in what he terms rotating flow (basically Types 2A and 2B in Table 2). He includes a limited discussion on swirl tape flow (Type 3C1) among the 193 references he cites. Kreith also includes a very pertinent caveat: "...new and unexpected phenomena may occur when operating conditions are extended beyond the ranges of the variables for which experimental data are available."

Eckert [76] has edited a recent survey of heat transfer literature for the 17 year period from 1953 through 1969 that includes heat transfer references for confined vortex flow and curved flow under the heading of "Channel Flow" (a total of 63 such references) and for rotating flow under the heading of "Convection from Rotating Surfaces" (183 references). In addition, more-recent bibliographies and surveys appear periodically in the International Journal of Heat and Mass Transfer.

A detailed discussion of the pertinent results of these citations will be deferred to the appropriate subsections to follow.

Aspects of Data Interpretation and Application

There are two aspects of data interpretation and application which are pertinent to the study here that are widely debated in the literature. The first deals with the applicability of isothermal data to the prediction or interpretation of conflagrant flow fields. The question arises because of the difficulty of obtaining data in a combustion environment and thus there is a great temptation to utilize the abundant data available with Class A1 flows for Class A2 or D2 flows. There is not yet a consensus for the validity of this concept and in the course of the survey the various divergent viewpoints and opinions will be noted.

The second aspect of data application debated in the literature is the validity of any data obtained by the use of probes, however small, inserted into the flow field. Although it is agreed that some disturbance of the flow field is inherently present as with almost any measurement system, it is not at all clear whether the peculiar nature of swirling flows is sufficiently insensitive to these devices that meaningful data can be obtained. The divergent opinions expressed in the literature will be discussed in the course of the survey for this issue also.

Literature Common to Vortex Flows

Vortex "Cores"

The subject of vortex "cores", sometimes called "concentrated vortex cores," is concerned specifically with the structure of the inner portion of a vortex flow wherein the effects of viscosity prevent the circulation from being preserved (otherwise an infinite tangential velocity would need to occur at the axis). There is a wide body of literature on this subject although most of it is directed toward either atmospheric vortex cores (i.e. whirls, dust devils, tornadoes, whirlwinds, waterspouts, typhoons, hurricanes, willy-willies, etc.) or aerodynamic vortex cores (i.e. the trailing vortex pair always present as a result of induced lift from a finite wing).

An early survey of the structure of vortex cores was given by Gartshore [77, 78] while Hall [79] has more recently summarised the state of knowledge on the subject. Hall begins his survey of the axisymmetric core of a spiraling fluid of high vorticity by presenting the complete equations of motion for a viscous, heat-conducting, compressible fluid; then he quickly notes that: "The above equations are couple, elliptic, and highly non-linear, and can not at present be solved without drastic simplification." There are three usual procedures, he points out, by which analytical results can be achieved:

(1) make use of quasi-cylindrical assumptions to transform the equation from an elliptic-type to a parabolic-type, or

(2) simply linearize the equations by dropping every non-linear term, or

(3) apply similarity transforms, which apply only to special boundary conditions, that permit the reduction of the partial differential equations to simply ordinary differential equations.

Hall then discusses in some detail the application of vortex core theory to the explanation of the Ranque-Hilsch Effect.

Kuchemann [80] and Riley [81] have recently reported on international conferences that have been devoted exclusively to papers on vortex cores.

Morton [82] has surveyed the area of vortex cores from a geophysical-application viewpoint Howard [83], Lighthill [84], and Carrier [85] are three widely-quoted reference papers on the subject of geophysical motions that are helpful in explaining how such vortex cores can develop. The study of fire whirls has received considerable recent attention, see Emmons [86] and Lee [87], and is of interest here because the combustion phenomenon present greatly influences the flow. Emmons points out the somewhat paradoxical result that fire whirls, together with tornadoes, achieve their violence primarily because turbulence is suppressed by the centrifugal forces present as a result of the rotating flow field. In fact, he indicates that it is entirely possible to laminarize a whirl flame due to the stabilizing effect of rotation. As will be discussed later this is in contrast to the experience of free vortex flames. Emmons summarizes the extent of knowledge about fire whirls as "very crude."

Vortex core literature from the aerodynamic perspective is so abundant that no attempt will be made to survey it here. Kuchemann [88] has written a survey article on the subject with an extensive bibliography. A recent NASA report by Baldwin and Chigier [89] presents a computer program for the prediction of vortex decay from aircraft. The subject of aerodynamic vortex cores has, in fact, almost become a fluid-dynamic field to itself even to the extent of short courses devoted exclusively to this area [90].

Vortex "Waves"

One of the interesting features of swirling flows is their capacity to sustain wave motion even for completely incompressible fluids. Perhaps the most well-known standing wave motion is that of the previously-mentioned Taylor-Proudman Column but there are a great many other examples (see Batchellor [68] for some unusual photographs). A detailed survey of this subject is outside the scope of this investigation and reference is made only to the books of Lyttleton [91] and Chandrasekhar [92] on the general subject of hydrodynamic stability and to Chapters 3 and 4 of Murthy [71] where a survey of this topic is available.

Vortex "Breakdown"

It is experimentally observed that under certain circumstances a vortex whose structure and velocity profiles has been changing gradually and uniformly with respect to its length abruptly forms a stagnation point at its axis with an associated reversed flow "bubble" that causes the streamlines to diverge suddenly. This phenomenon has come to be known as "vortex breakdown" although some investigators prefer the term "vortex jump". According to Murthy ([71], page 121) this unusual feature was observed almost two centuries ago; however, careful observation and investigation of vortex breakdowns, at least insofar as the literature reveals, has only been done in the past 15 years or so. Harvey [93] reported one of the earliest investigations on this subject; his results were purely visual. More recently, Mamworthy [94] has developed an apparatus that can produce the breakdown under a variety of conditions although it is primarily an end-wall interaction effect in his experiments. Because the occurrence of a breakdown is associated with a large region of sensitive, low-velocity flow, experiments have been hampered by the effect of measuring devices on the flow to be measured. However, within the past several years, the use of laser anemometry has been reported [95] which should provide much more useful data in the near future.

Explanations and interpretations of the breakdown phenomenon have been hotly debated in the literature. Hall [96], in a recent survey of the subject, has classified all the postulated theories into three camps:

(1) the separation theory—which explains the breakdown as a

rotating flow equivalent of two-dimensional, axial flow separation (a viewpoint championed by Hall himself [97]),

(2) the hydrodynamic instability theory—which explains the event in terms of a standing wave (see Ludwieg [98]), and

(3) the critical state theory—which takes the perspective that breakdown (usually called a "jump" by this group) is a finite transition between conjugate states much like a hydraulic jump in open channel flow (see Benjamin [99-101] and Bossel [102-104]).

Although no completely satisfactory theory exists as yet, it is still possible to summarize the circumstances under which breakdown usually occurs:

(1) A high value of swirl is essential. Hall [96] claims that the swirl angle (defined as the arctangent of the ratio of the tangential velocity to the axial velocity) must be greater than 40 degrees upstream of a breakdown; this means that the tangential velocity must be greater than 0.84 times the axial velocity.

(2) The axial pressure gradient can determine both the existence and location of the breakdown [102]. It appears that an adverse pressure gradient is not essential as Hall [96] reports that breakdown can occur in a simple tube for which there is a favorable gradient for values of swirl just below the breakdown value. Bossel [104] points out that for low values of swirl it is possible to have a large divergence for the outer streamtube contour, but at higher swirls a very small increase in streamtube radius can cause stagnation at the axis or a very small decrease in radius can cause accleration at the axis. It would seem, then, that breakdown would occur much more readily in unconfined vortex flows where the spread of the vortex jet is unconstrained than it would for confined vortex flows where the development of side-wall boundary layer would tend to diminish the radius of the vortex contour.

(3) When breakdown occurs, the influence of downstream disturbances becomes very pronounced [102] much in the manner of a hydraulic jump or a normal shock. This increased downstream-influence effect was explained by Lewellen ([105], pages 101, 102) as follows:

> In a confined vortex, breakdown may be expected to occur at varying positions along the axis as a function of swirl. For small values of swirl breakdown will not occur anywhere. For moderate values of swirl which permit the flow at the minimum exhaust cross section to still be slightly supercritical, breakdown should occur downstream of this cross section as flow expands, and becomes less supercritical (increasing its maximum swirl angle). As the swirl is increased, breakdown will move upstream toward the minimum exhaust cross section. When the swirl is sufficiently large for the breakdown to move upstream of the exhaust the flow becomes subcritical all along the

> axis and the breakdown must jump to the wall opposite the exhaust where it is associated with the eruption of the end wall boundary layer. . .

This statement by Lewellen will be discussed more thoroughly in Chapters 3 and 4.

(4) The breakdown is an essentially inviscid phenomenon with the Reynolds number and Mach number playing only a minor role. [102]

(5) Rotation in the recirculation bubble may be reversed. [102]

(6) The breakdown may be either axisymmetric or spiral in character ([105], page 95).

The form of vortex breakdown discussed to this point is essentially of a steady flow nature. Unsteady vortex cores and vortex bubbles have also been observed [106, 107]. Not only can the vortex core take on a spiral shape but it can process as well. It is thought that this phenomenon is related to the occurrence of the vortex whistle.

In Murthy [71] a connected account of the subject of vortex breakdown is presented. It appears that very little work has been done for non-isothermal flows in regard to the breakdown; further mention of this will be made in the subsection on vortex flames to follow.

Literature Survey of Free Vortex Flows

Isothermal Jets

The use of swirl with isothermal jets in practical devices dates back many years. Wotring [108] obtained a patent for using swirl to atomise oil for a burner in 1940. Through the years a wide variety of swirl atomiser configurations have been developed and reported in the literature; among the more recent are Nolan [109] who has reported on the use of such an atomiser to inject sewage sludge in a heat recovery incinerator, and Berman [110] who has presented a somewhat novel configuration for the use with liquid fuels which he terms a "swirl cup". Due to its limited application to the study here, no further mention is made of swirl atomizers.

Swirl jets can be generated in a variety of ways. Ullrich [111] used tangential inlets and vanes, Rose [112] a pipe rotating at 9500 revolutions per minute, Gore [113] a rotating perforated plate, Chigier [114] an annular chamber shown in Figure 1a (taken from [114]) with both orifice-exits and diverging channels, and Chigier [115] with what has come to be known as a "swirl generator". This swirl generator permits the mixing of any combination of tangential and axial air flow rates and is shown in Figure 1b (taken from [115]).

As a result of the swirl imposed upon a jet, tangential, axial, and radial velocity components are produced together with axial and radial pressure gradients. These gradients enhance jet mixing and produce a wider jet for the same length than for the case without swirl (or with reduced swirl).

There has been a modest production of theoretical examinations of swirl jets although until recently they have been strictly for laminar flows and usually only for very weak (in terms of intensity) swirls. Loitsyanskii [116] and Gortler [117] were two of the earliest efforts along this line. Steiger [118, 119] extended their analysis to permit moderate and strong swirls. These analyses predict that the tangential velocity of the jet will decay with the inverse square of the coordinate along the jet while the tangential and radial velocities will tend to decay with the inverse first power. Therefore, if the swirl ratio is

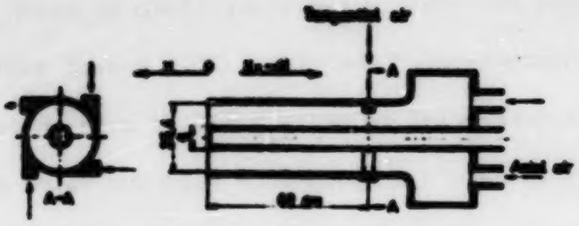
Tangential air
A
A
Axial air
A-A

(a) Annular Swirl Generator

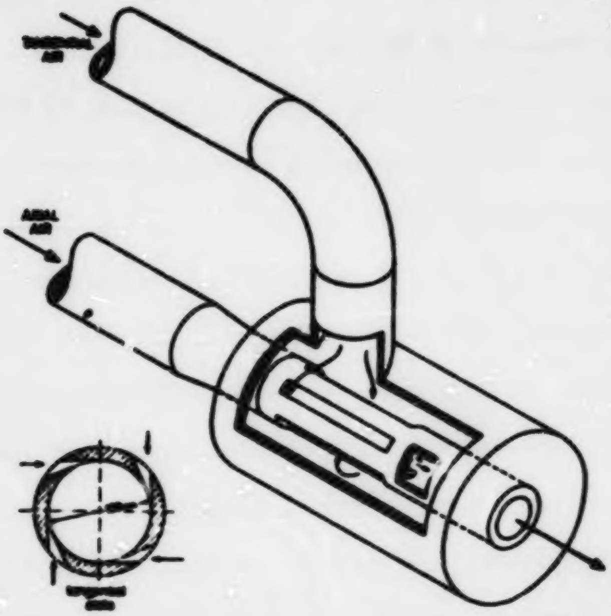
Tangential Air
Axial Air

(b) Orifice Swirl Generator

Figure 1. Chigier Swirl Generators (taken from [114, 115])

defined as the ratio of the local tangential to axial velocity components, this would decay as the inverse first power also. These analyses have been extended to turbulent flows by means of a great many simplifying assumptions. Shao-Lin [120] assumed similar profiles for the axial and tangential velocity together with an assumed jet entrainment velocity to obtain a close-form solution using the mixing-length theory. This was extended by Chigier [121, 115] who reduced the equations to functions of three empirically determined decay constants without the need for any entrainment velocity assumption. These decay constants are a function of the magnitude of swirl and have been experimentally examined by Chigier also [115].

Recent experimental work has been devoted to trying to obtain double-velocity correlations using hot-wire equipment [122, 123] to permit a better understanding of the turbulence structure of these jets. Lilley [124, 125] has developed a program that uses axial and tangential velocity profile data to infer the radial-axial and radial-tangential shear coefficients for small values of swirl. He has found that the shear stress, the turbulent intensity, and the rate of entrainment increase for increasing values of swirl in the near-jet region; in the far region (usually defined to be about 15 exit orifice diameters downstream), however, he has found that the shear stresses are actually lower than for the case of no swirl. From this he has concluded that the model of an isotropic, uniform mixing-length is appropriate only for very small swirls.

The restriction of small swirl values in the analytical schemes attempted is a result of the formation of vortex bubbles or recirculation zones for values above a critical number. These zones have been observed and documented by a number of sources [114, 115, 122] and are the source of insuperable analytical difficulties. It is the presence of this bubble, however, that makes swirl such an attractive feature for flames, a point to be discussed in the next subsection.

The primary correlating variable that has been reported is commonly referred to as the "swirl number" with the symbol "S". It was defined originally by Chigier [114] as the ratio $G_\phi/G_x R$, where G_ϕ is the axial flux of angular momentum, G_x is the axial flux of linear momentum, and R is the outer radius at the orifice exit. The value of S is found by integrating the axial and tangential velocity profile data for r (radius from the jet centerline) from zero to infinity at each axial station of the jet. The data appears to indicate that both G_ϕ and G_x are conserved with respect to jet length and hence S is also conserved. If the tangential velocity varies according to some known function of jet radius, and if the axial velocity can be similarly described, it is then possible to compute the value of swirl a priori. However, the only apparent success at this procedure was noted by Chigier [115] for the assumption of solid body rotation and uniform axial velocity at the orifice exit and even this success was limited to very small values of swirl (about 0.20 maximum) indicating that the exit flow is not so simply described.

The use of this swirl number has been successful in correlating the Chigier decay constants and the onset of recirculation. Chigier [115] has demonstrated that a recirculation zone can be expected to occur for swirl values greater than 0.64 (a magnitude which he calls "very strong swirl"). However, he also cautions ([114], page 789):

> ...these distributions showed that the basic nondimensional characteristics of swirling jets, i.e., pressures in swirl generator, exit profiles, minimum pressure, maximum reverse-flow velocity, and length of the internal vortex, were largely determined by the ratio of the moments. It became clear, however, that the shape of the nozzle as well as the method of introduction of the tangential air can also influence the behavior of the jets. It cannot therefore be claimed that the ratio $G_\phi/G_x R$ is the sole universal criterion for swirling jets but it is expected to be the significant criterion of similarity for all swirling jets having geometrically similar swirl generators.

Murthy [71] includes a discussion of Chigier's swirl number together with a confined vortex flow analogue of this parameter, $0.5\Gamma/m$, where Γ is the circulation around a particular contour, and m is the axial mass flux through that contour.

Vortex Flames

The subject of vortex flames dates back at least four decades to the development of the tangentially-fired furnace and the cyclone combustion chamber. Since these configurations are classed as confined vortex flows they will be discussed in the next section; however, several early papers dealing with flame stability are included here even though some of the results were obtained in ducted configurations.

The early interest in vortex flames was due to the enhanced turbulence achieved during furnace combustion processes. In the post World War II era, research began on the stabilizing influence of swirl on a flame which permitted shorter flame lengths at higher superficial velocities (defined as the velocity the gases would have experienced had they passed through the orifice or duct unburned and at room conditions). The earliest work was apparently done by Alexander at the

University of Illinois in the period 1949-1952, however there are no published papers during this period. The first known paper on this effect was by Hottel [126] in 1953. He was concerned about the possibility of modeling the conflagrant flow with an isothermal one. On the basis of qualitative observation Hottel concluded, "Combustion runs indicated no significant change from cold flow in the volume occupied by the fixed-vortex core." He explained the recirculation zone and the resulting shortened flame length as due to an adverse axial pressure gradient that must be present due to vortex decay. For his configuration, however, he concluded that no recirculation actually occurred.

Pistor [127] also examined a swirl flame in a ducted system and found, as Hottel had, that the flame formed an annulus with the unburned gases on the exterior. Albright [128] then published extensive results for swirl flames in free jets, straight ducts, and diverging ducts. For the ducted configurations, Albright also found hollow flames with the unburned gases on the exterior even though his apparatus produced much higher superficial velocities (up to 700 feet per second) and, apparently, a recirculation region. He found that the effect of swirl was to stabilize the flame whether it was a free jet or a confined one, but he found the effect more pronounced for the confined configurations. In fact, he was able to produce stable flames 20 inches long in only a half-inch diameter tube. Albright attributed this to the phenomenon of recirculation but the only evidence he offerred was that for conflagrant flows the core gas temperatures were lower than at the flame-annulus boundary which he explained by the hypothesis of relatively cool recirculation gases mixing with the products of combustion.

It should be noted that in his configuration the fuel (natural gas) was admitted only axially while the swirl was provided by supplying the air tangentially.

The continuation of this work was published a year later by Albright [129] for a larger diameter tube (2 inches) and a less intense vortex. For this work he measured velocity profiles by means of a 1/16-inch diameter pitot probe for both isothermal and conflagrant conditions and noted that although recirculation was observed for the air-only condition at the axis, no such pattern was found for the combustion condition. This led him to conclude contra Hottel [126], "The differences in the flow patterns . . . were probably caused primarily by heat release in the gases. Angular momentum was, however, unaffected by combustion." He makes no mention of the possible disturbance of the effect he is trying to measure by the device he is using to measure it. Kenny [130] continued this work on the same apparatus using propane to determine conbustion efficiency as a function of degree of swirl and duct length by means of a quenching-gas analysis device located at the duct exit. Drake [131] found that there was an optimum value of swirl to maximize combustion-completeness. Kerr [132, 133] presented correlations for combustion efficiency in an actual furnace installation as a function of a single, non-dimensional parameter characterizing the intensity of swirl.

The results of this early work may be summarized as follows:

(1) The presence of swirl tends to stabilise flames for both free and confined configurations.

(2) The flame front forms an annulus (identified by the location of maximum temperature isotherms) with the unburned gases on the

exterior and the products of combustion in the core region.

(3) For ducted configurations the flame front does not quite touch the wall and somewhat surprisingly does not appreciably heat the walls either (hence these flame systems were essentially adiabatic).

(4) When the apparatus was used under isothermal conditions recirculation zones (usually only at the core region) were observed that apparently were not present under combustion conditions.

(5) Two crucial questions were unresolved: how valid is it to interpret conflagrant flows by results observed with isothermal flows? and is it possible to insert probes into the vortex flow field and obtain uncorrupted, meaningful data particularly when recirculation is present or eminent?

It is this last pair of questions that remain to be answered to this day.

There has been a great deal of work done on the subject of vortex flames in recent years spurned by its widespread use in commercial furnaces. Much of it has been done under the sponsorship of the International Flame Research Foundation. Chigier [134] has measured the decay of the axial and tangential velocity components for a vortex flame (from a combination of propane, butane, and air) and found it (the decay) to be slower than for an isothermal jet. Chigier, in this paper, made all the usual observations regarding these flames: they are shorter, more turbulent, and become stabilized closer to the exit orifice all as a result of swirl; Professor Emmons, in his recorded comments of the paper [134], pointed out how these contradict all the maxims of what is known about fire whirls (see [86, 87]) which evidence lengthened flames and reduced turbulence (even to the point of laminarization). Although unable to convince Dr. Chigier, Professor Emmons reasoned that the difference could be accounted for by noting that for a fire whirl, which has a rotating core with a free vortex surrounding, the radial gradient of angular momentum is either positive or zero everywhere and hence from Rayleigh's stability criterion [61] the flow field is stable, whereas the vortex flame, which is characterized by a rotating flow field exiting into a stationary air mass, possesses a strong negative radial gradient of angular momentum at the jet boundary and is therefore unstable because of the same criterion and hence turbulence tends to be promoted rather than suppressed. He, Emmons, readily admitted, however, that "There are in fact so many effects present that it is impossible to solve the Navier-Stokes Equations in either case..."

Chervinsky [135], on the basis of his data, also concluded that an increase in the value of swirl resulted in an increased flame width, decreased flame length, increased decay rates of all velocity components, and increased turbulent intensity; he explained all these effects in terms of an increased eddy viscosity and spatial variation of the turbulent Prandtl Number.

This discrepancy in the effect of fluid rotation on flame length was apparently resolved by Beer [136] with his experiments for an axial jet exiting into a rotating cylindrical flow. The rotation tends to exert a stabilizing effect because of centrifugal forces even for isothermal conditions, but when combustion is also present the density stratification causes an additional stabilizing influence. Hence, he concludes that this configuration could well lead to a laminarized flow and confirms the observations of Emmons.

Analytical attempts to model swirl flames have been greatly impeded by their need to begin with the aero-chemical dynamics of high vorticity flames [137]. Beer and Chigier, in a recent (1972) book on the subject of combustion aerodynamics concluded that ". . .the theory is not yet able to predict flame stability."([138], page 130). Thus, as noted by Dr. Swithenbank [60], the turbulent swirl-flame is as yet unsolved.

The debate continues as to the validity of using isothermal results for combustion processes. Syred [139] has recently commented ". . .for the modeling of swirl combustors it has been common practice to extrapolate isothermal experiments to combustion conditions. Although there are similarities it now appears that certain fundamental differences may arise depending upon the type of burner and mode of entry." (italics mine) But, Chigier, in a paper published not only in the same era but in the same volume of the same journal [140], claimed that it is permissible to compare isothermal and combustion condition processes even when recirculation is present because "the gasdynamic and chemokinetic processes become decoupled" since, he reasons, the chemical energy release is much less than the turbulent energy of the flow and hence has a negligible effect on the turbulent flow field.

The debate on the effects of inserted probes, however, may soon reach a resolution. The development of laser anemometry for velocity measurement in flames began about 1971 (see, for instance, [141-143], and meaningful data should be forthcoming soon.

In the two years since the publication of Beer and Chigier's book [138], a number of advances in analytical techniques have been published. Rubel [144, 145] has used a simple scalar eddy viscosity model with a potential core formulation to accurately predict the behavior of swirling flames in the far-jet region for weak swirl intensities. He has found that the enhanced mixing present at the jet boundary as a result of swirl could result in as much as a 25% reduction in nitrogen oxide formation because of the early cessation of NO producing reactions. Since he invoked the boundary layer approximations, his analysis can not be extended to either the near jet region or to cases with strong swirls.

Lilley, in a wholesale assault on the problem [146-149], has been able to achieve the following:

(1) He has extended his work for isothermal swirling jets to conflagrant ones for the invoked boundary layer assumptions and restrictions of weak swirl, thus enabling the calculation (via a computer program) of the two significant shear stress components of the stress tensor, the radial component of the turbulent enthalpy flux vector, and the radial component of each turbulent chemical specie flux vector from experimental mean distributions of tangential and axial velocity components, temperature distribution, and mass specie distributions.

(2) He has utilized his program with the limited distribution data available to show that the turbulent stress distribution is anisotropic, inhomogeneous, and a function of the degree of swirl.

(3) The results of his program tend to confirm the suspicion that conflagrant flows are very different from isothermal ones. Specifically, he writes, "In particular, the turbulent viscosity was found to be highly nonisotropic, the $r\theta$ component being an order of magnitude less than the rz component. The variation of normalized μrz with swirl *was found to be the opposite of that found in the isothermal case, indication that the effect of the combustion was far more than just a density change*." ([146], pages 186, 187, italics mine--where θ is the tangential coordinate, z the axial coordinate, and μ the viscosity).

(4) In a very recent paper [148] he has incorporated a nonisotropic mixing-length and energy-length turbulence model together with an eddy-break-up turbulence controlled reaction model (all previous work, including that of Rubel, employed the Arrhenius Model), together with the usual boundary layer assumptions (thus restricting the analysis to weak swirls) in a finite difference computation scheme that appears to accurately portray a vortex flame albeit a weak one.

Hacker [150] has recently published a proposed blow-off model for strongly swirling flows in terms of the ratio of tangential velocity to axial velocity which he calls the swirl parameter. However, he claims that, "The presence of the reverse flow region is in all respects identical to the reverse flow region observed in cold swirling flows". It is interesting that this comment and the one by Lilley (given on the preceding page) were made only a month apart in the same journal.

Literature Survey of Confined Vortex Flows

Fundamental Studies

The literature survey of confined vortex flows is separated into two broad categories: fundamental studies and practical devices. Although it is sometimes difficult to classify a particular paper into one of the other of these categories, if the work is of a general nature not specifically for a restricted geometry it has been classified as a fundamental study; on the other hand if the work is directed primarily to understanding how a particular device operates or how it might be optimized, it has been classified under that device in the category of practical devices.

Two basic kinds of geometries have been investigated in the area of fundamental studies. One of them has come to be known in the literature as the "bath-tub" vortex problem; this terminology is unfortunate in that it implies the draining of a liquid with swirl and the associated free surface problem (see, for instance, Dergarabedian [151] or Sibulkin [152]). Since the literature on this configuration is devoted to single-phase fluids without a free surface it will be referred to as a "vortex chamber" here. A sketch of this geometry, taken from Lewellen [105], is shown in Figure 2a.

The second geometry for which a body of literature exists also has a terminology-difficulty—specifically, no name at all. It is shown in Figure 2b (taken from Murthy [71]) and is referred to here as a "vortex tube" although it is not to be confused with a Ranque-Hilsch Tube which operates under a very different fluid-dynamic environment. As is apparent from a comparison of Figures 2a and 2b, the vortex tube can be thought of as a vortex chamber with a relatively large exit orifice connected to a long cylindrical tube. In both devices the swirling motion may be generated in a variety of ways (tangential entry, inlet vanes, stationary propellers, etc.) the vortex tube is distinguished by the presence of vortex decay with respect to length.

The vortex chamber configuration has been extensively studied for more than 20 years and the literature contains hundreds of papers, many of them purely analytical, on the flow field for this geometry. The vortex tube, on the other hand, has had rather limited study (with the exception of the Ranque-Hilsch Tube device which bears some geometrical similarity) especially along analytical lines. Since the object of this study would be classed in the vortex tube category, it is pertinent to ask: to what extent may vortex chamber analysis be utilized? The answer may be given by identifying the distinguishing characteristics of these two geometries:

(1) Length to Diameter Ratio: For the vortex chamber this is of order 1 whereas in the vortex tube it is of order 10.

(2) Decay: Only for the vortex tube, since the tangentially-injected fluid is supplied over the entire length of the vortex chamber.

(3) Exit Boundary Condition: For the vortex chamber the ratio of the chamber diameter to the exit orifice is of order 10 and is a significant controlling factor; in the vortex tube there are really two exits, the chamber exit and the tube exit, both of which are of realatively large diameter. It is also important to note that for

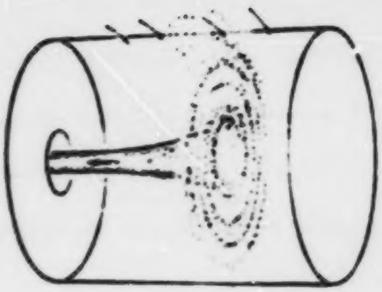

(a) Vortex Chamber (taken from [105])

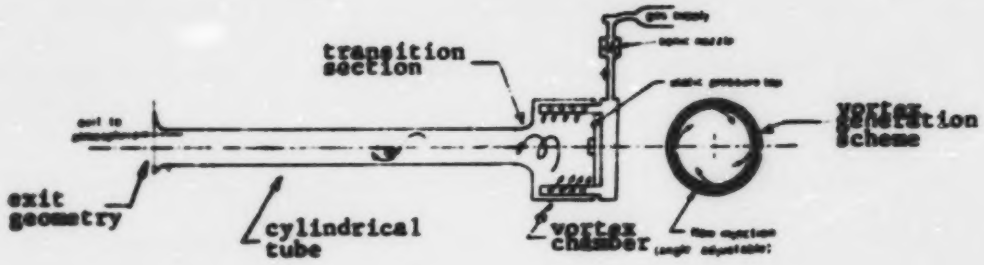
gas supply
transition
section
static pressure tap
exit to
atmosphere
vortex
generation
scheme
exit
geometry
cylindrical
tube
vortex
chamber
flow injection
(angle adjustable)

(b) Vortex Tube (taken from [71])

Figure 2. Two Fundamental Geometries

the vortex chamber the flow field is governed by a free expansion of the fluid out the exit orifice whereas in the vortex tube the flow exiting the chamber is constrained by the tube.

(4) Transition Section: vortex tubes have been constructed using a variety of transition sections whereas the vortex chamber has used the abrupt, end-plate-like configuration exclusively.

The conclusion of this comparison must be that the results of vortex chamber analysis are of limited applicability to vortex tube flow. In fact, as will be discussed subsequently, many of the results available for vortex tube flow are difficult to interpret because of variations in injection schemes, transition sections, length-to-diameter ratios, etc.

Vortex Chamber Studies

This geometry as shown in Figure 2a has become the classic geometry for confined vortex flows in the sense that virtually all the analytical approaches have adopted it as the object of investigation. Perhaps the very first investigators to do so were Einstein and Li [153] in 1951 in what has come to be the classic paper in the field as evidenced by the hundreds of times it has been cited since its publication.

There are two principal problem areas that are the object of most of the papers: the effects of the exit boundary conditions and the end wall boundary layers. Donaldson in a series of publications ([154-156], among many others) has developed a complete family of similarity solutions to the Navier-Stokes equations. The primary difficulty with the result, aside from being restricted to weak swirls, is that the required form of the boundary conditions do not appear to be capable of being satisfied by the geometry of Figure 2a (some have suggested a rotating, perforated pipe open at both ends through which the tangentially admitted air exits). Lewellen [157] has extended Donaldson's work to include the case of strong circulation.

The end wall boundary layer has been examined by a plethora of papers with the usual progression of initially laminar-only analysis to turbulent flow analysis. Rosensweig [158] has demonstrated that this end wall boundary layer is the dominant force in determining the axial velocity distribution even though it represents a small fraction of the total internal volume. Rott [159], in a survey paper, points out that it is this end wall boundary layer with its unique role of providing a strong interaction between the region of highly viscous flow and the outer region that makes rotating flows so much more complicated than simple linear flows. He also points out that this interaction is crucial to the understanding of tornadoes since the boundary layer "feeds" the observed high velocity core (where velocities as high as 700 feet per second have been observed). This boundary layer interaction phenomenon was recently extended by Serrin [160] to show how it can create the down drafts that can occassionally occur in tornado cores. This interaction remains the fertile ground of very recent research (see, for instance Chi [161] for a mixing length theory application and Hoffman [162] for an account of radial inflow effects) and it is certain to be the subject of much future work as well.

In general, the tangential velocity distribution inside a vortex chamber has been found to take the form of a Rankine vortex: solid body rotation from the center line axis to the point of maximum tangential velocity and near-free-vortex flow from then until near the outer boundary or vortex generating mechanism. Smithson [163], in a recent survey of velocity profiles, concluded that the velocity profile outside the core region can be expressed as $vr^n = c$, where v is the tangential velocity, r the radius from the centerline, c a constant, and n an experimentally determined constant which may vary in value from 0.2 to 0.8 depending on how the vortex has been generated; he has also stated what has been found by many others: namely that the radius at which the maximum tangential velocity occurs is located at a value of r "slightly less" than the exit orifice radius.

An extensive monograph, more than 200 pages with more than 400 references, was published on the subject of vortex chamber analysis in 1971 by Lewellen [105]. In this work he traces the complete development of literature on the subject (as can be inferred from his bibliography) with the purpose of applying the results to fluidic devices and containment configurations for nuclear rockets both of which tend to have geometries similar to the vortex chamber. Since this publication, numerous other papers have appeared of which several have already been cited [160-163].

It is very important to note that all of the literature cited in this subsection as well as the vast majority of Lewellen's bibliography are restricted to adiabatic, isothermal flows (i.e. Class A1). The few papers considered by Lewellen that were not of this class were for the nuclear rocket configuration which will be discussed in an appropriate subsection to follow.

Vortex Tube Studies

In contrast to the case for the vortex chamber geometry, relatively little literature exists for the vortex tube. Perhaps the reason is that most of the effort has been directed toward practical configurations, such as the cyclone separator and the Ranque-Hilsch Tube, rather than the development of a baseline apparatus for which the effects of swirl can be systematically examined. The results for cyclone separator studies must be excluded here (to be discussed in a later subsection) because the flow pattern is so vastly different due to the fact that the exit tube is usually of a re-entrant type and it is located at the same end of the chamber as the tangential inlet. The Ranque-Hilsch Tube results are not appropriate here, since the objective of such a device is energy separation it is characterized by a pair of flow exits (at the same end for a uniflow type and at opposite ends for a counterflow type) with very complex secondary and back flows occuring throughout the length of the tube; also, because the degree of temperature separation is a strong function of the inlet tangential velocity, virtually all of the devices investigated have extremely high tangential velocities (tangential Mach numbers of order 1) and thus compressibility effects are very pronounced.

The literature on the category of vortex tube studies can be surveyed in two groups: adiabatic systems for which the primary objective is either an analytical expression or experimental data for vortex decay (i.e. decrease in angular momentum with axial length) as a function of a Reynolds number and a parameter characterizing the level of swirl and diabatic systems for which an additional result is sought—that of a heat transfer correlation (usually in terms of Nusselt number) also as a function of these two dimensionless parameters. Since the objectives of these groups are different they will be surveyed separately.

One of the earliest works for adiabatic vortex decay was done by Talbot [164] in 1954 for laminar flow. He generated the swirl by the use of a section of rotating pipe, which of course resulted in solid body rotation, then permitting the tangential velocity component to decay as the flow was confined in a stationary cylindrical pipe. Both his analysis and experiments were restricted to the laminar regime. This work is cited here under the category of confined vortex flows instead of internal rotating flows because in the absence of the rotating pipe the flow pattern is observed to develop into a Rankine vortex wherein the solid body rotation region becomes confined to an ever-decreasing radius with the development of an annulus corresponding to a potential vortex. Laufer [165] in a NACA report did much the same thing for turbulent flows.

More recently, Thompson [166] has done both a theoretical and experimental study of free and confined vortex flows. For the confined vortex experiments he used a tube 5.72 inches in diameter and 30 inches long through which air was induced and swirl generated by the use of inlet vanes. There was no transition section connecting the vortex generator with the tube and the exit configuration consisted of a 1.25 inch diameter hole in an end plate. The length of the vortex chamber was 1 inch. Thompson noted that without the exit orifice in place, the flow pattern was one of solid body rotation over almost the entire cross-section whereas when it was installed there developed a potential flow region in the outer regions of the tube thus indicating the entire flow field can be sensitive to the exit boundary conditions. He noted complex axial velocity profiles with an annular region of reversed flow.

Musolf [167] and Kreith [168] presented data and analysis respectively on vortex decay. Kreith assumed that the Reynolds shear stress could be related to the velocity field by means of an eddy diffusivity that was neither a function of radius nor axial length. With this and several additional assumptions he was able to obtain a linear equation for the tangential velocity which compared favorably with the data available for axial distances up to 20 diameters. He noted that the swirl decays to approximately 10 to 20% of its original value in 50 diameters with the higher decay rate occuring for the lower Reynolds number. The data used for comparison was obtained by Musolf using a swirl tape (i.e. a twisted band of metal which is inserted into a simple cylindrical tube usually extending across the entire cross-section thus forcing the flow on a complex spiral path) at an inlet section with decay taking place in a simple tube.

Youssef [169] presented extensive data that were taken using air in a tube 12 inches in diameter and 184 inches long in which the swirl was generated by means of inlet vanes. Velocity profiles were obtained through the use of a 5 hole pressure probe. Lavin [170] used a geometry of a 3 inch diameter, 30 inch long tube to obtain similar data only at much higher velocities (the axial Mach number varied from 0.3 to 2.0). The swirl was induced by means of vanes located at a 30 inch radius and a complex transition section was used in which a shaped-plug insert was designed to aid in turning the flow from radially inward to an axial direction. One of Lavin's observations was especially noteworthy:

> . . . if the swirl ratio is sufficiently large, stagnation regions

> and regions of reversed flow can be formed near the entrance section. At flows with large Reynolds number this occurred when the ratio of maximum tangential velocity to the average axial velocity was in excess of four. When the Reynolds number was very small, this phenomenon was not noticed. (page 145)

Baker [171] obtained swirl decay data for two geometries one with a diameter of 5.75 inches and length of 270 inches using water and one with a diameter of 1.18 inches and length of 120 inches using liquid hydrocarbons. He found that the decay of swirl was exponential in which the angular momentum flux at any point downstream of a known angular momentum flux could be determined by multiplying the upstream flux by the quantity $\exp(-\rho\Delta x/D)$ where β is a decay parameter found to be a function of the axial Reynolds number, Δx is the axial distance between the two points, and D is the pipe diameter. Typical values of β were 0.02 for Reynolds numbers (based upon mean axial velocity and pipe diameter) of 2×10^5 and 0.04 for Reynolds numbers of 1.25×10^4. Thus he found that the decay increased for decreasing Reynolds number as has already been noted from earlier studies.

Wolf [172] and Rochino [173], in related papers, presented data and analysis for the flow of air in a 3 inch tube of 216 inch length for which the swirl was induced by means of inlet guide vanes. The degree of swirl was quite strong, in contrast to most of the results, with swirl angles (defined as the arc tangent of the ratio of tangential velocity to axial velocity) of 60 degrees--which implies that the tangential velocity exceeded the axial velocity by a factor of approximately 1.7. Their results may be summarized as follows:

(1) The radius at which the maximum tangential velocity was found, separated the regions of solid body rotation and potential flow. This location moved radially inward with increasing axial distance (i.e. as a result of vortex decay) thus making more of the pipe area of the

free vortex type.

(2) The distribution of axial velocity as a function of radius remained relatively unchanged with respect to length. This was attributed to the presence of an adverse pressure gradient at the axis and a favorable one at the wall, a combination which tended to hinder the development of the axial profile.

(3) The decay parameter (see Baker above) was found to vary as 140 times the axial Reynolds number to the minus 017 power--thus indicating that decay increased with decreasing Reynolds number. When this result was compared with an analytical expression developed by Dreith [168], the turbulent Prandtl number was predicted to be equal to 8.32 $Re^{0.3}$ where Re is the axial Reynolds number.

(4) Hot wire probes showed that the turbulent intensity was high at the axis (and relatively independent of length) and diminishing as the wall was approached in contrast to linear flows and thus showing that the turbulence structure is a strong function of radial position.

(5) Analytical predictions for decay could be obtained by using Taylor's modified vorticity transport theorem and Karman's similarity hypothesis. Two equations were presented for eddy viscosity as a function of radius: one for the region up to 0.9 of the pipe radius and the other for the annular area near the wall.

Recently, Yajnik [174] has presented the first part of his results for an inlet vane vortex tube of 100 diameters length. He has examined the turbulent law of the wall for weak swirls and found that the logarithmic variation was still valid although the thickness of the region so described was both a function of the swirl and the axial Reynolds number. He used a swirl parameter analogous to Chigier [114] only the upper limit on the integral is the pipe radius rather than infinity. Yajnik has also shown that for appropriately defined scales of axial velocity and angular velocity this swirl parameter reduces to the inverse of the Rossby number. The original apparatus used by Yajnik did not include a transition section between the vortex chamber and the cylindrical tube but apparently consisted of an abrupt contraction. This configuration caused an unsteadiness to be observed which was only eliminated by designing a transition section fairing described by a cubic curve. Yajnik noted that for values of swirl exceeding 0.155 (a very small value) flow reversal occurred, a flow regime he has chosen to avoid; hence, his results are restricted to very weak swirl levels.

In a very recent paper (July 1974), Love [175] has attempted to explain the increased pressure drop noted with swirl flows with respect to linear flows by accounting for the acceleration of an annular region of the pipe due to the stagnant or reversed flow region observed in the core region. The effect of the accelerated flow together with the effect of swirl decay is claimed to explain the increased friction factor noted. His predictions agree fairly well with that of Youssef and Baker.

The subject of swirl decay has been examined by a large number of recent Soviet papers, among them: Filippov [176], Gostinets [177], Liane [178], Veske [179], and Nurste [180]. Of particular interest here, Gostinets found that, "the turbulent swirled flow of liquid in the greater part of the pipecross section is actually close to helical and the vortex lines in it coincide with the streamline. The establishment of this fact confirms the possibility of using a model of a helical flow of an ideal liquid for calculating certain effects of real rotating flows". This point will be pursued further in Chapter 4. Also, Liane found an annular reversed flow in contrast to the core or axial reversed flow observed by several U. S. investigators (although Thompson [166] also reported an annular reversed flow region).

None of the investigators cited in this discussion of vortex decay of adiabatic confined vortex flows has dealt with the problem of flow perturbation by the use of inserted pressure probes. This effect is one possible explanation for the varying observations noted for regions of reversed flow. Also, a close comparison of results between apparatus' shows a significant variation in decay rates, velocity profiles, etc. It is entirely possible that this is a result of the lack of geometric scaling, as noted earlier in citing a quote by Murthy [71].

Among the earliest work examining heat transfer characteristics for vortex tubes were two papers by Gambill and Greene [181, 182]. Greene [182] reported "heat transfer coefficients one to two hundred per cent larger than that calculated for linear turbulent flow at the same pumping power". Blum [183] has also demonstrated a markedly improved heat transfer performance although diminished by vortex decay effects.

Virtually every additional paper on this subject (beside the three just mentioned) can be classed in one of two groups: work carried out at the Aerospace Research Laboratories using a heated inner cylinder and an adiabatic outer cylinder (often called the boundary condition of the "second kind") with air swirled initially either by vanes or tangential nozzles and work documented in recent Societ publications for a wide variety of configurations and boundary conditions.

The Aerospace Research Laboratories' (ARL) interest in confined vortex flow heat transfer stems from the prospect of stabilizing a long arc and transferring the contained electrical energy to the vortex flow. This concept was presented at the First Plasma Arc Seminar by Andrada [184]. Because of the operational difficulties of using the arc discharge to obtain data, the ARL work has similuated this energy addition through the use of an inner cylindrical tube which is heated via electric resistance. Scambos [185] presented the results of the first such simulation. His apparatus was similar to that used by Moore [186] and Holman [187] who were concerned with isothermal effects. Scambos observed that there was a reversed flow region that surrounded the inner cylinder and caused, he concluded, the observed increase in heat transfer coefficient with respect to length contrary to the usual trend. McKelvey [188] examining basically the same concept (but with a vortex tube of smaller length to diameter ratio) found that the Nusselt number was augmented by the vortex effect but not to the degree observed by Scambos; McKelvey also noted an increase in heat transfer coefficient with respect to length, and he also explained it on the basis of a reversed flow cell. Kelsey [189] examined the reversed flow cell in detail and concluded that it was not due to the heat addition process but apparently was a characteristic of the geometry. The only observable change in the flow field as a result of the heat addition process was a changed total temperature profile. Loosley [190] using an apparatus of even smaller length to diameter ratio and with two different diameter insert tubes found no evidence of a reversed flow region and was able to correlate mean Nusselt numbers with the Reynolds number (based upon hydraulic diameter) and Prandtl number. He did his experiments with inner cylinder diameters of one and two inches (vortex tube diameter was 4 inches) and found very little change in the correlation equation indicating that the heat transfer process was not sensitive to the annular gap. This work was continued by Talcott [191], Palanak [192], and Murthy [193, 194, 71] to account for the effect of inlet injection angle i.e. swirl intensity, in addition to axial Reynolds number. In these studies [191-194] the heat tranfer coefficient was found to be essentially independent of length, in contrast to earlier work. This led Murthy [193] to conclude, "In a study of this type, one should be forewarned that the conclusions drawn in the discussion will apply largely to the configuration under investigation." (page 10)

In the Soviet literature, Alimov [195] presents one of the earlier papers that is available in the United States. He used a tangential slot generator and concluded that the heat transfer could be correlated by the ratios of the areas of the tube cross-section and the slots. Migay [196] used a vane swirl generator with a relatively long tube. He concluded that the Nusselt number ratio of vortex to linear flow was approximately equal to the square root of the friction factor ratio for vortex to linear flow. He noted that "the initial swirl distribution has an appreciable effect on the heat transfer and friction characteristics." Bol'shakov [197] examined a configuration where tangential nozzles were distributed along the entire length of a cylindrical tube, thus obviating the need for a swirl generator, with the perspective of developing a gas-liquid heat exchanger. Koval'nogov [198] examined the effect of vortex decay and different tangential velocity distributions (as a function of radius) upon Nusselt number. The various velocity distributions were obtained by means of inlet propellers of various blading laws. He used a heated outer tube with cool swirling water. He has continued this investigation in a more recent publication [199] which does not appear to be available in the United

States. Sudaver [200] examined the flow of air swirled by means of inlet vanes flowing through an annular channel with the outer cylinder heated. Borisenko [201] also used an annular channel but with the inner cylinder heated. Bukhman [202] used a hot gas geometry to develop both local and mean Nusselt numbers but he made no attempt to correlate his results to the intensity of swirl employed. Schchukin [203] has used inlet vanes to examine heat transfer coefficients as a function of axial length in a paper not yet available in U. S. literature.

Theoretical attainments are decidedly meager for vortex heat transfer with decay effects. Kharitonov [204] and Ghil [205] have presented recent attempts but the analysis currently available is limited to providing coarse interpretations of the available data.

Many of the results of the papers cited in this subsection [181-203] will be referred to again in more specific detail in Chapter IV.

Practical Devices

The objective of this section is to present a broad overview of the literature of confined vortex flows that have been oriented primarily to the analysis or optimization of practical devices. Since vortex flows have been applied to an exceedingly wide variety of devices only the literature for the seven most-common types are presented here (as listed under 1B2 in Table 2).

Ranque-Hilsch Tube

One of the most-remarkable fluid-dynamic results of a confined vortex flow is usually termed the Ranque-Hilsch Effect after its original discoverer (Georges Joseph Ranque) and its re-discoverer (Rudolf Hilsch). In 1931, Ranque read a paper before the Societe Francaise de Physique (French Society of Physics) wherein he reported that it was possible to obtain a hot and cold stream of air out of an adiabatic pipe with a single inlet stream of ambient air; the response of the society was apparently something less than enthusiastic. In that same year Ranque applied for a French patent and in 1932, after it was issued, he applied for a United States patent as well. In 1933 his paper became available in the literature [206] and in 1934 his U. S. patent was granted [207]. Ranque then assigned the patent rights to a small company that he had formed--La Giration Des Fluides (or Whirl-Gas) of Montlucon. Despite these events his invention remained virtually unknown and in the period 1934 to 1944 no further mention of the device was made in the Societe's Journal.

After the end of World War II, when U. S. scientists were sent to Germany to examine the work of the German intelligentsia, it was found that Rudolf Hilsch, a physicist at the University of Erlangen, had been working on an operating model of Ranque's device from whose paper [206] he got the original idea. Hilsch then published his results in 1946 [208] one month before it was referred to in a brief article by Milton [209] in a U. S. journal (Milton had been one of the scientists sent to Germany and had observed Hilsch's work). From this year on there has been a veritable explosion of papers on the subject. Further details on the early history of this device can be found in Fulton [210].

This proliferation of literature is attested to by the fact that by 1951 a bibliography of literature on the subject was publishable [214].

In 1957, Westley [212] published the details of the practical performance parameters of the Ranque-Hilsch Tube which Lewellen [105] cited in 1971 as "one of the best sources of data for determining optimum performance of the tube".

There was a large number of early systematic experimental studies of the tube; among the more well-known were: Eckert [213, 214], Hartnett [215], Keyes [216], Schowalter [217], and Savino [218]. The theory of operation of the tube has also been the subject of a great many papers from Kassner's [219] in 1948 through Deissler [220, 221], Lay [222, 223], Sibulkin [224-226], and even in recent times with Linderstrom-Lang [227]. Despite this effort by investigators, Lewellen ([105], page 182) concluded that "the detailed prediction of the three-dimensional flow pattern in a highly turbulent vortex tube is still beyond the state of the art. Since the energy separation depends upon this flow pattern it is to be expected that the numerous attempts to predict the performance of a Ranque-Hilsch Tube, although each contributing to the understanding on the tube, have not met with complete success." Hall [79] even went further by saying, "the complexity of the flow in a Ranque-Hilsch Tube has made the accurate prediction of performance virtually impossible."

Even the data for the velocity profiles in these tubes is subject to strong suspicion. Reynolds [228] in commenting on the use of one-sixteenth inch diameter probes used by Sibulkin to obtain data used to substantiate his theory, said:

> ...the introduction of such pressure and temperature probes into the vortex produced large changes in the fields within the tube. These changes were not just local ones; large disturbances occurred throughout the tube...However, all the measurements made in vortex tubes until now have relied upon instruments of somewhat similar

> design and of about the same size as those used here. All the data must be equally suspect. (italics mine)

Holman [187] has found that the flow field was "significantly" disturbed by the introduction of probes of this size. Timm [229] has published a recent survey of the velocity profile data that is available for the tube flow.

Recent literature reveals that investigation of the Ranque-Hilsch tube continues unabated with new geometries (see Gulyaev [230] for the use of a diverging tube which he claims improves the refrigeration capacity by 25%) as well as new thermodynamic boundary conditions (see Martynov [231] for predictions of "more effective" performance for a diabatic tube).

A number of literature surveys strictly on the subject of Ranque-Hilsch tubes are available. In addition to Curley already cited, Westley [232] included 116 references in 1954, a bibliography which was updated by Dobratz [233] in 1964. Lewellen [105] includes in his bibliography the papers published since Dobratz' survey on the subject.

Both the theory and the data obtained for this device are not pertinent to this investigation. Not only is the geometry fundamentally different (relatively short tubes with a pair of exits) but the very high-velocity flow field and adiabatic boundary conditions are in contradistinction to that used here.

Cyclone Separator

The cyclone separator is unquestionably the most practical application of confined vortex flow charecteristics as it is widely-used in industry to separate particulate on the order of several microns in diameter from flue gas streams. Lewellen [105] claims that a German Patent had been issued in 1855 for such a device that looks very similar to those used today. The secondary flows characteristic of swirling flow play an important role in the particulate separation. By shaping the bottom of the separator into a conical form, the boundary layer formed on the walls, which contains most of the particulate to be separated, will tend to flow inward and downward because of the imposed radial pressure gradient and thus can be collected at the bottom of the separator without being reinjected into the air stream.

Ter Linden [234] gave an early account of the velocity distribution inside a separator and noted that the solid body rotation core extended to approximately 0.6 of the exit radius of the re-entrant pipe; this same figure has been reported by many others (e.g. [235]). Davies [236], in a survey paper on separation techniques, detailed the collection efficiency of a cyclone separator in comparison to alternate techniques (settling tanks, scrubbers, etc.). He pointed out that desirable operating characteristics required a geometry that included a high inlet velocity, small exit radius, large height to radius ratio, and a ratio of external radius to outlet radius of nearly one.

Smith [237, 238] has presented detailed analytical and experimental results for the cyclone separator. He showed by means of stability analysis that the boundary layer on the outer wall of the cyclone is unstable to a radially inward displacement, explaining the dust streaks that are sometimes found on the walls of operating separators. In his experimental work he found that in addition to the expected turbulent and laminar regimes that it was possible to produce a periodic regime. An apparent axiom for vortex flows is that the unexpected should be expected.

The Aerospace Research Laboratories has recently become interested in examining new configurations of cyclone separators, which they have termed "reverse-flow" chambers. Two of many reports on the operation of such a device were given by Fiorino [239] and Poplawski [240]. The objective is that through the use of new geometries better utilizing the inherent secondary flows and with very high inlet velocities (tangential Mach numbers exceeding one), sub-micron separation can be achieved.

Despite the cyclone's long history, it is still the topic of continued research (see, for instance, [241]). Two books on the subject that are often quoted for design information are Reitema [242] and Bradley [243]. Recently, fluid-dynamic separation principles have also been applied to gas centrifuges whose purpose is the enrichment of nuclear fuels.

Fluidic Devices

As with many applications of fluid dynamics, fluidic devices have undergone a history of early development and interest followed by a long dormant period and now have experienced a recent revival. Thoma [244] is usually credited with having invented the first use of vortex flow in a fluidic device, having obtained a patent for his vortex in 1928. The original idea was simply that the use of a small control jet oriented tangentially at the periphery of a short cylindrical chamber could greatly reduce a much larger flow rate by converting much of the linear flow energy into a vortex. Shortly thereafter, Heim [245] used this principle to develop a vortex diode.

For the next thirty years of its history, the literature is very meager. Starting in about 1960, however, there has been an exponential growth in research and publications on the subject. Mayer [246], in a survey article, gives a partial list of fluidic devices that operate upon some principle of vortex flow: vortex diode, swirl atomizer, vortex air thermometer, storm diverter, vortex combustor, vortex amplifier, vortex valve, and negative vortex oscillator. Lewellen [105] has expanded this list as well as provided an updated bibliography in his 1971 monograph.

Vortex fluidics has been the subject of a great many dissertations, among them Lawley [247] and Lee [248] of this institution, and can be found as the research subject of at least one article in almost any current journal related to controls (see, for instance, [249]).

These devices are operated under isothermal conditions in (usually) small, sandwich-like chambers. The small flow areas suggest that their flow patterns are strongly influenced by end wall boundary layer effects. Due to the many different purposes to which they are put, there is rarely any geometry which may be termed "usual" and as a result it is very difficult to translate the results, for a vortex structure obtained from data for one apparatus to another. The usual procedure is to completely ignore the internal flow dynamics, because of its hopelessly complex nature, and instead concentrate on obtaining macroscopic performance characteristics. Perhaps the most common of these characteristics is presented as a graph of the total flow through a vortex modulator as a function of the control flow (usually expressed in terms of the turn down ratio).

Containment/Stabilization

The earliest work in this area is usually attributed to Schoenherr [250] who in 1909 documented the stabilizing influence of a vortex flow upon a long arc discharge. Schoenherr was developing a process to synthesize nitric acid for which he needed a stabilized high temperature source. The stabilizing effect of vortex flow upon flames dates from about 1950 and has already been discussed at some length [126-130].

In the last 15 years a new application of this characteristic of vortex flow has become of great interest. This application is commonly referred to as "containment". It originally arose in connection with the development of a nuclear rocket,wherein the vortex flow of a gas such as hydrogen would contain the fissionable material in an annular volume while simultaneously being heated and accelerated by the energy of release. The first apparent mention of this concept in unclassified literature was by Grey [251] in 1959, although it is claimed to be the idea of Kerrebrock who proposed it in classified literature in 1958; in 1959, Kerrebrock [252] presented the concept at a conference in technically couched terms. Of interest here is that he noted a fundamental difference in velocity profiles which occurred because of the heat addition process--specifically, "Heat addition, through its effect on the gas temperature would provide a means for establishing a quite different variation of the tangential Mach number with radius than is found for any adiabatic flow". Later, in 1961, Kerrebrock [253] was much more direct in his application of vortex containment (it is interesting to note the difference in the titles of his papers.)

Very early in the investigation it was recognized that the apparent maximum tangential velocity achievable for confined vortex flows, i.e. a Mach number of approximately 1.5, would not be sufficient to achieve adequate containment. Lewellen [254] posed this problem in 1960 noting that the only other logical alternative, that of generating the vortex by rotating the tube walls, is also severely limited (here by structural considerations), has suggested using magnet hydrodynamic forces to augment the intensity of swirl. R. G. Ragsdale and J. M. Kendall each authored a large number of early publications on this subject. In [255] Ragsdale included a bibliography of the early literature on containment. Kendall [256] in a Jet Propulsion Laboratory report, examined the fluid dynamic reasons for bounds on the containment parameter (defined as the ratio of the tangential Mach number squared to the radial Reynolds number); he concluded that the end wall boundary layer was the most likely cause, especially in view of the rather short chambers being investigated (length to diameter ratio of order one).

In the past 5 years the interest in containment has expanded to include a vortex reactor [257], a control scheme permitting the same chamber to be used for both subsonic and supersonic combustion [258], and for use in electric propulsion rockets [259]. Murthy [259] in his survey paper includes 155 references on the subject of vortex stabilization and confinement in addition to the following caution: "the use of immersed probes is open to question on account of the disturbance introduced into the flow."

Despite the interest in containing an energy releasing volume, virtually all the data available is for isothermal operation, although

ARL, in their study of containment, have utilized a heated cylindrical rod at the axis to simulate a stabilized arc (this literature has already been discussed [184-194]).

Nozzles/Diffusers

Vortex flow has been found to offer enhanced performance for both nozzles and diffusers. Guderley in a series of papers [260-262] has shown that swirl in a Laval nozzle can be advantageous with respect to fuel consumption as a result of increased effectiveness of the nozzle. This question has also been recently examined by Boerner [263].

The effect of swirl upon improving the performance of a diverging, conical diffuser has been reported by So [264]. So found 5 distinct flow regimes for different intensities of swirl, giving some indication of the complexity of flow present in such arrangements. Chow [265] has discussed the general effect of non-uniform cross-section channels upon swirl flow in a recent paper.

Usually the diffuser investigations are for isothermal flows only while the nozzle investigations, because they involve propellant exhaust gases, are for non-isothermal and diabatic flows. The objective of the diabatic boundary for the nozzle flows is not, however, heat recovery (as is the case in the present study) but merely the protection of the nozzle wall; hence, the amount of heat transfer at the wall in comparison to the energy content of the gas stream is very small.

Cyclonic Combustion Chamber

Cyclonic combustion, as distinguished from tangentially-fired combustion, dates from the 1940's and is almost the exclusive means of burning low grade coal (in crushed, but not pulverized, form). The distinguishing features and early history of these two kinds of vortex combustion is presented in a number of reference works [266-268]. Discussion of the tangentially-fired combustion chamber will be deferred to the next subsection.

Perhaps the earliest paper on vortex combustion is due to Hurley [269] who reported its use in 1931. By 1943 a patent had been issued to Vroom [270] for:

> A pulverized fuel burner comprising a burner tube having an open outlet end adapted to connect with a combustion chamber, means including an inlet port in the peripheral wall of said burner tube supplying to said burner tube in a direction tangential to the inner surface thereof a stream of pulverized fuel suspended in carrier air, means causing said suspended fuel to advance helically in a peripheral layer in said burner tube to the outlet end thereof, a central axial air admission means including an air register admitting a secondary air stream at the inlet end of said burner tube out of the main path of the peripherally rotating layer of fuel, said air register having peripheral doors to impart a rotary motion to said secondary air stream, and means preventing direct contact between at least the main portion of the rotating stream of secondary air and the main portion of said fuel stream at the inlet end of said burner tube.

Parmale [271] received a patent for a modified form of cyclonic combustion chamber in which all the air and fuel was introduced tangentially with a slight backward (with respect to the outlet) component.

The original design, development, and commercial fruition of cyclonic combustion was described in a series of papers by Brunnert [272], Gilg [273], and Schroeder [274]. The abundance of unusable low-grade, Central Illinois coal led Babcock and Wilcox Company to develop a combustion chamber that would trap the high ash content of these coals. They found by orienting a cylindrical combustion chamber (originally only one foot in diameter) in a horizontal fashion with a slight [illegible] slope (usually about 5 degrees) and by injecting the air and suspended crushed coal that a liquid slag formed on the bottom of the chamber which was highly scrubbed by the tangential gases; this slag acted as a trap for the ash suspended in the tangential stream thus preventing its being passed to the boiler-tube section and then to the atmosphere. The slight slope to the chamber permitted a means of continually collecting the molten slag. The first full-scale use of such a chamber was at the Calument Station of the Commonwealth Edison System in September 1944; this chamber had an 8-foot diameter and an 11-foot length with a 5 degree slope. It was found that the same power generation capacity could be obtained with a furnace requiring 25% less floor area, 33% less volume, and 22% less weight. The operating temperature of the combustion chamber was on the order of 3000 degrees Fahrenheit; thus, although the chamber walls were water cooled, a negligible fraction of the heat of combustion was in fact recovered through these walls as is typical of these devices. The hot exhaust gases must be routed through the usual boiler tubes to achieve the rated steam capacity. Flushed with these early successes, a number of other configurations were attempted, among them a vertical furnace where the tangential impetus occurred at the top with a slight downward component and then exhausted through a re-entrant nozzle also at the top. This configuration was apparently not very successful (although it occasionally reappears in the literature [275]) and virtually every cyclonic combustion chamber currently in use (currently about 600 in the United States and Europe) closely resembles its first ancestor. An early book detailing the performance of cyclone combustion chambers in comparison to the alternatives was written by

Smith and Stinson [276]. They quote a typical capability of 50,000 British Thermal Units (Btu) per hour per cubic foot based upon the total furnace volume and 500,000 Btu per hour per cubic foot based upon the volume of the cyclone chamber itself.

This concept of vortex combustion has also been successfully demonstrated with natural gas and oil as the fuel although the method does not appear competitive with alternative techniques. Garner [277] and Stone [278] have reported on two early such demonstrations. Garner in particular noted that the pressure at the axis of the combustion chamber was sub-atmospheric and suggested that flow reversal might be the explanation. Recently, Dumoutet [279] has observed such recirculation patterns and in fact found that they were substantially different for a gas as the fuel than for crushed coal. Seidl [280] in a relatively old paper noted that for crushed coal the velocity profile outside the solid body rotating core could be described by $vr^n = c$ where v is the tangential velocity, r the radius, c a constant, and n, an experimentally observed constant, of about 0.5. He explained this value of n by suggesting that the coarse dust of the coal had an "altered" viscosity which prevented the development of a free vortex region (for which the value of n would have been 1.0). For calculation purposes he suggested using solid body rotation (i.e. $n = -1.0$) for the core region and constant velocity (i.e. $n = 0.0$) for the outer annulus region since this closely approximated the measured profile. Recently, however, Kalishevskii [281] has reported on observations of a peripheral reversed flow region.

Continued research on improving the cyclonic combustion process is being reported in the literature, particularly in Soviet journals (see, for instance, [282-284]). Mills [285] has also recently reported on the use of waste wood in a cyclone furnace (Cycloburner, Tradename of Energex, Ltd.). This was a refractory chamber of 3-foot diameter, 6-foot length which developed heat releases of up to 800,000 Btu per hour per cubic foot. Once again the primary heat recovery was external to the burner.

In addition to power generation, vortex combustion has recently become of interest for use in turbojet combustors [286, 287]. Osgerby [288] has written a survey paper on the subject of turbine combustion modelling that includes vortex combustion configurations. He includes more than 100 references in his review.

Tangentially-Fired Combustion Chamber

There are two broad classes of coal firing: grate/stoker and suspension. Of the suspension class there are four sub-classes: vertical firing, impact firing, horizontal firing, and corner or tangential firing [289]. It is this later subclass that is of interest here. Tangentially firing pulverized coal pre-dates the 1920's when corner nozzles were used in square, vertical, refractory furnaces. The effect of vortex combustion was observed early to enhance the turbulence level of the chamber and resulted in more efficient combustion. Starting in about 1925, water cooling all or most of the furnace chamber walls became structurally necessary in order to achieve the large furnace sizes desired [290] and today virtually all such furnaces are water-walled. But, as was the case for the cyclone combustion chamber, the degree of heat recovered by the wall cooling water is negligible in comparison to the heat of combustion and virtually all the heat-recovery process takes place external to the combustion chamber. Hence the temperature of the chamber tends to be very high with only a slight radial variation due to the cool, confining walls.

This combustion chamber configuration is by far the most common for use with pulverized coal. Nozzles are customarily located in each of the four corners of the square or rectangular chamber and are distributed along the height of the chamber as well. The nozzles are sometimes oriented such that the incoming suspension of coal and air has a small downward velocity component as well as a tangential one. Photographs of the vortex flame typically show a hot, annular turbulent flame with a relatively cool core. The injection scheme together with the combustion process tends to make the flame extremely turbulent and intense and undoubtedly causes very complex velocity profiles as the conflagrant gas spirals down and then up out of the chamber.

A comprehensive survey of the literature on this subject would easily result in hundreds of citations that would still shed very little light on the subject of this investigation. Instead, a brief survey of the literature on the use of tangentially-fired combustion chambers for the incineration of waste products will be presented.

The U. S. Bureau of Mines has sponsored a series of experimental research programs on the use of tangentially-fired chambers to incinerate wastes. The typical configuration involves the waste being fed in from the bottom (by means of stokers or on a charge basis) with only the air being injected tangentially. The results of these efforts have been reported by Corey [291-293], Weintraub [294], and Schwartz

[295] among others. The results of this series of papers may be summarized by noting that the use of tangentially-over-fired air was capable of significantly increasing the burning rate in a manner correlatable with the Reynolds number of the injection nozzles. There is an optimum such Reynolds number (usually stated as 35,000 based upon the diameter of the nozzle and the tangential velocity) in terms of maximum burning rate. Again, like all the previous work in this area, heat recovery at the walls of the combustion chamber was not the objective and was in fact avoided and, as a result, there is no experimental data for Nusselt number (for instance) as a function of inlet Reynolds number and geometry.

Literature Survey of Rotating Flows

Heat Transfer Surveys Available

A complete bibliography of the literature on the subject of heat transfer from rotating surfaces for the period through 1959 has already been cited--Eckert's monograph in the series Progress in Heat and Mass Transfer [76]. This bibliography has been continually updated in selected issues of the International Journal of Heat and Mass Transfer so that a relatively current body of literature is readily available to a researcher in the field.

Dorfman [296] published one of the earliest surveys on this subject in 1963. Kreith [75], already cited, updated this book in 1968 in the series Advances in Heat Transfer, providing 193 references. Dorfman [297] has very recently provided another update, including 242 references.

Despite these extensive surveys and the intense interest in the field, there are fewer than ten papers available on the heat transfer between an internally flowing fluid and a confining tube wall which is rotating about its own axis. It is this configuration that would be most closely similar to that under study here.

External Rotating Flow

Since this type of swirling flow is really not applicable to the present investigation, no attempt will be made to survey the literature available. A few citations will be included for the most recent work in this area in the interest of completeness.

Cham and Head in a series of recent papers [298-300] have developed an integral-profile technique for use on isothermal, turbulent boundary layers forming on a variety of rotating surfaces. Chin [301] has examined the problem of simultaneous mass and momentum transfer on a rotating hemispherical electrode. Koosinlin [302] in contrast to Cham, has used a finite difference technique to predict the flow field surrounding rotating free disks, cylinders, cones, etc. This technique is essentially that used by Lilley [125] for isothermal swirling jets.

Recent heat transfer research has been reported for a variety of configurations. Johnson [303] found that the heat transfer from a cylinder to a normal air stream could be increased approximately 15% by the use of vortex generators. Eisele [304] claims to have presented the first research on the heat transfer from a flat plate rotating as a propeller. Eastop [305] has correlated the heat transfer from a rotating sphere in an air stream solely in terms of a flow Reynolds number and a rotational Reynolds number. Koosinlin, Launder, and

Sharma in a series of papers [306-308] have extended their finite difference analytical technique to predict heat transfer as well as momentum transfer with a variety of rotating surfaces. They have defined a local swirling flow Richardson number that has been used to obtain a mixing length (via a linear relationship) to generate what are apparently accurate models of the actual external rotating flow heat transfer processes. At present their results are still restricted to small swirls (i.e. low values of rotational Reynolds number).

Internally Rotating Flow

There is a vast literature on internally rotating isothermal flows since many geophysical flows can be modeled by such geometries. Also, various unusual phenomena occur relating to vortex breakdown, such as the Taylor-Proudmann column, for this geometry that are widely reported. Only the most recent literature--that published within the last five years--will be cited here.

Bien [309] has examined a cylinder with one end wall fixed and the other rotating with a Helium-Neon laser anemometer using water as the working fluid. His experiment was interesting in that it showed the development of the Karman profile by the rotating disk and the Bodewadt profile by the stationary one. Carrier [310] has examined the flow over a rigid body locating in a rotating container by means of the modified Oseen method. Wagner [311] has modeled the radial passages in centrifugal pumps and compressors by means of a pipe rotating about an axis perpendicular to its centerline for both laminar and turbulent flow. His theory predicted and his experiments confirmed the presence of longitudinal vortices for this flow field. In an attempt to model air cooled multiple disk pumps and compressors, Bakke [312] presented hot-wire data obtained for a source flow between two rotating disks under a wide combination of disk speeds and source flow rates. He found that the flow tended to be stabilized as a result of centrifugal forces. Moore [313, 314] has examined the flow field surrounding the impeller of a centrifugal compressor and has noted the presence of: a potential flow region, top and bottom wall boundary layers, corner flows, and sidewall boundary layers. Huppert [315] has studied the flow field about an obstacle located on the bottom of a cylinder rotating about its vertical axis. He has explained how the observed streamline displacement around the obstacle is dependent upon the side walls through the influence of the Rossby number. Benton [316] has presented a survey paper on what he calls the "spin-up" problem. This is the change of a homogeneous fluid which is initially rotating as a solid body to a step change in the angular velocity of the rotating, confining cylinder. He has noted the development of three boundary layers--each of which is a function of the Ekman number but to a different power.

For diabatic conditions for internally rotating flows there are a large number of papers for configurations vastly different from that of interest here. Miyazaki [317], in a recent paper, has presented results obtained by rotating a rectangular tube about an axis other than its own axis of symmetry. This kind of a problem is usually classed as a special case of a thermosiphon as the flow field is greatly influenced by the heat transfer process through the bouyancy forces. The configuration of parallel disks within a casing is also the subject of recent research (see, for instance [318-320]) and is important to the design of cooling systems for gas turbines and compressors. Hammond [321] has summarized some of the literature available on the subject of rotary heat exchangers (sometimes called rotary regenerators).

Heat transfer in annular tube configurations has also been the subject of much research. The literature is very difficult to classify as there are a large number of possible operating conditions: one or both tubes rotating, heat transfer from the fluid to one or both of the tubes, heat transfer from one or both of the tubes to the fluid, and various relative gap thicknesses. Bjorklund [322] provided some of the earliest results for 4 values of annular gap and several combinations of cylinder rotation rates. For the inner cylinder only rotating he found that he could correlate the observed Nusselt number in terms of the Taylor number (which is essentially a rotational Reynolds number) only. One of the complications of annular configurations is the possiblity of the formation of Taylor vortices; Haas [323] has examined their effect upon heat transfer to a liquid flowing through the annulus. Zmeykov [324] has published recently some of the Soviet research for this configuration. Sharman [325] has examined the configuration for a heated outer cylinder and a cooled inner cylinder with air flowing in the gap. Scott [326] used an adiabatic, rotating inner wall with a heated, stationary outer wall to measure the turbulent transport properties, eddy diffusivities of momentum and heat, which were found to be functions of the swirl distribution (i.e. they varied as the flow developed down the rotating annulus). Citations of additional work with annular, rotating flows can be found in the surveys of Kreith [75] and Dorfman [296, 197].

As previously mentioned, the research in the area of simple rotating tubes is much more limited than other geometries, and may be summarized as follows:

(1) Water as the working fluid without entry-length effects--
Kuo [327] and Pattenden [328, 329]

(2) Air as the working fluid without entry-length effects--
Briggs [330] and Cannon [331]

(3) Air as the working fluid including entry-length effects--
Buznik [332-334]

Kuo [327] has presented data for a variety of rotating configurations: full as well as partially-full tubes and with and without inserts (either an annulus or a paddle system). The length to diameter ratio of the rotating tube was 8.0. Heat was supplied to the system by stationary Nichrome wires located parallel to the tube axis near the walls. He was able to correlate the measured Nusselt number in terms of the axial and rotational Reynolds numbers with the general result that Nusselt number increased with Reynolds number although it did so in steps on log-log paper. He attributed this to a transition phenomena from a region where the effects of gravitation are significant to a region where centrifugal effects are significant. It is interesting to note that the data for partially filled tubes indicated a higher Nusselt number than for the full-tube case.

Pattenden [328, 329] used a configuration similar to a single-pass, counter-flow heat exchanger only with the separating tube being rotated. He concluded from his experiments that "very high heat transfer coefficients can be obtained." Kreith [75] however, has concluded that Pattenden's experiments were of "limited accuracy" (page 241).

Briggs [330] has reported on extensive data taken with air being heated by the rotating tube. The principal effect of the tube's rotation was concluded to be a delay in transition from laminar to turbulent flow for, "Once fully established turbulent flow is attained the effect of rotation, at least for the range of variables considered is small." This result is in contrast with that reported above by Kuo and by Pattenden. Briggs was able to correlate his data for Nusselt number in terms of the axial Reynolds number and the number of revolutions per minute of the tube (investigated for the values of 0, 1900, and 3400 RPM). For Reynolds numbers exceeding about 20,000 the Stanton number was essentially independent of the speed of rotation. Briggs did not analyze any entry length effect (the length to diameter ratio of his apparatus was 56.5).

Cannon [331] has extended Briggs' work using essentially the same apparatus. Although he too did not account for entry-length effects, he has included both the case of the rotating air being heated as well as cooled (which he found to have only a minimal effect upon the observed Nusselt number suggesting that the flow field was essentially independent of thermal boundary conditions). Cannon's principal conclusion was that the effect of rotation was only to delay transition from laminar to turbulent flow because of its stabilizing influence on the wall boundary layer, specifically, "As the tube rotational speed is increased, with the through-flow velocity constant, the effect is to stabilize and make less frequent the bursts of turbulence. If rotational velocity is sufficiently high, the bursts disappear entirely."

Buznik in a series of papers reported in Soviet journals [332-334] has examined the entry-length effects upon heat transfer from a hot rotating tube to cool air flowing through it. He has used an apparatus with a length to diameter ratio of 16.25, capable of rotational speeds of up to 1170 revolutions per minute. He was able to correlate his data by using a Stanton number as a function of the two Reynolds numbers (axial and rotational) and the non-dimensional axial distance from the start of the test section. As found earlier by the work of Briggs and Cannon, the effect of rotation was to diminish the heat transfer coefficient from that obtained for purely linear flow.

The results of Briggs, Cannon, and Buznik will be compared to that obtained for this study in Chapter 4.

Literature Survey of Curved Flows

Flow Past Concave/Convex Walls

Since many of the characteristics of swirling flow inside stationary tubes can be analyzed as flow past concave surfaces, it is pertinent to examine the state of knowledge and literature on this subject. Gortler [335], in what has become a classic paper, predicted in 1940 that the laminar flow past a concave surface is unstable to the formation of longitudinal vortices which have since become known by his name (this work was later translated and published as a NASA report in 1954 [336]). Some time later, Gortler [337] demonstrated the analogy between instabilities caused by centrifugal body forces originating because of flow past a concave wall and by the bouyant forces originating in a thermally stratified boundary layer. Tani [338] showed the existence of a longitudinal vortex structure in a turbulent flow as well as for a laminar one.

Kreith in a series of papers [339-340] has shown both analytically and experimentally that flow past a concave wall enhances heat transfer (with respect to a flat wall) and flow past a convex wall inhibits heat transfer. He has demonstrated that the Nusselt number ratio for that obtained in a concave flow to that for a convex flow is approximately equal to the square-root of the ratio of wall shear stress for a concave flow to that of a convex flow. As noted in the subsection on vortex tube studies, Migay [196] made a similar observation for the Nusselt number ratio obtained with swirl to that obtained without swirl.

The actual fluid-dynamic cause of the enhancement is a subject of some debate. One line of reasoning explains the effect as a result of increased radial turbulent fluctuations at a concave wall (see, for instance, [342]). The alternative explanation accounts for the increased heat transfer by the presence of a vortex structure (see [343]). Schultz-Grunow [344] has shown for a laminar flow that by accounting for streamline curvature by using a higher order boundary layer approximation than that usually employed, it is possible to obtain an expression where the Nusselt number is equal to 0.5 β $u_o x/\nu$ where U_o is the free stream velocity, x the distance along the wall, ν the kinematic viscosity, and β a non-dimensional function of the Prandtl number. For a flat plate β is known to be equal to $0.664Pr^{0.348}$ where Pr is the Prandtl number. Schultz-Grunow has shown that β is equal to $0.692Pr^{0.355}$ for flow past a concave wall and $0.632Pr^{0.355}$ for a convex wall. Thus there appears to be sound analytical basis for increased heat transfer for concave walls at least for laminar flows.

Persen has examined the effect of longitudinal vortices on heat transfer in series of papers and reports [345-351]. His analysis as relevant to this study, has concluded that the presence of longitudinal vortices can not account for the increased heat transfer observed (he quotes an increase of "70 to 80%", although he does not cite a source) with the principal effect of the vortex structure being the more rapid development of the boundary layer when compared to a simple linear flow.

Recent data by Ellis [352] for the turbulence in a curved duct (with a 15 inch radius of curvature) has shown that the flow behavior is distinctly different than for the case of a plane wall. The turbulence intensity is amplified for flows past concave walls with increased rates of boundary layer growth and larger measured values of friction factor. Data for heat transfer in a simply curved duct are limited. Shchukin [353] has presented data for heat transfer as a function of length of the channel (of fixed curvature) for laminar flows.

A very extensive survey on the state of knowledge on the effect of streamline curvature upon turbulent flows has recently been prepared by Bradshaw [354]. This monograph includes more than 300 references of work in this area. The conclusions of this reference as pertinent to the present investigation may be summarized as follows:

(1) The changes in the flow produced by streamline curvature are both large and, to a degree, surprising. "These changes are usually an order of magnitude more important that normal pressure gradients and other explicit terms appearing in the mean-motion equations for curved flows". (page 1)

(2) The effect of curvature upon friction factor and heat transfer coefficient is about 10 times greater in turbulent flows than in laminar flows which implies that the change in the Reynolds stress term must be a factor of 10 greater than the change in the viscous term. However, at present there does not appear to be any reasonable

explanation as to how this could occur leading to the conclusion that curvature must change the very structure of the turbulent flow.

(3) Knowledge of curvature effects upon the flow field properties is still so minimal that heat transfer predictions are not yet achievable for turbulent flows. In particular, "Some apology is necessary for the neglect of heat transfer in this review. Quite simply, the uncertainty of the behaviour of the Reynolds analogy factor and the turbulent Prandtl number is so great even in plane flows that a discussion of the effect of streamline curvature on these quantities would be premature". (page 52)

(4) On the subject of data and interpretations of confined vortex flows, he writes:

> There seems to be little detailed information on the decay of pre-swirl in a simple pipe flow: any device for generating strong swirl will cause large changes in the axial velocity profile, whose return to full development will be inseparable from the decay of the swirl . . . . it is frequently unclear whether experiments on vortex flows in tubes are supposed to relate to classical vortices surrounded by an irrotational flow, to fully-turbulent pipe flow initially near a state of solid-body rotation, or to some unhappy compromise between the two. . . . Unfortunately it is not possible to classify experiments by the swirl generator used: the use of a twisted tape or rotating grid implies a rough approximation to solid-body rotation, but with *a vortex tube with radial entry, of the type originally intended to generate a classical vortex with $W \sim 1/r$ outside the core, can be used by design or accident to produce almost any swirl distribution*. (page 64, where W is the tangential velocity and r the radius from the centerline, italics mine).

(5) On the subject of conflagrant, swirling flows, Bradshaw notes: Swirling flames are an example of the class of flows in which a qualitative consideration of curvature effects is helpful in understanding the phenomena but which are rather too complicated to yield quantitative data for general use: turbulence measurements are difficult and numerical experiments may show up discrepancies other than those directly attributable to curvature effects. (page 65).

Bradshaw includes in his report a detailed history of the development of the theory of curved flow back to the time of Rayleigh's paper [61]. He concludes this section with the following observation: "The history of research on the effects of streamline curvature on turbulence is an object lesson in the effects of poor communication". (page 24)

Flow Through Helically-Formed Tubes

The problem of predicting the heat transfer through helically coiled tubes has been examined by a large number of investigators starting with Grindley [355] in 1908. From the beginning, the presence of secondary flows as a result of the curving geometry has been noted as the agent of the observed heat transfer enhancement. Eustice [356, 357] expanded upon the work of Grindley in 1910 and 1911. Somewhat later, 1925, Jeschke [358] published the first complete set of data for the flow through coiled tubing. About this same time Dean [359, 360], in his study of the flow characteristics in refrigeration tubing, found a non-dimensional grouping of flow variables--now known as the Dean number--that correlated the observed results. The classic work in this field, however, was done by White [361, 362] in 1929 and 1932 and was used by designers of heat transfer equipment as the authoritative work on the subject for nearly three decades.

McAdams in his reference work on heat transfer [363] has suggested a simple correlation for the average heat transfer coefficient for coiled tubes in terms of the result for simple linear tubes: a multiplying factor of 1 + 3.5/R, where R in the curvature ratio defined as the radius of curvature of the tubing coil (to the centerline of the tube) divided by the radius of the tube. Although simplistic, later research has basically supported this result.

Ito [364] has examined the turbulent regime for helical-flow to obtain an empirical law for friction factor supported by some theoretical considerations. He found that the critical Reynolds number (defined as the transition point from laminar to turbulent flow) could be correlated by the following expression: $2000/R^{0.32}$ where R is once again the curvature ratio. This shows that for a decrease in the curvature ratio, i.e. a more tightly wrapped coil, the transition from laminar to turbulent flow is delayed much in the manner of the effect of rotating a tube with an axial throughflow.

Seban [365] has extended Ito's work to include heat transfer effects upon friction factor as well as to obtain a Nusselt number correlation. Seban has shown that Ito's friction factor correlation can be used for non-isothermal flow if the fluid properties are evaluated at the mean film temperature. For the Nusselt number, Seban recommends the following relation: $f\ Re\ Pr^{0.4}/8$, where f is the friction factor determined by Ito's correlation, re is the Reynolds number based upon mean velocity and pipe diameter, and Pr is the Prandtl number of the fluid. Seban has noted that his expression yields very similar results to the simple correlation suggested by McAdams. In addition to causing a delay in transition to higher Reynolds numbers, Seban has also found that the tube curvature causes a significant peripheral variation in Nusselt number (by a factor of about 2 to 4 larger on the outside radius than on the inside radius). This result is consistent with what was noted as observed heat transfer enhancement for flow past concave walls and inhibition for flow past convex walls.

Rogers [366] has extended Seban's work and, although supportive of his conclusions, has suggested two alternative correlations for Nusselt number: one based upon evaluating the fluid properties at the film temperature and the other at the bulk temperature. Mori [367] has performed an analytical study for high Dean numbers (usually defined as the ratio of the Reynolds number to the square root of the curvature ratio) using a boundary layer/potential flow analysis that appears to be valid only for fluids with Prandtl number about 1. He quotes a 50% heat transfer increase over that obtainable with a simple straight tube with a curvature ratio of 20.

Kalb in several papers [368, 369] has examined the flow from a theoretical standpoint for two boundary conditions: constant axial heat flow with uniform peripheral wall temperature and for the case of uniform wall temperature. Patankar [370] has recently developed a numerical, finite-difference procedure to obtain predictions of laminar flow in helically coiled pipes. He notes that the principal effect of the curvature is to cause secondary flows which in turn result in a departure from Poiseuille flow. But he cautions, "further work is required to develop turbulent flow predictions".

This particular configuration has such wide spread application to industrial equipment that new studies and geometries are continually being reported in the literature (see [371, 372] for several recent Soviet papers). It appears, however, that the correlations currently available for both heat transfer and friction factor are sufficient to predict the performance of virtually any such flow with physical dimensions of practical interest.

Flow Through Tubes with Axially-Mounted Swirl Generators

The most common means of generating a swirling flow for confined applications is through the use of inserts of various sorts.

The most common insert is fabricated by simply twisting a metal tape and pulling it through a pipe; this configuration is usually referred to as a swirl tape flow.

The use of swirl tapes to augment heat transfer dates back at least to the work of Royds [373] in 1921. Sometime later, in 1931, Colburn [374] also examined the effect of internally twisted tapes along with stationary propellers. Since that time, data has been obtained by a large number of investigators [375-389] for a variety of fluids, pitch-ratios of tape twist, and thermodynamic boundary conditions. A summary of this work is presented in Table 4, taken from Bergles [73]. Not included in this table are data obtained for boiling (see, for example, [390, 391]) or for data obtained with other effects combined (see [392] where the effects of wall roughness and swirling flow produced by the swirl tape were found to be roughly additive in augmenting heat transfer).

One of the earliest attempts at explaining the observed heat transfer enhancement was by Kreith and Margolis in an early pair of papers [379-380]. They noted that it was possible to obtain a four-fold increase in Nusselt number and they attributed this increase to four effects:

(1) fin-like character: the presence of the internal metal tape attached to the tube wall acts much like an internal rib or fin and would act to augment the heat transfer regardless of any swirling velocity.

(2) wall curvature: as noted in the subsection on concave/convex flows, Kreith has presented analyses to show that heat transfer is augmented simply by passing a concave wall without a swirling velocity.

(3) Centrifugal force field: when the heat flow is from larger to smaller radii the body force field acting on the density gradient aids

TABLE 4

SUMMARY OF PRINCIPAL INVESTIGATIONS OF SWIRL TAPE FLOW

Investigator	Fluid	Inside Diameter (inch)	Tape Pitch*	Tape fit	Heating	Cooling	Pressure drop
Royds [373]	Air	2.625	Below 10	Loose		X	X
Colburn [374]	Air	2.625	2.67 - 3.05 (axial core)	Loose		X	X
Siegel [375]	Water	0.527	2.84	Snug	X		
Evans [376]	Non-luminous gases	3.00	2.9 - 5.9	Loose		X	X
Koch [377]	Air	1.97	2.45 -11.0	Unknown	X		X
Judd [378]	Isopropylated Santowax	0.48	2.6 - 7.3	Snug	X		
Kreith [380]	Air, Water	0.53	2.58 - 7.3	Snug	X	X	X
Greene [392]	Water	0.89	0.28 - 1.12 (axial core)	Unknown	X		X
Gambill [383]	Water	0.136 - 0.25	2.30 -12.03	Tight	X		X
Ibragimov [384]	Water, liquid metals	0.473	2.12 - 4.57	Tight	X	X	X
Smithberg [385]	Air, Water	1.382	1.61 - ∞	Snug	X		X
Gambill [386]	Ethylene glycol	0.136 - 0.25	2.30 -12.03	Tight	X	X	X
Seymour [387]	Air	0.87	1.8 -14.0	Tight	X		X
Lopina [388]	Water	0.194	2.48 - 9.2	Tight	X	X	X
Thorsen [389]	Air	0.587	1.58 - 4.0	Snug	X	X	X

* Defined as distance per 180° of twist.

convection (and, of course, vice versa when the heat flow is in the other direction).

(4) roughness character: the presence of the swirl tape causes an added turbulence level to the flow field much like wall roughness elements which tends to enhance the heat transfer.

Smithberg and Landis [385] were the first to attempt a detailed correlation of the data available, including their own, with an analytical model of some sort. Their study was limited to low heat transfer rates and low wall to fluid temperature differences. They used a flow field model of a forced vortex flow in the core region superposed on an essentially uniform axial flow, a combination they termed as "helicoidal." This model was then used to predict the friction factor by summing the effects of the axial flow, the tangential flow, and the momentum deficit due to vortex core mixing. Then by means of the Colburn analogy they were able to predict the heat transfer coefficient. This work was then extended by Throsen and Landis [389] for high heat transfer rates and large temperature differences in the radial direction. They were able to develop a diabatic friction factor correlation in terms of the friction factor for flow through a straight pipe that was valid for both heating and cooling, and two Nusselt number correlations (one for fluid heating and one for fluid cooling) that were functions of the Reynolds number and the Grashof number. Bergles [74] in assessing the worth of these two papers has concluded: "their semi-analytical prediction method appears to account for all of their observed variation in h_s with the swirl flow of air subjected to large radial temperature gradients". (h_s defined as the heat transfer coefficient for swirling flow).

Lopina and Bergles [388] developed a correlation based upon the premise that the observed heat transfer is due to the simple sum of three effects: turbulent flow in a spiral channel, centrifugal convection upon a density gradient, and the fin-effect. Their assumption and calculations agrees well with the data for fluid heating but for cooling a better prediction is obtained simply by neglecting the centrifugal convection effect rather than by trying to make it inhibitive of the heat transfer. Thus they sum three terms to predict the Nusselt number for fluid heating and two terms for fluid cooling.

Recently there has been literature published for swirl-generating inserts other than swirl tapes. Gutstein [393] in an extensive monograph has investigated a family of inserts: helical vanes with and without a centerbody and a wire-wrapped plug. Sketches of these geometries together with the swirl tape and the wire coil are presented in Figure 3, taken from his report. The distinguishing feature between the swirl tape configuration and the helical vane configuration is that in the latter case there is a single helical flow passage which would appear to be more amenable to analysis and would, perhaps, be characterized by a smaller pressure drop. The analytical model presented for the prediction of the measured Stanton number provided an excellent correlation for the helical vane configuration. However, when compared to the swirl tape data available in the literature, the correlating equation underpredicted the observed heat transfer.

In a configuration similar to Gutstein's, Seban and Hunsbedt [394] have obtained additional data supportive of his results. Their correlation used a "straightened-out" length of the flow channel based upon the known helix angle.

Klaczak [395] has recently reported on the use of spiral and helical turbulators to enhance the heat transfer in a tube. These configurations have not been examined in detail here since their effect is primarily through artificially increasing the wall roughness as there is very little induced swirl. Megerlin [396] has used spiral brush inserts to obtain heat transfer coefficients 5 times empty tube values. These data also include the effect of heat transfer enhancement due to entry-length effects (the length to diameter ratio of the apparatus was 9.5) whereas the data is usually available only in terms of mean Nusselt numbers obtained from fully developed flow in relatively long tubes.

Klepper [397] in a recent paper claims to present the first data for Nusselt number as a function of tube length in a decaying swirl flow generated by swirl tapes. All the other data reported in subsection (i.e. [373-397]) is for geometries in which the swirl generator, usually tapes, extends through out the entire heat transfer length; in addition, all the data but that of Megerlin appears to be obtained for sufficiently long tubes that any entry-length effect present has been minimized. Klepper, on the other hand, has examined sections for which the tube contains a length of swirl tape followed by an extended section that is only a simple tube. He has obtained data and a correlation under these combined effects of entry-length and swirl decay. The local Nusselt number is correlated to be equal to $0.023\ \mathrm{Re}^{0.8}\mathrm{Pr}^{0.4}(T_w/T_b)^{-0.5}\psi_1\psi_2$, where Re is the Reynolds number, Pr the Prandtl number, T_w/T_b the temperature ratio of the wall to the bulk fluid, and ψ_1 is the "Reynolds number modulus" for which he gives

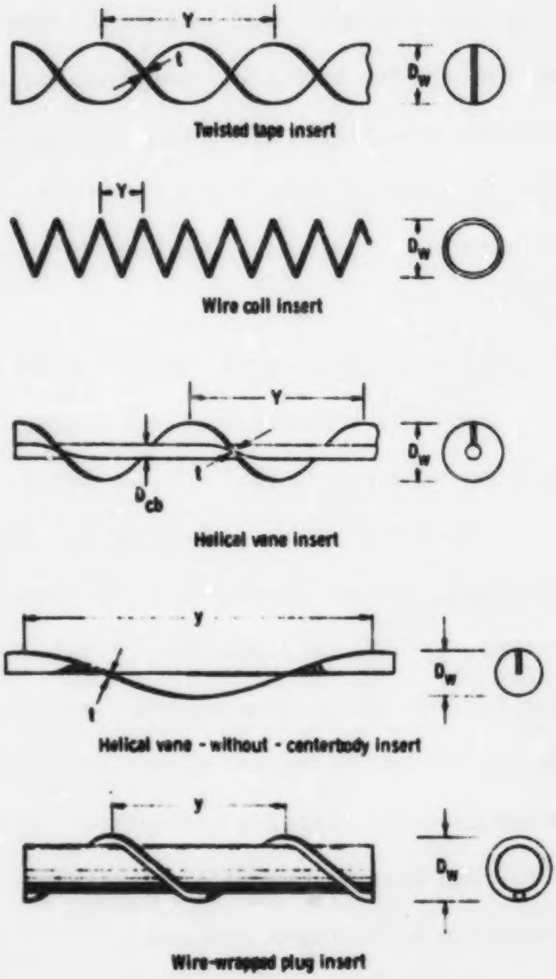
Y
t
D_w
Twisted tape insert
Y
D_w
Wire coil insert
Y
t
D_cb
D_w
Helical vane insert
y
t
D_w
Helical vane - without - centerbody insert
y
D_w
Wire-wrapped plug insert

Figure 3. Swirl Generators (taken from Gutstein [393])

an expression that is a function of Reynolds number only, and ψ_2 is the entry length factor which is given as a function of distance from the trailing edge of the swirl tape.

Further reference will be made to the data available for swirl tape heat transfer, particularly the work of Klepper, in Chapter IV.

Scope, Significance, and Objective of Research Investigation

In the area of incineration there appears to be three primary needs worthy of investigation:

(1) A dependable, clean, and inherently efficient incinerator concept that would dispose of solid wastes without unacceptable pollution levels.

(2) An incinerator configuration that would not require the usual complement of stack devices to meet air quality standards.

(3) A device that would efficiently recover the energy liberated by combustion.

The incineration configuration to be examined in this research effort is anticipated to meet these three requirements. The concept is that of a vortex furnace wherein the solid waste is used as fuel, augmented as necessary by auxiliary fuels, and fed to the furnace in a fluidized state carried by the feed air. The auxiliary fuel is utilized to maintain the combustion process at a sufficiently high temperature to insure the complete odor-free pyrolysis of the waste material.

The vortex can be effectively generated by supplying the air and fuel into a vortex chamber through tangentially opposing ports. The attached vortex tube would be a water-walled furnace column from which a significant fraction of the chemical energy liberated can be recovered. The outlet of the vortex tube would be connected to an enlarged section whose purpose would be to trap any unburned particulate much as a cyclone separator.

There are a number of unknown factors that would determine the performance of such an incinerator concept:

(1) Heat transfer from a confined, conflagrant vortex flow has never been examined in the literature and thus the amount of heat recovery as a function of vortex tube length (or, in this case, furnace column height) is at present both unknown and unknowable.

(2) Heat transfer under the conditions of vortex decay with entry-length effect has not been examined for swirl generation by means of tangential jets and thus its prediction is not yet possible.

(3) Gas temperature profiles in regions of confined, conflagrant vortex flow with significant heat recovery have never been reported in the literature.

The overall objective of this research effort was to obtain the data and correlations necessary for these unknown factors that would permit the prediction of the performance capability of a full-size incinerator utilizing this concept of vortex combustion with simultaneous heat recovery.

To this end, a laboratory-size incinerator has been designed, constructed, instrumented, and operated to obtain the first body of data for this concept. The configuration of the apparatus is described in detail in Chapter II, the results of the data in Chapter III, and the suggested correlations for heat transfer in a conflagrant, vortex flow are given in Chapter IV.

CHAPTER II

EXPERIMENTAL APPARATUS AND PROCEDURE

Experimental Apparatus

In order to achieve the outlined research objectives, a working model of a fluidized, vortex incinerator was fabricated and assembled within a separate four-foot concrete structure directly adjoining the Thermal/Fluid Sciences Laboratory. This structure effectively isolated the incinerator in a near-adiabatic enclosure as well as acted as a safety chamber in the event of a structural failure during operation. The controls for the operation of the incinerator were all located within the laboratory itself.

Figure 4 illustrates the overall configuration of the vortex incinerator installation.

Vortex Chamber

The vortex incinerator has two primary requirements essential for operation: an arrangement for the generation of the vortex and a combustion zone within which the flame front can be stabilized. As noted in the literature survey, there are a variety of means used to generate a vortex flow. The use of inlet vanes in conjunction with an induced flow scheme was rejected because the blower required would need to operate in a high temperature environment and thus necessitate a relatively expensive installation. Swirl tapes, helical vanes, etc., were also

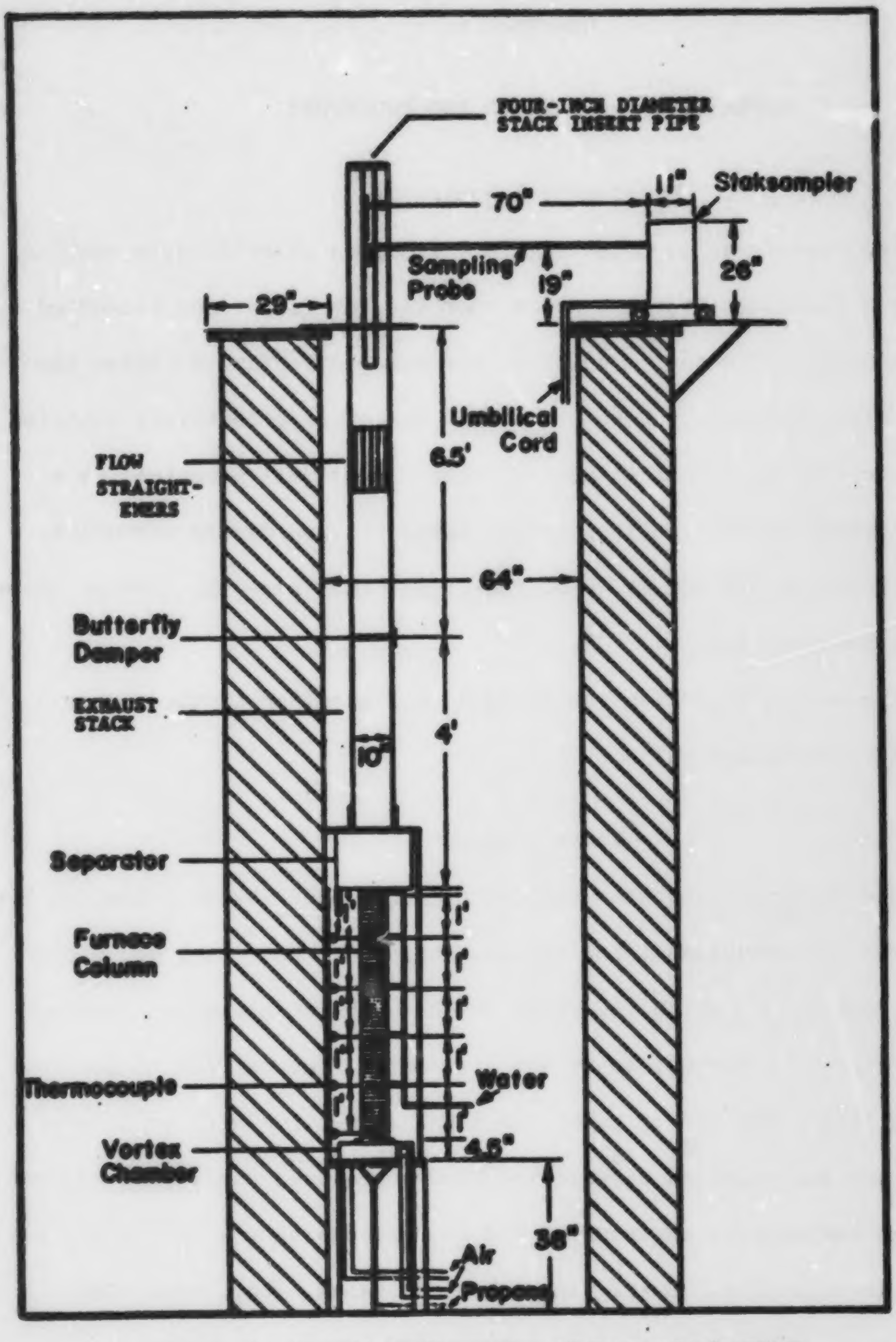
FOUR-INCH DIAMETER
STACK INSERT PIPE
70"
11"
Staksampler
Sampling
Probe
19"
26"
29"
6.5'
Umbilical
Cord
FLOW
STRAIGHT-
ENERS
64"
Butterfly
Damper
EXHAUST
STACK
10"
4'
Separator
Furnace
Column
1'
Thermocouple
Water
4.5"
Vortex
Chamber
38"
Air
Propane

Figure 4. Overall Configuration of Vortex Incinerator

rejected from consideration because: (1) manufacturing restrictions greatly limit the intensity of swirl that can be generated with these devices (it is not usually possible to obtain a tangential velocity component exceeding the mean axial velocity component), (2) the high temperature environment anticipated in a conflagrant flow would require sophisticated cooling techniques to maintain structural integrity of these devices, and (3) because these generation devices introduce an unnecessary uncertainty in the quantification of swirl level in that by their very nature it is only possible to specify the twist ratio whereas the degree of swirl experienced by the fluid motion is unknown. Since a large reciprocating air compressor and an associated storage pressure-vessel was available in the laboratory complex, the decision was made tangential air inlets to generate the vortex flow.

Due to the intense mixing and turbulence anticipated, it was also decided to use the vortex chamber as the combustion zone as well by introducing the fuel into the same area as the inlet air. A schematic of the vortex chamber is given in Figure 5.

The side walls of the chamber were constructed of one-eighth inch sheet steel rolled to an eighteen-inch diameter. The top and the bottom of the chamber were made of three-eighths inch steel plate; grooves (0.150 inch) were cut in the plates to permit insertion of the side walls. These seams were then welded. The two air inlets, made of 1½-inch/schedule 40 pipe, were welded to the side walls at opposite corners of the chamber as shown in Figure 5. A hole (5.76 inch diameter) was cut in the top plate and a 0.2 inch deep inset was cut around this edge to provide an opening and a supporting base for the furnace column. The

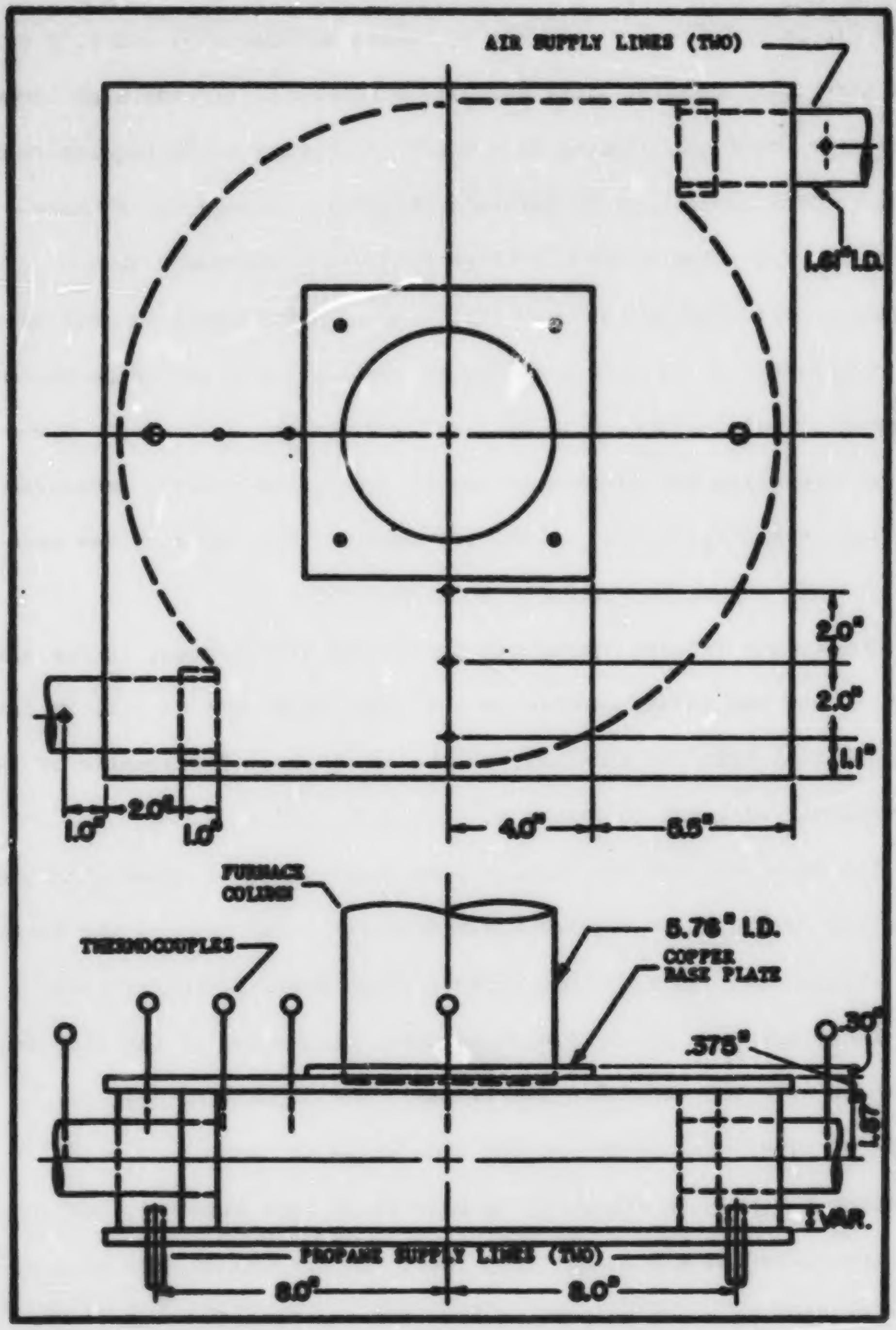
AIR SUPPLY LINES (TWO)
1.61" I.D.
TOP VIEW
2.0"
2.0"
1.1"
1.0"
2.0"
1.0"
4.0"
5.5"
FURNACE COLUMN
THERMOCOUPLES
5.76" I.D.
COPPER BASE PLATE
.30"
.375"
1.5"
SIDE VIEW
VAR.
PROPANE SUPPLY LINES (TWO)
8.0"
8.0"

Figure 5. Vortex Combustion Chamber

complete vortex chamber was mounted atop a steel table (workbench height) that had been constructed in the four-by-eight structure.

Fluidized wastes entered the chamber through one of the air inlets whereas the auxiliary fuel (propane was chosen) was supplied through a pair of one-half inch stainless steel tubes mounted in the bottom plate with Conax fittings (see Figure 5). These jets were located near the walls in order to insure that the entering refuse would be immediately exposed to the flame for ignition. The height of the jets with respect to the bottom plate was not found to have a significant effect upon the incinerator performance. It was necessary, however, to install reducers within the stainless steel tubes because of instabilities introduced into the propane feed system by pressure variations in the combustion chamber; apparently without the reducers this was a dynamically unstable system.

The initial propane inlet configuration was a single inlet located in the center of the bottom plate. In this position a very stable flame, more or less confined to the center of the chamber, was stretched vertically in a narrow, cylindrical shape (approximately 2 inches in diameter) through most of the furnace column much in the manner of that reported by Albright [128, 129]. As a result, most of the entering refuse escaped ignition, since the core of this flame was comparatively quiescent, and was collected unburned. For this reason, the configuration was changed to that described in the preceeding paragraph.

The three-quarter inch hole remaining in the center of the bottom plate was then used as a drain line (to remove trapped water after rains) and as a slag collector during slagging tests. The bottom plate acquired a convex shape (when viewed from above) after several runs which permitted any liquids to collect above the central hole.

A small hole (one-eighth inch NPT) was tapped in the side wall of the chamber to provide a means of starting the incinerator. A separate propane tank (the standard size used for portable hand-torches) was used for this purpose by means of an attached section of copper tubing that was crimped off at the end except for a very small hole; when ignited, a flame of approximately six inches in length could be provided by this arrangement.

Various additional one-eighth inch NPT ports were provided in the top plate of the chamber permitting the insertion of Honeywell MegopaK Thermocouple Assemblies.

Figure 6 is a photograph of the vortex combustion chamber as installed with the furnace column attached.

Furnace Column/Heat Recovery System

Since the primary objective of this investigation was to assess the heat transfer capability of the vortex incineration concept, it was necessary to design a heat removal scheme that would enable the recovery of an economically significant fraction of the heat of combustion. This component is a combination cylindrical tube attached to a vortex generator (see Figure 2b) and a heat sink and is referred to here as a "furnace column".

The basic objectives in its design were to make the column long (to allow enough residence time to remove a reasonable amount of thermal energy), of small diameter (to maximize vortex velocities and hence maximize convection coefficient), and to use a good conductor (so that energy transmitted to the interior wall by the hot gases would be readily transmitted through the column's wall to the heat recovery medium). In

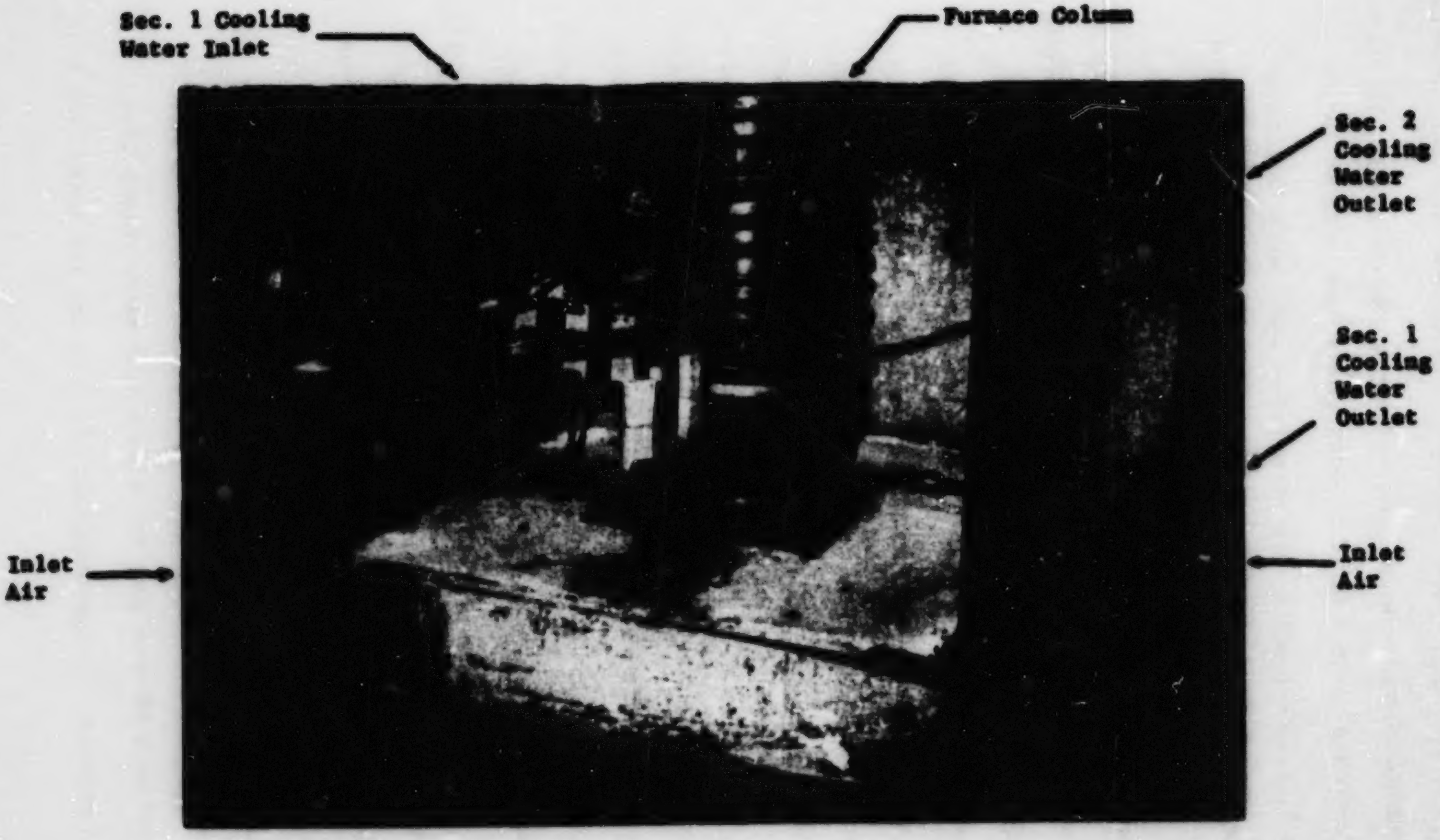
Sec. 1 Cooling
Water Inlet
Furnace Column
Sec. 2
Cooling
Water
Outlet
Sec. 1
Cooling
Water
Outlet
Inlet
Air
Inlet
Air

Figure 6. Vortex Combustion Chamber and Furnace Column

addition, the size of the column was restricted to that available off-the-shelf at reasonable cost. As a result of these considerations, the furnace column was selected to be a six-foot long copper tube with an inside diameter of 5.76 inches and a three-sixteenths-inch wall thickness.

Water was chosen as the heat recovery medium and the system was designed to insure that boiling would not occur (again, in order to maximize heat transfer). As a result, the column was divided into one-foot sections with each section cooled by a separate water supply. Only five feet of the column was actually cooled; the remaining one foot extended inside the separator. In a full-size, commerical installation these cooling coils could--and probably should--be located inside the furnace column to maximize heat recovery. Due to the relatively small diameter of this column it was not possible to install the coils internally. The cooling water flowed through one-quarter inch (outside diameter) copper refrigeration tubing that was wrapped spirally around the furnace column at a rate of approximately sixteen turns per foot (this corresponds to approximately a nine-sixteenths-inch gap between adjacent tubing). The flow direction was selected to achieve a slight counter-flow effect. To facilitate removal of the column, each section of cooling coil terminated in a six-inch leader which was connected to the water system with a Swagelok union. Figure 7 is a schematic of a typical one-foot section of cooling coil and Figure 8 is a photograph of the installed furnace column.

The five water supply lines were fed by a single two-horsepower pump that acted as a booster pump to a main city water supply line. The discharge pressure was approximately 125 psig and the total flow to

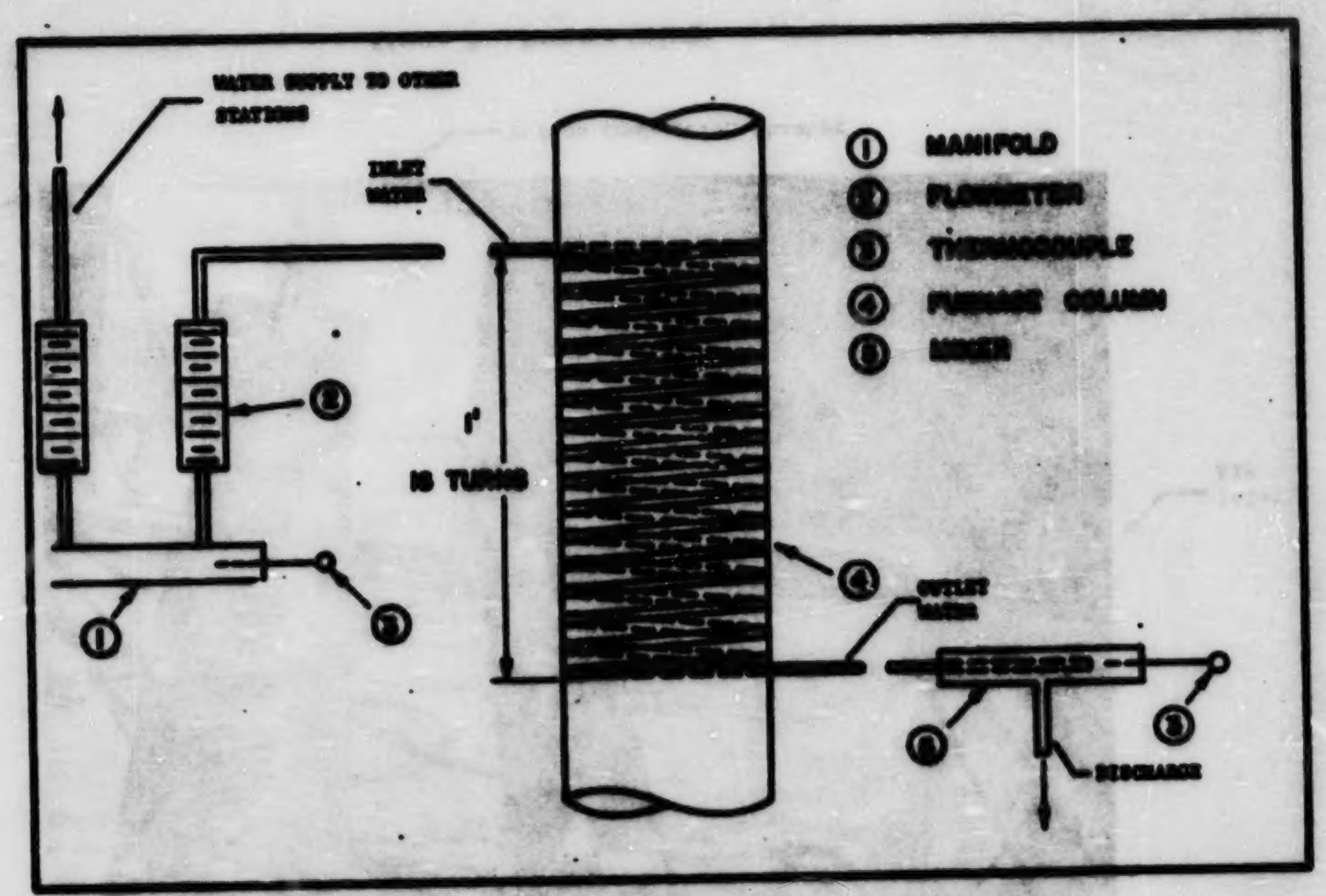
WATER SUPPLY TO OTHER STATIONS
INLET WATER
1'
18 TURNS
① MANIFOLD
② FLOWMETER
③ THERMOCOUPLE
④ FURNACE COLUMN
⑤ MIXER
①
②
③
④
OUTLET WATER
⑤
③
DISCHARGE

Figure 7. Furnace Column Cooling Water Schematic (Typical Section)

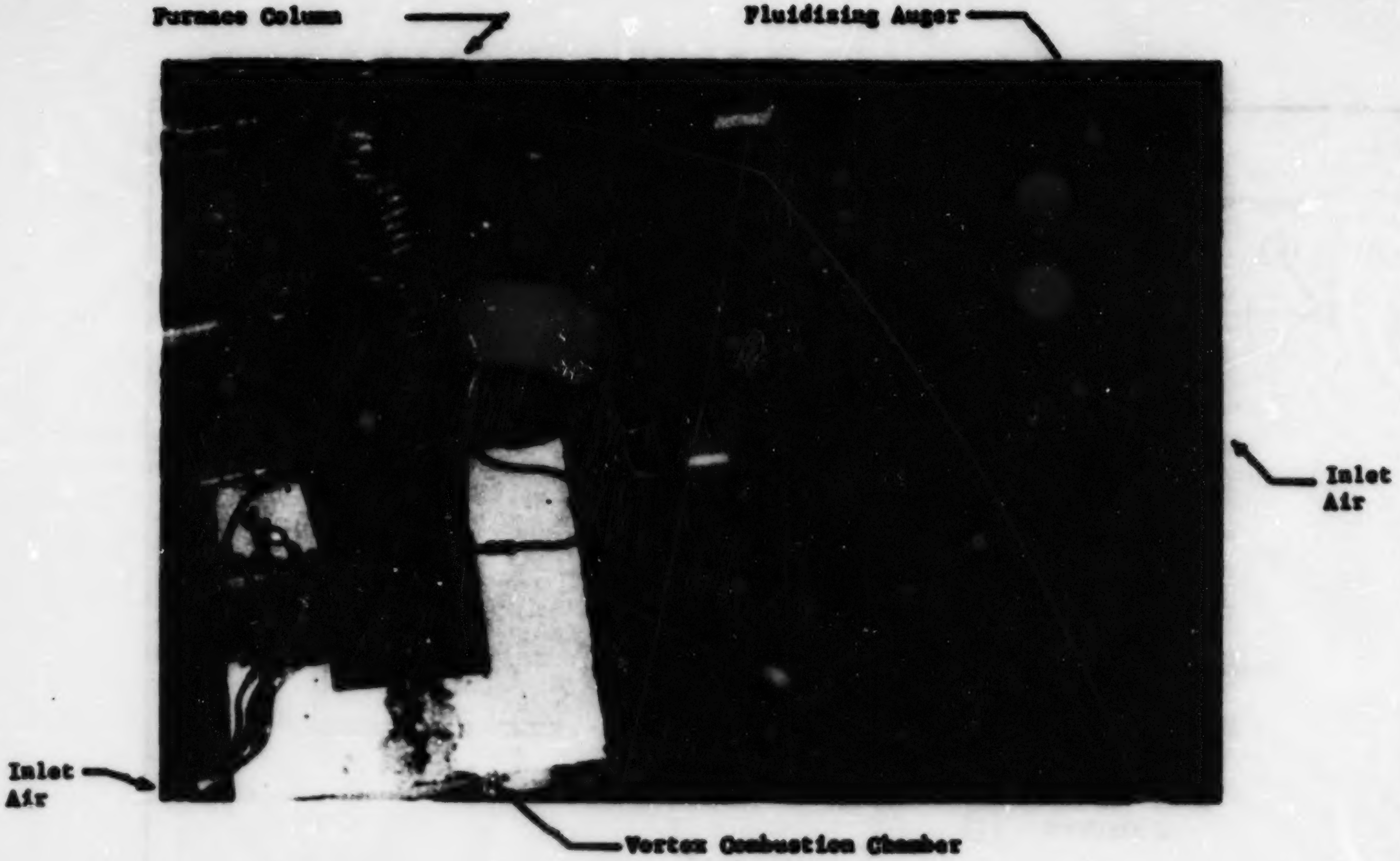
Furnace Column
Fluidizing Auger
Inlet Air
Inlet Air
Vortex Combustion Chamber

Figure 8. Furnace Column

all five sections was approximately 240 gallons per hour (nominally 60 gph went to the bottom section and with 45 gph supplied to each of the other four sections). The discharge water from each section was routed to a mixing chamber where its temperature was measured and then it was simply discharged.

Initially the cooling coils were thought to be amenable to attachment to the column by means of silver solder. However, the copper furnace column was such a good heat conductor that the silver simply would not melt (its melting point is about 1200°F). It was then necessary to use lead-tin solder (melting point 400°F) which worked satisfactorily. There was some a priori concern that the column would heat up to the solder's melting point during operation, but by insulating it from the very hot vortex chamber, and by insuring an adequate flow rate of water, this problem never materialized.

An eight inch square copper plate (with a 5.76 inch hole), one-quarter of an inch thick (hereafter referred to as the "copper base plate") was then silver-soldered to the base of the furnace column. This base was in turn attached to the top of the vortex combustion chamber with a one-eighth-inch thick asbestos separating gasket (to minimize gas leakage and conduction heat transfer from the hot vortex chamber).

At the midpoint of each one-foot section, a one-eighth inch tap was provided between the refrigeration tubing. MegopaK thermocouples were then installed permitting the measurement of the gas temperature at five different vertical stations (6, 18, 30, 42, and 54 inches above the vortex chamber) as well as at various radial positions at each station; thus each "station" is located at the mid-point of each respective "section". Figure 9 illustrates the location of these thermocouple taps and Figure 10 the method of obtaining temperature measurements as a function of radial position. Static pressure taps were also installed at various points along the column although it became exceedingly difficult to obtain any reliable data (due to condensation) and hence they were not used further.

An additional tap was also provided for installation of an aspirated thermocouple. This device will be discussed further in Appendix E.

Separator

One of the advantages of using vortex flow in an incineration concept is that it provides a ready means of separating particulate matter. The separator designed for this incinerator is illustrated in Figure 11.

The entrapment of particulate is achieved by providing a cylindrical section approximately one-foot high with an inside diameter of eighteen inches rather than the 5.76 inch diameter of the furnace column. At the bottom of the separator an annular trough three inches wide and three inches deep was provided to prevent the separated particulate from being picked-up and reintroduced into the primary flow pattern. A 1½ -inch diameter port was installed in the bottom of this trough to permit continuous ash removal (via a suction pump) in the event it became necessary. Because of the small volumes of refuse incinerated by this apparatus, this port was never utilized; only occasional emptying of the trough was necessary and this was done simply by removing the separator itself, and dumping the accumulated particulate.

The separator was constructed of 16 gauge galvanized steel and

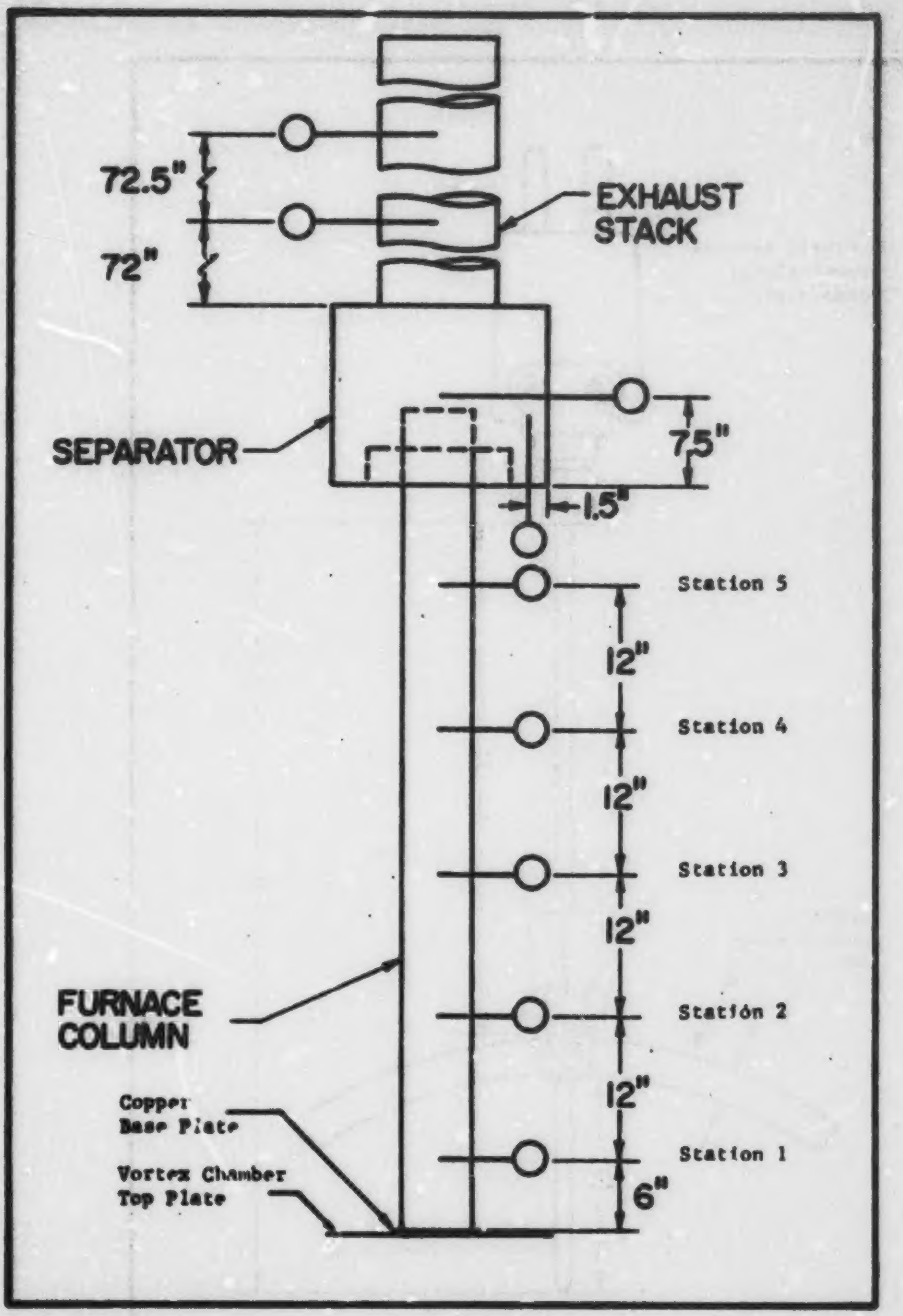
72.5"
72"
EXHAUST STACK
SEPARATOR
7.5"
1.5"
Station 5
12"
Station 4
12"
Station 3
12"
Station 2
12"
Station 1
6"
FURNACE COLUMN
Copper Base Plate
Vortex Chamber Top Plate

Figure 9. Thermocouple Locations

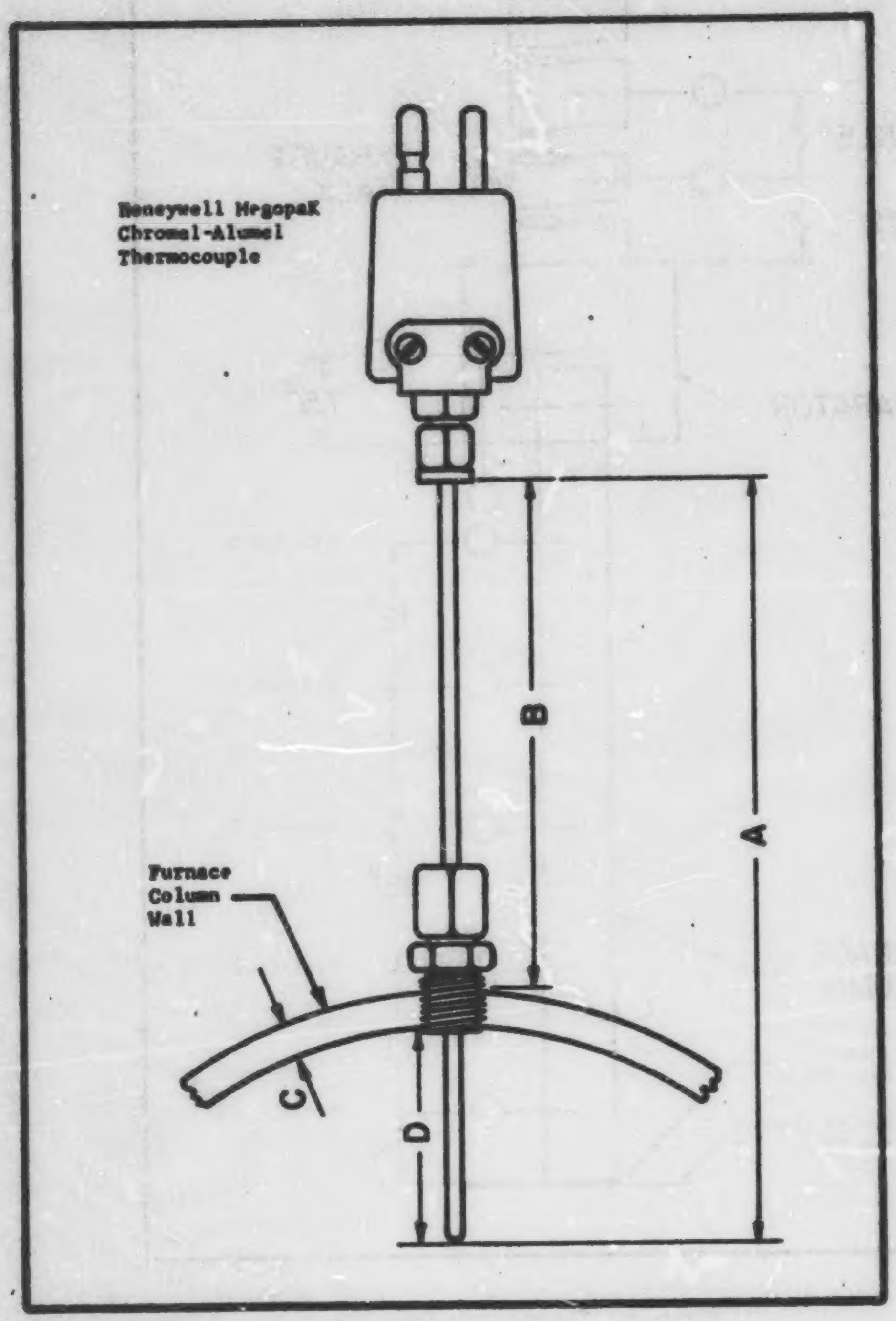

Honeywell MegopaK
Chromel-Alumel
Thermocouple
Furnace
Column
Wall
A
B
C
D

Figure 10. Gas Temperature Measurement System

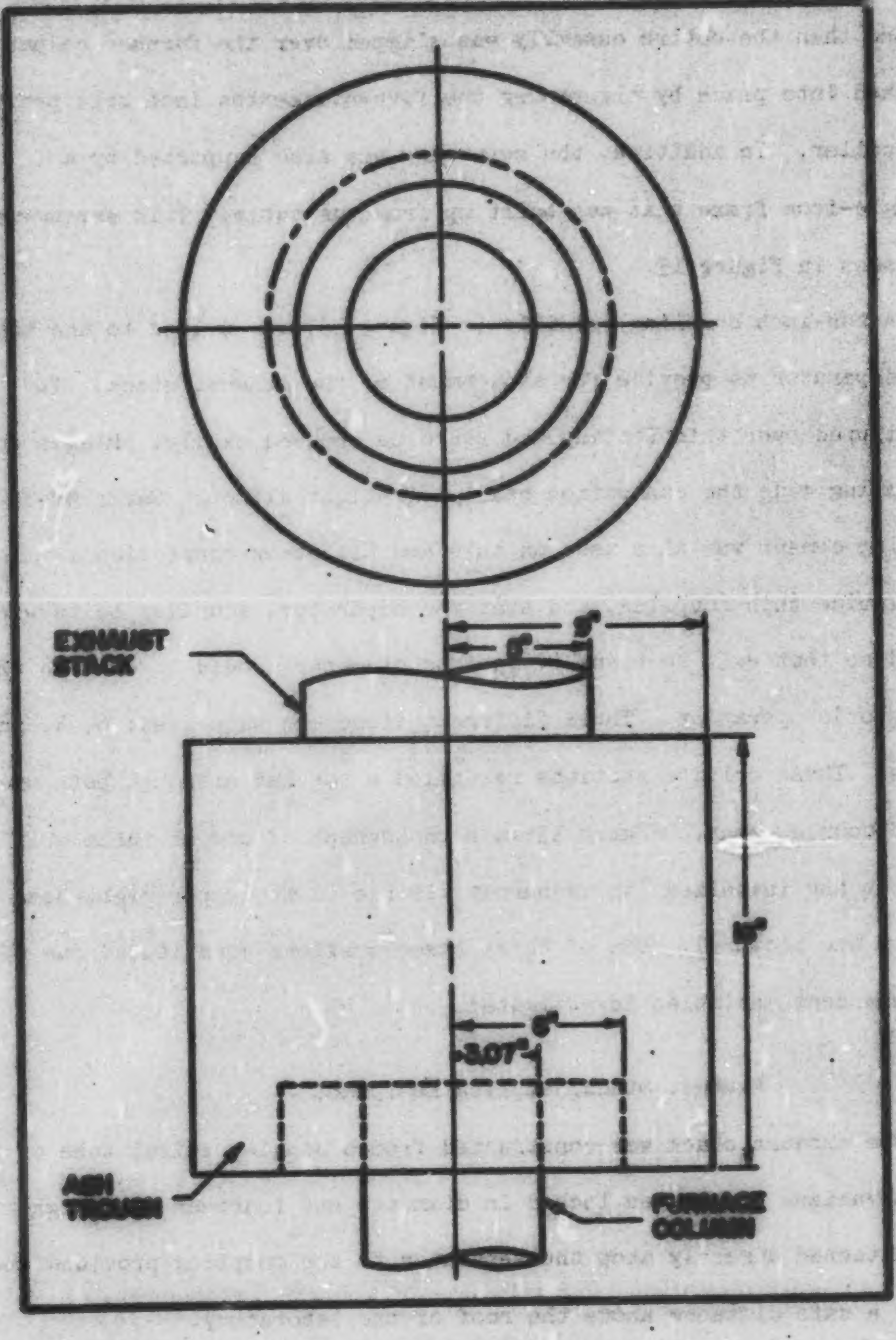
EXHAUST STACK
9"
5"
15"
6"
3.07"
ASH TROUGH
FURNACE COLUMN

Figure 11. Separator

was attached to the furnace column by means of the collar shown in Figure 12. The collar was bolted directly to the bottom of the separator and then the entire assembly was slipped over the furnace column and locked into place by tightening the five-sixteenths inch bolt provided in the collar. In addition, the separator was also supported by a 1 inch angle-iron frame that was built up from the table. This arrangement can be seen in Figure 13.

A ten-inch coupling (visible in Figure 13) was welded to the top of the separator to provide for attachment of the exhaust stack. The stack slipped over this fitting and could be removed easily. Ridges on the coupling made the connection nearly air-tight although Carey MW-50 insulating cement was also used on this and all other connections.

Inside this coupling, and atop the separator, mounting bolts were provided so that exit sections of various diameters could be used in the incinerator's operation. Three different diameters were used: 6, 4, and 2 inches. These orifice sections resembled a top hat although both ends were, of course, open. Figure 13 is a photograph of one of these orifices as it is being installed (it is barely visible in the upper right-hand corner of the picture). Use of these three orifices constituted one of the independent variables investigated.

Exhaust Stack/Sampling Equipment

The exhaust stack was constructed from a single, spiral tube of 20 gauge galvanized steel, ten inches in diameter and fourteen feet high. It was attached directly atop the separator to the coupling provided and it ended a safe distance above the roof of the laboratory.

A butterfly damper was installed in the stack approximately thirty

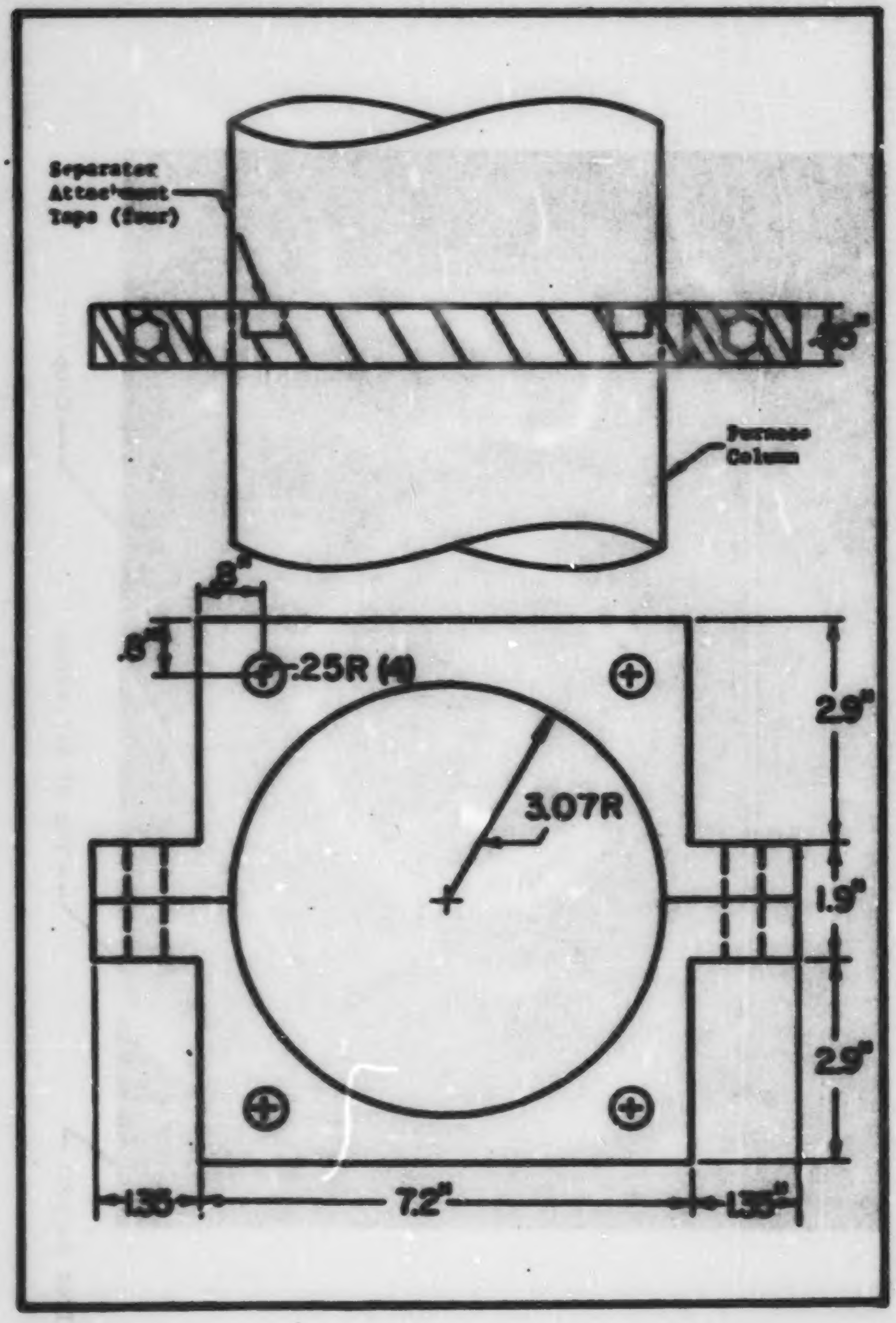
Separator
Attachment
Taps (four)
.45"
Furnace
Column
.8"
.8"
.25R (4)
3.07R
2.9"
1.9"
2.9"
1.35
7.2"
1.35"

Figure 12. Collar

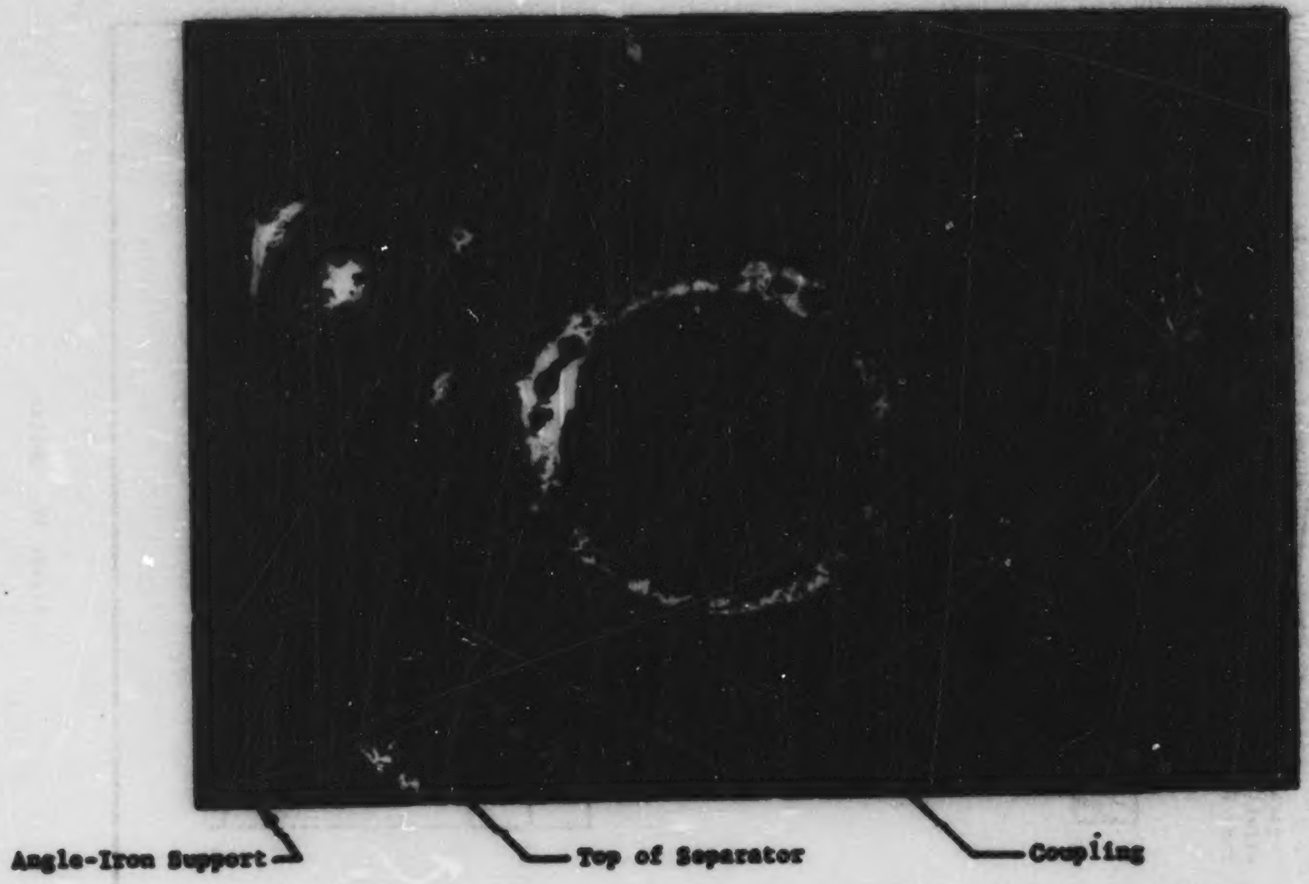
Angle-Iron Support
Top of Separator
Coupling

Figure 13. Separator and Exhaust Stack Coupling (Exit Orifice Removed)

inches above the separator. Its original purpose was to provide a means of assessing the performance of the incinerator under various back pressures. However, the use of the damper was awkward and the resulting charges in back pressure did not appear to be adequately reproducible, and, since the effect was observed to be minimal, it was left in the full open position for all the data taken.

A photograph of the exhaust stack together with the separator and the top of the furnace column is shown in Figure 14.

A commercially manufactured sample train—Research Appliance Corporation "Staksamplr" Model 2343—was installed on the roof of the laboratory to isokinetically sample the stack. The installation was done to conform to the requirements given in Specifications for Incinerator Testing at Federal Facilities [398, 399]. Figure 15 is a photograph of the actual installation.

In order to satisfy the requirements of the Staksamplr two modifications to the exhaust stack were necessary. First, flow straighteners were installed (see Figure 4) that would convert the vortex flow into a simple axial flow; these straighteners consisted of a bank of half-inch, thin-wall, aluminum tubes six inches long. Second, a four-inch diameter insert pipe was installed (also illustrated in Figure 4) to provide stack velocities high enough (17 feet per second minimum) to permit the sample to operate isokinetically; the top of the stack was plugged except for the four-inch opening thus effectively reducing the flow diameter from ten inches to four. It should be noted that virtually all the temperature and heat transfer data presented in Chapter III were obtained with this insert removed; it was installed primarily for the sampling efforts. However,

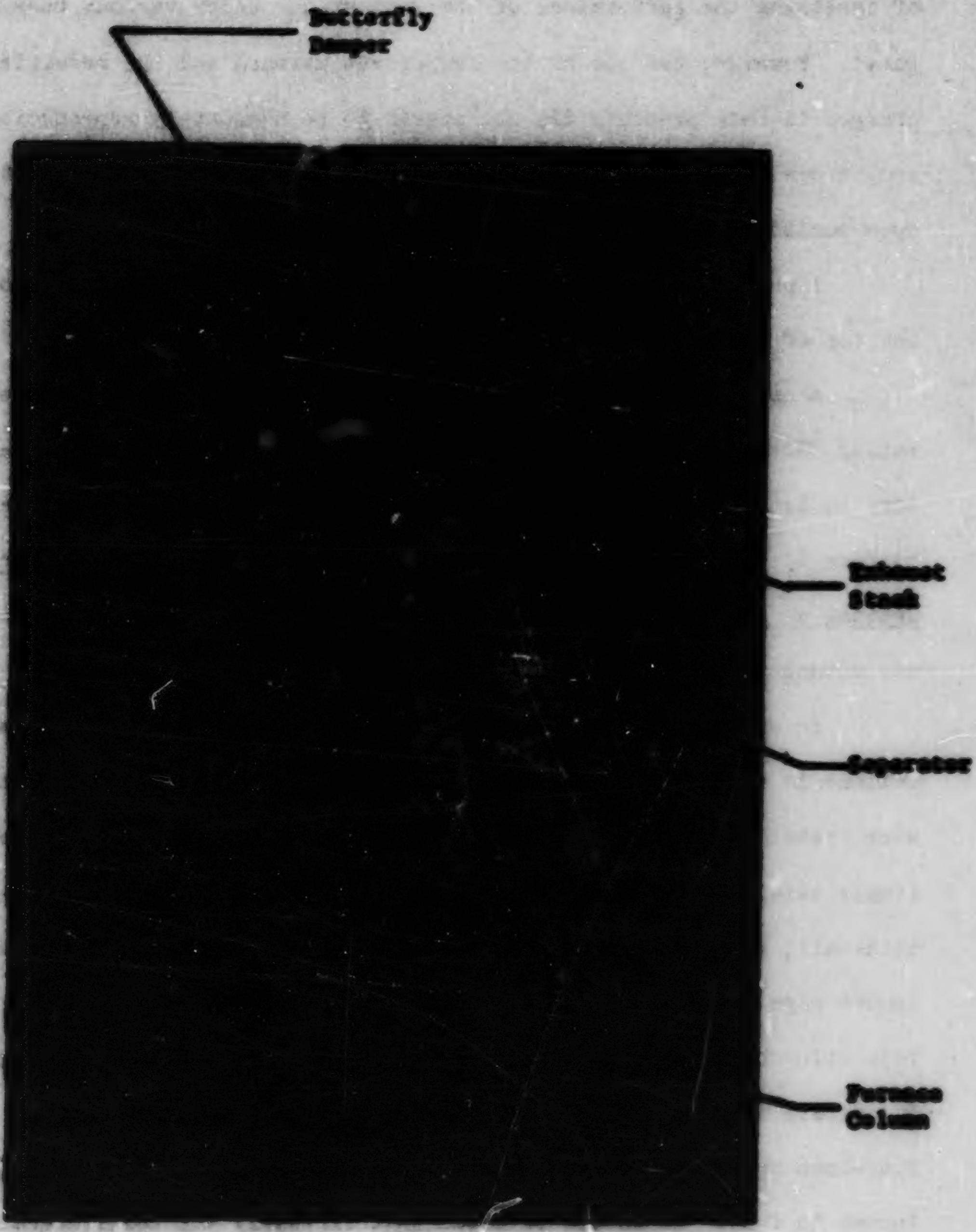
Butterfly Damper
Exhaust Stack
Separator
Furnace Column

Figure 14. Exhaust Stack, Separator, and Furnace Column

Figure 15. "Staksamplr" Installation

since an orifice was always used at the separator exit, the operating performance of the incinerator was not noticeably affected by its presence or absence.

Fluidizer

In order to operate this apparatus as an incinerator, some method of ingesting the refuse was necessary. The most convenient means of doing this was to fluidize the refuse in one of the air supply lines to the vortex chamber. The use of the word "fluidized" should be distinguished from its use by chemical engineers with respect to fluidized beds; the objective here was not to mobilize the refuse en masse, but merely to use the air as a carrier for the fuel much as in an automobile carburetor. In a full-size commerical incinerator it would be feasible to provide separate ports where the refuse, truly "fluidized," could be ingested.

The device designed to accomplish this objective is visible in Figure 8. It should be noted that the refuse was fluidized into only one of the two air lines; however, the turbulence level in the vortex combustion chamber was sufficient that no uneven burning effects were detected.

The fluidizer was constructed from a plexiglass tube four-feet long and six-inches in diameter which was mounted vertically as shown in Figure 8. This tube acted as a hopper whereby a charge of refuse could be stored. The refuse was injected to the three foot horizontal section of plexiglass by means of a reducer/tee section which was machined from a single block of plexiglass. All joints were fused with acetone.

Plexiglass was chosen so that feed rates could be determined (to insure a uniform rate of ingestion) and also to provide a means of detecting clogging as different kinds of refuse were tested.

Initially it had been hoped that simple gravity feed in conjunction with the venturi effect would be sufficient to cause the refuse to leave the hopper. These attempts, however, were unsuccessful as the natural packing of the refuse prevented any significant amount of the material from dropping through the tee section. Even pressurizing the hopper did not measurably improve the situation. Finally an auger driven at 3½ revolutions per minute by an electric motor providing 8.125 foot-pounds of torque achieved the desired results, although stirring rods (attached to the auger) were necessary to prevent the auger from simply boring out a cavity in the refuse. The drive shaft consisted of a five-sixteenths steel rod which was inserted through the lid sealing the top of the hopper. These components are shown in the photograph given as Figure 16. Thus the operating procedure required charging the hopper with refuse, sealing the lid, and then actuating the motor prior to each data run. Sealing the top of the hopper was necessary because it was discovered that non-uniform feed rates would result because of the changing height of the refuse column when the lid was left off.

Initially it had been hoped that a variety of products would serve as refuse: shredded computer cards, shredded leaves, shredded newsprint, digested paper, sawdust, wood chips, grass clippings, potato peelings, etc. Several difficulties were encountered as many of these substances were tried but the principal problem was that of the effect of scale. Specifically, because this laboratory was not full-size, various dimensions were, necessarily, restricted; one of these dimensions—air inlet diameter—proved to be crucial here. The inside diameter of the air inlet pipe was 1.6 inches; this dimension in turn limited the maximum diameter of the outlet of the fluidizing hopper. This situation prevented most of

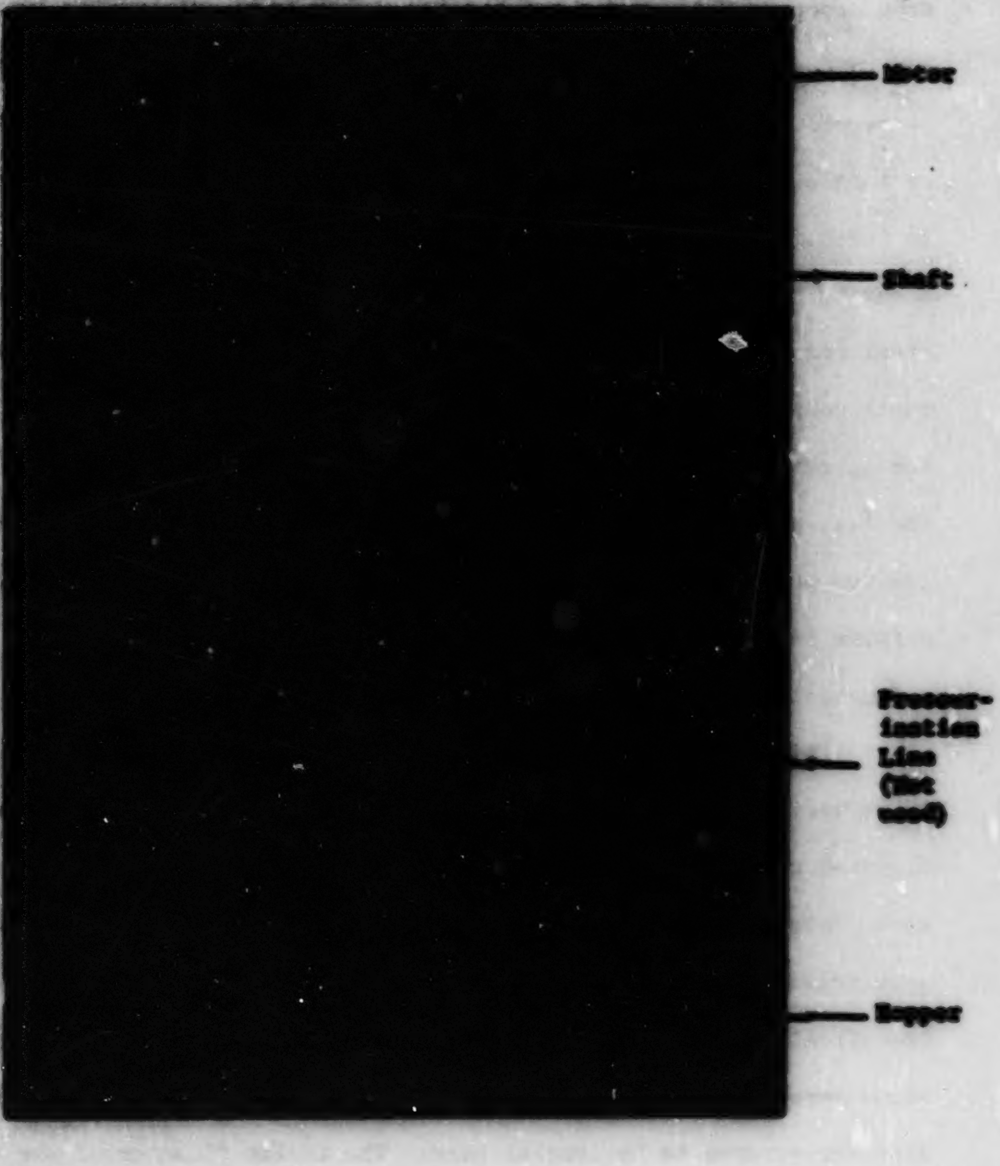
Motor
Shaft
Pressurization Line (Not used)
Hopper

Figure 16. Fluidizer Motor/Drive Shaft

the previously mentioned materials from being fluidised. With the shredding facilities available (a Sears Lawn and Garden Shredder) the newsprint, cards, etc., could never be made small enough to work. As a result, all the refuse data was taken using a mixture of woodchips, sawdust and wood shavings which was obtained by sweeping a local cabinet maker's floor; when the term "refuse" or "sawdust" is used throughout this report it refers to this mixture. Figure 17 is a photograph of this "sawdust".

When the sawdust mixture was used, the hopper was capable of holding about four pounds and the motor/auger caused it to be ingested at a rate of about thirty-five pounds per hour. This permitted approximately five minutes of operation per charge—which turned out to be very limiting when stack sampling was attempted.

Air/Propane Supply System

The air supply system necessary to drive the vortex (as well as oxidise the fuel) was provided by a 4000 cubic foot storage tank which was pressurised to approximately 150 psig prior to each run. This supply was divided into two separate lines each with its own regulating valve.

Propane was selected as the fuel since it was readily available in one-hundred pound tanks. The propane was filtered and regulated prior to being supplied to the combustion chamber.

The use of propane was necessary for two reasons. First, some means of igniting the refuse initially was required; in the case of low heating value refuse (or wet refuse), auxiliary fuel such as propane would also be necessary to maintain combustion (although this was not the problem here). Second, because of the inconvenience of the use of the refuse and

Figure 17. Sawdust Mixture

the associated short operating times, propane alone as the fuel was used to assess the performance of the incinerator. Thus all the quantitative data presented in Chapter 3 (heat recovery, heat transfer, and temperature profiles) was obtained using propane as the sole fuel.

Instrumentation and Calibration

Temperature data were obtained using 27 chromel-alumel and 8 copper-constantan thermocouples. All of the thermocouples together with the associated extension wire was purchased from Honeywell, Inc. Sixteen of the chromel-alumel thermocouples were of the MegopaK-Type (Model No. 2K2M13-G6-5-T, one-eighth-inch outside diameter, 304 stainless steel sheath material, integral measuring junction, compression fitting attachment, and Quick Konnect electrical connection); the remaining eleven chromel-alumel thermocouples (used to obtain furnace column wall temperatures) were fabricated from bulk thermocouple wire. All the copper-constantan thermocouples were also of the MegopaK-Type (Model No. 2T2M13-G6-5-T, similar in all respects to the chromel-alumel assemblies except for calibration-type).

These data were permanently recorded on either of two multichannel strip charts or on a twenty-four channel digital recorder. Details of the recording equipment and the calibration procedure are presented in Appendix A.

The temperature of the inlet air and propane was measured (to determine mass flow) and also of the five inlet and outlet cooling water lines (to determine heat recovery). In addition, the furnace column wall temperature was measured at eleven locations while the combustion gas temperature measured at five stations (see Figure 9) for thirteen radial positions. Various additional temperature measurements were made in the vortex combustion chamber, the separator, and the exhaust stack.

Manometers were used to measure the inlet pressure of the two air supply lines and the propane supply line. Together with the temperature data this permitted a determination of the density.

Eight Fisher and Porter Rotameters were used to determine the flow rate of the two air supplies, the propane supply, and the five cooling water supplies. The water and propane flow meters were calibrated using a simple weight-change procedure.

The calibration procedure and results for these measurements are also presented in Appendix A.

Procedure

The start-up procedure for the operation of the vortex incinerator was very straight-forward. First, the air storage tank pressure was checked to ascertain whether an adequate supply of compressed air was available, if the pressure was below approximately 100 psig, the Ingersoll-Rand reciprocating air compressor was activated until the tank was pressurized to approximately 200 psig. Next, the cooling water supply valve was opened and the boost pump energized. After a wait of several minutes a steady-state, bubble-free flow of water was established in the cooling system as observed through the glass tubes in the rotameters. Then one of the two tangential air supply valves was cracked open to provide a slight flow of air. The propane starter tank with the crimped-off copper line (as already described in the subsection on the vortex chamber) was ignited and positioned on the steel table so that a six-inch flame would extend past the open one-eigth inch NPT port on the side of the vortex chamber. Next the main propane supply valve was cracked open resulting in a slight vacuum within the vortex chamber which in turn sucked in the pilot flame from the portable propane tank and thus ignited the incinerator. The air and propane supply valve were then brought open in steps until each of the rotameters were indicating 30% of full-scale. This operating condition is one of three that were examined in detail and is referred to as Condition 3 in Chapters III and IV. Once steady-state combustion had been confirmed, the pilot propane tank was shut-off and the NFT port plugged.

The strip chart recorder-motors were then started (their electronic sections were usually left on overnight) and the incinerator temperatures were monitored for the attainment of steady state conditions. This usually required about thirty minutes. Once the incinerator was fully warmed-up, only about ten minutes was required to stabilize the temperatures as various changes in operating conditions were imposed.

Once steady-state operation was confirmed for the flow conditions to be examined, data were recorded and a run number assigned. The data customarily recorded for a run were as follows:

(1) The flow rates of
    (a) each of the two tangential air supplies,
    (b) of the propane supply, and
    (c) of each of the five cooling water supplies;
(2) the total pressure of
    (a) each air supply line, and
    (b) the propane supply line;
(3) the temperatures of
    (a) the air supply,
    (b) the propane supply,

- (c) the water inlet supply
- (d) each of the five cooling water outlet lines, and
- (e) the furnace column wall and vortex gas as it was instrumented at the time;

(4) the barometric pressure.

The radial temperature profiles of the conflagrant, vortex flow were obtained at the 5 vertical stations by positioning the sheathed thermocouples at thirteen different insertion depths. This was done by using dial calipers to measure dimension B on Figure 10. Since dimensions A and C were known, the penetration depth, D, could be readily determined. The radial positions examined together with the data is presented in Chapter III.

To facilitate data reduction, two programs were written for the Monroe Desk Calculator Model 1655, card-punched, and de-bugged thus assuring an error-free algorithm. The details of these programs are given in Appendix B.

CHAPTER III

RESULTS AND DISCUSSION

Independent Variables Investigated

There were four variables selected as independent whose influence on heat transfer and temperature profiles was examined:

(1) air/fuel ratio,

(2) total mass flow rate,

(3) exit orifice diameter,

(4) inlet air-line diameter.

The incinerator has operated successfully at air/fuel ratios from 15.3 to 33.5 and total mass flow rates from 60 to 355 pounds per hour in thirty different combinations; these combinations are henceforth referred to as Conditions. A complete tabulation of these 30 Conditions is given in Table 5. It was decided to examine the effect of air/fuel ratio and mass flow rate by taking data for three of these thirty combinations: these were Conditions 3, 8, and 12. Condition 3 is very close to stoichiometric (slightly fuel rich), whereas Conditions 8 and 12 both represent an excess-air state (approximately 130% of theoretical). The nominal flow rates and air fuel ratios for these three Conditions is given in Table 6.

The third independent variable, the effect of exit orifice diameter, was examined by taking data with three different-sized exit sections (as described in Chapter II): 2, 4, and 6-inch diameters. These are referred

TABLE 5

SUMMARY OF OPERATING CONDITIONS

Condition	Air Flow Rate (lbm/hr)	Propane Flow Rate (lbm/hr)	Air/fuel Ratio
1	77.4	3.88	19.9
2	119.7	5.19	23.1
3	119.7	7.83	15.3
4	167.0	5.20	32.2
5	267.0	7.84	21.3
6	167.1	10.55	15.8
7	220.4	7.83	28.1
8	216.5	10.45	20.7
9	216.6	13.17	16.4
10	216.8	6.48	33.5
11	354.9	10.45	26.6
12	276.5	13.36	20.7
13	276.2	16.19	17.1
14	347.2	13.39	25.9
15	60.2	3.92	15.3
16	78.8	3.92	20.1
17	78.8	5.24	15.0
18	98.6	5.25	18.8
19	119.6	5.25	22.8
20	131.3	5.25	25.0
21	143.5	5.25	27.3
22	143.5	6.58	21.8
23	143.5	7.93	18.0
24	143.6	9.30	15.4
25	155.9	5.23	29.8
26	168.9	5.24	32.3
27	182.4	7.92	23.0
28	195.0	7.93	24.6
29	207.9	7.92	26.2
30	221.5	7.92	28.0

TABLE 6

INDEPENDENT VARIABLES INVESTIGATED

Mass Flow Rate and Air/Fuel Ratio

Condition	Air/Fuel Ratio	Propane Flow Rate (lbm/hr)	Total Flow Rate (lbm/hr)
3	15	7.9	125
8	20	10.5	220
12	20	13.3	280

Exit Configuration

Exit Configuration	Exit Diameter (inches)	Exit Velocity Ratio
1	2	9.00
2	4	2.25
3	6	1.00

Inlet Configuration

Inlet Configuration	Inlet Area (sq. ft.)	Inlet Velocity Ratio
A	0.00418	3.36
B	0.00616	2.28
C	0.00140	1.00

to as exit Configurations 1, 2, and 3 respectively. For simple axial flow, Configuration 1 should cause an exit velocity 9 times that of Configuration 3 based upon continuity considerations (when at the same temperature). In addition, the presence of different exit diameters could cause a change in the distribution of the solid-body rotation and potential-vortex regions as described by Thompson [166]. It is also possible that the change in the exit diameter could be the cause of a drastic alteration of the flow field in the manner described by Lewellen [105] and quoted in Chapter I, wherein the flow could be made to experience a "jump" at the bottom plate of the vortex chamber for one exit Configuration whereas remain supercritical throughout the furnace column with a breakdown in the exhaust stack for another exit Configuration. The exit Configurations examined are also summarized in Table 6.

The fourth independent variable, the effect of inlet air-line diameter, was examined by installing sleeves of different internal diameters in the tangential air supply-lines attached to the vortex chamber. The effect of the sleeves was to increase the vortex velocity at the same mass flow rate. Without any sleeve, the inside diameter of each supply line was 1.602 inches which corresponds to an area of 0.0140 square feet; this arrangement is referred to as inlet Configuration C. The largest internal-diameter sleeve used had a bore of 1-1/16 inches (flow area of 0.00616 square feet) and is referred to as Configuration B. The smallest sleeve diameter that was successfully utilized was 7/8 inches (flow area 0.00418 square feet) and is designated Configuration A. Two smaller diameter sleeves were fabricated (1/2 and 3/4 inch), but it was not possible to ignite the air/propane mixture with the high inlet velocities generated (velocity ratios of 10.3 and 4.6, respectively, with respect to Configuration C). Based upon the continuity relation Configuration A has an inlet velocity 3.36 times that of C while B has a velocity of 2.28 times C. The geometry and velocity characteristics of the three inlet Configurations are also summarized in Table 5.

Whenever data is presented without a specification of the exit and inlet Configuration it should be presumed to be 3-C (i.e. exit Configuration 3 and inlet Configuration C).

Heat Recovery/Vortex Gas Temperature-Profile Data

Since the demonstration of efficient heat recovery at sufficiently high gas temperatures was the major objective of the investigation, these data constitute the primary achievement of the experimental phase. There are two heat recovery rates of interest: the total heat recovery rate which is obtained by summing the rates recovered at each of the five cooling-coil sections, and the heat flux recovered as a function of furnace column height (or, equivalently, vortex tube length) which is obtained by dividing the heat recovered at each section by the area of each section (1.508 square feet).

Effect of Exit Configuration and Condition

Since it was desired to examine the effect of three exit Configurations and three Conditions there were nine possible operating combinations. Thus, in order to obtain a thirteen-point radial temperature profile of the vortex gas, at the five selected vertical locations identified in Figure 9 (called Stations), it was necessary to perform thirteen runs for each of the nine operating combinations or a total of 117 runs. In addition to obtaining the temperature profile data, heat recovery rates were determined for each of these runs yielding 13 data points for each operating combination (although, due to equipment failures of one sort or another, the average number of data points actually reduced to obtain heat recovery rates was between 11 and 12 for each combination). The flow rate and associated heat recovery data for Conditions 3, 8, and 12 for exit Configuration 1 are presented in Table 7; there are 13 points for Condition 3, 12 for Condition 8, and 11 for Condition 12. The data for exit configuration 2 is given in Table 8 and for exit Configuration 3 in Table 9. All these data are for inlet Configuration C. Since a reasonable number of data points were available for the same Condition and Configuration, it was possible to perform a statistical analysis to obtain the mean, the standard deviation, and the standard deviation of the mean. These results are given in Table 10 for all 9 combinations of heat recovery data.

The temperature profiles of the vortex gas obtained in these 117 runs are presented in Tables 11 (for Configuration 1-C), 12 (for Configuration 2-C), and 13 (for Configuration 3-C) for each Station.

If the velocity profiles were known, it would be possible to obtain the mixed-mean temperature (sometimes also called the mixing-cup temperature or the bulk temperature) defined ([400], page 105) by the following relation:

$$T_m \equiv \frac{1}{\bar{\bar{U}} A_c} \int_0^r U \, T \, r \, dr \qquad (1)$$

However, since these data would be exceedingly difficult to obtain as well as of dubious value due to the disturbance effect of the inserted probes, a calculated or assumed profile is necessary to perform the above integration. As indicated in Chapter I, there does not yet exist an analytical means

TABLE 7

CONFIGURATION 1 HEAT RECOVERY DATA

Flow Rate (lbm/hr) Air	Flow Rate (lbm/hr) C_3H_8	Air/Fuel Ratio	Heat Flux Recovered (Btu/hr-ft^2) Sec. 1	Sec. 2	Sec. 3	Sec. 4	Sec. 5	Total Heat Recovered (Btu/hr)
119.7	7.83	15.29	20,120	12,380	9,290	6,630	6,190	82,350
117.9	7.86	15.00	16,170	9,960	9,510	7,080	6,410	74,070
116.8	7.83	14.92	19,760	12,160	9,730	7,080	6,510	83,300
116.5	7.84	14.86	19,410	12,930	9,730	7,080	6,410	83,780
115.5	7.70	15.00	17,050	10,780	8,400	5,970	5,530	71,980
116.5	7.83	14.88	18,920	12,930	8,620	6,630	5,970	80,030
116.4	7.89	14.75	19,620	14,300	10,390	7,960	7,520	90,160
116.7	7.88	14.81	22,040	15,010	9,290	7,080	6,410	90,220
117.2	7.89	14.85	21,880	13,890	9,510	7,300	6,520	89,120
116.1	7.80	14.88	20,670	13,170	8,850	6,630	6,190	83,710
115.9	7.74	14.97	20,530	13,030	8,960	6,630	5,860	82,960
116.8	7.84	14.90	21,150	14,400	9,290	7,300	6,740	88,790
116.3	7.86	14.80	22,430	14,370	9,400	7,080	6,630	90,340
216.5	10.45	20.72	28,030	15,260	11,940	9,730	9,290	111,970
216.0	10.52	20.52	25,150	12,610	11,500	9,290	9,100	102,020
215.6	10.55	20.44	30,190	16,800	11,500	9,290	9,200	116,090
213.5	10.50	20.33	29,470	15,570	11,720	9,290	9,290	113,610
214.0	10.51	20.36	27,880	14,610	11,050	8,630	8,400	106,420
214.3	10.60	20.22	29,440	15,640	12,270	9,730	9,510	115,500
214.3	10.59	20.24	31,200	17,190	12,390	9,730	9,510	120,790
214.9	10.59	20.29	30,780	16,700	11,940	9,290	9,510	117,960
213.5	10.44	20.45	29,340	15,700	11,140	8,960	8,960	111,740
212.8	10.40	20.46	29,820	15,990	11,610	9,180	9,190	114,290
215.3	10.52	20.47	31,640	17,430	11,940	9,290	9,290	120,020
213.5	10.54	20.26	33,420	18,200	11,940	9,510	9,400	124,360
276.5	13.36	20.70	32,340	18,800	14,380	11,500	11,500	133,490
273.8	13.17	20.79	34,140	19,240	14,600	10,840	10,990	135,430
275.8	13.32	20.71	33,530	19,770	15,040	11,500	11,500	137,740
274.0	13.26	20.66	33,060	19,160	14,600	11,050	11,050	134,090
274.9	13.37	20.56	35,390	21,300	15,590	12,160	12,160	145,670
274.8	13.35	20.58	35,190	20,820	13,270	11,940	12,160	140,820
274.9	13.34	20.61	36,790	21,900	16,580	13,160	12,940	152,870
273.3	13.17	20.75	34,100	20,360	15,700	12,610	11,940	142,820
272.5	13.22	20.61	35,080	20,780	15,150	12,270	11,940	143,590
275.6	13.32	20.69	36,260	21,540	15,260	12,390	12,160	147,200
273.2	13.25	20.62	36,510	21,540	15,700	12,390	12,490	148,730

TABLE 8

CONFIGURATION 2 HEAT RECOVERY DATA

Flow Rate (lbm/hr) Air	Flow Rate (lbm/hr) C_3H_8	Air/ Fuel Ratio	Heat Flux Recovered (Btu/hr-ft^2) Sec. 1	Sec. 2	Sec. 3	Sec. 4	Sec. 5	Total Heat Recovered (Btu/hr)
115.5	7.92	14.58	24,340	14,280	11,130	7,950	7,850	98,850
115.5	7.88	14.66	24,880	16,870	11,540	8,180	7,740	104,370
115.0	7.85	14.65	24,340	15,290	11,130	8,180	7,410	100,050
115.7	7.88	14.68	24,340	15,080	10,900	8,400	7,860	100,400
115.5	7.84	14.73	23,110	14,490	10,780	7,410	7,850	95,970
115.3	7.86	14.67	23,650	15,010	10,940	7,850	7,410	97,810
113.9	7.90	14.42	23,290	15,970	10,410	7,960	6,970	97,420
113.7	7.87	14.45	23,290	14,750	11,380	7,850	7,300	97,390
115.5	7.89	14.64	23,630	14,920	10,760	8,070	7,520	97,870
115.5	7.87	14.68	23,790	14,920	10,810	7,960	7,190	97,520
115.5	7.85	14.71	24,520	16,630	11,250	8,400	7,740	103,360
115.0	7.81	14.72	24,140	16,430	11,370	8,180	7,740	102,330
207.6	10.65	19.49	32,220	19,850	13,810	10,440	9,980	130,140
205.8	10.57	19.47	34,370	18,900	13,800	10,610	10,640	133,190
205.8	10.50	19.60	30,960	16,820	12,710	9,960	10,060	121,390
207.4	10.58	19.60	32,220	18,400	13,290	10,440	10,390	127,850
205.8	10.51	19.58	31,410	20,360	13,170	10,390	10,170	128,930
205.8	10.52	19.56	31,060	17,190	13,310	9,980	9,950	122,900
205.8	10.62	19.38	30,710	20,080	12,590	9,770	9,770	125,060
205.8	10.59	19.43	31,730	19,560	13,080	10,280	9,980	127,640
207.6	10.59	19.60	31,140	17,120	12,840	9,730	9,730	121,[illegible]
206.6	10.57	19.55	31,940	17,540	13,090	9,990	10,390	125,080
206.0	10.54	19.54	32,310	19,810	12,840	10,220	10,500	129,200
205.8	10.49	19.62	31,580	18,280	13,220	10,170	9,770	125,190
264.2	13.41	19.70	35,620	20,940	15,850	12,380	13,160	147,710
261.3	13.33	19.60	38,300	24,690	16,020	12,940	13,050	158,340
260.2	13.24	19.65	35,620	23,350	16,020	12,490	13,160	151,760
264.2	13.32	19.83	36,870	21,550	16,170	13,160	13,270	152,340
261.5	13.22	19.78	36,350	23,960	16,460	13,270	13,430	156,030
262.6	13.20	19.89	37,060	21,060	15,980	12,600	12,600	149,740
261.3	13.39	19.51	35,880	23,240	15,400	12,380	12,600	150,230
261.3	13.34	19.59	37,240	24,320	15,730	12,720	12,720	154,980
264.2	13.35	19.79	36,050	21,270	15,400	12,600	12,500	147,360
264.3	13.34	19.81	36,300	23,720	15,810	12,160	12,380	151,390
261.3	13.27	19.69	38,480	24,960	16,110	12,720	12,600	158,130
261.1	13.24	19.72	35,760	23,350	15,440	11,830	12,160	148,600

TABLE 9

CONFIGURATION 3 HEAT RECOVERY DATA

Flow Rate (lbm/hr) Air	Flow Rate (lbm/hr) C_3H_8	Air/ Fuel Ratio	Heat Flux Recovered (Btu/hr-ft^2) Sec. 1	Sec. 2	Sec. 3	Sec. 4	Sec. 5	Total Heat Recovered (Btu/hr)
114.2	7.81	14.62	23,830	15,090	10,170	7,410	7,080	95,880
114.0	7.82	14.58	23,450	14,640	10,590	7,630	6,970	95,430
113.8	7.71	14.76	24,000	15,330	10.540	7,520	6,970	97,050
114.5	7.74	14.79	22,590	15,330	10,540	7,410	6,860	94,600
116.8	7.88	14.82	24,350	16,700	11,420	8,400	7,740	103,460
116.8	7.85	14.88	23,430	15,650	11,370	8,620	7,960	101,080
116.8	7.89	14.80	24,520	16,090	11,420	8,180	7,740	102,470
114.6	7.85	14.60	23,450	15,890	11,300	8,400	7,520	100,370
115.5	7.89	14.64	23,800	16,100	11,180	8,400	7,960	101,700
115.5	7.82	14.77	22,140	14,920	10,640	7,960	6,860	94,280
115.5	7.94	14.55	22,570	15,160	10,810	7,960	7,300	96,210
115.5	7.88	14.66	23,120	15,850	11,260	8,400	7,960	100,420
113.7	7.82	14.54	21,350	14,300	10,340	7,630	6,970	91,370
205.3	10.51	19.53	31,540	18,440	12,830	9,840	9,840	124,390
209.6	10.50	19.96	30,790	17,670	12,340	9,180	9,400	119,700
204.9	10.34	19.82	31,760	18,440	12,210	9,730	9,510	123,130
205.8	10.35	19.88	31,760	17,240	12,330	9,400	9,400	120,840
208.5	10.58	19.71	32,700	17,770	12,950	10,440	10,280	126,880
205.4	10.54	19.49	31,000	15,650	12,350	9,620	9,330	117,550
209.0	10.58	19.75	32,220	16,900	12,950	10,440	10,280	124,850
204.4	10.50	19.47	31,140	15,940	12,590	9,780	10,060	121,410
208.5	10.56	19.74	31,860	17,430	13,070	10,500	10,500	125,710
206.2	10.50	19.64	31,130	17,120	12,840	10,220	10,060	122,710
207.6	10.68	19.44	31,710	17,850	12,960	10,280	10,280	125,290
205.8	10.60	19.42	31,760	17,670	13,310	10,440	10,280	125,860
205.8	10.53	19.54	30,560	16,940	12,830	10,060	9,780	120,900
260.2	13.23	19.67	35,920	21,460	15,610	11,940	12,160	146,410
259.7	13.22	19.64	34,940	20,820	15,370	11,940	12,160	143,610
258.8	13.01	19.89	37,760	23,720	15,980	11,940	12,160	153,150
265.1	13.38	19.81	37,670	22,010	16,140	12,830	12,830	153,030
260.1	13.28	19.59	35,910	20,780	15,410	12,160	12,380	145,730
262.0	13.36	19.60	37,050	22,030	16,220	13,050	13,270	153,240
260.2	13.17	19.76	35,800	21,060	15,490	12,610	12,610	147,140
262.4	13.22	19.85	36,870	21,780	16,220	13,050	13,270	152,590
264.2	13.46	19.63	36,470	21,810	15,890	12,830	13,050	150,880
261.3	13.34	19.59	36,050	21,080	15,770	11,500	11,500	144,620
259.8	13.28	19.56	35,370	20,450	15,490	12,500	12,500	145,230

TABLE 10

MEAN, STANDARD DEVIATION, AND STANDARD DEVIATION OF THE MEAN OF THE HEAT RECOVERY DATA

Configuration	Condition		Flow Rate (lbm/hr)		Air/ Fuel Ratio	Heat Flux Recovered (Btu/hr-ft^2)					Total Heat Recovered (Btu/hr)
			Air	C_3H_8		Sec. 1	Sec. 2	Sec. 3	Sec. 4	Sec. 5	
1	3	$\bar{x}$ =	116.79	7.830	14.916	19,981	13,023	9,305	6,958	6,376	83,908
		σ =	1.06	0.056	0.135	1,843	1,464	520	476	480	5,980
		σ_m =	0.29	0.016	0.037	511	406	144	132	133	1,659
	8	$\bar{x}$ =	214.52	10.518	20.397	29,703	15,975	11,745	9,327	9,221	114,564
		σ =	1.15	0.063	0.143	2,101	1,471	408	326	310	6,169
		σ_m =	0.33	0.018	0.041	637	425	118	94	89	1,781
	12	$\bar{x}$ =	274.48	13.285	20.662	34,763	20,474	15,079	11,983	11,894	142,041
		σ =	1.23	0.074	0.073	1,455	1,085	869	698	592	6,363
		σ_m =	0.37	0.022	0.022	439	327	262	210	178	1,919
2	3	$\bar{x}$ =	115.13	7.858	14.633	23,943	15,385	11,033	8,033	7,548	99,442
		σ =	0.66	0.029	0.101	552	863	325	271	293	2,675
		σ_m =	0.19	0.008	0.029	162	251	94	78	85	772
	8	$\bar{x}$ =	206.32	10.561	19.535	31,804	18,662	13,145	10,165	10,114	126,505
		σ =	0.77	0.050	0.076	969	1,276	382	281	309	3,623
		σ_m =	0.22	0.014	0.022	280	368	110	81	89	1,046
	12	$\bar{x}$ =	262.29	13.304	19.713	36,621	23,033	15,883	12,596	12,802	152,209
		σ =	1.52	0.068	0.112	992	1,453	309	406	397	3,841
		σ_m =	0.44	0.020	0.032	286	420	89	117	114	1,109
3	1	$\bar{x}$ =	115.17	7.838	14.693	23,277	15,465	10,891	7,994	7,376	98,025
		σ =	1.14	0.063	0.114	908	664	448	434	450	3,753
		σ_m =	0.32	0.017	0.032	252	184	124	120	125	1,041
	8	$\bar{x}$ =	206.68	10.521	19.645	31,533	17,389	12,735	9,995	9,923	123,017
		σ =	1.73	0.093	0.178	593	735	339	436	406	2,791
		σ_m =	0.48	0.026	0.049	164	204	94	121	113	774
	12	$\bar{x}$ =	261.26	13.268	19.690	36,346	21,545	15,781	12,395	12,535	148,694
		σ =	1.99	0.121	0.117	907	899	327	526	544	3,875
		σ_m =	0.60	0.036	0.035	273	271	99	159	164	1,168

TABLE 11

CONFIGURATION 1

VORTEX GAS TEMPERATURE PROFILES

Condition	Distance from Wall (inches)	Radius Ratio r/r_{wall}	Vortex Gas Temperatures (°F)				
			Sta. 1	Sta. 2	Sta. 3	Sta. 4	Sta. 5
3	0	1.000	139	165	139	104	99
	0.25	0.913	803	854	532	386	323
	0.50	0.826	1424	1222	1014	743	576
	0.75	0.740	1587	1346	1103	913	692
	1.00	0.653	1681	1433	1196	977	829
	1.25	0.566	1699	1468	1226	1019	867
	1.50	0.479	1712	1481	1245	1052	896
	1.75	0.392	1699	1468	1226	1044	901
	2.00	0.306	1684	1428	1205	1023	884
	2.25	0.219	1609	1394	1218	1048	909
	2.50	0.132	1578	1394	1226	1078	943
	2.75	0.045	1538	1364	1188	1057	947
	2.88	0.000	1573	1359	1175	1040	922
8	0	1.000	173	186	169	156	156
	0.25	0.913	998	1048	875	501	422
	0.50	0.826	1569	1368	1192	930	778
	0.75	0.740	1706	1490	1286	1090	964
	1.00	0.653	1772	1560	1351	1158	1036
	1.25	0.566	1794	1600	1368	1184	1057
	1.50	0.479	1799	1591	1359	1188	1057
	1.75	0.392	1794	1578	1365	1184	1052
	2.00	0.306	1767	1547	1346	1158	1027
	2.25	0.219	1726	1529	1359	1184	1052
	2.50	0.132	1708	1547	1415	1256	1133
	2.75	0.045	1663	1538	1415	1295	1201
	2.88	0.000	1645	1490	1376	1269	1166
12	0	1.000	186	265	296	139	130
	0.25	0.913	1107	1158	998	731	701
	0.50	0.826	1667	1699	1312	1124	989
	0.75	0.740	1790	1587	1415	1226	1107
	1.00	0.653	1850	1609	1463	1273	1162
	1.25	0.566	1873	1699	1481	1299	1175
	1.50	0.479	1873	1690	1472	1260	1171
	1.75	0.392	1850	1654	1450	1286	1149
	2.00	0.306	1841	1645	1459	1290	1154
	2.25	0.219	1808	1632	1481	1316	1192
	2.50	0.132	1776	1654	1534	1381	1260
	2.75	0.045	1740	1645	1534	1420	1338
	2.88	0.000	1731	1600	1499	1407	1312

TABLE 12

CONFIGURATION 2

VORTEX GAS TEMPERATURE PROFILES

Condition	Distance from Wall (inches)	Radius Ratio r/r_{wall}	Vortex Gas Temperatures (°F)				
			Sta. 1	Sta. 2	Sta. 3	Sta. 4	Sta. 5
3	0	1.000	160	136	121	104	104
	0.25	0.913	1006	888	684	462	426
	0.50	0.826	1485	1196	968	752	641
	0.75	0.740	1645	1329	1078	901	778
	1.00	0.653	1694	1424	1188	981	854
	1.25	0.566	1717	1468	1226	1023	888
	1.50	0.479	1712	1499	1235	1052	922
	1.75	0.392	1721	1494	1239	1069	934
	2.00	0.306	1699	1468	1243	1078	943
	2.25	0.219	1672	1450	1239	1090	951
	2.50	0.132	1627	1424	1231	1082	955
	2.75	0.045	1569	1398	1196	1065	951
	2.88	0.000	1543	1368	1171	1044	939
8	0	1.000	191	238	130	117	117
	0.25	0.913	1162	1002	824	680	580
	0.50	0.826	1582	1303	1107	913	837
	0.75	0.740	1717	1428	1231	1065	968
	1.00	0.653	1753	1512	1316	1133	1031
	1.25	0.566	1772	1560	1342	1166	1057
	1.50	0.479	1772	1573	1338	1175	1052
	1.75	0.392	1767	1569	1338	1179	1057
	2.00	0.306	1744	1538	1338	1184	1061
	2.25	0.219	1721	1520	1355	1209	1078
	2.50	0.132	1690	1503	1351	1213	1099
	2.75	0.045	1632	1481	1321	1201	1103
	2.88	0.000	1600	1446	1290	1179	1094
12	0	1.000	208	300	191	147	143
	0.25	0.913	1265	1112	930	786	688
	0.50	0.826	1663	1411	1222	1040	960
	0.75	0.740	1785	1534	1351	1171	1078
	1.00	0.653	1818	1614	1415	1235	1137
	1.25	0.566	1836	1659	1433	1265	1158
	1.50	0.479	1841	1672	1441	1290	1171
	1.75	0.392	1832	1650	1437	1286	1162
	2.00	0.306	1818	1627	1454	1299	1179
	2.25	0.219	1794	1600	1468	1321	1196
	2.50	0.132	1767	1591	1463	1329	1222
	2.75	0.045	1721	1565	1437	1312	1222
	2.88	0.000	1690	1525	1411	1290	1213

TABLE 13

CONFIGURATION 3

VORTEX GAS TEMPERATURE PROFILES

Condition	Distance from Wall (inches)	Radius Ratio r/r_{wall}	Vortex Gas Temperatures (°F)				
			Sta. 1	Sta. 2	Sta. 3	Sta. 4	Sta. 5
3	0	1.000	156	147	121	104	104
	0.25	0.913	960	840	680	500	420
	0.50	0.826	1446	1154	972	795	684
	0.75	0.740	1663	1342	1082	913	803
	1.00	0.653	1717	1441	1158	989	862
	1.25	0.566	1726	1485	1201	1031	905
	1.50	0.479	1721	1494	1222	1061	930
	1.75	0.392	1712	1472	1218	1061	930
	2.00	0.306	1699	1450	1222	1061	926
	2.25	0.219	1636	1389	1175	1031	888
	2.50	0.132	1573	1372	1175	1027	888
	2.75	0.045	1529	1364	1166	1031	892
	2.88	0.000	1547	1381	1184	1036	905
8	0	1.000	191	156	130	117	121
	0.25	0.913	1100	1000	825	680	550
	0.50	0.826	1520	1282	1112	913	807
	0.75	0.740	1703	1415	1231	1040	917
	1.00	0.653	1776	1525	1299	1116	993
	1.25	0.566	1762	1547	1303	1133	1019
	1.50	0.479	1749	1556	1303	1158	1036
	1.75	0.392	1740	1529	1299	1149	1031
	2.00	0.306	1726	1520	1312	1154	1027
	2.25	0.219	1681	1481	1286	1158	1014
	2.50	0.132	1627	1476	1290	1158	1014
	2.75	0.045	1569	1441	1256	1137	1010
	2.88	0.000	1582	1468	1278	1158	1031
12	0	1.000	203	296	191	139	139
	0.25	0.913	1200	1110	930	780	650
	0.50	0.826	1600	1402	1209	1023	930
	0.75	0.740	1772	1538	1329	1145	1040
	1.00	0.653	1836	1618	1394	1222	1107
	1.25	0.566	1836	1645	1411	1252	1137
	1.50	0.479	1818	1636	1407	1269	1149
	1.75	0.392	1799	1605	1389	1252	1133
	2.00	0.306	1790	1582	1411	1256	1133
	2.25	0.219	1755	1570	1410	1260	1125
	2.50	0.132	1694	1551	1394	1260	1124
	2.75	0.045	1654	1538	1381	1265	1141
	2.88	0.000	1659	1556	1394	1282	1162

of predicting the velocity field in confined vortex; even the limited data available is often contradictory which suggests that the flow is disturbed significantly by the measuring probe or is extremely sensitive to the geometry of the vortex apparatus or both. The results of Wolf [172] and Rochino [173], already reported in Chapter I, indicate that the axial profile does not tend to develop with respect to length as is characteristic of simple linear flows. Thus the profile can be expected to remain relatively flat for all axial stations (except very near the wall). Thus, there appears to be a reasonable basis to assume that the axial velocity is simply a constant with respect to both radius and length providing, of course, flow reversal does not occur. This assumption--which is frequently made (see [388] for instance) is often termed the "slug-flow" model-- permits removing the velocity from inside the integral in Equation (1) where it cancels the mean velocity factor in the denominator. The temperature obtained by means of this assumption is referred to here as the "average" temperature at each furnace column station since it represents the result of a simple temperature-area average. The details of the calculation procedure are presented in Appendix C with the results given in Table 14; the data termed "Average Furnace Column Temperature" are obtained simply by finding the mean of the five average temperatures (one for each Station) available for each Configuration/Condition combination.

Effect of Inlet Configuration and Condition

The heat recovery and temperature data obtained for the three inlet Configurations investigated utilized exit Configuration 3 exclusively (as the exit configuration data was for inlet Configuration C exclusively). The expected result of the use of the insert sleeves (i.e. inlet Configurations A and B) was that of higher heat transfer rates and higher

TABLE 14

AVERAGE VORTEX GAS TEMPERATURES

Configuration	Condition	Vortex Gas Temperature (°F)					Average Furnace Column Temperature (°F)
		Sta. 1	Sta. 2	Sta. 3	Sta. 4	Sta. 5	
1	3	1363	1201	976	792	658	928
	8	1480	1333	1152	940	828	1147
	12	1560	1459	1269	1074	977	1263
2	3	1424	1205	991	811	710	1028
	8	1500	1299	1108	954	859	1144
	12	1572	1397	1211	1058	964	1240
3	3	1413	1192	978	822	716	1024
	8	1474	1280	1092	937	826	1122
	12	1543	1384	1190	1037	931	1217

vortex gas temperatures due to the higher inlet air velocities and increased mixing. However, the data showed that just the opposite occurred leading one to reaffirm "expect the unexpected". The reason for this anomalous behavior is that, apparently, a change in the location of the combustion process took place. The sleeves, in addition to increasing the tangential velocity, also decreased the static pressure of the vortex chamber as a result of Bernoulli's Principle. This lowered pressure caused the combustion process to occur much lower in the vortex chamber/furnace column apparatus and was observable by the noticeably-increased radiation from the walls of the uncooled vortex chamber. This effect was so pronounced that it caused the wood supports of the steel table on which the incinerator rests to ignite. Thus, although the combustion intensity and heat transfer were probably enhanced because of the sleeves, the effect of the lowered pressure caused the heat transfer to take place at a point where no heat recovery capacity had been provided; thus the losses from the system were greatly increased and the observed heat recovery and gas temperatures diminished.

As a result, the data are not particularly useful in correlating the effect of the sleeves upon heat transfer, and only one set of data was obtained for the nine combinations of inlet Configuration and Condition; these data are presented in Table 15. Also, because only one set of data was obtained, no temperature profiles were measured. The gas temperature was, however, measured at one radial position for each station and this is given as Table 16. These data confirm the early explanation for diminished heat transfer in that they show a much cooler gas flowing through the furnace column for increasing inlet tangential velocity.

TABLE 16

INLET CONFIGURATION EFFECT UPON HEAT RECOVERY

Inlet Configuration	Condition	Flow Rate (lbm/hr) Air	Flow Rate (lbm/hr) C_3H_8	Air/Fuel Ratio	Heat Flux Data - Btu/Hr-ft^2 Sec. 1	Sec. 2	Sec. 3	Sec. 4	Sec. 5	Total Heat Recovery Btu/hr
C	3	115.2	7.96	14.47	19,380	13,980	10,080	7,450	6,640	86,080
	8	208.4	10.69	19.49	28,570	15,920	11,700	9,290	9,390	112,900
	12	268.0	13.45	19.93	33,080	19,480	12,460	11,190	11,170	131,770
B	3	116.0	7.93	14.63	16,740	13,780	9,120	6,750	5,710	78,570
	8	208.0	10.66	19.51	30,690	16,110	11,530	9,500	9,030	115,900
	12	266.4	13.46	19.79	35,640	20,560	14,780	11,300	11,280	140,940
A	3	115.5	7.86	14.69	16,230	12,800	8,270	5,720	4,650	71,090
	8	208.6	10.54	19.79	26,940	15,360	10,410	8,350	7,380	103,210
	12	268.3	13.27	20.22	33,370	19,860	11,920	9,740	9,420	127,140

TABLE 16

VORTEX GAS TEMPERATURES* FOR 3 INLET CONFIGURATIONS

Configuration	Condition	Temperature (°F)					
		Sta. 1	Sta. 2	Sta. 3	Sta. 4	Sta. 5	
A	3	1331	1101	854	658	559	
	8	1567	1355	1107	896	739	
	12	1654	1512	1276	1097	934	
B	3	1415	1201	945	742	639	
	8	1658	1490	1241	1029	905	
	12	1763	1658	1433	1224	1097	
C	3	1678	1518	1260	1070	926	
	8	1715	1594	1377	1152	1044	
	12	1751	1667	1461	1252	1129	

* All these data were measured at 1.25 inches from the furnace column wall.

A comparison of the data presented in Tables 10 and 15 for the same inlet/exit Configuration (C-3) reveals a small discrepancy. Since these data were obtained for identical Configurations and Conditions it would be expected that recovery rates should be nearly equal (at least within a standard deviation as given in Table 10); however, the data taken during the inlet Configuration investigation is approximately 10% lower than that observed for the exit Configuration investigation. Although this difference is not great, it appears to be consistent and not easily explainable. Two possible explanations are suggested: (1) due to the elapsed time between data taking periods (about one year) it is possible that there has been a slight aging effect (corrosion in the water tubes, carbon build-up on the inside walls of the furnace column, etc.), and/or, (2) the fuel provided in the one-hundred pound supply-tanks, although claimed to be propane (C_3H_8), may in fact be "watered-down" by the dealer (who carries other fuels such as LNG) with lower heating-value hydrocarbons as a result of the scarcity and high cost of C_3H_8.

Discussion of Heat Recovery Data

The objective of any investigation of the effect of independent variables upon a dependent variable is to develop a correlation relation. The usual means of expressing the mass flow rate independent variable is through the use of a Reynolds number. The difficulty here is that there are many possible definitions of Reynolds number. The usual form of internal-flow Reynolds number is given by

$$Re_D = \frac{\rho \bar{U} D}{\mu} = \frac{4 m}{\pi D \mu} \qquad (2)$$

where $\overline{U}$ is the average axial velocity, D the tube diameter, and m the axial flow rate all in consistent units.

The second form given in Equation (2) will be used here since the total mass flow rate of air plus propane is known and will be referred to as the "axial Reynolds number". The absolute viscosity is somewhat difficult to determine since it is both a function of temperature and gas composition and there is no simple expression available that can account for these two effects. Maxwell [401], however, has obtained data for the absolute viscosity of "flue gas" as a function of flue-gas temperature. He has found that it is relatively insensitive to the percentage of excess air and is thus approximately only a function of the temperature. The calculation of the axial Reynolds number, using [401] to find the viscosity for the average furnace column temperature, is given in Appendix D.

The total heat recovery rate and the total heat recovered per pound of propane as a function of the axial Reynolds number evaluated at the average furnace column temperature is presented in Figures 18 and 19 for the data given in Tables 7-9 (i.e. exit Configuration/Condition effect). It should be noted that the heat recovery data cannot be expressed directly in terms of Nusselt or Stanton numbers because it includes the effects of radiation and conduction. To determine the convective portion of the heat recovered requires further analysis and will be performed in Chapter IV. On these figures, the left-most group of 3 data parts are for Condition 3, the middle group for Condition 8, and the right group for Condition 12. What should be noted from Figure 19 is that the heat recovery rate is relatively insensitive to the average axial Reynolds number when expressed on a per pound of propane basis. For Configurations 2 and 3 there is an approximate linear degradation in heat recovery with increasing Reynolds

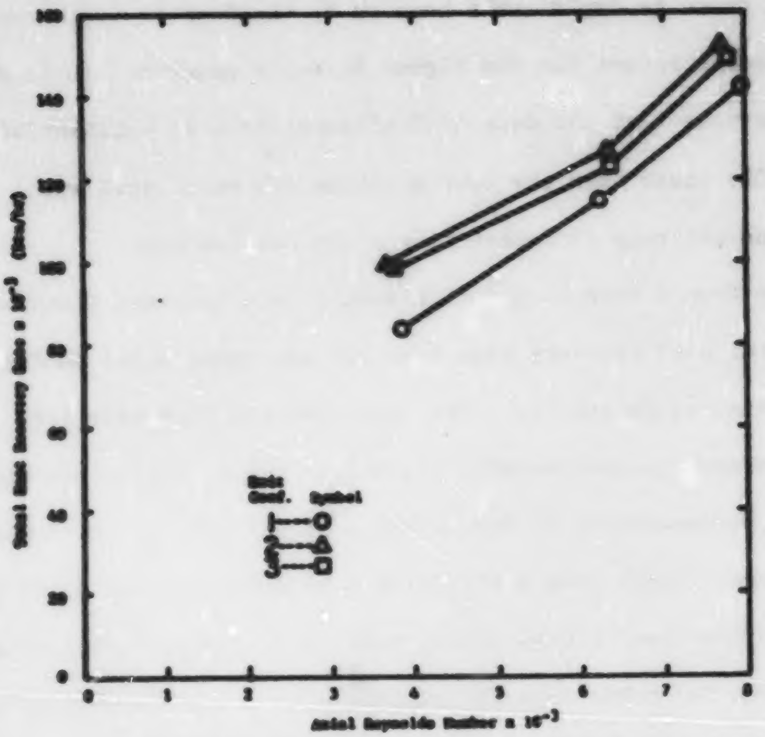

Figure 18. Total Heat Recovery Rate vs. Axial Reynolds Number

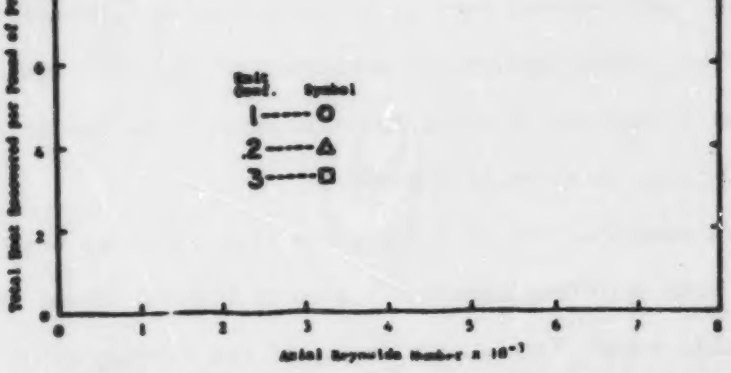

Figure 19. Total Heat Recovered per Pound of Propane vs. Axial Reynolds Number

number although the change is only about 10% for a doubling in Reynolds number. This trend is explainable because of the shorter residence times within the furnace column for the higher Reynolds numbers. It is also significant to note that the data of Configuration 1 is substantially (i.e. about 20%) lower than the Configuration 2/3 data; this would suggest that an entirely different flow field has resulted for the change from a four-inch exit diameter to a two-inch diameter.

The total heat recovery rate data for the three inlet Configurations are given in Figures 20 and 21. The measured recovery rate for the smallest sleeve is considerably below that for no sleeve but the large sleeve (Configuration B) does yield a higher rate at the largest Reynolds numbers. These data are difficult to interpret--as noted earlier--because of the increased energy losses from the uncooled vortex chamber.

There are two other Reynolds numbers that can be meaningfully defined: the "exit Reynolds number" where D in Equation (2) represents the diameter of the exit orifice and the viscosity is evaluated at the average temperature at the exit section and the "inlet Reynolds number" where D is the inlet air-line diameter and the viscosity is found from air-property tables using the measured inlet air temperature. These calculations are also performed in Appendix D.

The total heat recovery rate as a function of exit Reynolds number, for the exit-effect investigation, is presented in Figure 22 while the recovery rate as a function of inlet Reynolds number, for the inlet-effect investigation, is given in Figure 23.

Figure 22 suggests a cause for the observed decreased heat recovery rates obtained with exit Configuration 1 seen in Figures 18 and 19: namely, that exit Reynolds number is higher than any of the Configuration 2/3

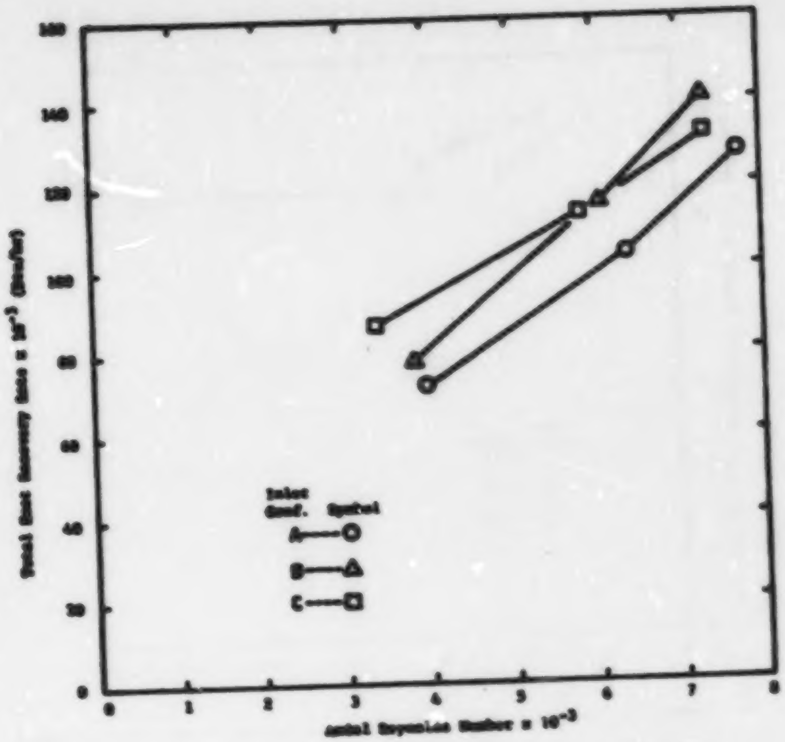

Figure 20. Total Heat Recovery Rate vs. Axial Reynolds Number

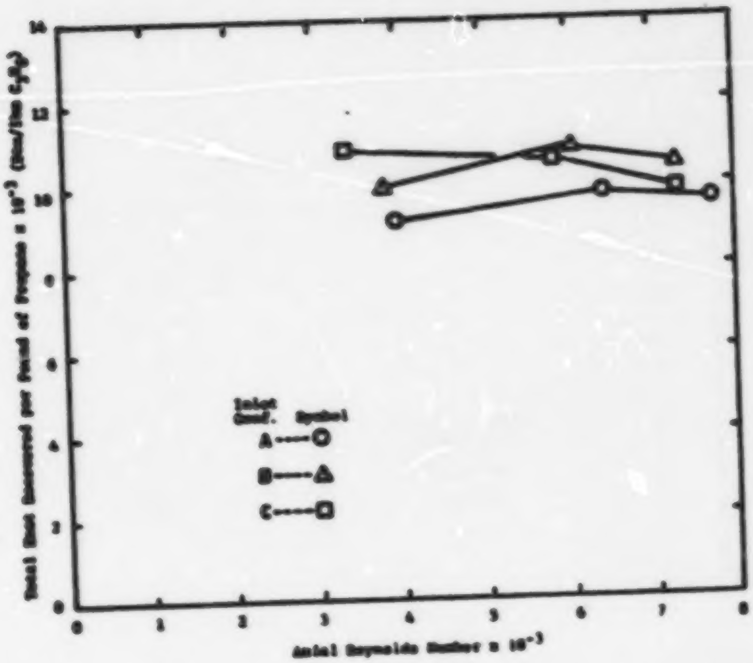

Figure 21. Total Heat Recovered per Pound of Propane vs. Axial Reynolds Number

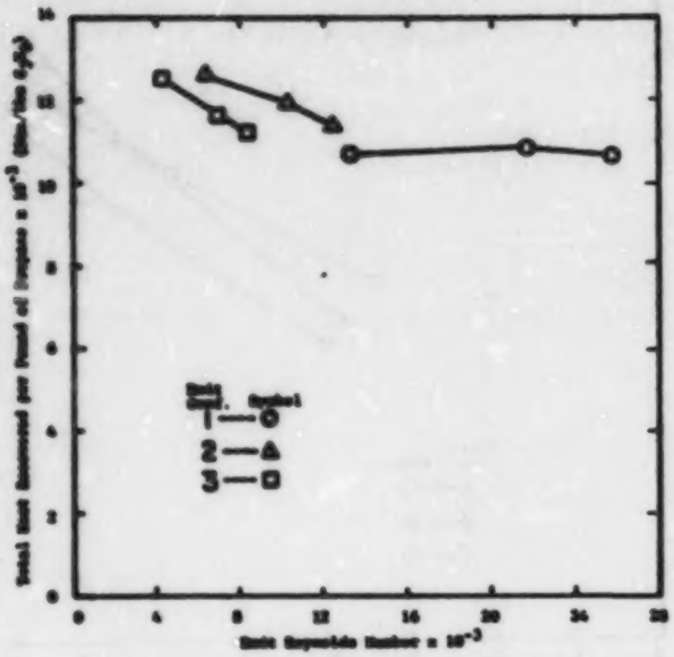

Figure 20. Total Heat Recovered per Pound of Propane vs. Exit Reynolds Number

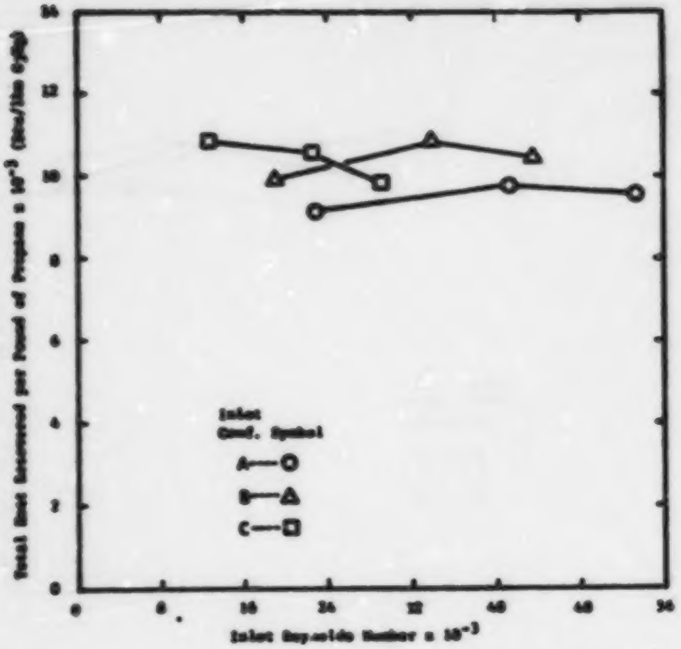

Figure 21. Total Heat Recovered per Pound of Propane vs. Inlet Reynolds Number

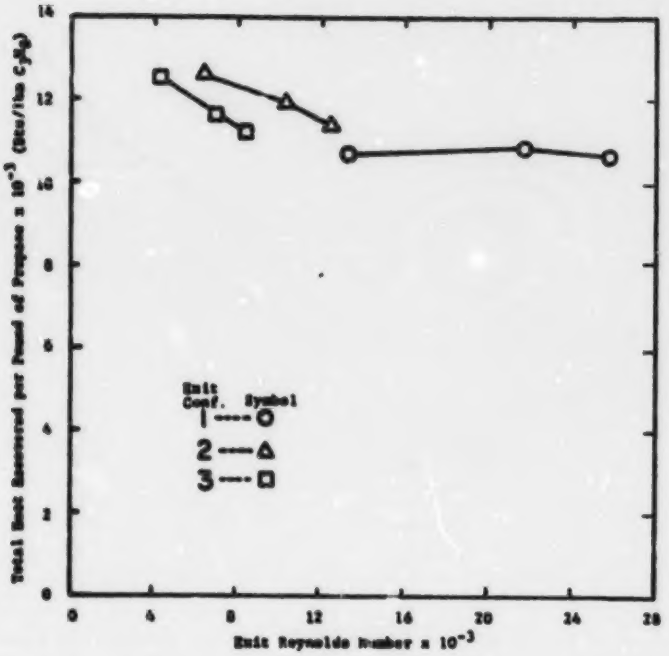

Figure 22. Total Heat Recovered per Pound of Propane vs. Exit Reynolds Number

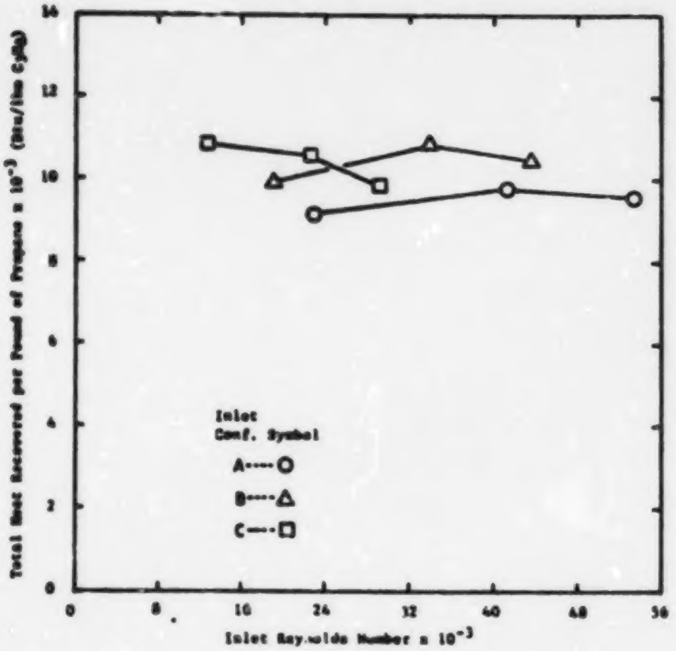

Figure 23. Total Heat Recovered per Pound of Propane vs. Inlet Reynolds Number

data. Note also, for Configuration 2/Condition 12 and Configuration 1/ Condition 3 the exit Reynolds numbers are nearly equal and despite the differences in geometry, flow rate, and air/fuel ratio, the heat recovered per pound of propane is nearly equal as well. By comparing Figures 19 and 22 the following can be concluded:

(1) If the heat recovery rate per pound of propane were independent of the exit geometry, then the data for the three Configurations investigated should fall nearly on a common line. This is true, however, only for the Configuration 2/3 data; this suggests that for the larger exit diameters—on the order of the furnace column diameter (5.76 inches)—the effect of the exit Configuration is small.

(2) Since Figure 19 has shown that there is, in fact, an exit Configuration effect for the 2-inch diameter exit, then a plot of heat recovery rate per pound of propane versus an appropriate dimensionless parameter representing the exit diameter change (and the exit Reynolds number is one such parameter) should reveal that Configurations 2/3 are operating in approximately the same flow regime with Configuration 1 in a distinctly different regime. This is precisely demonstrated by Figure 22.

The total heat recovery rate is given as a function of the inlet Reynolds number in Figure 23. Again this graph tends to explain the earlier graph for which the axial Reynolds number was used for the abscissa. Configuration A is operating at the highest inlet Reynolds number and thus the lowest recovery rates (in comparison with Configuration C). Configuration B does not, however, follow the pattern and instead shows a peak in heat recovery rate at an inlet Reynolds number of approximately 35,000. Corey [291] reported a tangential inlet Reynolds number of 15,000 as optimum in his tangential-overfire studies of solid waste incineration; although his configuration and objectives were very different, it is interesting to note a comparable value of Reynolds number.

In order to assess the entry-length/vortex-decay effects associated with heat transfer from a confined vortex it is necessary to examine the heat flux recovered as a function of furnace column height (or, equivalently, vortex-tube length). These data have already been given in tabular form in Table 10. In order to present these results graphically it is desirable to obtain yet another Reynolds number: the "length Reynolds number" defined by

$$Re_L = \frac{m L}{A \mu} = \left(\frac{4 m}{\pi D \mu} \right) \left(\frac{L}{D} \right) \qquad (3)$$

which is simply equal to the axial Reynolds number defined in Equation (2) multiplied by the length-to-diameter ratio of each heat recovery section (i.e. L equals one-foot, two-feet, etc., where D is the furnace column diameter in feet, 0.4800). These calculations are presented in Appendix D.

The heat flux data for each of the five furnace column sections is presented as a function of the length Reynolds number for the nine combinations of exit Configuration and Condition in Figure 24. It is clear that there is a very pronounced effect of length Reynolds number upon the local heat flux although there are a number of causes:

(1) the radiation flux density is the highest at the lowest sections because of the larger radiation view factor with respect to the radiating flame and the vortex chamber walls,

(2) the conduction heat transfer component is the largest at the bottom section because the furnace column is separated from the very hot vortex chamber by only a one-eighth-inch asbestos gasket,

(3) the largest gas temperature occurs at the lowest sections thus causing a greater potential for heat transfer,

(4) the flow is undeveloped both fluid-dynamically and thermally and thus there is an entry-length enhancement effect, and

(5) the vortex strength is at its maximum value at the lowest sections since it has had the least opportunity to decay for those locations.

It should also be noted that the Condition 12 data indicate higher heat fluxes at comparable Reynolds numbers than the Condition 3/8 data but it

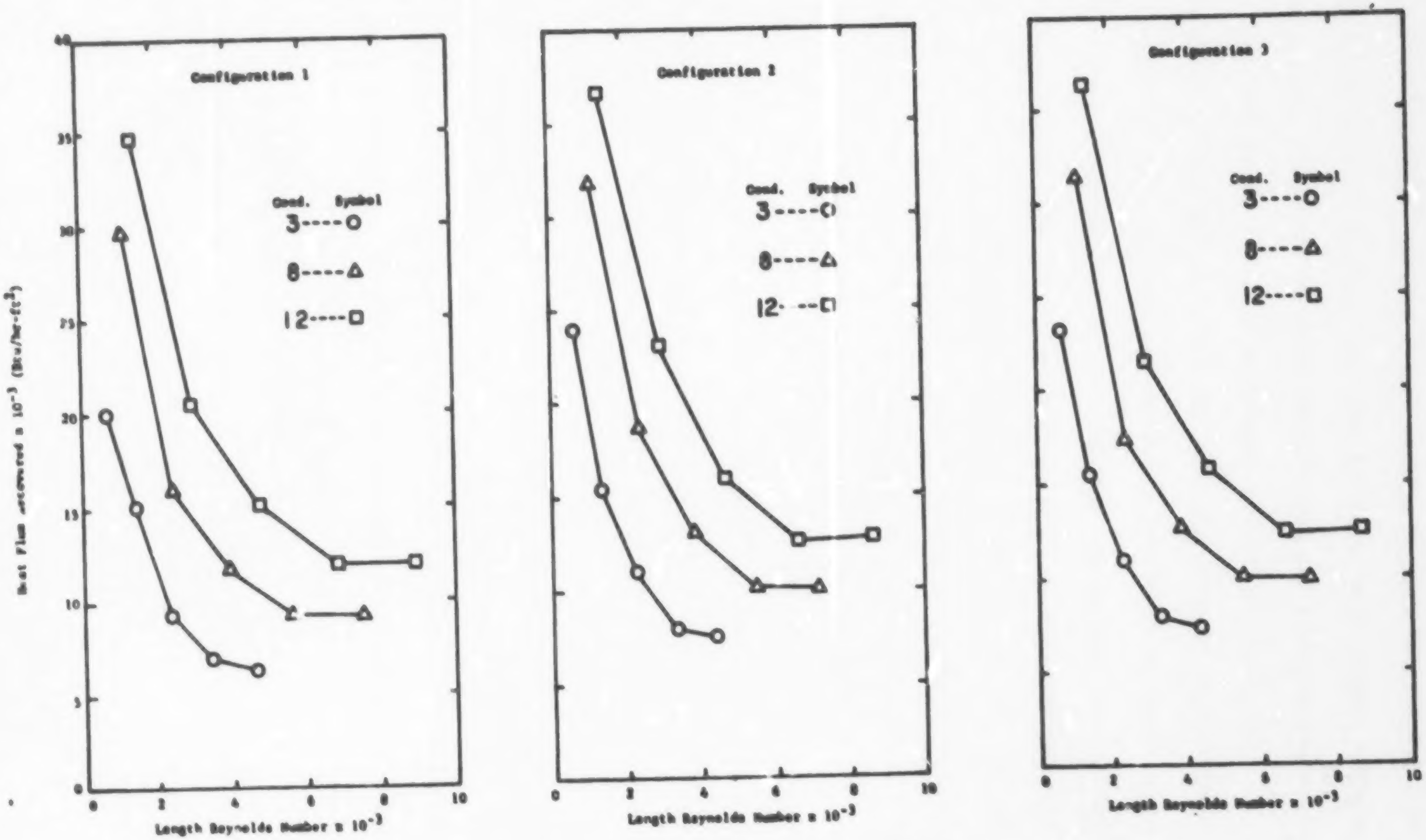

Figure 24. Heat Flux Recovered vs. Length Reynolds Number

is only because the ordinate is given on a per unit time basis rather than on a per unit of mass of propane basis, because Condition 12 has the highest propane flow rates and thus the greatest rates of enthalpy addition, it should evidence the highest heat recovery fluxes on a per unit time basis.

One final observation regarding Figure 24 should be made. The effectiveness of each additional one-foot cooling section diminishes exponentially—at least for the first four sections. It is clear, then, that greatly increasing the length of the furnace column would not result in marked improvement in total heat recovery. What is not clear is whether the leveling-off between sections 4 and 5 is due to the total decay of the vortex, the attainment of fully-developed flow, or the effect of the exit boundary conditions (or some combination of all three effects).

To examine the combustion/recovery efficiency of each cooling section, it is necessary to examine the local heat flux on a per unit mass of propane basis. This result is given in Figure 25. Since there are five flux data points available for each combination of Configuration and Condition (and there are 9 such combinations) this figure presents 45 data points. It is interesting to note that all of the Condition 8/12 data (triangles and squares) fall in a fairly narrow band regardless of the exit Configuration with the data for Configuration 1 congregated on the low side of the band and the data for Configuration 3 on the high side. For length Reynolds numbers exceeding 60,000 the heat flux remains almost exactly constant at about 900 Btu/ft^2-lbm C_3H_8.

Every data point for Condition 3 lies entirely outside the band of the Condition 8/12 data. This effect is examined in detail in Chapter IV where Nusselt and Stanton numbers are calculated and the effects of radiation, conduction, and different mixed-mean temperatures are accounted

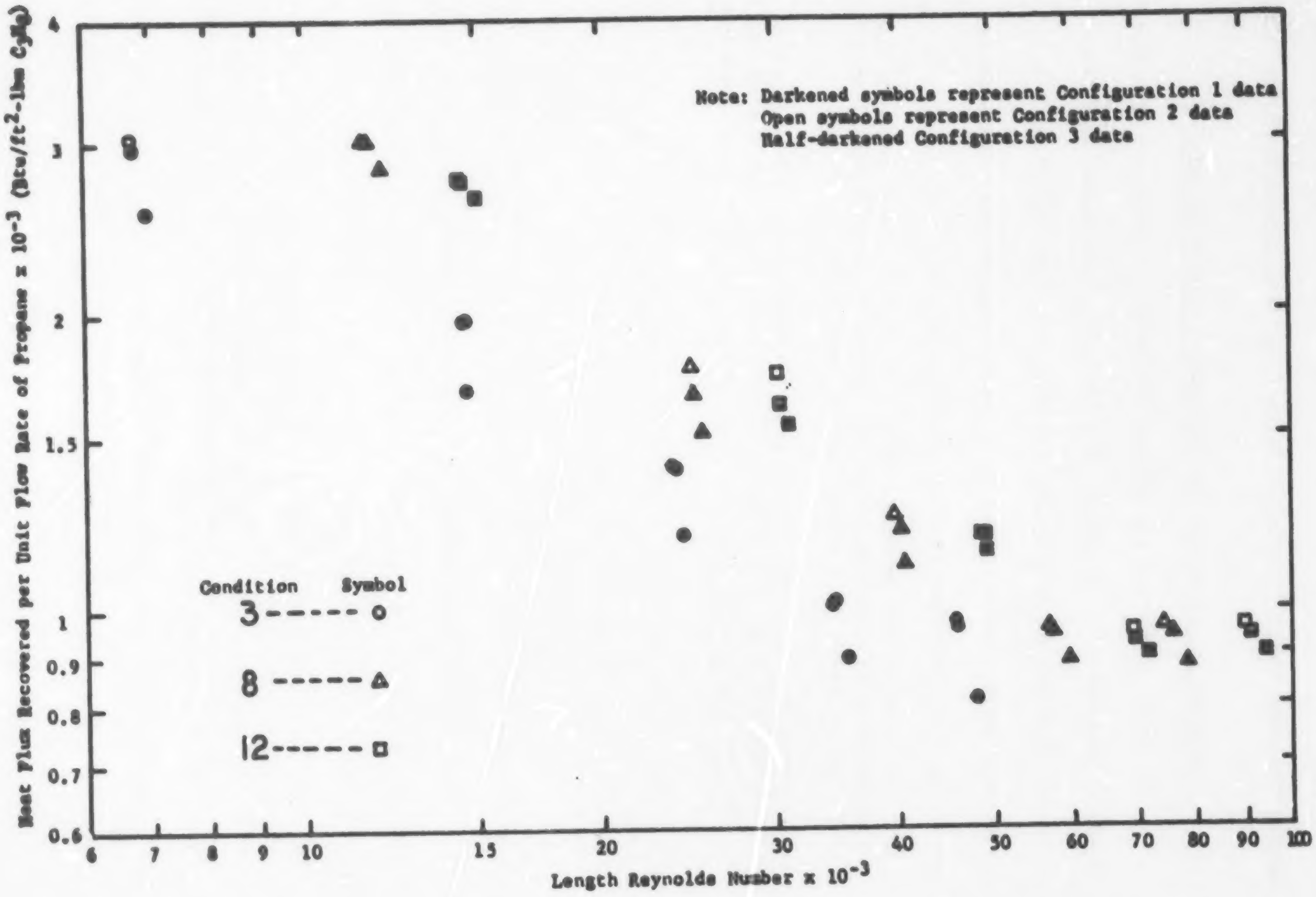

Note: Darkened symbols represent Configuration 1 data
Open symbols represent Configuration 2 data
Half-darkened Configuration 3 data

Figure 25. Heat Flux Recovered per Unit Flow Rate of Propane vs. Length Reynolds Number

for. Although the level and slope of the Condition 3 data is considerably different from that of Condition 8/12, the data suggest the existence of a similar constant heat flux region at approximately the same level (900 Btu/ft^2-lbm C_3H_8) and length Reynolds number.

Discussion of Vortex Gas Temperature-Profile Data

In order to assess the effect of changing Condition upon the radial temperature profile data, the data for Configuration 2 from Table 12 are given in Figure 26; the data for Configurations 1 and 3 illustrate similar results and are, therefore, not also graphically presented. Several observations should be noted:

(1) The temperature profiles reveal an almost linear decrease in temperature with increasing furnace column height (Station) at a given radius ratio as a result of the heat removal process.

(2) The radial profiles show a peak temperature at a radius ratio of approximately 0.5 for Stations 1 and 2 for all three Conditions, but at the higher Stations the peak appears to shift inward nearing the centerline for Station 5.

(3) The primary effect of Condition is simply to increase the temperature level of the gas with the same approximate profile shape despite the fact that there is both a change in air/fuel ratio and mass flow rate. The increase in temperature is to be expected since the energy addition rate increases with increasing condition (higher flow rates of propane) faster than the energy removal rate increases (since the cooling-water system is unchanged).

To illustrate the effect of exit Configuration at the same Condition, some of the data of Tables 11, 12, and 13 are presented in Figure 27. The following can be noted:

(1) The data for Configuration 2/3 are similar and portray analogous behavior to that described previously for Figure 26; the temperature-level at Stations 1 and 2 are nearly equal although at the higher Stations, Configuration 3 data show that the gas is appreciably cooler than for Configuration 2.

(2) The profiles obtained for Configuration 1 are noticeably different from any of the other profiles for Stations 3-5 with a sharp peak located near the centerline; the data for Stations 1 and 2 show similar

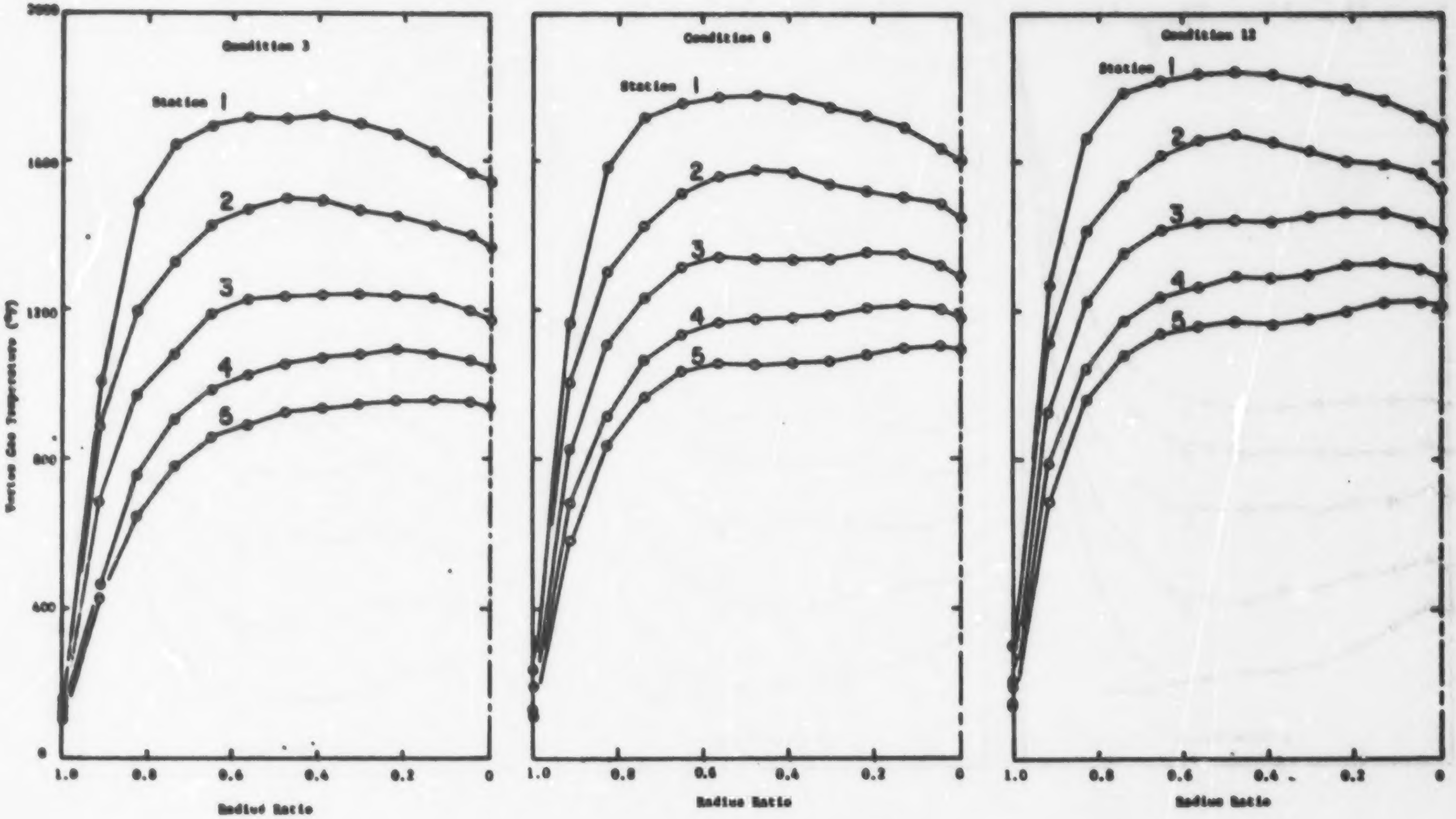

Figure 26. Vortex Gas Temperature Profiles for Configuration 2

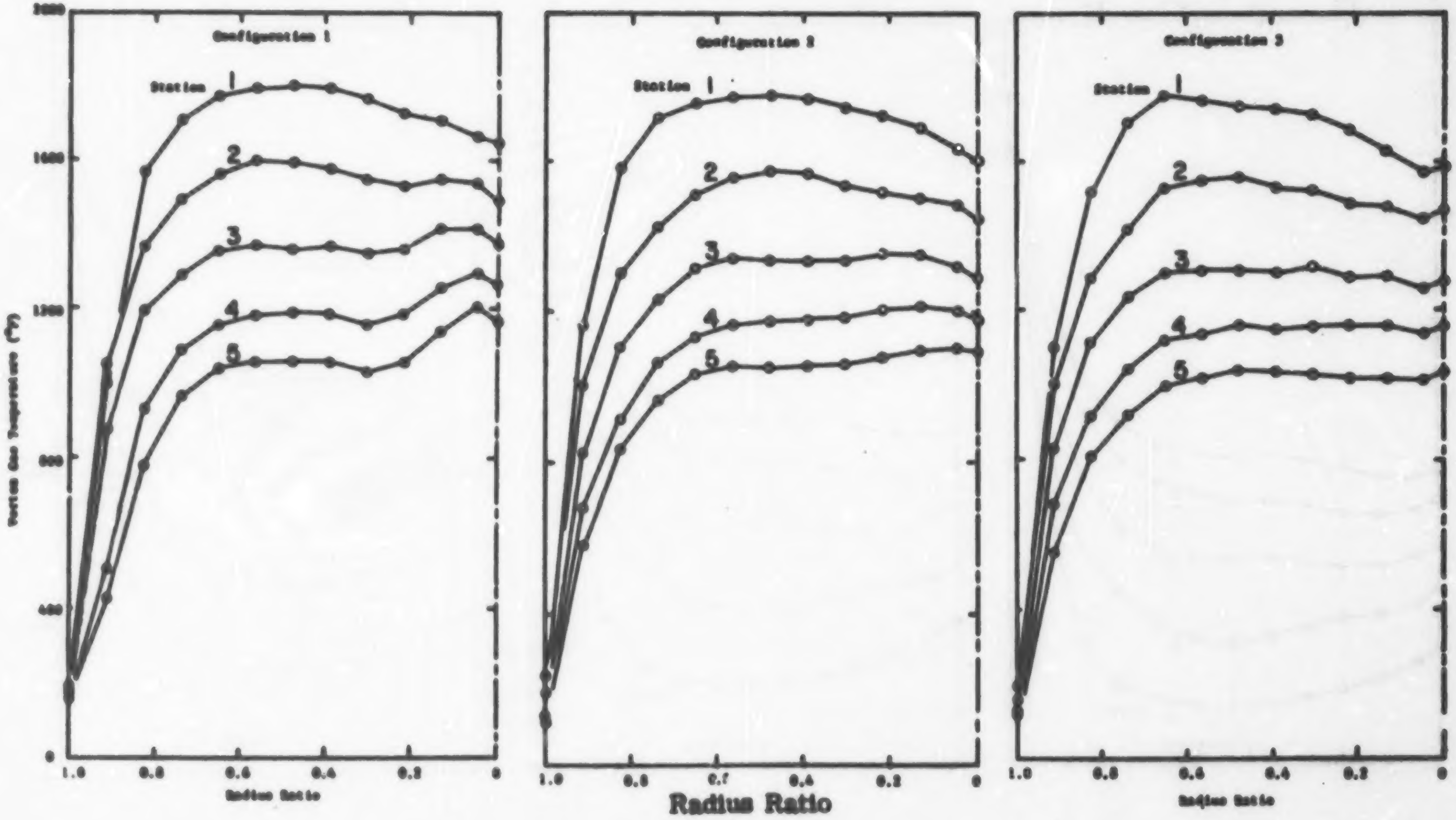

Figure 27. Vortex Gas Temperature Profiles for Configuration 8

shapes to the comparable Configuration 2/3 profiles.

(3) The temperature levels for all three Configurations are very nearly equal and suggest that the effect of changing exit diameter is not large.

The presence of an annular peak in the temperature profile suggests that combustion is occurring in an annular region as observed by others [126, 128-130]. The temperature decreases toward the centerline because of radiant energy lost from the hot gases to the cool walls and it decreases toward the walls because of convective heat transfer. Thus the absence of an annular peak for Stations 3-5 would imply that combustion is complete and only energy removal processes are occurring. Visual observation confirms the implication that flame front is confined to approximately the bottom one-foot section of furnace column.

These temperature profile data were obtained using Honeywell MegopaK, sheathed, chromel-alumel thermocouples. They are subject to two principal errors: radiation error and conduction error.

The radiation error present is due to the fact that the thermocouple sensing-tip "sees" a relatively cool furnace column wall and thus there is a net radiant energy loss resulting in a temperature reading that is also too low. The severity of this effect is extremely difficult to assess because the vortex gas separating the tip of the thermocouple and the wall is both emitting and absorbing; thus, for measurements near the centerline of the furnace column, the measuring junction is to some degree shielded from the wall by the presence of the high temperature annular flame. Near the wall, however, the absence of a flame permits the maximum radiation exchange. Therefore, the maximum radiation error occurs for radius ratios near one. In Appendix E an estimate of the radiation present in Tables 11-14 is given.

Wall Temperature Data

Because of the difficulty in obtaining accurate readings of the wall temperature using the MegopaK-type thermocouple, separate thermocouples were fabricated and bonded into a hollowed-out cavity on the exterior furnace of the column wall between the cooling water tubing at 6-inch intervals for a total of 11 vertical positions.

The temperature data obtained with these thermocouples is not as useful as was hoped because of a sensitive dependence upon the water inlet-temperature which, in Dallas, can be as high as 90°F in August and as cool as 50°F in January. Thus the wall temperature of the furnace column would be expected to shift by approximately the same amount as the shift in water temperature.

The data for Configuration 3-C for two different water inlet temperatures is presented in Table 17 as a function of Condition and furnace column height. It is clear that the wall temperature is affected principally by the water temperature although for the same inlet temperature there is a marked increase with increasing Condition.

Two additional wall temperature measurements were also made: the top plate of the vortex chamber and the top of the copper base plate of the furnace column. This latter location differs from that of the 0-foot location for the furnace column wall temperature data given in Table 17 in that it is located on top of the horizontal plate that is directly atop the asbestos gasket (separating the vortex chamber from the furnace column) whereas the 0-foot thermocouple is mounted on the cylindrical portion of the furnace column near the copper plate but between the cooling water tube-spiral (see Figure 30). These data are necessary to determine the

TABLE 17

FURNACE COLUMN WALL TEMPERATURE vs. FURNACE COLUMN HEIGHT

Condition	Water Inlet Temperature (°F)	Furnace Column Height (ft)										
		0	½	1	1½	2	2½	3	3½	4	4½	5
3	82	256	154	145	134	126	123	119	117	115	114	114
8		298	171	158	141	134	128	126	124	121	121	126
12		330	186	169	152	141	137	134	130	128	130	134
3	62	N.O.*	138	124	112	103	N.O.*	92	92	90	90	92
8		N.O.	148	127	114	107	N.O.	101	98	96	96	101
12		N.O.	161	140	125	114	N.O.	109	105	103	105	109

* Thermocouple was not operative at the time.

conduction heat transfer from the hot vortex chamber to the relatively cool furnace column. The data obtained for Conditions 3, 8, and 12 for Configuration 3-C are summarised below:

TABLE 18

VORTEX CHAMBER/COPPER PLATE TEMPERATURES

	Condition		
	3	8	12
Vortex Chamber Top Plate Temperature (°F)	1001	1060	1088
Furnace Column Copper Base Plate Temperature (°F)	492	555	573

These data will be used in Chapter IV to calculate the conduction heat transfer component of the heat recovered at each cooling water section.

Orsat Data

An Orsat sample and analysis was obtained for Conditions 3, 8, and 12 for Configuration 3-C using a Model No. 39-547 Burrell Gas Analysis Apparatus according to the instructions of the manufacturer [402]. The gas samples were taken from a tap located just above the separator. The volumetric results of the analysis on a dry products basis, are summarized in the following table:

TABLE 19

ORSAT DATA

	Condition		
	3	8	12
Propane Flow Rate (lbm/hr)	7.83	10.45	13.36
Air/Fuel Ratio	15.3	20.7	20.7
Percent Stoichiometric Air	98.0	132.4	132.4
Percent CO_2	10.0	9.2	9.6
Percent O_2	6.0	7.6	7.6
Percent CO	0.75	0.1	0.2

Slagging Effects

Since one of the principal problems of incinerators is coping with the slag that is invariably created by burning wastes, the effect of slagging on this incinerator concept was investigated by using aluminum, in various forms, and fluidizing it in one of the inlet air supplies. Forms of aluminum tried were:

(1) metal lathe-generated "curly-cues"
(2) milling machine-generated "slivers"
(3) aluminum foil sheet squares
(4) aluminum foil balls
(5) aluminum shot (about pea-size)

All forms of the aluminum "slag" were successfully ingested into the vortex chamber, although only the shot was used in large quantities (about 20 pounds). As might be expected, the less dense forms of aluminum (slivers, curly-cues, and squares) occasionally exited the furnace column without melting and were subsequently trapped in the separator. The other forms of aluminum (balls and shot) appeared to be too dense to be carried out of the vortex chamber at the air velocities being used (maximum of approximately 100 feet/second). In no instance did slag form on the inside cool wall of the furnace column.

To collect the slag, the natural concave shape of the bottom of the vortex combustion chamber was utilized together with a collecting tank attached to a hole in the bottom-center of the chamber as described in Chapter II.

Unfortunately, the aluminum shot unexpectedly piled up on the floor of the chamber without melting as was anticipated although, initially, a small amount did melt and flow. The problem was caused by the shallowness of the vortex chamber (approximately 3.7 inches high) that permitted the cool inlet air to blow over the aluminum shot and thus keep it relatively cool despite being in contact with the hot chamber wall. It appears, however, that this problem could be solved by making the chamber sufficiently high (perhaps a foot or so) with the air inlets still near the top so that the ingested aluminum could always be maintained above its melting temperature as a result of contact with the hot chamber walls and the hot combustion gases. By liquefying the slag, the concave shape of the chamber floor would permit collection simply by using gravity feed.

Sawdust as Fuel/Stack Sampling Results

Sawdust was used as fuel in the operation of this incinerator on approximately fifteen occasions. Most of these runs were concerned with determining the qualitative performance and feasibility of the fluidizing system.

Once an effective fluidizing system was developed (rotating auger with stirrers) feed rates were determined. The hopper would hold almost exactly four pounds of sawdust mixture when it was lightly packed. At the fixed motor rotation speed (54 rpm), this charge would be ingested in about six minutes and forty-five seconds—which corresponds to a feed rate of approximately 35 pounds per hour. The feed rate was relatively uniform (after a starting transient) with the varying sawdust height in the hopper until the sawdust level reached the top of the tee/contraction section. This meant that approximately uniform conditions could be anticipated for a period of five to six minutes.

Sawdust was ingested into the incinerator in two modes: in conjunction with propane and as the sole fuel (after warm-up and ignition using propane). The incinerator operated successfully in both modes. With the sawdust/propane combination it was always possible to adjust the air flow rate so that the exhaust stack was visually clear.

Quantitative data were very difficult to obtain due to the short feed times for the hopper capacity. A Configuration 3/Condition 8 baseline run was performed to determine total heat recovery with a result of 118,200 Btu/hr. Then the sawdust feed motor was turned on and data taken; it should be noted that the air/propane settings were not changed resulting in a somewhat more fuel-rich condition than before. The resulting heat recovery rate immediately after the sawdust ingestion began was 136,900 Btu/hour or an increase of 18,700 Btu/hour which corresponds to 534 Btu/pound of sawdust. However, the heat recovery rate steadily decreased with time until near the end of the five-minute period it was virtually identical to the propane-only figure. This decrease occurred despite what was a fairly uniform feed rate. Since the usual procedure was to allow a minimum of ten minutes of operation for the removal of transients when changing from one Condition to another, it is difficult to interpret this result.

Originally, it had been hoped that the Staksamplr could be used to quantitatively assess the efficiency of combustion and the performance of the separator. The specifications for its use dictate a thirty minute sample of typical operation and it was thought that even though the sawdust capacity of the hopper was limited to about five minutes, the requirement could still be fulfilled by doing it in six steps. As it turned out this was not practical. Due to the small scale of operation any momentary burst of sawdust from the hopper would result in an equally momentary black cloud. These bursts would occur at the beginning and end of each hopper load as well as on one or two occasions in between as a result of the fact that the mixture was not homogeneous and the slow feed rates. Thus, each sample taken resulted in a black piece of filter paper at the end of the first five-minute sequence even though for 99 percent of the time the exhaust was clear.

As a result of these difficulties it was concluded that a commercial stack sampling procedure is just not feasible for a laboratory-size apparatus because of scale effects. What is needed is a much simpler procedure that would require sample times only on the order of fifteen to thirty seconds.

CHAPTER IV

DATA ANALYSIS AND ANALYTICAL INVESTIGATIONS

Philosophy of Approach

Purely analytical attempts at finding the fluid velocity, the temperature profiles, or heat transfer rates encounter incredible complications because of the many effects present. From the very nature of a vortex flow with an axial velocity component, three dimensional considerations are essential. Also, because the walls are of a non-refractory nature due to the heat recovery system, severe radial temperature gradients are present which require consideration of variable-property effects. In addition, as is apparent from the Reynolds number calculations presented in Appendix D, the flow stream is fully turbulent. Further, there is the added consideration of combustion effects; not only does this result in an energy addition but there are also mass specie concentration effects, gas radiation and absorption effects, and finite-rate combustion chemistry effects.

As noted in the survey of the available literature (presented in Chapter I), no solution exists for this flow field. The analytical efforts presented in this Chapter have been directed primarily toward both gleaning from the data the maximum amount of information possible and developing a correlation relation between heat transfer and Reynolds number. The models employed are necessarily quasi-simplistic and must rely upon the data for their sustenance.

Heat Recovery Efficiency

Although the data for heat recovery have already been presented in Chapter III, it is important to assess the performance demonstrated by this laboratory-sized incinerator in terms of some useful benchmarks. What is in view here is not the amount of heat transfer but the quality of heat transfer.

The significance of these heat recovery data can best be displayed by expressing the results in terms of the theoretically achievable values by calculating recovery "efficiencies". There are two obvious possibilities for a theoretical standard:

(1) the "absolute" theoretical standard corresponding to a furnace column of infinite height for which the exhaust gas temperature would be 77°F with water appearing as a liquid in the products, and

(2) the "practical" theoretical standard for which the theoretical heat recovery is based upon measured furnace column exit temperatures with water assumed to appear as a vapor in the products.

Since both of these standards represent useful concepts, the data will be presented in terms of each.

It is first necessary to calculate the theoretical enthalpy of combustion based upon the known air/fuel ratio; the procedure for doing this is presented in virtually every thermodynamics textbook (see, for instance, Wark [403] Chapters 14 and 15). For the theoretical standard, the sensible enthalpy of the products need not be calculated since they are taken to be at the reaction temperature (77°F). The sensible enthalpy of the reactants together with the sensible enthalpy of the products required for the practical standard can be found by means of known property tables such as the JANAF Thermochemical Tables [404, 405] for the measured average gas temperature. These calculations are performed in Appendix F.

The absolute efficiency can now be found by ratioing the actual heat recovered per pound of propane (available from Table 10) to the "Net Enthalpy of Combustion" given in Table F-3. The practical efficiency is found by using the "Net Enthalpy of Reaction at the Exit" given in Table F-5 as the standard to ratio with the heat recovery data. These two efficiencies, so calculated, are presented in Figure 28 as a function of the average axial Reynolds number (calculated in Table D-1 and used in Figures 18 and 19) of the furnace column.

Several observations can be noted from the graphs given as Figure 28. First, the relatively high efficiency levels of the incinerator indicate that the heat recovery concept of vortex heat transfer is effective even for the modest length-to-diameter ratio used in this apparatus (slightly greater than 10). The maximum efficiency on an absolute basis was 70% while values in excess of 80% were obtained for practical efficiencies. It is relevent to note that the efficiency of simple boilers--whose sole objective is to recover heat--is often quoted ([268, 406] for example) to be on the order of 85% on an absolute standard. In comparison, the heat recovery performance of this model incinerator is considered to be highly satisfactory.

Several additions observations can be made:

(1) The absolute efficiency decreases with increasing mean axial Reynolds number of the furnace column. Since this trend is also present for the practical efficiency curve (with the exception of Configuration 1) it can be concluded that this efficiency degradation is not due entirely to increased sensible enthalpy loss in the flue gas as a result of higher mean axial velocities (although this effect does play a significant role).

(2) The change in slope of the efficiency curves at the middle value of Reynolds number (which represents Condition 8) could be a result of an air/fuel ratio effect. By extending a straight line beyond the Condition 8 and 12 data it is clear that the Condition 3 data lie

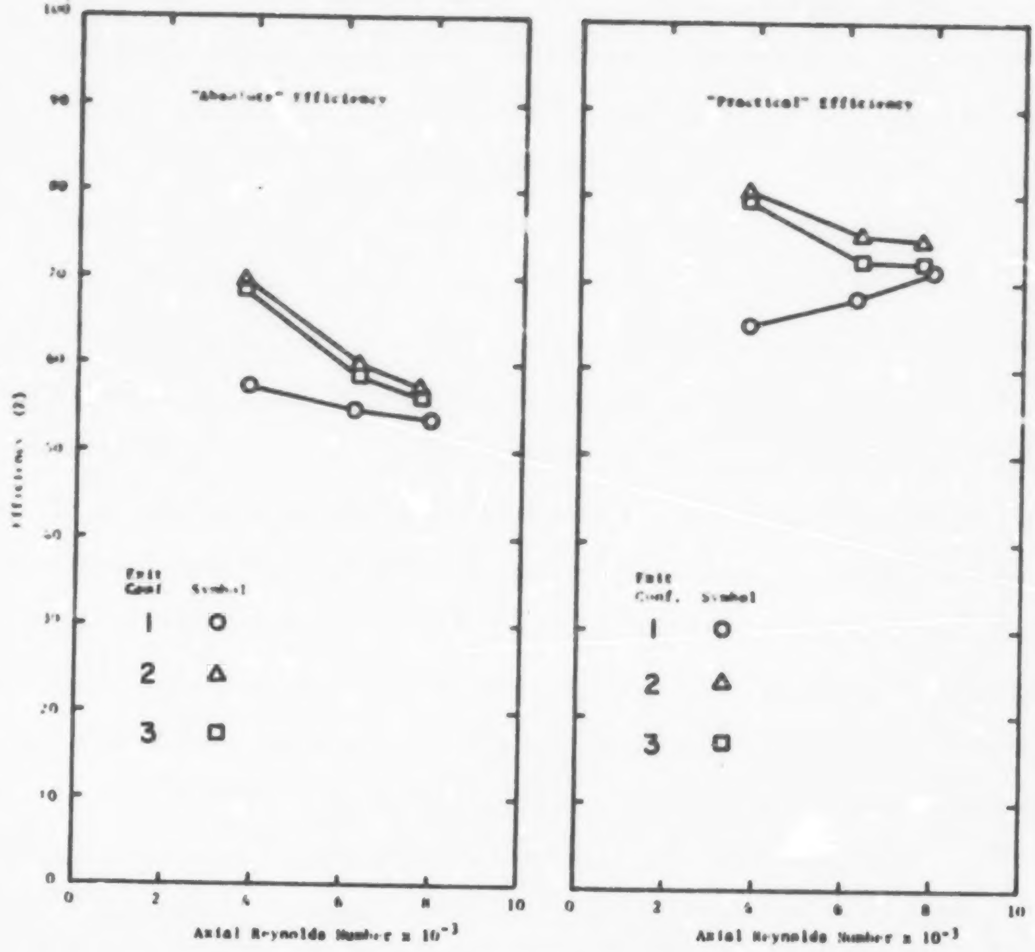

Figure 28. Absolute and Practical Efficiency vs. Axial Reynolds Number

above this line for all six possibilities which is expected since Condition 3 is near-stoichiometric. If this is in fact the case, then the degredation of recovery efficiency observed is due in part to the increase in air/fuel ratio and in part because of the increase in Reynolds number with the latter factor the most-predominant.

(3) The effect of the exit Configuration is small for the change from the four to the six-inch exit diameter. A dramatic change occurs, however, for the change from the four to the two-inch diameter. This suggests a fundamental change in the operating characteristics of the incinerator, perhaps as a result of a vortex breakdown. The middle-sized exit diameter (Configuration 2) actually demonstrates a higher recovery efficiency than either the size larger or the size smaller for all eighteen data points. On the basis of Thompson [166] and others it is known that a reduced exit orifice size increases the region of free vortex flow and thus increases the maximum tangential velocity experienced. Thus it is expected that the smaller exit diameters would cause a higher heat transfer rate due to a higher velocity gradient (although in this configuration the effect of the intervening separator between the end of the furnace column and the actual exit orifice is unclear). This is exactly what the data show for the change from Configuration 3 to 2. However, for the change from 2 to 1 an abrupt decrease is observed, suggesting the likelihood of a breakdown or vortex jump.

(4) It should also be noted that these recovery efficiencies have been obtained without any attempt at optimizing the performance either in terms of determining an optimum Condition/Configuration or in attempting hardward modifications. In particular, since no attempt to recover heat from the vortex chamber has been made, a marked improvement in these efficiencies can be expected as a result of an installation of an additional cooling coil. It is predicted that recovery efficiencies on the order of 80% on the absolute basis (90% on the practical) can be obtained as a result of this single modification.

For many years a great many investigators have attempted to correlate furnace heat recovery in terms of some universal parameter on a basis that would be applicable to all types and configurations. Hudson [407] proposed one of the earliest such correlations in 1890. His was a purely empirical equation that related absolute furnace efficiency in terms of air/fuel ratio and a quantity that has come to be known as the "available heat"; the available heat is defined as the net enthalpy of bustion (see Appendix F) divided by the radiant wall surface area.

Broido [408] presented in 1925 what has become a widely-known curve correlating efficiency with available heat. In that same year, Orrok [409] suggested a modification of Hudson's correlation (now referred to as a Hudson-Orrok equation) and Wohlenberg [410-412] presented the first of his several papers attempting to ground the subject on a firmer theoretical basis. Hurvich [413] has given an equation for a modified Boltzmann number in terms of an experimentally determined coefficient accounting for the fraction of the total heat transferred via radiation for coal-fired furnaces. Konokov [414] has approached the same question with somewhat different assumptions. Greyson [415] has presented a survey of these correlations with suggested modifications together with a compendium of data from various boiler furnaces in operation in the United States.

All of the above relations have been developed with the large, typical power generation furnace in mind. These devices are characterized by large furnace volumes of extremely high-temperature gas with a relatively low velocity and small wall area. As a result, radiation heat transfer is predominant in the furnace chamber area in contrast to the case in view here. Hence, these correlations generally do not agree with the results of this investigation.

However, if the total heat recovery data of Table 10 are plotted as a function of the available heat and compared with the classic Broido curve there is remarkably close agreement. These results are given in Figure 29 for absolute efficiency in terms of two available heats: one based upon the internal area of the furnace column (7.540 square feet) and the other using the total internal area of the furnace column plus the vortex chamber (12.36 square feet). The Broido curve was obtained

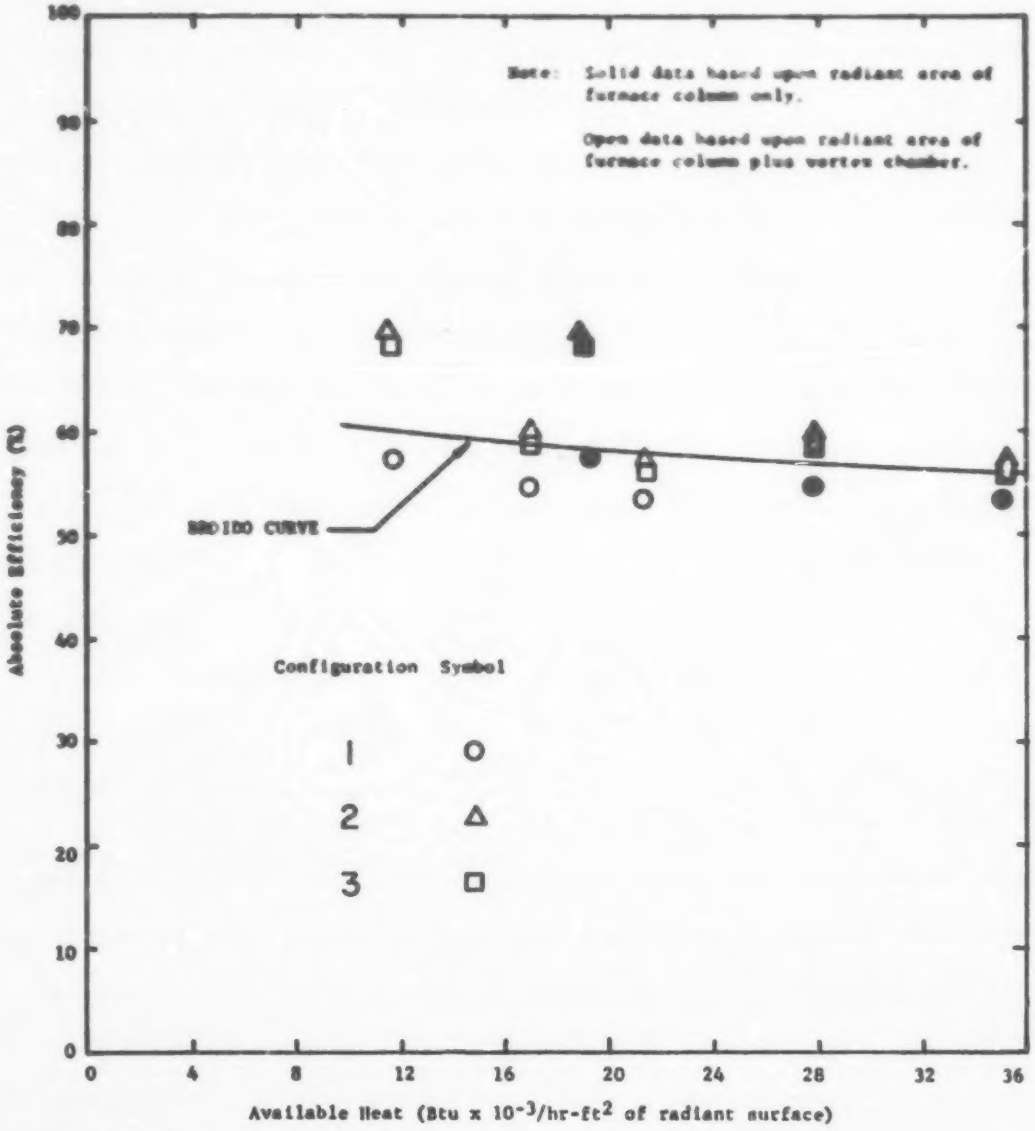

Note: Solid data based upon radiant area of furnace column only.

Open data based upon radiant area of furnace column plus vortex chamber.

Figure 29. Comparison of Incinerator Efficiency vs. Available Heat With Broido Curve

from Reference [408] (page 1132) which was presented for available heats from 10,000 to 250,000 Btu/hr-ft^2; the good agreement shown in Figure 29 is especially surprising because only the very lowest portion of the Broido curve applies to heat rates measured for this incinerator.

The lowest available heat data presented by Greyson [415] corresponds to the maximum shown in Figure 29. This point was taken from measurements made at the Willow Island Station (which is a pulverized coal furnace) and demonstrated approximately the same absolute efficiency as was achieved with the vortex incinerator--namely, 55%.

A final basis of comparison for the heat recovery performance is the total heat recovery rate (in Btu/hour) per furnace volume (in cubic feet); the volume of the vortex chamber alone is 0.5508 ft^3 and that of the vortex chamber plus the furnace column is 1.456 ft^3. Thus the heat recovery data of Table 10 ranged from a low of 57,700 Btu/hr-ft^3 (for Configuration 1/Condition 3 using the total volume of the vortex chamber plus the furnace column) to a high of 276,300 Btu/hr-ft^3 (for Configuration 2/Condition 12 using just the volume of the vortex chamber).

Energy Balance

There are three energy fluxes that comprise the energy balance of the incinerator: the total heat recovery rate, the enthalpy rate associated with the internal energy of the flue gas leaving the furnace column, and the over-all energy losses from the system. The total heat recovery rates are given in Table 10 and the gas enthalpy rates in Table F-5. The calculation of the energy losses from the system is presented in this section.

The sources of energy loss are as follows:

(1) radiation from the vortex chamber that does not reach the exterior of the furnace column,

(2) free convection from the vortex chamber,

(3) conduction from the vortex chamber through its supporting pins to the steel table (the conduction to the furnace column is not a loss from the system),

(4) radiation from the furnace column/copper base plate,

(5) free convection from the furnace column/copper base plate,

(6) conduction from the furnace column to the separator.

Also, the actual enthalpy of reaction is somewhat less than the theoretical value calculated in Table F-5. This is because of two effects: the Second Law of Thermodynamics which limits the degree of completion of any reaction (usually expressed in terms of the attainment of the minimum of the Gibbs function) and the incompleteness of combustion that results from the imperfect mixing that occurs in all combustors. The Orsat data given in Chapter III, however, demonstrates that the actual chemical energy released is very close to the theoretical values already calculated in Appendix F.

Although the energy recovered and released are known to relatively high precision, the calculation of the energy losses from the incinerator can only be, at best, a reasonable approximation. Many of the material properties (such as surface emissivity) can only be estimated and a number of assumptions are necessary to obtain any result whatever due to the complicated geometry, heat transfer processes, and absence of data in some cases. As a result, no distinction will be made for Configuration in the calculations since both the heat recovery data and the sensible enthalpy calculations show that the effect is small. Also, although the calculations are performed to the nearlest 100 Btu/hour, it should be noted that two significant digits is about the best accuracy that can be obtained.

Radiation Loss

From the Vortex Chamber

The radiation loss from the vortex chamber will be calculated in three components due to the difference in surroundings: the radiation from the top plate, from the side walls, and from the bottom plate.

A portion of the radiant energy emitted from the top plate of the vortex chamber strikes the external wall of the furnace column and hence is not a loss from the system. The remainder of the radiant energy is exchanged principally with the concrete walls of the enclosure of the incinerator. A calculation of the configuration factor (sometimes referred to as the "view" factor of the "angle" factor) is necessary to account for the latter fraction. The numerical integration procedure to find this factor is presented in Appendix G; the result appropriate here is the factor of 0.138 from the top plate square annulus to the entire furnace column--thus the configuration factor to the concrete enclosure is 0.862. The top plate must be viewed as a square annulus because the copper base plate of the furnace column is located on the top-center of the vortex chamber and this plate is at a comparatively low temperature. The area of this annulus is simply the area of the top plate (19 inches square) less the area of the copper base plate (8 inches square) and is equal to 2.06 square feet.

The emissivity of the plate can be estimated to be 0.80 (taken from [416] "sheet steel with strong, rough oxide layer"). The temperature of the concrete walls (which act as an approximate diffuse, gray enclosure) can be estimated to be 70°F (530°R) although it is obvious that this value was dependent upon the time of operation of the incinerator as well as the seasons of the year. The final quantity required before the calculation of the radiation exchange between the top plate and the enclosure is the temperature of the plate itself. These data were given in Table 18 and are as follows: 1461, 1520, and 1548°R for Conditions 3, 8, and 12. Although the plate was not at a uniform temperature, these data were taken at a location away from both the hottest and the coolest area and so will be taken to represent the temperature of an equivalent isothermal plate; to do otherwise would unduly complicate the calculation.

The equation for the heat exchange between an object and its enclosure (for the diffuse, gray assumption) is given by ([416], page 263):

$$q_R = \sigma A \epsilon F (T_v^4 - T_e^4) \qquad (4)$$

The results of the calculation (in Btu/hour) for Conditions 3, 8, and 12 are as follows: 10,900, 12,800; and 13,800 Btu/hour for Conditions 3, 8, and 12 respectively.

The radiation loss from the side-walls of the vortex chamber can be readily calculated since the configuration factor is 1.0 because the furnace column is not viewable. The emissivity, wall, and enclosure temperatures will be assumed to be the same as that used above. The side wall area is 1.865 square feet. Again using Equation (4) results in the following loss rates in Btu/hour for Conditions 3, 8, and 12: 11,400; 13,500; and 14,500.

The radiation loss from the bottom plate of the vortex chamber is complicated somewhat by the fact that the steel table underneath the has a square hole (7.5 inches square) and two round holes (2.75 inches in diameter). Thus, there is a total area of 0.473 square feet that views the concrete floor, whereas the remaining area (2.03 square feet) views the steel table which is located approximately ¼-inch below and parallel to the bottom plate. For the area that views the concrete floor, the radiation loss may be calculated in exactly the same manner as given above using Equation (4). The resulting loss rates are: 2900, 3400, and 3700 Btu/hour for Conditions 3, 8, and 12.

The radiation loss for that portion of the plate that views the steel supporting table can be estimated by treating the table as a flat radiation shield of the same approximate emissivity and thus the radiation rate equation can be expressed as ([416], page 264):

$$q_R = \frac{0.5\ \sigma\ A\ (T_v^{\,4} - T_e^{\,4})}{1/\varepsilon + 1/\varepsilon - 1} \tag{5}$$

Using the same temperatures and emissivity as before (the table is assumed to have the same emissivity as the vortex chamber--namely 0.80) results in radiation rates of 5200, 6100, and 6600 Btu/hour for Conditions 3, 8, and 12.

Thus the total radiation loss from the vortex chamber can be found from summing these four separately calculated rates and is tabulated below:

TABLE 20

RADIATION LOSS FROM VORTEX CHAMBER (Btu/hour)

Condition	From the Top Plate	From the Side Wall	From the Bottom Plate To Floor	From the Bottom Plate To Table	Total
3	10,900	11,400	2,900	5,200	30,400
8	12,800	13,500	3,400	6,100	35,800
12	13,800	14,500	3,700	6,600	38,600

From the Furnace Column/Copper Base Plate

In addition to the radiation loss from the vortex chamber just calculated, there is a loss from the furnace column via radiation because it is relatively warm with respect to the concrete enclosure. There are two radiating areas that must be considered: the cylindrical portion of the column and the copper base plate.

The configuration factor from the cylindrical tube of the furnace column to the concrete enclosure can be found directly from Table G-1: since the factor from the cylinder to the top plate of the vortex chamber is 0.0232, the factor to the enclosure must be 0.9768. The radiating area is simply the circumference (6.4 inches to the outside of the cooling-water tubing) times pi times the height (5 feet) or 8.38 square feet. The emissivity will be taken to be 0.78 ([416], for "plate, heated long time, covered with thick oxide layer"). The temperature of the furnace column wall has been tabulated in Table 17. Because the total radiation loss from the furnace column walls is relatively small, it is sufficiently precise to choose an equivalent isothermal column temperature rather than calculate the loss in sections. Since most of the heat recovery data was obtained for relatively warm water inlet temperatures, the higher wall temperatures given in Table 17 will be used. The equivalent temperature point to be used will be that for the one-foot height; a low location was selected because of the strongly non-linear relationship of emitted energy with wall temperature (thus a simple area-average would have predicted too low a radiation loss). Once again using Equation (4) results in the following radiation loss rates in Btu/hour: 600, 700, 800 for Conditions 3, 8, and 12.

The radiation loss from the copper base plate requires a determination of the configuration factor that views the concrete enclosure. From Table G-1 the factor from the base plate to the entire cylinder is given to be 0.155; thus the factor to the enclosure must be 0.845. The temperature of the base plate was given in Table 18 (952, 1015, and 1033°R for Conditions 3, 8, and 12). The area of the base plate is 0.263 square feet. Thus the radiation loss from the copper base plate is: 200, 300, and 300 Btu/hour for Conditions 3, 8, and 12.

Thus the total radiation loss from the furnace column is 800, 1000, and 1100 Btu/hour for Conditions 3, 8, and 12.

Free Convection Loss

From the Vortex Chamber

Since these losses are approximately an order of magnitude smaller than that given in Table 20, the calculation procedure is only intended to provide a gross estimate. Because the walls of the vortex chamber are oriented differently, the calculation for the free convection losses from the top, sides, and bottom will be performed separately.

The calculation procedure will follow that given in Chapter 7 of Reference [416] using 70°F as the ambient air temperature. The vortex wall temperature will be assumed to be that given in Table 18. Knowing these two temperatures permits calculating the film temperature and thus all the required fluid properties (the volume coefficient of expansion, the density, the absolute viscosity, the thermal conductivity, and the Prandtl number). The Grashof number, defined by the following equation, may then also be found:

$$Gr = \frac{\rho^2 g \beta \Delta T L^3}{\mu^2} \qquad (6)$$

where L here is the length of the plate (approximately 19/12 feet). By forming the products of the Grashof and Prandtl numbers the equation for the free convection conductance may be found from Table 7-1 of Reference [416]; this product, for Conditions 3, 8, and 12, is as follows: 3.44×10^8, 3.26×10^8, and 3.16×10^8.

From Reference [416], the convection conductance can then be found from:

$$h = 0.14 \, (k/L) \, (Gr \, Pr)^{0.333} \tag{7}$$

This calculation results in values of h of 1.57 Btu/hr-ft^2-°F for all three Conditions. The convection rate may now be found from the defining equation for convection conductance:

$$q = h \, \Delta T \tag{8}$$

Performing this calculation results in the following convection losses in Btu/hour for Conditions 3, 8, and 12: 3000, 3200, and 3300.

The procedure for determining the convection losses from the sidewalls of the vortex chamber is the same as that given for the top plate only now the length, L, is the height of the sides (0.312 feet). This results in three new products of Grashof-Prandtl numbers: 2.64×10^6, 2.50×10^6, and 2.43×10^6. The associated convection conductance equation is now given by:

$$h = 0.54 \, (k/L) \, (Gr \, Pr)^{0.250} \tag{9}$$

This calculation yields values of convection conductance of: 1.77, 1.78, and 1.78. Using Equation (5) to find the convection loss in Btu/hour for Conditions 3, 8, and 12 yields: 2400, 2600, and 2700.

The convection loss from the bottom plate is a much more complicated calculation since the steel table greatly affects the flow field induced by thermal bouyancy effects. It is known that for narrow, horizontal gaps with the top plate heated, the formation of free convection currents is inhibited. Since the steel table is positioned only about a half-inch below the bottom plate of the vortex chamber, it is assumed that the free convection losses from this surface are so small as not to warrant inclusion.

Thus the total convection loss from the vortex chamber is: 5400, 5300, and 6000 Btu/hour for Conditions 3, 8, and 12.

From the Furnace Column/Copper Base Plate

There are two surfaces from which free convection losses occur from the furnace column: the cylindrical tube and the copper base plate.

The length of the equivalent plate for the copper base plate will be taken to be 6 inches instead of 8 inches because of the effect of the furnace column located at its center. Using the temperature data of Table 18 and 70°F ambient air results in Prandtl number/Grashof number products in the laminar range (i.e. between 10^4 and 10^9). According to McAdams [363] the convection conductance for air with an upward facing heated plate is given by:

$$h = 0.27\ (\Delta T/L)^{0.250} \qquad (10)$$

Substituting the appropriate values yields convection conductances of: 1.46, 1.51, and 1.52 for Conditions 3, 8, and 12. Using these values in Equation (8) for a surface area of 0.263 square feet results in loss rates of: 200, 200, and 200 Btu/hour for conditions 3, 8, and 12.

The free convection loss from the furnace column, if calculated in the manner given above, would be on the order of 200 Btu/hour. However, since the air flowing upward along the furnace column has been heated by the vortex chamber top plate and the copper base plate, it is no longer valid to assume a 70°F ambient temperature. Since the ambient temperature is probably very near the wall temperature and the magnitudes involved are very small anyway, the convection losses from the furnace column cylindrical portion will be ignored.

Conduction Loss

From the Vortex Chamber

There are two conduction heat transfer rates associated with the vortex chamber: the conduction through the asbestos gasket to the furnace column and the conduction through the four supporting pins to the steel table. Since the former does not constitute a heat transfer component leaving the system it need not be evaluated here.

The vortex chamber is supported by four steel bolts of length 0.75 inches and diameter 0.325 inches. The heat transfer area is 0.00230 square feet and the length is 0.625 feet. The thermal conductivity of 0.5% carbon steel at 752°F is 24 Btu/hr-ft-°F [416]. The conduction heat transfer can be evaluated directly for the Fourier Law for constant thermal conductivity and a uniform temperature gradient:

$$q = k\,A\,(\Delta T/L) \tag{11}$$

The temperature of the steel table is estimated to be 275°F, 300°F, and 325°F for Conditions 3, 8, and 12. Using this estimate together with the measured plate temperature data to determine ΔT the conduction rate is determined to be as follows (Btu/hour): 200, 300, and 300 for Conditions 3, 8, and 12.

The conduction across the top gap can be estimated by using the thermal conductivity of air at the film temperature (approximately 0.03 Btu/hr-ft-°F) and the area of the bottom plate (2.51 square feet). The heat transfer length used is 0.5 inches since the plate has a significant sag, the average separation distance from the top of the steel table is less than the 0.75 inches that the four corners are supported. The calculated conduction heat transfer is 500, 600, and 600 Btu/hour for Conditions 3, 8, and 12 across the film gap.

Thus, the total conduction heat transfer from the vortex chamber bottom plate is 700, 900, and 900 Btu/hour for Conditions 3, 8, and 12.

From the Furnace Column

The only possible conduction loss from the furnace column would be up to the separator through the attachment collar. However, because the separator is uncooled, its temperature has been measured to be several degrees above the wall temperature at the top of the furnace column. Thus the conduction heat transfer component is very small (because of the small temperature difference) and would represent an energy addition to the system and not a loss. In any case it is neglected.

Total Energy Losses

The calculations of this section are summarized in Table 21. By summing the losses from the vortex chamber and furnace column for the three modes of heat transfer it is seen that the energy leakage rate is: 37,500; 43,700; and 46,800 Btu/hour for Conditions 3, 8, and 12.

The energy recovered from the system has been measured and tabulated in Table 10. Since the energy losses were calculated on the basis of mean values for all three Configurations, it is necessary also to use the mean for each Condition of this data given in this table. This averaging must also be performed on the final component of the energy balance: the net enthalpy of reaction at the exit given in Table F-5. Since this value is given in terms of Btu/pound C_3H_8, it must be multiplied by the average propane flow rate for each condition as found from Table 10.

The results of these calculations together with the results of Table 21 are given in Table 22.

TABLE 21

SUMMARY OF ENERGY LOSSES FROM SYSTEM

(Btu/hour)

		Condition		
		3	8	12
Vortex Chamber:	Radiation	30,400	35,800	38,600
	Convection	5,400	5,800	6,000
	Conduction	700	900	900
	Total	36,500	42,500	45,500
Furnace Column:	Radiation	800	1,000	1,100
	Convection	200	200	200
	Conduction	0	0	0
	Total	1,000	1,200	1,300
Total		37,500	43,700	46,800

TABLE 22

ENERGY BALANCE TABLE

	Condition		
	3	8	12
Mean Energy Recovery Rate (Btu/hr)	93,800	121,400	147,600
Calculated Energy Loss Rate (Btu/hr)	37,500	43,700	46,800
Predicted Rate of Energy Leaving the System (Btu/hr)	131,300	165,100	194,400
Net Enthalpy of Reaction Within the System (Btu/hr)	125,300	168,600	202,700
Percent of Net Enthalpy of Reaction Unaccounted For	+4.8	-2.1	-4.1

Table 22 shows that the system (vortex chamber/furnace column) balances very well for all three Conditions. Apparently the loss analysis has overpredicted the true loss rate since for Condition 3 the total energy rate leaving the system exceeds that entering.

Several important conclusions can be made from this balance:

(1) The incinerator system has been properly identified with all the associated energy rate satisfactorily measured and/or computed.

(2) The sensible enthalpy of products at the exit, which is used to find the net enthalpy of reaction (which represents the net energy into the system), is accurately found on the basis of enthalpy calculations for the theoretical products using the JANAF Tables [404, 405] and the average temperature found by the area average method of Appendix C. This implies that the average temperature so calculated is in fact the true mixed-mean temperature.

(3) The implication that the average temperature at the exit of the furnace column is the true mixed-mean temperature confirms that the temperature data as measured with the sheathed, MegopaK thermocouple is not greatly in error due to conduction and radiation effects, and that the assumption of a uniform axial velocity profile at that point in the furnace column is an adequate assumption.

(4) The credence so given to the temperature profile data at the top of the furnace column is very important since the maximum radiation error would be expected at that location due to the absence of a shielding effect since no flame occurs that high in the column. Since the conduction error would not be substantially different for any of the Stations, it is expected then that the temperature data given in Tables 11 through 13 is, in fact, accurate.

Determination of Convective Heat Transfer Component

As noted in Chapter III, the heat recovery fluxes presented in Tables 7 through 10 included the effects of conduction heat transfer from the hot vortex chamber top plate and of radiation from the vortex chamber as well as from the hot vortex gas itself. In order to determine a Nusselt number (or Stanton number) it is necessary to evaluate these two components of heat flux and subtract them from the known total flux to find the convection-only component. These calculations are presented in this section.

Conduction Flux Component

A schematic illustrating the conduction heat transfer path is given as Figure 30. The data obtained from the two thermocouples shown in this figure have been presented in Table 18.

The conduction heat transfer rate can be computed using Fourier's Law based upon a constant thermal conductivity and a uniform temperature gradient; this equation has been presented as Equation (11). The thermal conductivity used will be simply that of the asbestos gasket (approximately 0.096 Btu/hr-ft-°F) since the conductivity of the copper base plate is so high in comparison that its effect in determining the total thermal resistance may be neglected. The heat transfer area is simply the area of the base plate (64 square inches) less the area of the furnace column opening (26.06 square inches) or 0.263 square feet. The heat transfer length (L in Equation H-8) is the thickness of the gasket which is 1/8-inch or 0.0104 feet.

The results of this calculation in Btu/hour for Conditions 3, 8, and 12 are: 1240, 1230, and 1260. As can be seen by comparing this rate with the flux recovered at the bottom furnace column section, the conduction component of heat transfer is small; it is also interesting to note that the variation in the calculated heat transfer for these three Conditions is less than 2%.

In addition, because there is a wall temperature gradient with respect to furnace column height, there is a conduction heat transfer component from section to section. Since this value is quite small, only a very approximate calculation will be performed.

The same Fourier Law equation can be used as was used for the

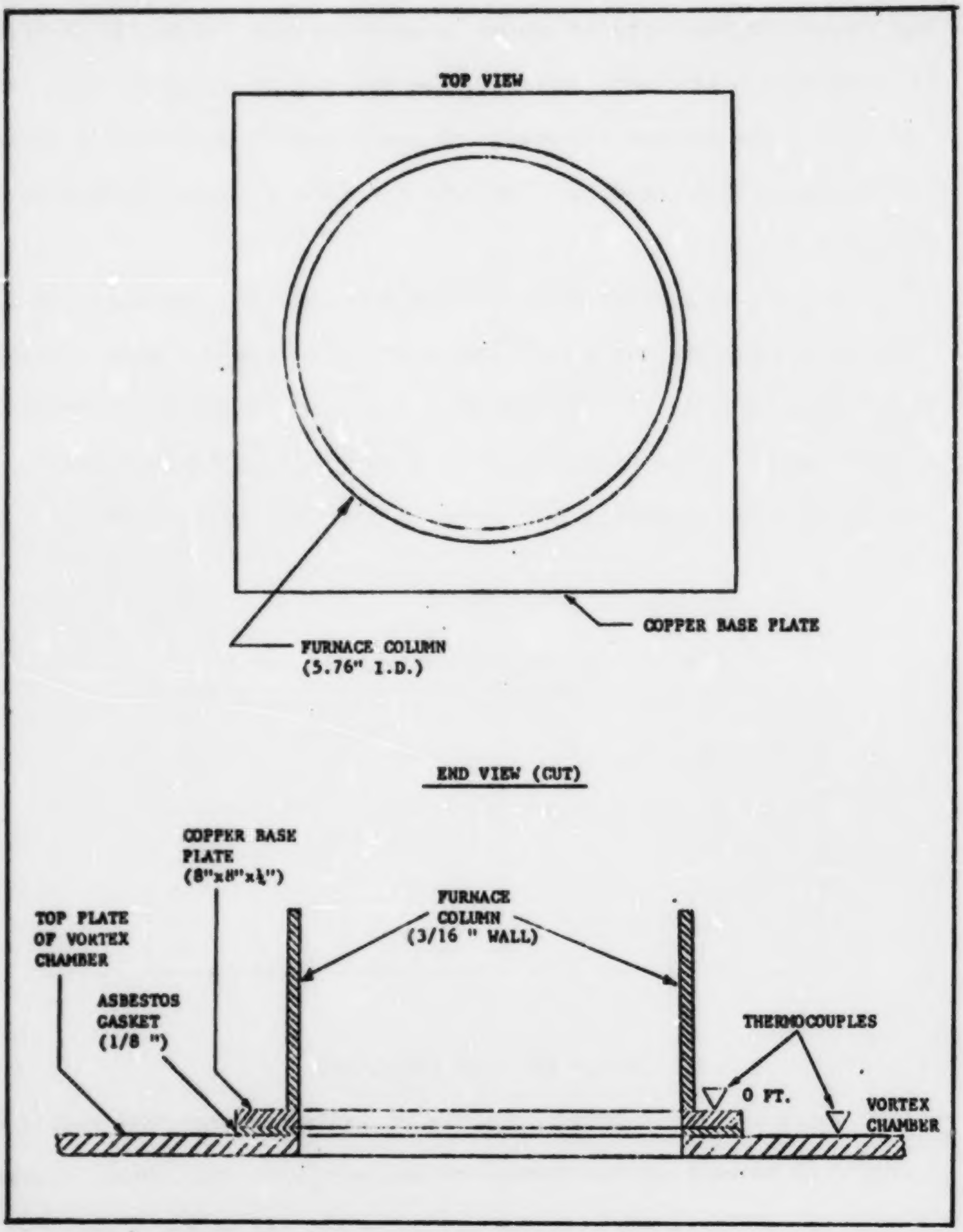
TOP VIEW
FURNACE COLUMN
(5.76" I.D.)
COPPER BASE PLATE
END VIEW (CUT)
COPPER BASE
PLATE
(8"x8"x¼")
FURNACE
COLUMN
(3/16 " WALL)
TOP PLATE
OF VORTEX
CHAMBER
ASBESTOS
GASKET
(1/8 ")
THERMOCOUPLES
0 FT.
VORTEX
CHAMBER

Figure 30. Conduction Heat Transfer Schematic

vortex chamber/copper base plate calculation--Equation (11). Now the heat transfer area is the annular area of the furnace column (the cross-sectional area of the furnace column wall) which is 0.0243 square feet. The thermal conductivity of copper is approximately 220 Btu/hr-ft-°F. The temperature gradient, $\Delta T/L$, will be computed by using the wall temperature difference between mid-points of cooling-water sections for ΔT and the length is then one-foot. The data for a water inlet temperature of 82°F will be used.

The net conduction rate into any given section can simply be determined by subtracting the outlet conduction rate from the inlet conduction rate. This quantity is then converted to a flux (units of Btu/hr-ft^2) by dividing by the surface area of each section (1.508 square feet). The results of this calculation procedure is presented in Table 23.

TABLE 23

CONDUCTION FLUX TO EACH SECTION (Btu/hr-ft^2)

Section	Condition		
	3	8	12
1	750	710	710
2	30	60	70
3	20	30	30
4	10	10	20
5	0	30	30

Radiation Flux Component

There are three primary sources of radiant energy that supply an energy flux to each of the furnace column sections: the vortex chamber walls (the top plate via exterior radiation and the bottom plate via interior radiation), the copper base plate, and the vortex gas itself (principally water and carbon dioxide molecules). In addition, the furnace column itself radiates to the concrete enclosure and this constitutes a loss to the system. Each of these components are calculated in this subsection.

Vortex Chamber Walls

First, the radiation flux that originates externally due to the vortex chamber top plate will be calculated. In Appendix G, the procedure and results of the necessary configuration factor calculation to each furnace column section was presented; again the top plate must be treated as a square annulus because a relatively cool copper base plate sits atop this surface. These factors are given in Table G-2. The emissivity will again be taken as 0.80, the area as 2.06 square feet, and the wall temperature as given in Table 18 (1461, 1520, and 1548°R for Conditions 3, 8, and 12, respectively). The temperature of the furnace column is taken to be the recorded wall temperature data given in Table 17 at the midpoint of each section for the higher water inlet temperature (since most of the heat recovery data was obtained for this water inlet temperature). The results of this calculation is given in Table 24 below (the heat rate is converted to a flux by dividing by the area of each section--1.508 square feet):

TABLE 24

EXTERNAL RADIATION FLUX TO EACH SECTION (Btu/hr-ft^2)

Section	Condition		
	3	8	12
1	980	1150	1240
2	110	130	140
3	30	40	40
4	10	10	10
5	10	10	10

Thus the total radiation energy transfer to the furnace column from the vortex chamber top plate is 1720, 2020, and 2170 Btu/hour for Conditions 3, 8, and 12, respectively.

In addition to the above calculation, the vortex chamber bottom plate also radiates to each furnace column section internally. The effect of this radiation is much more difficult to calculate since separating the plate and the column sections is an absorbing/emitting medium. However, since the vortex bottom plate is significantly cooler than the vortex gas (about 1000°F compared to 1800°F) its radiant energy is concentrated in a relatively long-wavelength band, and thus, it is not significantly affected by the absorption/emission phenomena present in the hot gas; this assumption permits the calculation of the plate and gas radiation rates separately and then simply adding them to find the total internal radiation rate to each furnace column section.

The emissivity of the plate will be taken as 0.80 as before. The plate temperature is somewhat higher than the data given in Table 18 since there is a temperature drop across the thickness of the plate. Using the conduction path as the plate thickness (0.031 feet), the heat transfer area as the plate thickness (0.031 feet), the heat transfer area as the area of the bottom plate (2.5 square feet), the thermal conductivity of the plate as 20 Btu/hr-ft-°F ([416] for 0.5% carbon steel at 1112°F), and the calculated heat rate out the bottom plate due to radiation and conduction that was performed in the previous section (which yielded 8800, 10400, and 11200 Btu/hour for Conditions 3, 8, and 12), and substituting into the Fourier Law, Equation (11), results in estimated temperature drops across the bottom plate of approximately 6°F for all three Conditions. Since this value is less than the uncertainty in the original temperature measurement, the effect of the temperature drop across the bottom plate will be neglected.

The configuration factors from the bottom plate (which is viewed as a disk located at the base of the furnace column, the same area as the cross-sectional area—namely, 0.181 square feet) to each of the furnace column sections have been calculated in Appendix G and are as follows: 0.948, 0.0491, 0.00254, 0.00013, and 0.00000 for sections 1 through 5, respectively. In addition, because the bottom section can view more of the vortex chamber cavity because it can "see around the corner" the effective emissivity of the bottom plate is greater than 0.80 taken as its surface property; since the maximum value of effective emissivity would be 1.0 (for the assumption that the vortex chamber cavity is acting as a black body radiator), a reasonable estimate of 0.95 will be used for furnace column section 1 only (the remaining sections will use 0.80).

The furnace column wall temperature used in this calculation will be the mid-height temperature of each section as given in Table 17 for the 82°F water inlet temperature.

Substitution of these values into Equation (4) results in the radiation rate from the vortex chamber bottom plate to each furnace column section; this rate is converted to a flux by dividing by the area of each section (1.508 square feet) and is tabulated in Table 25:

TABLE 25

INTERNAL PLATE RADIATION FLUX TO EACH SECTION

(Btu/hr-ft^2)

Section	Condition		
	3	8	12
1	820	960	1040
2	40	40	50
3	0	0	0
4	0	0	0
5	0	0	0

Furnace Column/Copper Base Plate

The radiation loss from the furnace column can be found in the same manner as in the previous calculations. The radiating wall temperature will again be chosen as the mid-height data for the 82°F water inlet temperature tabulated in Table 17. The emissivity of the copper will again be taken to be 0.78. The enclosure will be assumed to be diffuse, gray at 70°F. The external radiation area of each section will be based upon the diameter to the outside of the copper refrigeration tubing (i.e. 3.20 inches) and results in 1.676 square feet. The configuration factors from each furnace column section to the copper base plate/vortex chamber top plate can be found from Table G-1; however, since the largest factor--

that of section 1 to the top plate—is only 0.0232 (thus implying that the factor to the enclosure is 0.9768), the configuration factor for each furnace column section will be taken as 1.0.

Using these values in Equation (4) results in the following calculated radiation flux loss from each furnace column section (where the rate has been converted to a flux by dividing by 1.508 since all the flux calculations have been normalized on the inside surface area of each furnace column section):

TABLE 26

EXTERNAL RADIATION FLUX LOSS FROM EACH SECTION

(Btu/hr-ft^2)

Section	Condition		
	3	8	12
1	90	120	140
2	70	80	90
3	50	60	70
4	50	60	60
5	40	50	60

In addition to the just-calculated radiation loss from each furnace column section, the copper base plate located at the bottom of the furnace column acts as a radiant energy source to each section in addition to the conduction transfer calculated in an earlier subsection. The emissivity of the base plate will be taken as 0.78 as has been done for all the copper surfaces. The temperature of the plate has been given in Table 18. The temperature of each furnace column section will be taken as before.

The radiating area of the base plate is 0.263 square feet. The configuration factors from the plate to each section have been found in Appendix G: 0.154, 0.001, 0, 0, and 0 for sections 1 through 5 respectively.

Substitution in Equation (4) and dividing by 1.508 to get a flux results in the following:

TABLE 27

RADIATION FLUX FROM COPPER BASE PLATE TO EACH SECTION

(Btu/hr-ft^2)

Section	Condition		
	3	8	12
1	20	30	30
2	0	0	0
3	0	0	0
4	0	0	0
5	0	0	0

Conflagrant Vortex Gas

The calculation of the effective emittance of the conflagrant vortex gas and the associated radiation flux is considerably more difficult than any of the previous calculations. The estimate of the radiation load in industrial furnaces has been examined for many years without complete success. In addition to the papers of Hudson, Orrok, Broido, Wohlenberg and others [407-415] previously cited, additional, more-recent work is noted: the work of Myers [417] who attempted to account for the effect of furnace-wall fouling upon radiation transfer for a pulverized coal plant, Yagi [418] who has examined radiation from the viewpoint of individual soot particles by adding the flux due to the soot to that due to the gas which he claims to be valid for optically thin gases, Beer [419] who has recently updated the state of knowledge for the prediction of radiation from flames in furnaces, Brovkin [420] who has assessed the error caused by treating a non-isothermal radiating gas by a model using a set of isothermal zones, and Edwards [421] who has presented a very detailed and thorough treatment of the subject for those cases where the mole fraction composition is known throughout the volume.

The method of analysis adopted here is that given by Siegel and Howell [422] in Chapter 17 of their book--namely, the mean beam length technique. This approach is warranted here because the radiation component of the total heat transfer process is relatively small. Although it is customary to increase the calculated gas emittance by some rule-of-thumb factor to account for chemiluminescent effects (see [423] page 2-60) this procedure will not be adopted here because of the absence of soot and the small amounts of carbon liberated by the reaction process.

In Table 17-1 of Reference [422], mean beam lengths corrected for finite optical thicknesses are given for various geometries of gas volume. For a cylinder of infinite height radiating to its convex bounding surface the length is given to be 0.95D where D is the cylinder diameter; for the furnace column this results in a mean beam length of 0.456 feet. Although the furnace column is not particularly long in comparison to its diameter (about a factor of 10), the beam length is not very sensitive to the relative length as long as the cylinder in question is not so short such that end effects are important--this point is usually taken to be when the cylinder height is less than or equal to its diameter. Further, the emittance which is determined on the basis of this beam length estimate is not very sensitive to changes in the value of beam length. For these reasons the value of 0.456 feet will be used for the mean beam length.

In keeping with the previous calculations for radiation and conduction flux to each section, no distinction will be made for exit Configuration. Since the temperature profiles of Configuration 3 were noted to be of a value intermediate between Configurations 1 and 2, they will be used in the determination of the gas emittance and the calculation of the radiation flux.

The component pressures of the radiant constituents in the conflagrant vortex gas can be estimated using the ideal gas approximation from the ratio of the molal coefficient to the total number of moles of product; the pressure of the gaseous products will be assumed to be one atmosphere (this value is nearly independent of Condition since the change in velocities is so small that the total and static pressures are virtually identical) and the reaction will be assumed complete at each section. Using the coefficients given in Table F-1 for Configuration 3 for the theoretical reaction results in partial pressures (in units of atmospheres) for carbon dioxide of 0.0971, 0.0940, and 0.0939 for Conditions 3, 8, and 12, and for water vapor 0.1622, 0.1254, and 0.1251 for these same Conditions. Water vapor and carbon dioxide are the two principal radiating molecules present in the theoretical products (although carbon monoxide also radiates, it is present in such small concentrations that it does not warrant inclusion in this analysis).

By forming the products of the partial pressure and the mean beam length for both of these molecules and using the average temperature data given in Table 14 for each Station and Condition the emissivities of carbon dioxide and water vapor can be found from Figures 17-11 and 17-13 of Reference [422]. Next the band overlap correction ($\Delta\varepsilon$) may be found using Figure 17-15 of this same reference (it turns out to be negligible for all cases). Finally, the pressure correction coefficients (C_{CO_2} and C_{H_2O}) may be found from Figures 17-12 and 17-14; the correction coefficient for carbon dioxide is 1.0 for all Conditions and the coefficient for water vapor is 1.14 for Condition 3 and 1.08 for Conditions 8 and 12.

The emittance of the vortex gas is now found through the use of Equation 17-62 of References [422]:

$$\varepsilon_g = C_{CO_2}\,\varepsilon_{CO_2} + C_{H_2O}\,\varepsilon_{H_2O} - \Delta\varepsilon \qquad (12)$$

The heat flux to each of the furnace column sections may now be found using:

$$q = \sigma\,(\varepsilon_g T_g^4 - \alpha_g T_w^4) \qquad (13)$$

where α_g is the absorptance of the gas for the radiation emitted from the wall and is evaluated at the wall temperature. Since the wall temperature is very small with respect to the gas temperature, this term will be ignored.

The calculations of the emissivities of carbon dioxide and water vapor, the gas emittance, and the radiation flux to each section are presented in Table 28.

Summary of Radiation Flux Calculations

The net radiation flux to each section can now be estimated by summing the components due to five sources: the vortex chamber top

TABLE 28

CALCULATION OF RADIATION FLUX FROM VORTEX GAS TO EACH SECTION

Section		Condition		
		3	8	12
1	Average Temperature (°R)	1873	1934	2003
	Emissivity of CO_2	0.060	0.058	0.057
	Emissivity of H_2O	0.048	0.036	0.035
	Emittance of Vortex Gas	0.115	0.097	0.096
	Radiation Flux (Btu/hr-ft^2)	2430	2330	2620
2	Average Temperature (°R)	1652	1740	1844
	Emissivity of CO_2	0.061	0.060	0.059
	Emissivity of H_2O	0.055	0.041	0.039
	Emittance of Vortex Gas	0.124	0.104	0.101
	Radiation Flux (Btu/hr-ft^2)	1580	1630	2000
3	Average Temperature (°R)	1438	1552	1650
	Emissivity of CO_2	0.059	0.060	0.060
	Emissivity of H_2O	0.062	0.048	0.045
	Emittance of Vortex Gas	0.130	0.112	0.109
	Radiation Flux (Btu/hr-ft^2)	960	1110	1380
4	Average Temperature (°R)	1282	1397	1497
	Emissivity of CO_2	0.057	0.059	0.060
	Emissivity of H_2O	0.069	0.051	0.049
	Emittance of Vortex Gas	0.136	0.114	0.113
	Radiation Flux (Btu/hr-ft^2)	630	740	970
5	Average Temperature (°R)	1176	1286	1391
	Emissivity of CO_2	0.055	0.056	0.058
	Emissivity of H_2O	0.072	0.055	0.051
	Emittance of Vortex Gas	0.137	0.115	0.113
	Radiation Flux (Btu/hr-ft^2)	450	540	730

plate, vortex chamber bottom plate, the furnace column (a loss to the system), the copper base plate, and the vortex gas.

This calculation is given in Table 29.

Convection Flux Component

In the preceeding subsections the energy fluxes to each section attributable to conduction and radiation have been estimated. In Table 10 the total energy flux recovered at each section has been given on the basis of recorded data. The question that remains is as follows: Can the convection flux component be assumed to be that quantity that remains as a result of subtracting the conduction and radiation sources to each section from the total known to be present?

The difficulty in answering this question is that there can be a significant interaction between these heat flux modes: in particular, the interaction between radiation and convection at a surface. This subject has been the topic of a large number of papers, among them are the works of Viskanta [424], Macken [425], and Bratis [426]. Despite the many efforts in the field, the state of knowledge is still incomplete (for instance the work of Bratis [426], although extremely recent, is restricted to laminar flows of a free convection boundary layer along a vertical flat plate being irradiated by a high temperature parallel flat plate). Fortunately, the effect of radiation is small upon the Navier-Stokes equation; Viskanta [424] writes in connection with Rosseland's radiation pressure tensor term that it is, "ordinarily negligible in engineering applications even at moderately high temperatures." The principal effect appears in the energy equation in a manner uncoupled from the equation of motion. Thus the procedure adopted here

TABLE 29

CALCULATION OF TOTAL RADIATION FLUX TO EACH SECTION

(Btu/hr-ft^2)

Section		Condition		
		3	8	12
1	External Vortex Plate	980	1150	1240
	Internal Vortex Plate	820	960	1040
	Column Loss	(90)	(120)	(140)
	Copper Base Plate	20	30	30
	Vortex Gas	2430	2330	2620
	Total	4160	4350	4790
2	External Vortex Plate	110	130	140
	Internal Vortex Plate	40	40	50
	Column Loss	(70)	(80)	(90)
	Copper Base Plate	0	0	0
	Vortex Gas	1580	1630	2000
	Total	1660	1720	2100
3	External Vortex Plate	30	40	40
	Internal Vortex Plate	0	0	0
	Column Loss	(60)	(60)	(70)
	Copper Base Plate	0	0	0
	Vortex Gas	960	1110	1380
	Total	930	1090	1350
4	External Vortex Plate	10	10	10
	Internal Vortex Plate	0	0	0
	Column Loss	(50)	(60)	(60)
	Copper Base Plate	0	0	0
	Vortex Gas	630	740	970
	Total	590	690	920
5	External Vortex Plate	10	10	10
	Internal Vortex Plate	0	0	0
	Column Loss	(40)	(50)	(60)
	Copper Base Plate	0	0	0
	Vortex Gas	450	540	730
	Total	420	500	680

is one in which the components are assumed to be merely additive and so the convection flux can be found by subtracting the radiation and conduction fluxes from the total heat recovery flux.

The results of this subtraction procedure are given in Table 30. Because of the uncertainty associated with the calculations of the radiation flux and since the calculations were performed independent of Configuration, these results are given only to three significant figures.

Nusselt Number Correlation

Evaluation of Convection Conductance

The convection conductance, h, is defined by Equation (8) where the ΔT is usually taken as the temperature difference between the mixed-mean temperature and the wall temperature. Since the velocities present in this incinerator are relatively low, the difference between the adiabatic wall temperature and the measured wall temperature is negligible. Because the wall temperature data of Table 17 is particularly sensitive to water inlet temperature, the wall temperature used in formulating ΔT will be that measured a radius ratio of 0.0 for the vortex gas (as given in Tables 11-13). The average temperature of Table 14 will be used for the mixed-mean temperature.

The results of this calculation is given in Table 31 for convection conductance for each Station/Configuration/Condition combination. The mean convection conductance has been found by dividing the total convective heat recovery rate by the average temperature difference for all five Stations for each combination of Configuration/Condition.

TABLE 30

CONVECTION FLUX AT EACH STATION

Configuration	Condition	Convection Heat Flux ($Btu/hr\text{-}ft^2$)					Total Convection Rate (Btu/nr)
		Sec. 1	Sec. 2	Sec. 3	Sec. 4	Sec. 5	
1	3	15,000	11,300	8,360	6,360	5,[illegible]	71,000
	8	24,600	14,200	10,600	8,630	8,690	101,000
	12	29,300	18,300	13,700	11,000	11,200	126,000
1	3	19,000	13,700	10,100	7,430	7,130	86,500
	8	26,700	16,900	12,000	9,470	9,580	113,000
	12	31,100	20,900	14,500	11,700	12,100	136,000
3	3	18,400	13,800	9,940	7,390	6,960	85,200
	8	26,500	15,600	11,600	9,300	9,390	109,000
	12	30,800	19,400	14,400	11,500	11,800	133,000

Mean Nusselt Number Correlation

The mean Nusselt number is defined here by the following equation:

$$\overline{Nu}_D = \overline{h}\, D / k \qquad (14)$$

where $\overline{h}$ is defined to be the mean convection conductance as calculated in Table 31, D is the diameter of the furnace column (0.480 feet), and k is the thermal conductivity evaluated at the average furnace column gas temperature as given in Table 14. The calculation of this latter quantity is complicated by the fact that the conductivity is both a function of the gas temperature as well as composition. However, Maxwell [401] has measured the thermal conductivity of "flue gas" which he found to be insensitive to the degree of excess air and a function only of temperature similar to what was used for the viscosity in Appendix D.

The details of the calculation procedure are given in Appendix H.

Correlations for Nusselt number are typically given as functions of both Reynolds and Prandtl numbers for simple axial flow inside a tube. The well-known Dittus-Boelter equation for turbulent flow in a smooth tube with cool walls is as follows (taken from page 176 of Reference [416]):

$$\overline{Nu}_D = 0.023\, Re_D^{0.8}\, Pr^{0.3} \qquad (15)$$

where the fluid properties are evaluated at the mixed-mean temperature.

When the mixed-mean and wall temperatures are significantly different, the Dittus-Boelter equation is usually modified as follows (sometimes known as the Sieder-Tate relation, taken from page 178 of Reference [416]):

$$\overline{Nu}_D = 0.027\, Re_D^{0.8}\, Pr^{0.333}\, (\mu/\mu_w)^{0.14} \qquad (16)$$

TABLE 31

EVALUATION OF CONVECTION CONDUCTANCE
(Btu/hr-ft^2-°F)

Configuration	Condition	Local Convection Conductance					Mean Convection Conductance
		Sec. 1	Sec. 2	Sec. 3	Sec. 4	Sec. 5	
1	3	12.3	10.9	10.0	9.24	10.7	11.0
	8	18.8	12.4	10.8	11.0	12.9	13.7
	12	21.3	15.3	14.1	11.8	13.2	15.7
2	3	15.0	12.8	11.6	10.5	11.8	12.7
	8	20.4	15.9	12.3	11.3	12.9	15.2
	12	22.8	19.1	14.2	12.8	14.7	17.3
3	3	14.6	13.2	11.6	10.3	11.4	12.6
	8	20.7	13.9	12.1	11.3	13.3	14.8
	12	23.0	17.8	14.4	12.8	14.9	17.2

where all fluid properties are evaluated at the mixed-mean temperature except μ_w which is evaluated at the wall temperature.

The mean Nusselt number found in Appendix H together with the Seider-Tate relation are graphed at a function of the axial Reynolds number in Figure 31.

Length Nusselt Number Correlation

Just as a length Reynolds number was defined in Chapter III, a similar length Nusselt number can be defined using a characteristic length, L (equal to one-foot for the bottom furnace column section, two-feet, for the next section, and so on), instead of the furnace column diameter D.

$$Nu_L = \frac{h\,L}{k} = Nu_D\,(L/D) \qquad (17)$$

The convection conductance, h, used in this Nusselt number is the local value as given in Table 30 for each furnace column section.

This calculation is performed in Appendix H and the results are presented in Figure 32 as a function of the length Reynolds number found in Table D-5.

Nusselt has suggested the following correlation for heat transfer in the entry-length section of a tube (taken from [416] page 178):

$$Nu_D = 0.036\,Re_D^{0.8}\,Pr^{0.333}\,(L/D)^{-0.055} \qquad (18)$$

By substituting Equation (17) for Nu_D and Equation (3) for Re_D the following form of Nusselt's Equation can be found:

$$Nu_L = 0.036\,Re_L^{0.8}\,Pr^{0.333}\,(L/D)^{0.145} \qquad (19)$$

The Prandtl number has been evaluated using air property tables for the 45 average vortex gas temperatures tabulated in Table 14. The

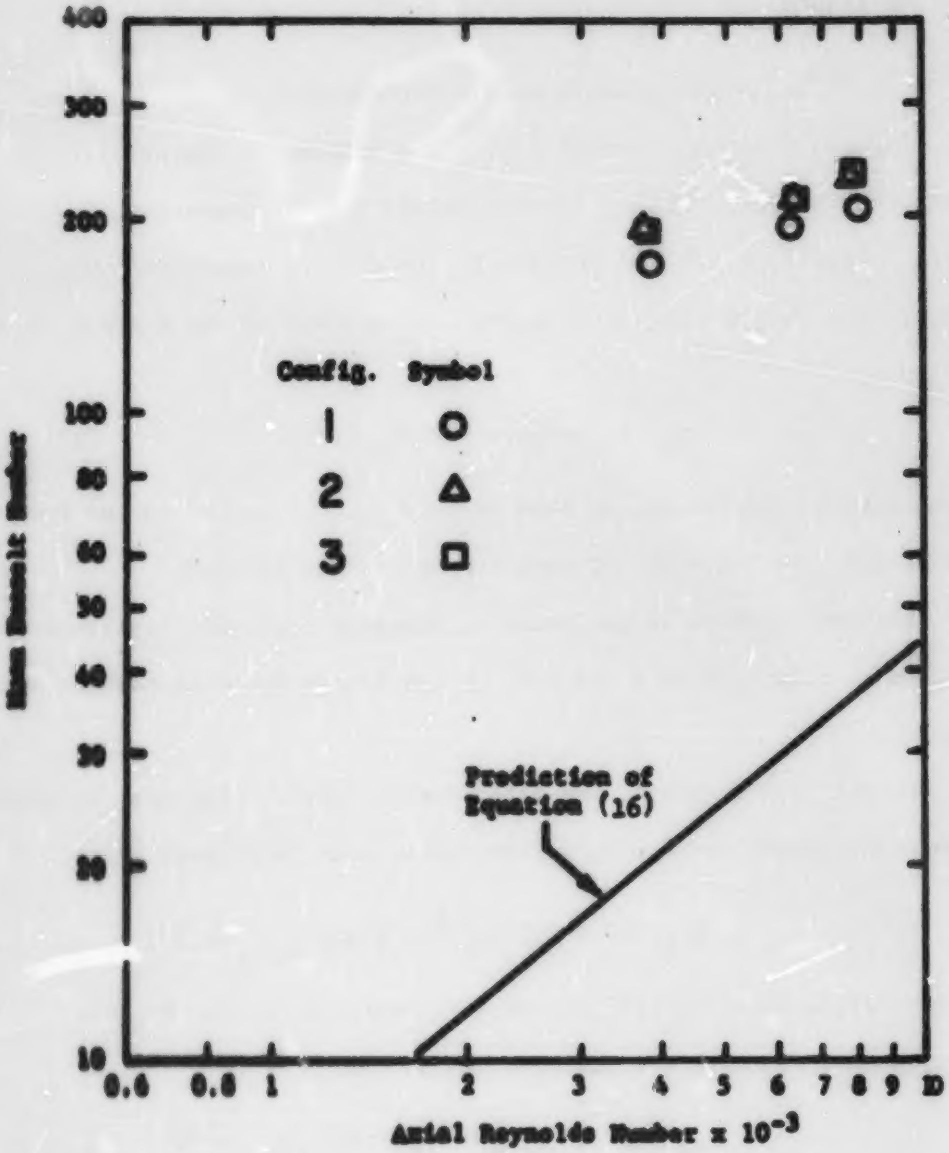

Figure 31. Mean Nusselt Number vs. Axial Reynolds Number

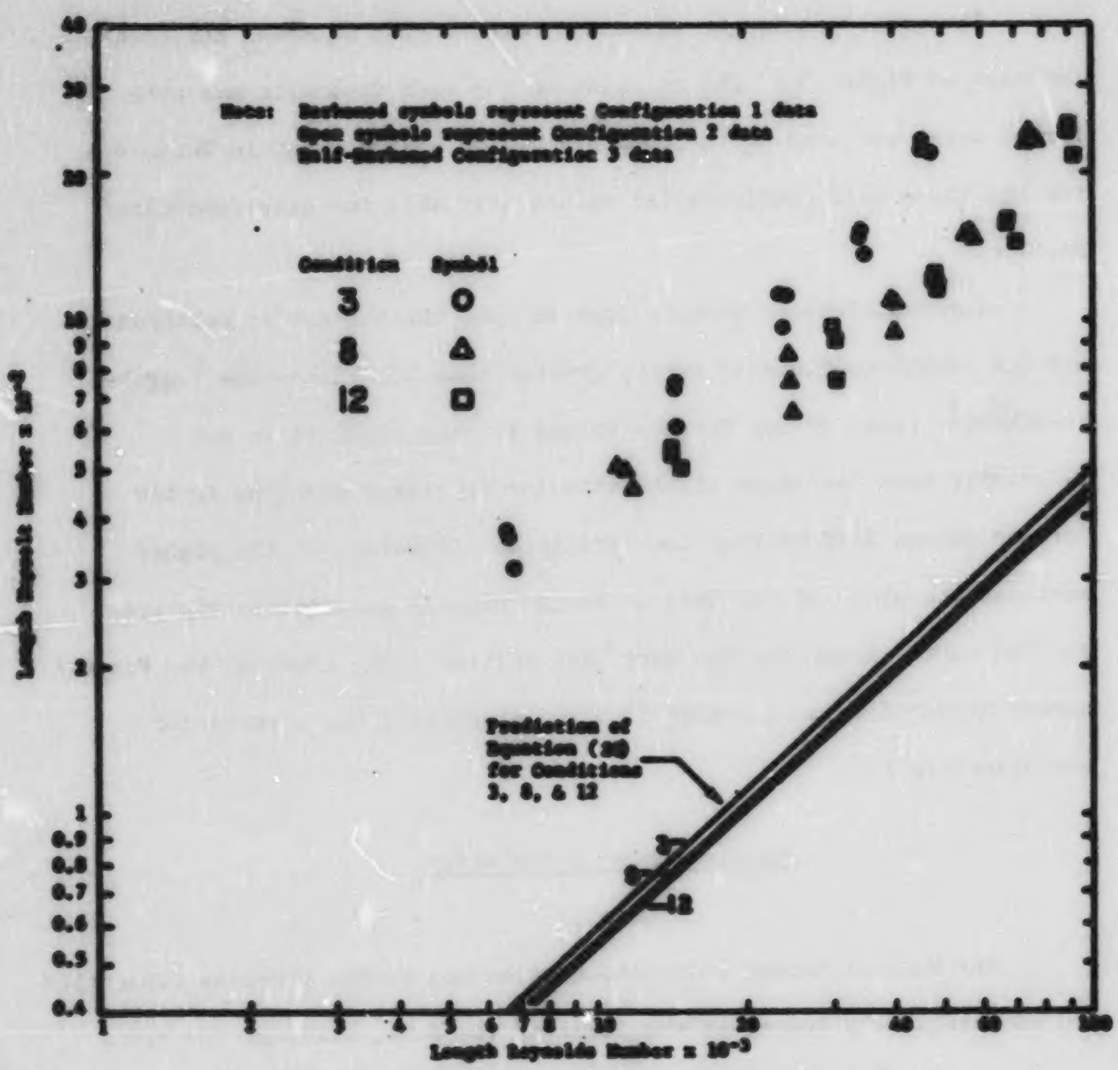

Figure 32. Length Nusselt Number vs. Length Reynolds Number

variation is very small and the Prandtl number raised to the 0.333 power is equal to 0.881 plus or minus 0.25% for all the data. Substituting this value into Equation (19) results in:

$$Nu_L = 0.0317 \, Re_L^{0.8} \, (L/D)^{0.145} \qquad (20)$$

The predicted length Nusselt number of this equation has been included in Figure 32. The calculation for each Condition was performed using the mean of the length Reynolds number given in Table D-5 for the three exit Configuration values available for each Condition/Station.

The restrictions usually imposed upon the Nusselt correlation are for length-to-diameter ratios greater than 10. Since the length-to-diameter ratio of the furnace column is only 10.42 it is not surprising that the slope of the data for the lower sections in the furnace column differs from that predicted. However, at the higher sections the slope of the data is almost exactly parallel to the prediction curve except for the very last section. The level of the Nusselt number measured is much higher than the prediction (by a factor of approximately 7).

Stanton Number Correlation

Concept

The Nusselt number correlation attempted in the previous subsection did not adequately represent the level of the data, although the slope is of the correct order.

The concept to be developed here stems from viewing the swirling flow within the furnace column as an external flow problem rather than an entry-length section of an internal flow field. The furnace column walls are replaced by an equivalent flat plate by unwrapping the column in what has come to be known as the "helicoidal model."

The Stanton number is defined as:

$$St = h / (\rho c_p W) \qquad (21)$$

where W is defined to be the free-stream velocity. The convection conductance used in the above equation is the local value as given in Table 31 for each section.

The Stanton number is usually correlated in the following manner:

$$St\ Pr^{2/3} = j = \text{function } (Re_x) \qquad (22)$$

where j is the Colburn j-Factor (defined as given) and Re_x is the length Reynolds number defined as:

$$Re_x = \rho W x / \mu \qquad (23)$$

where x is the distance along the surface which is the distance from the leading edge of the equivalent flat plate in this case. To avoid confusion with the length Reynolds number defined in Equation (3)--which is based upon the mean axial velocity and the furnace column height--this Reynolds number will be referred to as the free-stream Reynolds number (since it is based upon the free-stream velocity and the equivalent flat plate distance).

Thus, in order to develop a plot of the Colburn j-Factor as a function of the free-stream Reynolds number, the free-stream velocity must be determined and the equivalent flat plate distance found.

Characterization of Swirl Intensity

There are many possible definitions of dimensionless parameters that would characterise the intensity of swirl present in the flow field. The one chosen here is defined in terms of the following:

(1) the axial flux of angular momentum, K

(2) the axial flux of axial momentum, I

(3) and the wall radius of the furnace column, R.

In terms of these quantities, the swirl parameter S is defined as:

$$S = K / (I\ R) \qquad (24)$$

The axial flux of angular momentum is equal to the following:

$$K = 2\pi \int_0^R \rho\, U\, V\, r^2\, dr \qquad (25)$$

where U is the axial velocity, V the tangential velocity, and r the distance from the centerline of the furnace column. If the density is independent of the radius and the two assumptions that constitute the helicoidal model are made—namely, slug flow (i.e. U is also independent of r) and solid-body rotation (therefore V is equal to a constant times the radius)—then the axial flux of angular momentum can be expressed as follows:

$$K = m\, V_w\, R / 2 \qquad (26)$$

where m is the total mass flow rate, V_w the tangential velocity at the furnace column wall (in reality the velocity must be evaluated a short distance from the wall because the no-slip condition of continuum flow requires that the velocity at a solid surface be identically zero), and R the radius of the furnace column wall (0.240 feet).

The axial flux of axial momentum is equal to the following:

$$I = 2\pi \int_0^R \rho U^2 r \, dr + 2\pi \int_0^R p \, r \, dr \qquad (27)$$

where p is the static pressure expressed in units of psfg. By making the assumptions of density independent of radius, slug flow, and negligible contribution of the pressure integral term, this expression can be reduced to:

$$I = m \overline{U} \qquad (28)$$

where m is the total flow rate and $\overline{U}$ is the mean axial velocity.

Thus for the assumptions of density independent of radius and helicoidal flow, the swirl parameter can be expressed as follows:

$$S = 0.5 \, V_w / \overline{U} \qquad (29)$$

Greenspan [70] has defined the Rossby number as the ratio of the inertia forces (a characteristic velocity) to the coriolis forces (the product of the angular velocity and a characteristic length). If $\overline{U}$ is taken to be the characteristic velocity, R the characteristic length, and the quantity V_w/R as the angular velocity then the Rossby number is simply the following:

$$Ro = \overline{U} / V_w \qquad (30)$$

Thus, in terms of these assumptions the swirl parameter is simply the inverse of twice the Rossby number:

$$S = 1 / 2 \, Ro \qquad (31)$$

If the effect of pressure integral of Equation (27) is taken into account using Bernoulli's Law to relate the static pressure in terms of the tangential velocity and assuming that the total pressure is simply atmospheric pressure, then the following result for the swirl parameter is obtained:

$$S = \frac{0.5\ V_w / \overline{U}}{1 - 0.25\ (V_w / \overline{U})^2} \qquad (32)$$

Other authors have defined the swirl parameter somewhat differently. Persen [346] has defined it as the ratio of the maximum tangential velocity divided by the mean axial velocity; he called this expression the "vortex strength." Love [175] has defined a "local vorticity characteristic" as one-half the circulation evaluated at the wall times the wall radius divided by the axial volumetric through-flow. If the assumption of helicoidal flow is made, then Love's definition reduces to simply two times the result of Equation (29). Lewellen [105] has defined an "interaction parameter between the circulation and the stream function" as the circulation times the wall radius divided by the mass flow rate divided by the density; when the helicoidal assumptions are substituted and the circulation is evaluated at the wall the result is four times that given for the swirl parameter in Equation (30). Murthy's result [71] is similar to that used by Love. Chigier [114,115], Lilley [121], and Yajnik [174] used definitions of swirl intensity that would result in the same equation as developed here for the same assumptions. However, if the pressure integral term is ignored, then all the swirl parameter definitions reduce to essentially the same result, differing only by a factor of 2 or 4. The justification for ignoring the pressure integral term can be seen by comparing Equations (29) and (32). For tangential velocities equal to or greater than twice the mean axial velocity, the swirl parameter found by Equation (32)—which includes the effect of the pressure integral term—is undefined becoming infinite for values twice the mean axial velocity and negative for larger tangential velocities. Equation (29) will be used here.

The free-stream velocity to be used in the Stanton number definition is defined to be:

$$W = (\bar{U}^2 + V_w^2)^{\frac{1}{2}} \qquad (33)$$

By eliminating the tangential velocity through the use of Equation (29), the free-stream velocity can be expressed as a function of the mean axial velocity and the swirl parameter:

$$W = \bar{U} \; (1 + 4 S^2)^{\frac{1}{2}} \qquad (34)$$

Using Equations (26) and (29) to eliminate V_w and solving for S results in the following expression:

$$S = K / m \bar{U} R \qquad (35)$$

The axial flux of angular momentum, K, can be approximated by assuming that its value at the tangential inlet air-line is the value at the start of the furnace column. This assumption is termed the perfect conversion assumption since it assumes that the angular momentum injected into the vortex chamber is not dissipated in the contraction of the flow field as it enters the bottom of the furnace column. By employing this assumption, K can be found directly from the following equation:

$$K = m_a V_a R_a \qquad (36)$$

where the subscript a designates conditions at the air inlet section. Thus m_a is the flow rate of the air only (m is the flow rate of the air plus the propane), V_a is the velocity of the air in the inlet air pipe, and R_a is the radius of the centerline of the inlet air pipe with respect to the centerline of the furnace column (which can be found to be 0.638 feet from Figure 5). Thus, S can be expressed as follows:

$$S = 2.66 \left[\frac{AFR}{1 + AFR}\right]\left[\frac{Va}{\overline{U}}\right] \qquad (37)$$

where AFR is the air/fuel ratio, and the values for R and R_a have been substituted to obtain the factor 2.66.

Calculation of Mean Axial Velocity

The mean axial velocity is found from the use of the continuity relationship:

$$\overline{U} = m / (\rho A_c) \qquad (42)$$

The mass flow rate in the above equation is the total of the air and propane flow rates given in Table 10, the area is the area of the furnace column (0.181 square feet), and the density is the mean density of the products of reaction evaluated at the average gas temperature.

By assuming that the perfect gas law holds for the reaction products, the mean axial velocity can be related directly to the average gas temperature:

$$\overline{U} = (m R_g T_m) / (p A_c) \qquad (43)$$

where R_g is the gas constant of the products of combustion and p is the pressure of the gas (which is assumed to be atmospheric throughout these calculations).

If the reaction is assumed to be complete at the first furnace column section, then the gas constant can be found from Table F-1 and the following relation:

$$R_g = \frac{R^*}{\sum_i x_i M_i} = \frac{1}{\sum_i (x_i / R_i)} \qquad (44)$$

where R^* is the universal gas constant (1545 ft-lbf/lbm-°R), x_i the mole fraction of each product constituent, M_i the molecular weight of each constituent, and R_i the gas constant of each constituent. Performing the calculation indicated above results in the following values of R_g:

TABLE 32

GAS CONSTANT OF PRODUCTS

(ft-lbf/lbm-°R)

Configuration	Condition		
	3	8	12
1	55.13	54.35	54.34
2	55.36	54.38	54.38
3	55.31	54.38	54.38

Since the angular momentum flux is being evaluated based upon conditions at the bottom of the furnace column, the mean axial velocity will also be evaluated at that section. Thus the average gas temperature as given in Table 14 for Station 1 will be used in Equation (43). The results of the calculation for the mean axial velocity are as follows:

TABLE 33

MEAN AXIAL VELOCITY

(ft/sec)

Configuration	Condition		
	3	8	12
1	9.08	17.2	22.9
2	9.30	16.8	22.1
3	9.24	16.6	21.7

Calculation of Inlet Air Velocity

The inlet air velocity may be found using the equation of continuity and the perfect gas law similar to the procedure used to find the mean axial velocity. The pressure measured in the inlet air supply-line is the total pressure whereas the static pressure is required to determine the density in the perfect gas law; however, by assuming that the total and static pressures are equal, and using Bernoulli's Equation for incompressible flow to find the velocity and thus the difference between static and total pressure, the validity of the original assumption can be substantiated.

Using the total air flow rate (for both inlet air lines) given in Table 10, and twice the area of each inlet line (0,0140 square feet) together with the density calculated as outlined above, the velocity in the inlet air-line can be calculated. The results are tabulated below:

TABLE 34

INLET AIR VELOCITY

(ft/sec)

Configuration	Condition		
	3	8	12
1	13.9	20.9	23.3
2	13.6	20.1	22.5
3	13.7	20.3	22.6

Calculation of Free-Stream Velocity

By substituting the calculated values of mean axial velocity and inlet air velocity together with the tabulated values of air/fuel ratio (from Table 10) the swirl parameter can be found from Equation (37). Use of Equations (33) and (29) then permit the determination of the free-stream velocity and the tangential velocity.

These results are presented in the following table:

TABLE 35

SWIRL PARAMETER CALCULATION

Configuration	Condition	S	W (ft/sec)	V_w (ft/sec)
1	3 8 12	3.82 3.08 2.58	69.9 107 120	69.4 106 118
2	3 8 12	3.64 3.03 2.58	68.4 103 116	67.7 102 114
3	3 8 12	3.69 3.10 2.64	68.9 104 116	68.2 103 115

Equivalent Flat Plate Length

In order to determine an equivalent flat plate length x for each furnace column section (given in terms of length L) some assumption is necessary. The one made here is that the helix pitch of the equivalent plate is determined by the ratios of the tangential to axial velocities via:

$$x = L \left(V_w / \overline{U} \right) = 2 L S \tag{45}$$

The heat flux recovered at each section will be ascribed to the mid-height of that section; thus the value of L for the first section is 0.50 feet, the second 1.50 feet and so on. Therefore the entire five-foot high furnace column is approximately equivalent to a 30-foot flat plate, the precise value dependent upon Configuration and Condition.

The free-stream Reynolds number may now be found using Equation (23) together with the values of W and x found in this section. These calculations are performed in Appendix D, and the results tabulated in Table D-6.

Entry Length Effect Upon Convection Conductance

The convection conductances calculated in Table 31 were obtained by using the convective heat flux measured for each furnace column section. Thus they are mean convection conductances with respect to the height of each section. Since the Stanton number correlation obtained in this section is to be evaluated as a function of the free-stream Reynolds number evaluated at the mid-point of each section, this mean value needs to be adjusted so that it too reflects the local value at the mid-height point.

To do this it is necessary to know how the convection conductance varies with respect to x and hence L. For simple linear flows past a flat plate this variation is to the minus one-fifth power, and this relation will be used to evaluate h_x, defined as the convection conductance at the mid-height of each section. If β is defined as the ratio of h_x to h (which is the mean conductance over the whole section), and if the variation of h_x is assumed to be as $x^{-0.2}$, then β can be expressed as follows:

$$\beta = \frac{0.80\,(x_t - x_b)\,x^{-0.2}}{x_t^{0.8} - x_b^{0.8}} \tag{46}$$

where x is the equivalent flat plate distance at the mid-height of each section, x_t at the top of the section, x_b at the bottom of the section.

Performing the above calculation for each section and Configuration/Condition results in the following values which are dependent only upon section: 0.919, 0.995, 0.998, 0.999, and 0.999 for sections 1 through 5 respectively.

Calculation of Colburn j-Factor

All the quantities necessary to form the product $St_x\ Pr^{2/3}$ have been defined where St_x indicates that the convection conductance to be used is h_x as defined above.

This calculation is presented in Appendix I with all the fluid properties evaluated at the film temperature which is defined to be the mean of the average fluid temperature and the wall temperature.

The j-Factor is graphed as a function of Re_x as calculated in Table D-6, in Figure 33. The least-squares curve-fit calculation has been performed in Appendix J in accordance with the procedure outlined in Reference [427].

On the basis of the Reynolds analogy, the Colburn j-Factor for turbulent flow past a flat plate is given as (from [416] page 153):

$$St_x\ Pr^{2/3} = 0.0288\ Re_x^{-0.20} \tag{47}$$

The prediction of this equation is given in Figure 33.

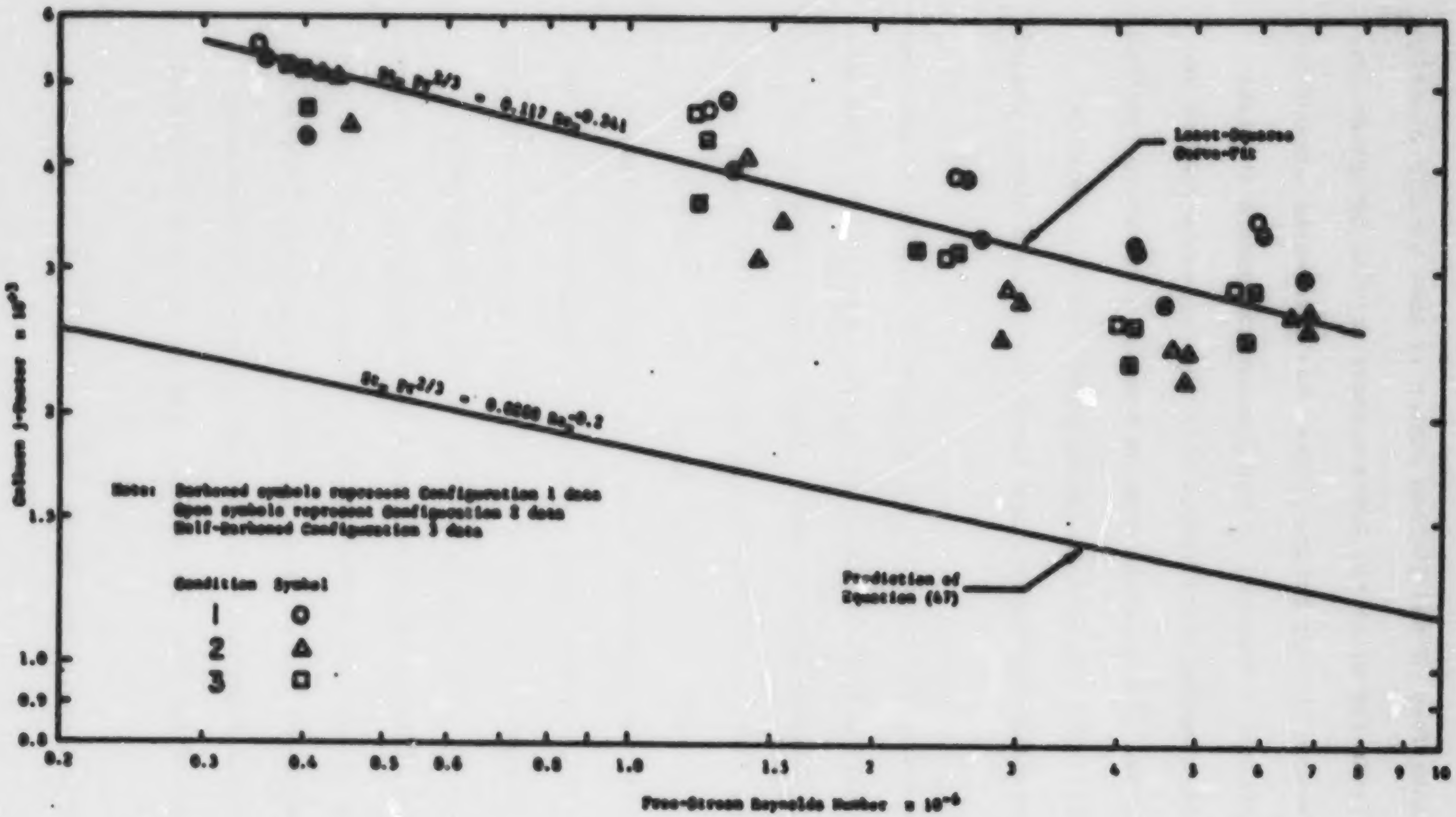

Figure 33. Colburn j-Factor vs. Free-Stream Reynolds Number

Chemical Reaction Effect

The preceding form of the Stanton number is that usually specified for non-reacting flows for which the thermodynamic driving potential is, in fact, the difference in temperature between the mixed-mean temperature and the wall temperature. However, in the present instance a chemical reaction process is occuring simultaneous with the convective/radiative heat transfer process. The question remains then: is the above temperature difference still the appropriate thermodynamic driving potential upon which the convection conductance and hence the Stanton number should be normalized?

This problem--usually termed "heat transfer in chemically reacting flows"--has been dealt with in a number of papers. Bartz [428] examined the turbulent heat transfer from a rocket combustion gas to a cooled nozzle wall. Chung [429] in a review work, has documented the state of knowledge for laminar reacting boundary layers noting, "for very few published works exist for turbulent non-equillibrium boundary layers." He identified the key parameter as the gas phase Damkohler number. For vanishing Damkohler number, the reaction rates are much slower than the transport rates and the condition is usually termed as "chemically frozen flows." For infinite values of Damkohler number just the reverse is true with the reaction rate dominating the transport rate; this case is usually referred to as "local chemical equillibrium flows." Because the maximum velocities experienced in this vortex flow are relatively small (on the order of 100 feet per second) this later state is assumed to hold true.

Chung [430] has shown that for the case of infinite Damkohler number, the "total enthalpy difference is basically the driving potential for heat transfer in a chemically reacting flow." If the kinetic energy of the flow field is negligible with respect to the chemical enthalpy (which is the case here) then this driving potential is simply the difference between the net enthalpy of reaction (which is the sum of the chemical enthalpies and the sensible enthalpy) evaluated at the mixed-mean temperature and at the wall temperature.

Conolly [431] has presented a means for accounting for an "equilibrium Prandtl number" in terms of the frozen Prandtl number and the Lewis number thereby accounting for diffusion effects upon the energy transport process. However, by assuming that the Lewis number for the gas is approximately one (which is a reasonable assumption for most gases) then equilibrium Prandtl number reduces to the frozen Prandtl number.

In general, the heat transfer process in the presence of flames is extremely complicated and has not been solved even for relatively simple cases. Emmons [432] in a recent survey paper has identified 16 significant dimensionless parameters (not including geometrical ones) that governing the heat transfer process in fires. The approach utilized here is to account for the effect of chemical reaction by defining an enthalpy potential.

Thus, the Stanton number can be expressed as follows:

$$St_x = \beta \, q_{conv} \,/\, \rho \, W \, \Delta H \qquad (48)$$

where β has been defined in Equation (46), q_{conv} is the convective heat transfer flux as given in Table 30, ρ the gas density evaluated at the film temperature, W the free-stream velocity (given in Table 35), and ΔH the enthalpy potential for heat transfer.

The enthalpy potential is expressed here in the following manner:

$$\Delta H = \Delta H_c + H_r^* - H_p^* \qquad (49)$$

where ΔH_c is the net enthalpy of combustion (defined in Appendix F and calculated in Table F-3), H_p^* is the sensible enthalpy of the products (determinable from the JANAF Tables [404, 405] as a function of product's temperature) and H_r^* is the sensible enthalpy of the reactants (similarly a function of the temperature).

If the flow field is assumed to be such that the reactants are heated to the mixed-mean temperature and the products are generated at the wall temperature, then the quantity H_r^* is evaluated at the average temperature as tabulated in Table 14 and the quantity H_p^* is evaluated at the gas temperature at the wall as given in Table 11-13.

The Stanton number obtained using this value of enthalpy potential is called the "modified Stanton number" here. Multiplying this Stanton number by the Prandtl number raised to the 2/3 power results in the modified Colburn j-Factor. These calculations are given in Table I-2 and graphically presented as a function of the free-stream Reynolds number in Figure 34. The least-squares line is calculated in Appendix J.

In Figure 35 the same data as given in Figure 34 is presented with the exception of the 9 data-points at section 5 (the top-most section of the furnace column). Two least-squares lines are shown: one through the data of sections 1 and 2 (the bottom two sections) and one for sections 2 through 4. These equations are calculated in Appendix J.

Also shown in Figure 35 is the prediction of the Colburn j-Factor for laminar flows which is given by (taken from page 153 of Reference [416]):

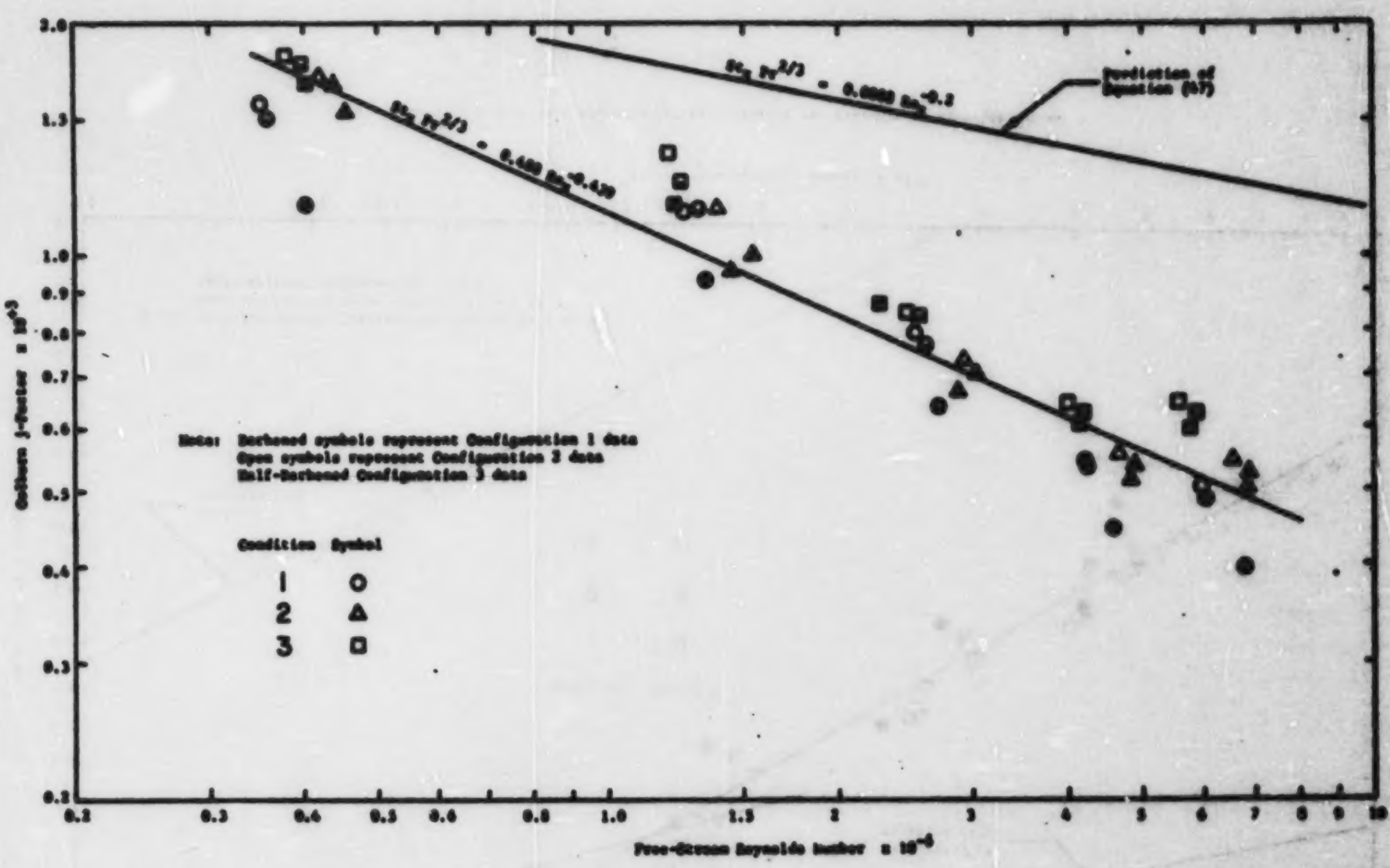

Figure 34. Modified Colburn j-Factor vs. Free-Stream Reynolds Number

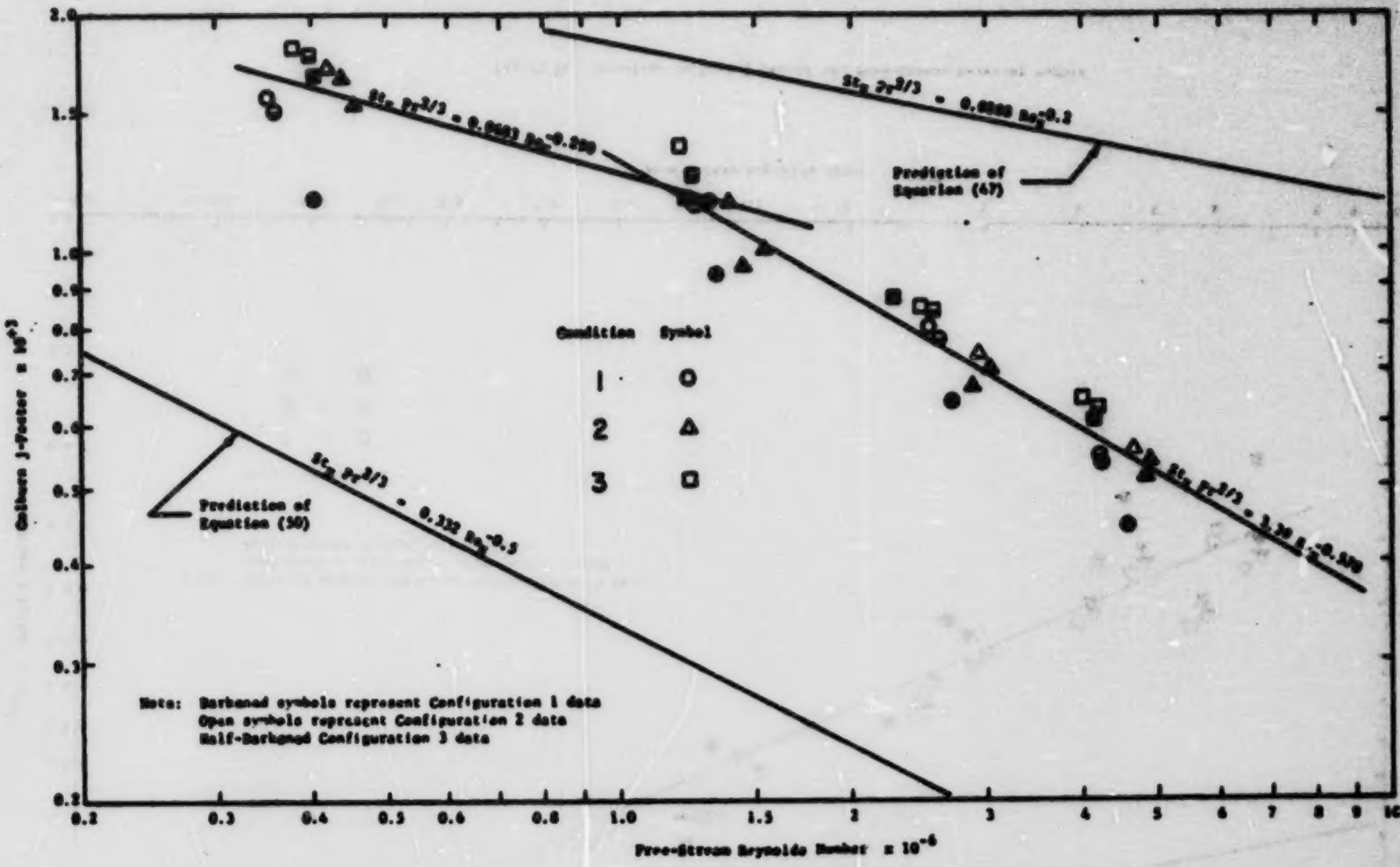

Figure 35. Modified Colburn j-Factor vs. Free-Stream Reynolds Number

$$St_x \, Pr^{2/3} = 0.332 \, Re_x^{-0.50} \qquad (50)$$

The data of sections 1 and 2 agrees with the slope of the turbulent flow prediction, Equation (47), whereas the slope of the data for sections 2 through 4 more closely agrees with the laminar flow prediction given above. This change in slope is also present in Figure 33 although the effect is not as dramatic.

There are three likely causes of the slope change:

(1) vortex decay,

(2) entry-length effects, and

(3) chemical reaction variation.

This latter effect would alter the formulation of the enthalpy potential equation as given in Equation (49) for each section. Since the slope change seen in Figure 35 is much larger than that of Figure 33, the change in the chemical reaction process with respect to furnace column height is the most-likely cause of this effect.

APPENDIX A

EQUIPMENT CALIBRATION

Temperature Measurement

Three different temperature measuring devices were used for data recording during the experimental phase of this investigation:

(1) A Honeywell Model No. Y153X82-C-II-III-13, 24-channel, 0 to 50 millivolt strip-chart recorder compensated for chromel-alumel thermocouple material (Type T).

(2) A Daystrom Model No. 6702, 12-channel, minus 100 to plus 150 degrees Fahrenheit strip-chart recorder compensated for copper-constantan thermocouple material (Type T).

(3) A Hewlet-Packard Model No. 680, single-channel, 0 to 100 volts in ten calibrated spans (only the 0 to 50 millivolt span was used) strip-chart recorder.

(4) A Hewlet-Packard 24-channel digital recording system consisting of the following:

(a) a Model No. 2901A input Scanner,
(b) a Model No. 2402A Integrating Digital Voltmeter, and
(c) a Model No. 5050B Digital Recorder.

The two Hewlett-Packard recorders were not compensated for a specific thermocouple material or reference temperature and required the use of an ice-bath together with an insulated junction box.

The Honeywell and Daystrom strip-chart recorders, items 1 and 2 in the above list, were calibrated with a Leeds and Northrup Millivolt Potentiometer (Model Number 8686-2, Serial Number 1789249) in accordance with the procedure given in Reference [433]. The results of the calibration are given in Table A-1 for the Honeywell recorder for two of its 24 channels and Figure A-1 for the Daystrom recorder for one of its 12 channels.

TABLE A-1

HONEYWELL RECORDER CALIBRATION (Serial No. D 1168326002)

Channel Number	Potentiometer Input (mv)	Recorder Output (mv)	Reference Temperature (°F)
6	0	0.0	69.2
	5	5.0	
	10	10.0	
	15	15.0	
	20	20.0	
	25	25.0	
	30	30.0	
	35	35.0	
	40	40.0	
	45	44.9	
	46	45.9	
	47	46.9	
42	0	0.1	68.0
	1	1.0	
	2	2.0	
	3	3.0	
	4	4.0	
	5	5.0	
	10	10.0	
	15	15.0	
	20	20.0	
	25	25.0	
	30	30.0	
	35	35.0	
	40	40.0	
	45	44.9	
	46	46.0	
	47	46.9	

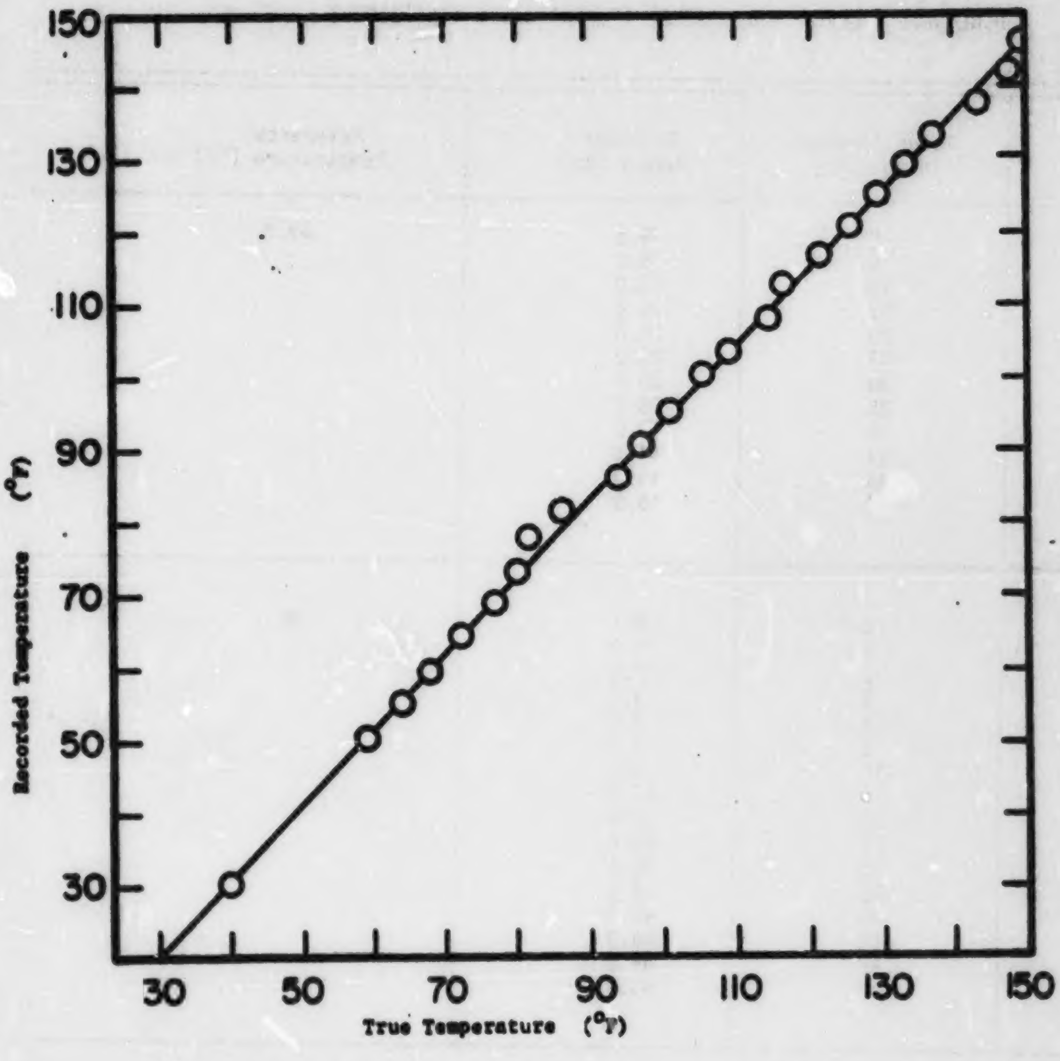

Figure A-1. Daystrom Recorder Calibration (Serial No. 17219-1)

The Hewlett-Packard strip-chart recorder, item 3, was calibrated using a Honeywell Rubicon Potentiometer (Model Number 2745, Serial Number 115587). Use of the internal adjustments accessible on the recorder always made it possible to obtain a linear, accurate (within the pen-width) indication of the input voltage; hence, no calibration curve is presented for this recorder.

The Hewlett-Packard digital recording system, item 4, included a self-contained calibration device which was used to check the accuracy of the measurement system. Since the calibration never deviated more than one one-thousandth of a millivolt, no correction was applied to the data obtained with this device.

Two types of thermocouple materials were used: chromel-alumel (Type K) and copper-constantan (Type T). All the Type T data were measured exclusively on the Daystrom recorder, whereas the Type K were measured on all of the other three recorders. All thermocouple materials were purchased from Honeywell, Inc. The stated accuracy [434] of the thermocouples were as follows:

(1) copper-constantan: ±1½°F in the range used.

(2) chromel-alumel: ±4°F for temperatures below 530°F, and

±0.75% of the actual temperature recorded for temperatures above 530°F.

The stated accuracy [434] of the standard grade extension wire were as follows:

(1) copper-constantan: ±1½°F, or

±0.75% of the temperature difference between the connection heat and the reference junction,

whichever is less.

(2) chromel-alumel: ±4°F, or

±2.5% of the temperature difference between the connection heat and the reference junction,

whichever is less.

For the Honeywell and Daystrom strip-chart recorders the reference junction temperature was approximately room temperature. The maximum connection head temperature experienced was approximately 110°F. Thus for these recorders the limits of error for the extension wire were ±0.30°F for the copper-constantan and ±1.0°F for the chromel-alumel. However, most of the thermocouples were located sufficiently far from the incinerator that the connection head temperature was very nearly that of the reference temperature. For the two Hewlett-Packard recorders the junction temperature was 32°F; thus the limits of error for the extension wire for these recorders were (based upon the maximum connection head temperature of 110°F) ±0.60°F for the copper-constantan and ±2.0°F for the chromel-alumel.

End-to-end calibration checks for the entire temperature measuring system, thermocouple/extension wire/recorder, were performed using an ice-bath and boiling water together with a highly-accurate Mercury thermometer. In addition, intermediate temperature points were also checked by using a variac with a resistance-heated container of water. The results of this calibration indicated that the temperature could be measured within approximately ±0.5°F over this range.

Pressure Measurement

In addition to the barometric pressure, three system pressure measurements were also made: each of the two air supply lines and the propane supply line. These pressure measurements were made just upstream of the flow control valve and the rotameter in such a fashion as to obtain the total pressure.

The two air pressures were measured on a Meriam Instrument Company mercury manometer (Type W, Model Number 33KA35, Serial Number T20133) of range 0 to 100 inches. The propane pressure was measured with a U-type Meriam Instrument Company water manometer (Model Number 10AA25) of range 0 to 30 inches.

The barometric pressure was obtained from a Precision Thermo. and Inst. Company of Philadelphia precision barometer located within the laboratory.

Flow Measurement

Eight rotameters were utilized to measure the required flow rates: one for each air supply (two), one for the propane supply, and one for each cooling water section(five). All of these flow meters were series 10A3000 Glass Tube Indicating Rotameters manufactured by the Fisher and Porter Company of Warminster, Pennsylvania. The specified [435] accuracy and repeatability were ±2% and 0.25% of full-scale, respectively.

The two air flow meters were rated for 41.0 SCFM (standard cubic feet per minute) of air at STP (standard temperature and pressure—here taken to be 70°F and 14.7 psi) at 100% of scale. These rotameters were accurate to within ±0.82 SCFM and repeatable to within ±0.1025 SCFM. These devices were calibrated against a square-edged orifice of rated accuracy ±0.5%. The calibration procedure consisted of setting the control valve to provide the desired reading on the rotameter, then measuring the temperature and pressure of the air stream, with the system described in the preceeding Chapter II; the scale reading in percent was converted to

SCFM using the pressure and temperature data according to the procedure outlined by the manufacturer [436]. At the same time, the pressure drop across the square-edged orifice, the pressure, and the temperature were used in accordance with standard procedures [437] to obtain the actual flow rate in cubic feet per minute. Thus it was possible to develop a calibration curve which would yield actual flow rate in cubic feet per minute from the calculated flow rate (in SCFM) by means of the known scale reading (in %) and the measured pressure and temperature. These calibrations, for air flow meters number 1 and 2, are given as Figures A-2 and A-3.

The propane flow meter was rated for 4.6 SCFM of air at STP: thus its stated accuracy and repeatability was ±0.092 and ±0.0115 SCFM of air, respectively. Since the propane was supplied in one-hundred pound tanks, it was more convenient to calibrate the rotameter by a weight-change procedure using a standard beam-balance scale. The calculated flow rate (including the specific gravity correction) in accordance with the manufacturer's specification [436] was found to agree to within 1% of the measured weight change; as a result, no calibration curve was used.

Each water flow rate rotameter was rated for 1.52 GPM (gallons per minute) of water at STP; thus, the stated accuracy and repeatability was ±0.0304 and ±0.00376 GPM of water, respectively. Each of the five rotameters were calibrated by means of a weight change procedure which entailed collecting the water through-flow in portable tanks and obtaining the tare weight on a beam-balance scale. The water flow was achieved by means of the boost pump described in Chapter II on the city water supply line. Due to transients in water pressure, there were inevitable momentary drop-offs in flow rate. This flow disturbance together with the start-up and shut-

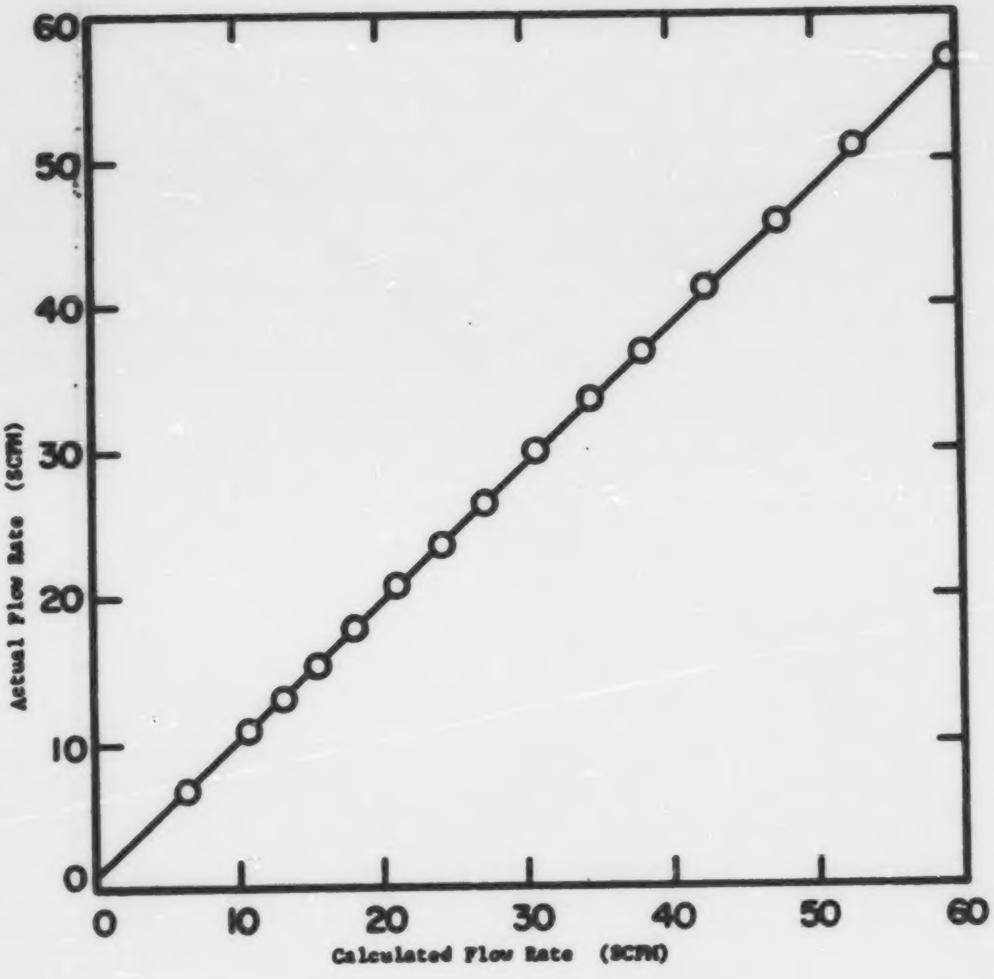

Figure A-2. Air Rotameter No. 1 Calibration

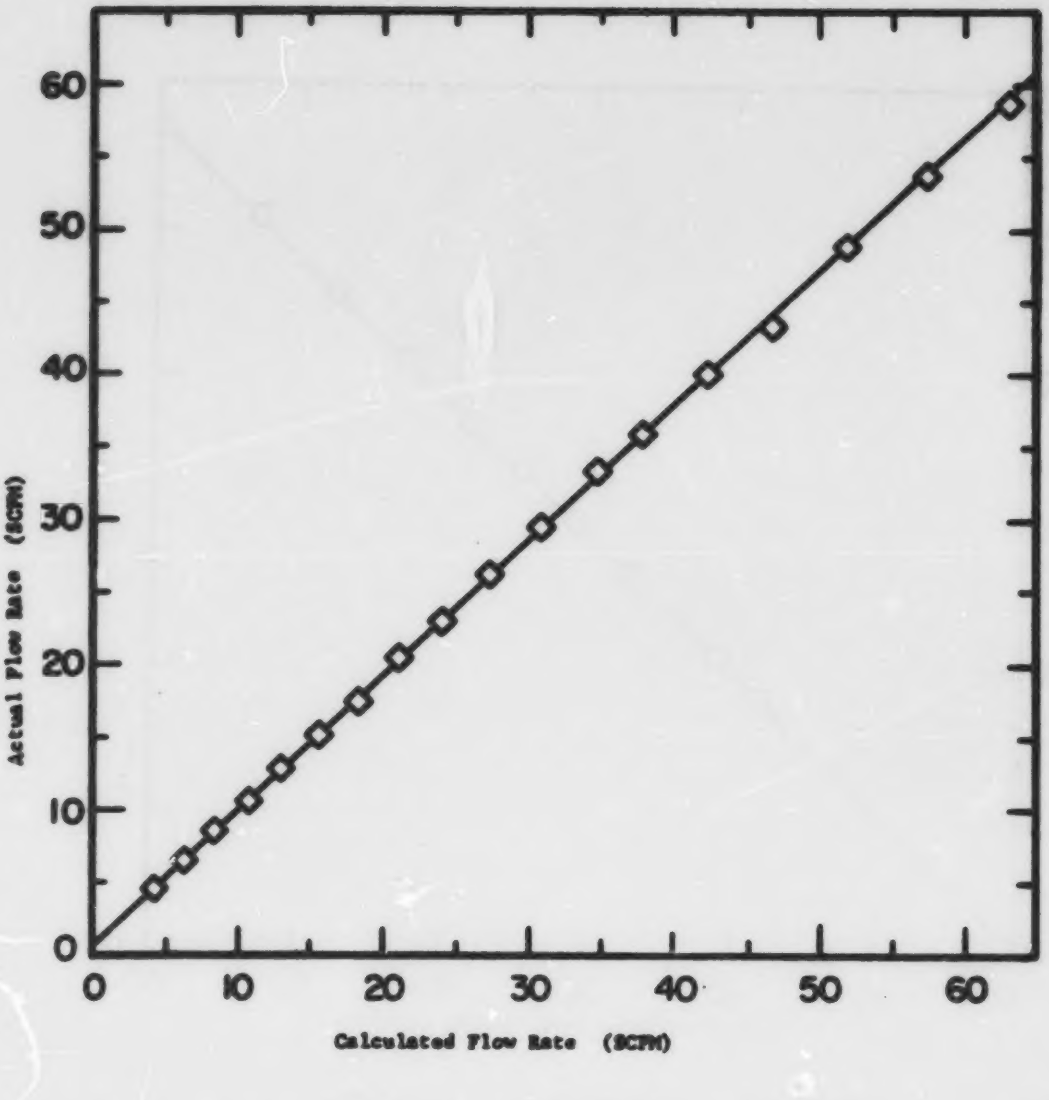

Figure A-3. Air Rotameter No. 2 Calibration down transients associated with this procedure resulted in a somewhat lower level of confidence in the calibration obtained, although the degree of agreement was within the stated accuracy of the rotameter over the range of interest (approximately 45 to 70% of full-scale). In addition, since in the actual operation of the incinerator these same momentary drop-offs in flow could be expected to occur, even an absolutely precise calibration curve could not account for these effects. Hence it was decided that the predicted flow rates using the observed percent of full-scale reading would be used without further modification to obtain the water flow rate. The water flow rate in gallons per hour was thus obtained from the rotameter reading in percent by multiplying by a factor of 0.912.

APPENDIX B

DATA REDUCTION PROCEDURE

General Procedure

Due to the large number of data runs that required reduction, it became both expedient and necessary to develop a data analysis algorithm. Available in the laboratory was a Monroe Model 1655 Electronic Programmable Display Calculator together with a card reader that provided a programming capability of 126 steps [438]. Once the programs had been written, debugged, and punched-out then all future operations required only that the cards be fed into the reader and stored in the machine's internal memory pripr to each data reduction session.

The data was supplied through the key-board to the operating program with the results presented in the electronic display.

Heat Recovery Program

The heat recovery program was designed to utilize the cooling water temperature and flow rate data to determine the heat transferred to each section of cooling water and the total heat recovered in all five cooling sections. The basis of the program was the following equation:

$$q = m \, c_p \, \Delta T \qquad \text{(B-1)}$$

where q is the heat transfer rate in Btu/hour, m the water flow rate in pounds per hour, c_p the specific heat at constant pressure (the value of 1.0 was used for all the calculations), and ΔT the temperature difference of the water outlet temperature minus the inlet temperature.

The program was designed so that the water inlet temperature, which was common to all five cooling-water lines, was loaded first. Then in sequence each cooling-coil section's outlet temperature and flow rate in gallons per hour (obtained by multiplying the rotameter percent reading by the factor 0.912) were loaded. The program then provides the heat transferred to each section and the total of all five sections in units of Btu per hour. To obtain the heat flux recovered at each section it was then only necessary to divide each section's heat recovery rate by the area of each section (1.508 square feet).

Flow Rate Program

The purpose of the flow rate program was to utilize the rotameter percent full-scale data for the two air and one propane control valve settings to obtain the actual mass flow rate for each of these quantities. The required input was the rotameter reading, the pressure, and the temperature of each flow supply and the barometric pressure. The program proceeds in the following fashion. It utilizes the rotameter reading in percent (defined as D), the rated rotameter capacity in SCFM (defined as C, which is equal to 41.0 for the air rotameters and 4.6 for the propane rotameter), and the pressure and temperature of the flowing gas. Three correction factors are required as follows:

(1) the specific gravity correction factor (defined as H) which is equal to the square root of the specific gravity of the gas to the specific gravity of air(thus it is equal to 1.00 for air and 1.22 for propane),

(2) the pressure correction factor (defined as I) which is equal to the square root of the ratio of 14.7 to the actual flowing gas pressure in pounds per square inch absolute, and

(3) the temperature correction-factor (defined as J) which is equal to the square root of the ratio of the actual flowing gas temperature in degrees Rankine to the standard temperature (530°R).

The predicted flow rate according to rotameter theory [436] is then:

$$SCFM = D \times C / (H \times I \times J) \qquad \text{(B-2)}$$

At this point in the program there is a halt and the above calculated value is corrected by the calibration curves given in Figures A-2 and A-3 (for propane, the calculated value is uncorrected). After the correction is inserted into the program, the actual flow rate in pounds per hour is computed directly by using the equation of state together with the continuity equation.

The air/fuel ratio is obtained simply by dividing the total flow rate of the two air supplies by the flow rate of the propane.

APPENDIX C

CALCULATION OF AVERAGE TEMPERATURE

The concept of mixed-mean temperature is commonly used [400] to correlate convective heat transfer coefficient for internal flows. This temperature is defined by Equation (1) given in Chapter III—but for the assumption of uniform axial profile, it can be written in the following form:

$$T_m = \frac{1}{A_c} \int_0^R T\, r\, dr \qquad \text{(C-1)}$$

The justification of the assumption of a uniform axial profile has been presented in Chapter III. The temperature so obtained will be called the "average" gas temperature since it represents a simple area-average of the temperature data presented in Tables 11-13.

This average is obtained in the following fashion:

(1) the temperature data for two adjoining radii (say at 0.25 and 0.50 inches from the wall) are averaged, then

(2) the area of the annulus bounded by these two radii is calculated (for these radii it would be 3.936 square inches), then

(3) the product of the averaged temperature and its respective annular area is formed;

(4) this procedure is continued for all twelve annuli, then the twelve temperature-area products are summed and the total is divided by the total area of the cross-section (26.058 square inches) yielding the "average" temperature.

The results of this calculation procedure are presented in Tables C-1 through C-5 for each of the five thermocouple stations and for each combination of Exit Configuration and Condition.

TABLE C-1

AVERAGE VORTEX GAS TEMPERATURE AT STATION 1

Distance From Wall (inches)	Annular Area (sq. in.)	Average Annular Temperature for Configuration 1			Average Annular Temperature for Configuration 2			Average Annular Temperature for Configuration 3		
		Cond. 3	Cond. 8	Cond. 12	Cond. 3	Cond. 8	Cond. 12	Cond. 3	Cond. 8	Cond. 12
0.00										
	4.328	471	586	646	583	676	736	558	646	702
0.25										
	3.935	1114	1284	1387	1246	1372	1464	1203	1310	1400
0.50										
	3.542	1506	1638	1728	1565	1650	1724	1554	1612	1686
0.75										
	3.149	1634	1739	1820	1670	1735	1802	1690	1740	1804
1.00										
	2.757	1690	1783	1862	1706	1762	1827	1722	1769	1836
1.25										
	2.366	1706	1796	1873	1714	1772	1838	1724	1756	1827
1.50										
	1.971	1706	1796	1862	1716	1770	1836	1716	1744	1808
1.75										
	1.579	1676	1780	1846	1710	1756	1825	1706	1733	1794
2.00										
	1.186	1632	1746	1824	1686	1732	1806	1668	1704	1772
2.25										
	0.793	1594	1717	1792	1650	1706	1780	1604	1654	1724
2.50										
	0.401	1558	1686	1758	1598	1661	1744	1551	1598	1674
2.75										
	0.053	1556	1654	1736	1556	1616	1706	1538	1576	1656
2.88										
Sum of Temperature-Area Products		35,507	38,571	40,631	37,093	39,096	40,949	36,824	38,398	40,201
Average Temperature (°F)		1363	1480	1560	1424	1500	1572	1413	1474	1543

TABLE C-2

AVERAGE VORTEX GAS TEMPERATURE AT STATION 2

Distance From Wall (inches)	Annular Area (sq. in.)	Average Annular Temperature for Configuration 1			Average Annular Temperature for Configuration 2			Average Annular Temperature for Configuration 3		
		Cond. 3	Cond. 8	Cond. 12	Cond. 3	Cond. 8	Cond. 12	Cond. 3	Cond. 8	Cond. 12
0.00										
	4.328	510	617	712	512	620	706	494	578	703
0.25										
	3.935	1038	1208	1428	1042	1152	1262	997	1141	1256
0.50										
	3.542	1284	1429	1643	1262	1366	1472	1248	1348	1470
0.75										
	3.149	1390	1525	1598	1376	1470	1574	1392	1470	1578
1.00										
	2.757	1450	1580	1654	1446	1536	1636	1463	1536	1632
1.25										
	2.366	1474	1596	1694	1484	1566	1666	1490	1552	1640
1.50										
	1.971	1474	1584	1672	1496	1571	1661	1483	1542	1620
1.75										
	1.579	1448	1562	1650	1481	1554	1638	1461	1524	1594
2.00										
	1.186	1411	1538	1638	1459	1529	1614	1420	1500	1576
2.25										
	0.793	1394	1538	1643	1437	1512	1596	1380	1478	1560
2.50										
	0.401	1379	1542	1650	1411	1492	1578	1368	1458	1544
2.75										
	0.053	1362	1514	1622	1383	1464	1545	1372	1454	1547
2.88										
Sum of Temperature-Area Products		31,293	34,744	38,007	31,406	33,856	36,393	31,048	33,355	36,051
Average Temperature (°F)		1201	1333	1459	1205	1299	1397	1192	1280	1384

TABLE C-3

AVERAGE VORTEX GAS TEMPERATURE AT STATION 3

Distance From Wall (inches)	Annular Area (sq. in.)	Average Annular Temperature for Configuration 1			Average Annular Temperature for Configuration 2			Average Annular Temperature for Configuration 3		
		Cond. 3	Cond. 8	Cond. 12	Cond. 3	Cond. 8	Cond. 12	Cond. 3	Cond. 8	Cond. 12
0.00										
	4.328	336	522	647	402	477	560	400	478	560
0.25										
	3.935	773	1034	1155	826	966	1076	826	968	1070
0.50										
	3.542	1058	1239	1364	1023	1169	1286	1027	1172	1269
0.75										
	3.149	1150	1318	1439	1133	1274	1383	1120	1265	1362
1.00										
	2.757	1211	1360	1472	1207	1329	1424	1180	1301	1402
1.25										
	2.366	1236	1364	1476	1230	1340	1437	1212	1303	1409
1.50										
	1.971	1236	1362	1461	1237	1338	1439	1220	1301	1398
1.75										
	1.579	1216	1356	1454	1241	1338	1446	1220	1306	1400
2.00										
	1.186	1212	1352	1470	1241	1346	1461	1198	1299	1410
2.25										
	0.793	1222	1387	1508	1235	1353	1466	1175	1288	1402
2.50										
	0.401	1207	1415	1534	1214	1336	1450	1170	1273	1388
2.75										
	0.053	1182	1396	1516	1184	1306	1424	1175	1267	1388
2.83										
Sum of Temperature-Area Products		25,432	30,009	33,061	25,812	28,871	31,558	25,477	28,443	30,994
Average Temperature (°F)		976	1152	1269	991	1108	1211	978	1092	1190

TABLE C-4

AVERAGE VORTEX GAS TEMPERATURE AT STATION 4

Distance From Wall (inches)	Annular Area (sq. in.)	Average Annular Temperature for Configuration 1			Average Annular Temperature for Configuration 2			Average Annular Temperature for Configuration 3		
		Cond. 3	Cond. 8	Cond. 12	Cond. 3	Cond. 8	Cond. 12	Cond. 3	Cond. 8	Cond. 12
0.00										
	4.328	245	328	435	283	398	466	302	398	460
0.25										
	3.935	564	716	928	607	796	913	648	796	902
0.50										
	3.542	828	1010	1175	826	989	1106	854	976	1084
0.75										
	3.149	945	1124	1250	941	1099	1203	951	1078	1184
1.00										
	2.757	998	1171	1286	1002	1150	1250	1010	1124	1237
1.25										
	2.366	1036	1186	1280	1038	1170	1278	1046	1146	1260
1.50										
	1.971	1048	1186	1273	1060	1177	1288	1061	1154	1260
1.75										
	1.579	1034	1171	1288	1074	1182	1292	1061	1152	1254
2.00										
	1.136	1036	1171	1303	1084	1196	1310	1046	1156	1258
2.25										
	0.793	1063	1220	1348	1086	1211	1325	1029	1158	1260
2.50										
	0.401	1068	1276	1400	1074	1207	1320	1029	1148	1262
2.75										
	0.053	1048	1282	1414	1054	1190	1301	1034	1148	1274
2.88										
Sum of Temperature-Area Products		20,641	24,505	27,997	21,133	24,866	27,562	21,422	24,417	27,023
Average Temperature (°F)		792	940	1074	811	954	1058	822	937	1037

TABLE C-5

AVERAGE VORTEX GAS TEMPERATURE AT STATION 5

Distance From Wall (inches)	Annular Area (sq. in.)	Average Annular Temperature for Configuration 1			Average Annular Temperature for Configuration 2			Average Annular Temperature for Configuration 3		
		Cond. 3	Cond. 8	Cond. 12	Cond. 3	Cond. 8	Cond. 12	Cond. 3	Cond. 8	Cond. 12
0.00	4.328	211	289	416	265	348	416	262	336	394
0.25	3.935	450	600	845	534	708	824	552	678	790
0.50	3.542	634	871	1048	710	902	1019	744	862	985
0.75	3.149	760	1000	1134	816	1000	1108	832	955	1074
1.00	2.757	848	1046	1168	871	1041	1148	884	1006	1122
1.25	2.366	882	1057	1173	905	1054	1164	918	1028	1143
1.50	1.971	898	1054	1160	928	1054	1166	930	1034	1141
1.75	1.579	892	1040	1152	938	1059	1170	928	1029	1133
2.00	1.186	896	1040	1173	947	1070	1188	907	1020	1129
2.25	0.793	926	1092	1226	953	1088	1209	888	1014	1124
2.50	0.401	945	1167	1299	953	1101	1222	890	1012	1132
2.75	0.053	934	1184	1325	945	1098	1218	898	1020	1152
2.88										
Sum of Temperature-Area Products		17,148	21,576	25,459	18,492	22,384	25,124	18,650	21,522	24,261
Average Temperature (°F)		658	828	977	710	859	964	716	826	931

APPENDIX D

REYNOLDS NUMBER CALCULATIONS

There are many possible definitions of Reynolds number because of the many choices available of characteristic dimension, characteristic velocity, and temperature at which fluid properties are evaluated. The absolute viscosity of the vortex gas is evaluated as a function of gas temperature using the flue gas viscosity curve of Maxwell ([401], page 191) which is given as Figure D-1.

Axial Reynolds Number

For the axial Reynolds number, the quantity D in Equation (2) given in Chapter III is the furnace column diameter, 0.4800 feet. This Reynolds number must be calculated separately for the exit and inlet Configuration investigations because the total mass flow rates varied slightly as well as the vortex gas temperature.

The axial Reynolds number for the exit Configuration investigation is presented in Table D-1 where the absolute viscosity has been evaluated at the average furnace column temperature which is obtained by finding the mean of the five Station average temperatures.

The axial Reynolds number for the inlet Configuration investigation is presented in Table D-2. Since temperature profiles were not available for these data, the average of the temperature measurements given in Table 16 was used to evaluate viscosity.

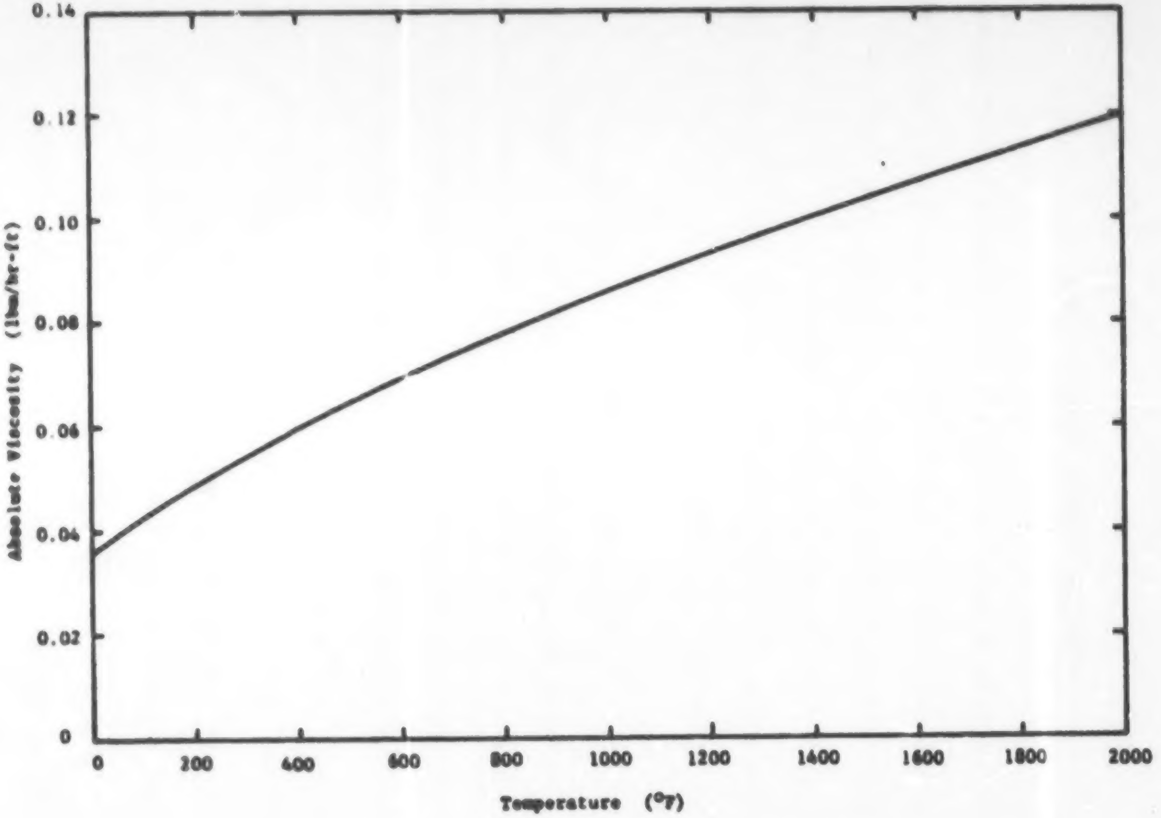

Figure D-1. Absolute Viscosity of Flue Gas at 1 Atm.

TABLE D-1

AXIAL REYNOLDS NUMBER CALCULATION FOR 3 EXIT CONFIGURATIONS

Exit Configuration	Condition	Average Furnace Column Gas Temperature (°F)	Absolute Viscosity (lbm/hr-ft)	Total Flow Rate (lbm/hr)	Axial Reynolds Number
1	3	980	0.0850	124.6	3890
	8	1147	0.0915	225.0	6520
	12	1268	0.0958	287.8	7970
2	3	1028	0.0871	123.0	3750
	8	1144	0.0912	216.9	6310
	12	1240	0.0940	275.6	7780
3	3	1024	0.0880	123.0	3710
	8	1122	0.0908	217.2	6350
	12	1217	0.0939	274.5	7760

TABLE D-2

AXIAL REYNOLDS NUMBER CALCULATION FOR 3 INLET CONFIGURATIONS

Inlet Configuration	Condition	Average* Furnace Column Gas Temperature (°F)	Absolute Viscosity (lbm/hr-ft)	Total Flow Rate (lbm/hr)	Axial Reynolds Number
A	3	981	0.0823	123.1	3970
	8	1133	0.0911	219.0	6380
	12	1295	0.0968	281.5	7710
B	3	988	0.0859	123.9	3830
	8	1265	0.0959	218.7	6050
	12	1435	0.1016	279.9	7310
C	3	1290	0.0967	123.4	3390
	8	1376	0.0998	219.2	5820
	12	1457	0.1022	281.6	7310

*This average was obtained by finding the mean of the temperature data at the flow stations at 1.75 inches from the wall.

Exit Reynolds Number

In order to assess the effect of changing the exit orifice diameter (exit Configurations 1-3) it is useful to formulate a Reynolds number based upon the total flow rate and the orifice diameter with the viscosity evaluated at the average gas temperature at Station 5 (presumed to be approximately the same as the temperature at the exit orifice location) using the flue gas curve given as Figure D-1. The Reynolds number so calculated is referred to as the "exit Reynolds number". The calculation procedure and the results are given in Table D-3.

Inlet Reynolds Number

To assess the inlet Configuration effect, an "inlet Reynolds number" analogous to that described in the preceeding paragraph is also defined. Here the characteristic dimension is the bore of the inlet air-line and the viscosity is found from tables available for the properties of air ([439], page 555) as a function of the measured air temperature at the inlet. This calculation is given in Table D-4.

Length Reynolds Number

In order to assess entry-length effects, the Reynolds number can be calculated using furnace column height as the characteristic dimension instead of a diameter. The resulting equation is given as Equation (3) in Chapter III. Since there are five discrete heat transfer sections (i.e. cooling-water sections) there are five discrete values of L: 1, 2, 3, 4, and 5 feet. The Reynolds number so obtained is referred to here as the "length Reynolds number" and as is apparent from Equation (3) is equal to the axial Reynolds number times the local value of L divided by the

TABLE D-3

EXIT REYNOLDS NUMBER CALCULATION

Exit Configuration	Exit Orifice Diameter (ft)	Condition	Average Gas Temperature at Station 5 (°F)	Absolute Viscosity (lbm/hr-ft)	Total Flow Rate (lbm/hr)	Exit Reynolds Number
1	0.1667	3	688	0.0718	124.6	13,260
		8	880	0.0795	225.0	21,620
		12	977	0.0853	287.8	25,780
2	0.3333	3	710	0.0743	123.0	6,320
		8	888	0.0808	216.9	10,250
		12	984	0.0848	275.6	12,410
3	0.5000	3	716	0.0746	123.0	4,200
		8	886	0.0794	217.2	6,970
		12	931	0.0836	274.5	8,360

TABLE D-4

INLET REYNOLDS NUMBER CALCULATION

Inlet Configuration	Inlet Air-Line Diameter (feet)	Condition	Average Air Inlet Temperature (°F)	Absolute Viscosity (lbm/hr-ft)	Average Air Flow Rate (lbm/hr)	Inlet Reynolds Number
A	0.07292	3	67.0	0.04384	57.98	22,930
		8	65.5	0.04383	104.2	41,420
		12	66.0	0.04377	136.0	53,460
B	0.08854	3	68.2	0.04391	58.01	19,000
		8	71.0	0.04409	104.0	33,920
		12	70.0	0.04403	133.2	43,500
C	0.1335	3	68.8	0.04395	57.77	12,540
		8	70.2	0.04406	104.3	22,590
		12	68.5	0.04393	134.2	29,140

furnace column diameter (D). However, since the length Reynolds number is intended to be a local parameter with respect to furnace column height, the property of absolute viscosity should be evaluated at the local average temperature (given in Tables 11-13 for each of the five Stations which are located at the mid-heights of each respective furnace column section). This calculation is presented in Table D-5.

Free-Stream Reynolds Number

The free-stream Reynolds number has been defined by Equation (23) in Chapter IV. The values of free-stream velocity have been presented in Table 35. The equivalent flat-plate distances for the mid-height of each furnace column section can be found from using Equation (45) with the tabulated values of swirl parameter given in Table 35. The value of L used in this equation is the mid-height of each section since the equivalent flat-plate distance sought is at this point. The fluid properties are evaluated at the film temperature which is defined as the mean of the average temperature (given in Table 14) and the gas temperature at the wall (given in Tables 11-13). The viscosity is evaluated using Figure D-[illegible] and the density using the perfect gas law for gas constants given in Table 32.

TABLE D-5

LENGTH REYNOLDS NUMBER CALCULATION

Configuration	Condition	Furnace Column Section	L/D	Average Gas Temperature (°F)	Absolute Viscosity (lbm/hr-ft)	Local Axial Reynolds Number	Length Reynolds Number
1	3	1	2.08	1363	0.0993	3330	6,930
		2	4.17	1201	0.0937	3530	14,720
		3	6.25	976	0.0854	3870	24,190
		4	8.33	792	0.0778	4250	35,400
		5	10.42	658	0.0719	4600	47,900
	8	1	2.08	1480	0.1032	5780	12,000
		2	4.17	1333	0.0982	6080	25,400
		3	6.25	1152	0.0919	6490	40,600
		4	8.33	940	0.0838	7120	59,300
		5	10.42	828	0.0794	7520	78,400
	12	1	2.08	1560	0.1058	7220	15,000
		2	4.17	1459	0.1026	7440	31,000
		3	6.25	1269	0.0960	7950	49,700
		4	8.33	1074	0.0890	8580	71,500
		5	10.42	977	0.0853	8950	93,300
2	3	1	2.08	1424	0.1014	3220	6,700
		2	4.17	1205	0.0938	3480	14,500
		3	6.25	991	0.0860	3790	23,700
		4	8.33	811	0.0788	4140	34,500
		5	10.42	710	0.0741	4400	45,800
	8	1	2.08	1500	0.1037	5550	11,500
		2	4.17	1299	0.0970	5930	24,700
		3	6.25	1108	0.0902	6380	39,900
		4	8.33	954	0.0844	6820	56,800
		5	10.42	859	0.0808	7120	74,200
	12	1	2.08	1572	0.1062	6880	14,300
		2	4.17	1397	0.1003	7290	30,400
		3	6.25	1211	0.0940	7780	48,600
		4	8.33	1058	0.0883	8280	69,000
		5	10.42	964	0.0848	8620	89,800
3	3	1	2.08	1413	0.1009	3230	6,720
		2	4.17	1192	0.0932	3500	14,600
		3	6.25	978	0.0853	3830	23,900
		4	8.33	822	0.0792	4120	34,300
		5	10.42	716	0.0745	4380	45,600
	8	1	2.08	1474	0.1030	5550	11,600
		2	4.17	1280	0.0963	5980	24,900
		3	6.25	1092	0.0897	6420	40,100
		4	8.33	937	0.0838	6880	57,300
		5	10.42	826	0.0794	7260	75,600
	12	1	2.08	1543	0.1052	6920	14,400
		2	4.17	1384	0.0999	7290	30,400
		3	6.25	1190	0.0931	7820	48,900
		4	8.33	1037	0.0876	8310	69,200
		5	10.42	931	0.0837	8700	90,700

TABLE D-6

FREE-STREAM REYNOLDS NUMBER CALCULATION

Configuration	Condition	Furnace Column Section	Equivalent Flat-Plate Distance (ft)	Film Temperature (°F)	Gas Density (lbm/ft^3)	Absolute Viscosity (lbm/hr-ft)	Free-Stream Reynolds Number $\times 10^{-5}$
1	3	1	3.82	751	0.0317	0.0760	4.01
		2	11.5	683	0.0336	0.0730	13.3
		3	19.1	558	0.0377	0.0672	27.0
		4	26.7	448	0.0423	0.0621	45.8
		5	34.4	378	0.0458	0.0587	67.5
	8	1	3.08	826	0.0303	0.0794	4.53
		2	9.24	780	0.0314	0.0774	14.4
		3	15.4	660	0.0348	0.0721	28.6
		4	21.6	548	0.0386	0.0668	48.1
		5	27.7	492	0.0409	0.0640	68.2
	12	1	2.58	873	0.0292	0.0812	4.01
		2	7.74	862	0.0295	0.0809	12.2
		3	12.9	782	0.0314	0.0776	22.5
		4	18.1	606	0.0365	0.0695	41.1
		5	23.2	554	0.0384	0.0670	57.4
2	3	1	3.64	792	0.0305	0.0780	3.50
		2	10.9	671	0.0338	0.0727	12.5
		3	18.2	556	0.0376	0.0670	25.2
		4	25.5	458	0.0416	0.0623	41.9
		5	32.8	407	0.0441	0.0600	59.4
	8	1	3.03	846	0.0298	0.0800	4.19
		2	9.09	769	0.0317	0.0768	13.9
		3	15.2	619	0.0361	0.0698	29.1
		4	21.2	536	0.0391	0.0661	46.5
		5	27.3	488	0.0411	0.0639	65.1
	12	1	2.58	890	0.0288	0.0819	3.79
		2	7.74	849	0.0297	0.0802	12.0
		3	12.9	701	0.0335	0.0737	24.5
		4	18.1	603	0.0366	0.0693	39.9
		5	23.2	554	0.0384	0.0670	55.5
3	3	1	3.69	785	0.0307	0.0785	3.58
		2	11.1	670	0.0339	0.0712	13.1
		3	18.5	550	0.0379	0.0669	26.0
		4	25.8	463	0.0415	0.0628	42.3
		5	33.2	410	0.0440	0.0601	60.3
	8	1	3.10	833	0.0301	0.0797	4.38
		2	9.30	718	0.0330	0.0744	15.4
		3	15.5	611	0.0363	0.0697	30.2
		4	21.7	527	0.0394	0.0658	48.6
		5	27.9	474	0.0417	0.0634	68.7
	12	1	2.64	873	0.0292	0.0813	3.96
		2	7.92	840	0.0299	0.0798	12.4
		3	13.2	691	0.0338	0.0736	25.3
		4	18.5	588	0.0371	0.0686	41.8
		5	23.8	535	0.0391	0.0662	58.7

APPENDIX E

ASSESSMENT OF RADIATION AND CONDUCTION ERROR

Because the walls of the furnace column are water-cooled there is a large temperature difference between the measuring tip of the sheathed thermocouples used to obtain the data given in Tables 11-14 and the wall. This temperature difference causes two errors: radiation error and conduction error.

Radiation Error

The first attempt to assess the extent of the radiation error was through the use of a radiation shield fabricated and installed on a single sheathed thermocouple. The shield was made from a three-eighths inch diameter steel tube, six inches long. The tube was attached to the Megopak thermocouple by means of six machine screws arranged in the form of two sets of three "spokes" each that were screwed in through tapped holes in the shield until they pinched the sheath. The thermocouple itself was installed at Station 2 and had a 90 degree bend so that the shielded portion was vertical (permitting it to measure the temperature at a unique distance from the wall) with the measuring tip located exactly midway between Stations 1 and 2 (i.e. exactly one foot above the vortex chamber).

This thermocouple/shield was then used to measure the gas temperature at Conditions 3, 8, and 12 at each of three radii for Configuration 3-C. The shield was then removed and the same thermocouple was used to obtain unshielded data to permit a direct comparison. These data are given in Figure E-1.

These data suggest a maximum radiation error of about 90°F and this occurs at a distance of 1.5 inches from the furnace column wall. At Conditions 8 and 12 at a radius of 0.5 inches there is an anomalous result in that the shielded data fall above the unshielded data; although this shift is only approximately 40°F, it is not readily explainable. These data would also tend to suggest that there exists an annular-like flame front in that the radiation error at a radius of 1.5 inches from the wall is greater than at either 0.5 inches or 2.88 inches.

To examine this radiation error correction further, an aspirated thermocouple was obtained from ARI Industries, Inc. The manufacturer's specification control drawing [440] is given as Figure E-2. A Millipore pump (model 0211 lubricated pump manufactured by Gast Manufacturing Corporation) was used to provide the necessary suction. Once again the data were taken at Conditions 3, 8, and 12 and at several radii. Because the aspirated thermocouple was larger (¼-inch NPT required) than the nominal spacing between the cooling-water tubing, it was necessary to install the thermocouple where a larger than normal gap was available. Fortunately such a point was available at the approximate height of the Station 1 thermocouple (i.e. 6 inches above the vortex chamber). The results of the aspirated thermocouple investigation are given in Figure E-3; the data of Table 13 has also been included on this figure to provide a comparison.

The clear result of the aspirated data is that there is an extremely large temperature difference due (presumably) to radiation error (the peak temperature also has shifted inward). However, the energy

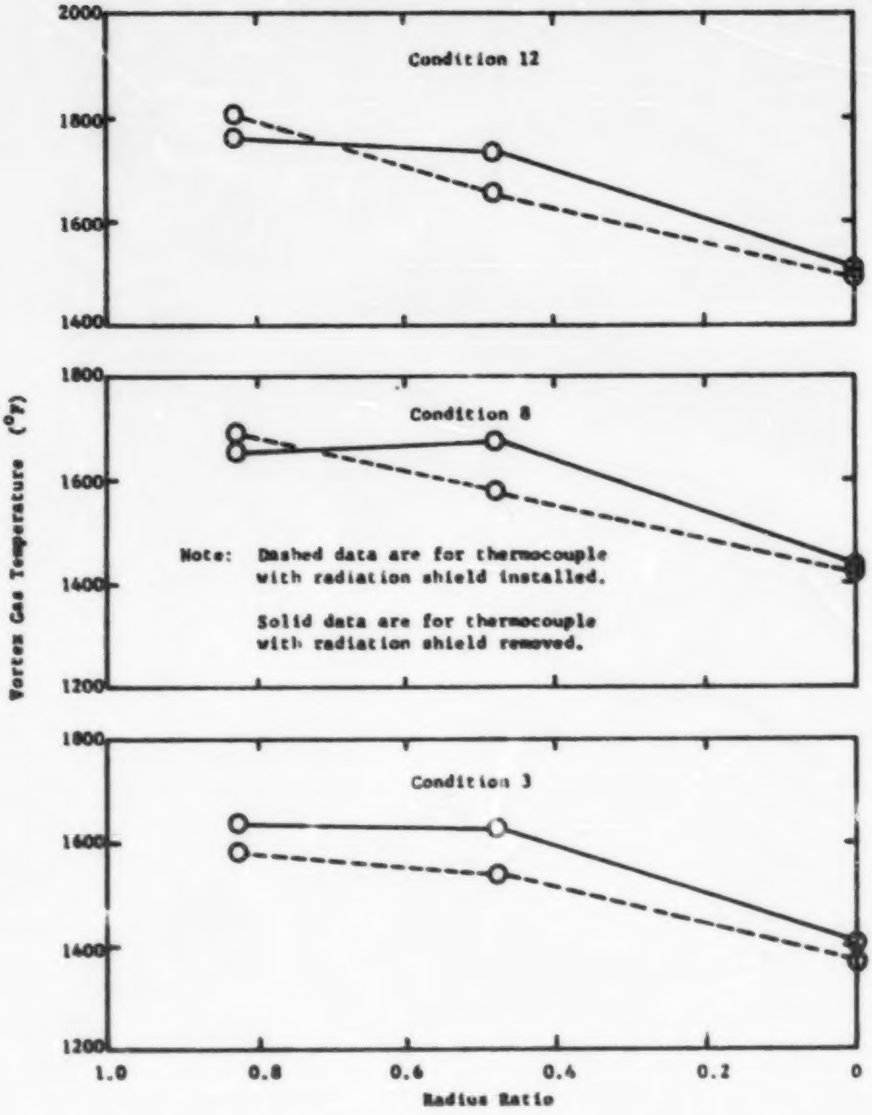

Figure E-1. Comparison of Shielded and Un-Shielded Thermocouple Data

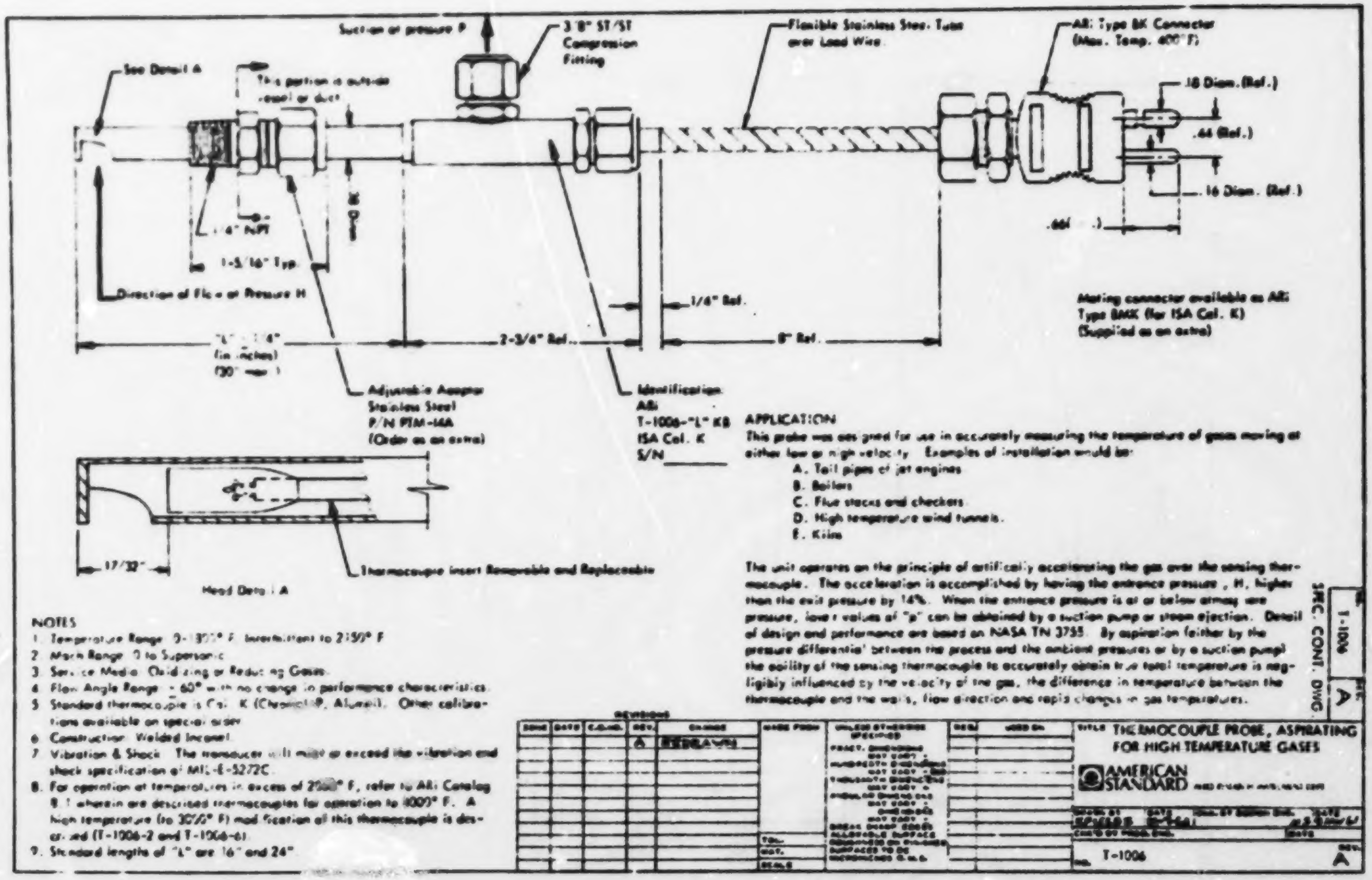

Suction or pressure P
3/8" ST/ST Compression Fitting
Flexible Stainless Steel Tube over Lead Wire
ARi Type BK Connector (Max. Temp. 400°F)
.18 Diam. (Ref.)
.44 (Ref.)
.16 Diam. (Ref.)
.66
See Detail A
This portion is outside vessel or duct
.38 Diam.
1/4" NPT
1-5/16" Typ.
Direction of Flow or Pressure H
1/4" Ref.
"L" ± 1/8" (in inches) (30" max.)
2-3/4" Ref.
8" Ref.
Mating connector available as ARi Type BMK (for ISA Cal. K) (Supplied as an extra)
Adjustable Adapter Stainless Steel P/N PTM-14A (Order as an extra)
Identification: ARi T-1006-"L" KB ISA Cal. K S/N
17/32"
Thermocouple Insert Removable and Replaceable
Head Detail A
T-1006
A
SPEC. CONT. DWG.
REVISIONS
A
REDRAWN
THERMOCOUPLE PROBE, ASPIRATING FOR HIGH TEMPERATURE GASES
AMERICAN STANDARD
T-1006
A

APPLICATION

This probe was designed for use in accurately measuring the temperature of gases moving at either low or high velocity. Examples of installation would be:

A. Tail pipes of jet engines
B. Boilers
C. Flue stacks and checkers.
D. High temperature wind tunnels.
E. Kilns

The unit operates on the principle of artificially accelerating the gas over the sensing thermocouple. The acceleration is accomplished by having the entrance pressure, H, higher than the exit pressure by 14%. When the entrance pressure is at or below atmospheric pressure, lower values of "p" can be obtained by a suction pump or steam ejection. Detail of design and performance are based on NASA TN 3755. By aspiration (either by the pressure differential between the process and the ambient pressures or by a suction pump) the ability of the sensing thermocouple to accurately obtain true total temperature is negligibly influenced by the velocity of the gas, the difference in temperature between the thermocouple and the walls, flow direction and rapid changes in gas temperatures.

NOTES

1. Temperature Range: 0-1800° F. Intermittent to 2150° F
2. Mach Range: 0 to Supersonic
3. Service Media: Oxidizing or Reducing Gases.
4. Flow Angle Range: ± 60° with no change in performance characteristics.
5. Standard thermocouple is Cal. K (Chromel-P, Alumel). Other calibrations available on special order.
6. Construction: Welded Inconel.
7. Vibration & Shock: The transducer will meet or exceed the vibration and shock specification of MIL-E-5272C.
8. For operation at temperatures in excess of 2150° F, refer to ARi Catalog 8.1 wherein are described thermocouples for operation to 4000° F. A high temperature (to 3050° F) modification of this thermocouple is described (T-1006-2 and T-1006-6).
9. Standard lengths of "L" are 16" and 24".

Figure E-2, Asp'rated Thermocouple (taken from [440])

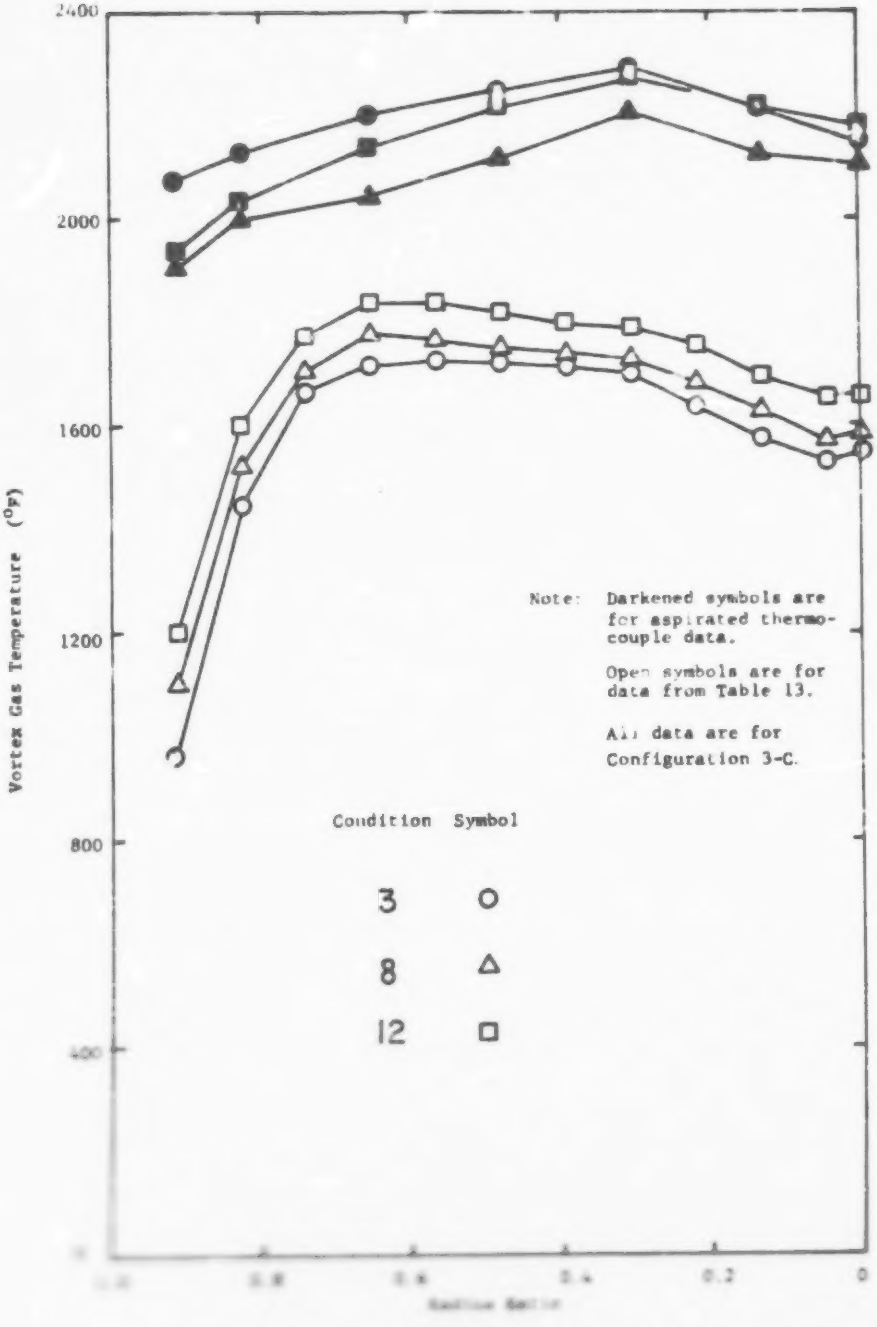

Figure [illegible]. Comparison of Aspirated and [illegible] Thermocouple Data balance calculation performed in Chapter IV shows that the temperature measured with sheathed thermocouples is in fact correct. The difficulty with all aspirated thermocouples is that one can never be sure where the gas being measured has come from because of the suction pump. This is especially the case in a vortex flow where recirculation zones and a low pressure core could interact in dramatic ways with this instrument. In particular, it is entirely possible that the suction pump alters the flow field such that the actual temperature being measured is not that of the vortex at Station 1 but of the very hot gases from the vortex chamber which were being drawn into the thermocouple inadvertantly.

Thus, it is believed that the radiation error is small as shown by the shielded thermocouple data and the energy balance (see Chapter IV).

Conduction Error

The conduction error will be estimated by using the equation of temperature for a long fin given in Reference [416] (page 32):

$$T_{true} = \frac{T_g - T_o e^{-mx}}{1 - e^{-mx}} \qquad \text{(E-1)}$$

where T_{true} is the actual vortex gas temperature, T_g the measured gas temperature, T_o the temperature at the base of the thermocouple, x the distance from the base to the measuring tip of the thermocouple, and m defined by

$$m = (h\,P / k\,A)^{\frac{1}{2}} \qquad \text{(E-2)}$$

where h is the convection conductance from the gas to the thermocouple tube, k is the effective thermal conductivity of the tube, P is the perimeter of the tube, and A is the cross-sectional area of the tube.

The diameter of the measuring tube is 1/8 inches; thus the ratio of P over A is 384 ft^{-1}. The effective thermal conductivity can be estimated by analogy to a parallel resistance electrical circuit since the cross-section is composed of asbestos insulation, metal sheathing, the actual thermocouple wire, and the insulation of the thermocouple wire. By combining the insulation with the asbestos and the wire with the sheathing, the following relation may be written for the effective thermal conductivity:

$$k = (k\ A)_{asb}/A_{tot} + (k\ A)_{sheath}/A_{tot} \qquad \text{(E-3)}$$

From the manufacturer's specifications [434] the ratio of the asbestos to the total area is 0.493, and the ratio of the sheath to the total area is 0.507. From Reference [416] the conductivity of the asbestos insulation can be estimated to be 0.093 Btu/hr-ft-°F (for loosely packed asbestos at 210°F) and that of the sheath as 10 Btu/hr-ft-°F (for SS 304 at 400°F). Substitution of these values into Equation (E-3) results in an effective conductivity of 5.12 Btu/hr-ft-°F.

The convection conductance for the flow past the thermocouple tube can be estimated by empirical expressions for heat transfer for air cross-flowing cylinders (page 196 [416]). The Reynolds number of the flow is as follows:

$$Re_{cyl} = W\ D/\nu \qquad \text{(E-4)}$$

where W is the free-stream velocity, D the diameter of the cylinder, and ν the kinematic viscosity evaluated at the film temperature. From Table 35, it is seen that the free-stream velocity is on the order of 100 feet per second. For air at 200°F, the kinematic viscosity is 0.864 ft^2/hour. Thus the Reynolds number for the cylinder is approximately 4340. From Table 6-1 of Reference [416], this implies that the convection conductance is given by the following:

$$h = 0.683\ Re_{cyl}^{0.466}\ Pr^{1/3}\ k_f\ /D \tag{E-5}$$

where k_f is the thermal conductivity of air evaluated at the film temperature, and Pr is the Prandtl number similarly found. Performing the above calculation results in a predicted value of h of 52 Btu/hr-ft^2-°F.

Therefore the value of m defined by Equation (E-2) may be determined as follows:

$$m = (52)\ (384)\ /\ (5.12)\ =\ 62.5 \tag{E-6}$$

The conduction error will be evaluated for the worst-case position that of a distance of 0.25 inches from the wall. The actual value of x to be used in Equation (E-1) is, however, somewhat larger than simply the penetration depth of the thermocouple tube because the tube is mounted in a compression fitting which in turn is held in place in the vortex chamber wall by a one-eighth-inch NPT adapter. Thus the point of actual wall contact with the thermocouple tube is effectively further removed from the tip than simply the penetration distance. Since the length of the compression/NPT fitting is 1.25 inches, the value of x is estimated to be equal to 1.50 inches for a 0.25 inch- penetration. Substitution into Equation (E-1) yields the following:

$$T_{true} = T_g - (4.05 \times 10^{-4})\ T_w \tag{E-7}$$

Thus for a measured gas temperature of 1200°F at 0.25 inches from the wall with a wall temperature of 200°F, the true temperature is estimated as 1199.9°F indicating that the conduction error is in fact negligible.

For increasing penetration depths this error decreases to even smaller values.

APPENDIX F

THERMOCHEMISTRY CALCULATIONS

Enthalpy of Combustion

The enthalpy of combustion can be determined from the tabulated values of enthalpy of formation once a chemical reaction can be written for the process. The reactants are known quite precisely because they are supplied to the system at a measured ratio: propane (C_3H_8) and "air" (approximately $O_2 + 3.76\ N_2$). The products are not so known and some assumptions must be made. It will be assumed that the only products formed are: CO_2, H_2O, N_2, O_2 (for those reactions with excess air), and CO (for those reactions with deficient air). At the temperatures measured in the furnace column the assumption of no formation of nitrogen-oxide molecules (or other more-complicated molecules) is well justified.

The basic chemical equation is as follows:

$$C_3H_8 + x(O_2 + 3.76N_2) \rightleftarrows yCO_2 + zO_2 + uCO + vH_2O + 3.76xN_2 \qquad \text{(F-1)}$$

The value of x can be determined from the air/fuel ratio from the known molecular weights of propane (44.09) and "air" (28.97):

$$x = AFR(44.09/28.97) = 1.522\ AFR \qquad \text{(F-2)}$$

The results of the specie balance for the nine combinations of exit Configuration and Conditions are given in Table F-1.

TABLE F-1

MOLAR COEFFICIENTS OF THE THEORETICAL CHEMICAL REATION BASED UPON THE MEASURED AIR/FUEL RATIO

Configuration	Condition	Reactants		Products				
		C_3H_8	$(O_2+3.76N_2)$	CO_2	O_2	CO	H_2O	N_2
1	3	1	4.769	2.537	0	0.463	4	17.930
	8	1	6.521	3.0	1.521	0	4	24.519
	12	1	6.606	3.0	1.606	0	4	24.839
2	3	1	4.678	2.356	0	0.644	4	17.589
	8	1	6.245	3.0	1.245	0	4	23.481
	12	1	6.302	3.0	1.302	0	4	23.696
3	3	1	4.697	2.394	0	0.606	4	17.661
	8	1	6.281	3.0	1.281	0	4	23.617
	12	1	6.295	3.0	1.295	0	4	23.669

The theoretical enthalpy of combustion at 77°F for all the Condition 8 and 12 data is the same since it is independent of the degree of excess air. The Condition 3 enthalpy of combustion is, however, dependent upon the air/fuel ratio because of its influence upon the formation of carbon monoxide as seen in Table F-1. The theoretical enthalpy can be calculated from the following expression:

$$\Delta H_{c,77} = \sum_i(\nu_i \; \Delta H_f)_{prod} - \sum_i(\nu_i \; \Delta H_f)_{reac} \qquad \text{(F-1)}$$

where $\Delta H_{c,77}$ is the enthalpy of combustion, ΔH_f the enthalpy of formation, and ν_i are the coefficients of the reaction. Using the values tabulated in Wark [403] for the enthalpies of formation, the resulting enthalpies of combustion are as follows:

TABLE F-2

THEORETICAL ENTHALPY OF COMBUSTION AT 77°F

(Btu/lbm C_3H_8)

	Condition		
Configuration	3	8	12
1	18,666	19,944	19,944
2	18,166	19,944	19,944
3	18,271	19,944	19,944

Sensible Enthalpy of Reactants

Since the enthalpy of combustion has been evaluated at the reference state (77°F), it is necessary to account for the sensible enthalpy change associated with the reactants when they are not supplied at that temperature. The mean supply temperature of the reactants has been measured, so the JANAF Tables [404, 405] can be used together with the molar coefficients of Table F-1 to calculate the sensible enthalpy of the reactants. The net enthalpy of combustion is defined as the sum of the enthalpy of combustion as calculated in Equation (F-1) and the enthalpy of the reactants as follows:

$$\Delta H_{cnet,77} = \Delta H_{c,77} + H^{*}_{reac}(T_{supply} - 77) \qquad (F\text{-}2)$$

where H^{*} designates the sensible enthalpy.

These calculations for sensible enthalpy of reactants and net enthalpy of combustion are presented in Table F-3.

Sensible Enthalpy of Products

A similar procedure to that followed to find the sensible enthalpy of the reactants can be used for the products. The temperature at which the sensible enthalpy of each products is evaluated is the average temperature of the vortex gas at that station (given in Table 14). The net enthalpy of reaction is then defined as follows:

$$\Delta H_{R} = \Delta H_{cnet} - H^{*}_{prod}(T_{m} - 77) \qquad (F\text{-}3)$$

These calculations are performed in Table F-4.

Net Enthalpy of Reaction at the Exit

Since each of the Station thermocouples is located at the mid-point of each respective cooling-water section, the net enthalpy of reaction calculated at Station 5 in Table F-4 is not quite equal to the net enthalpy of reaction available for the entire furnace column due to the six inches of cooling section remaining above Station 5. This can be accounted for satisfactorily by subtracting one-half of the enthalpy difference between Stations 4 and 5 from the value at Station 5. This

TABLE F-3

SENSIBLE ENTHALPY OF REACTANTS

Configuration	Condition	Propane		Air		Sensible Enthalpy* of Reactants (Btu/lbm C_3H_8)	Net Enthalpy of Combustion ** (Btu/lbm C_3H_8)
		Supply Temperature (°F)	Sensible Enthalpy * (Btu/lbm C_3H_8)	Supply Temperature (°F)	Sensible Enthalpy* (Btu/lbm C_3H_8)		
1	3	60.0	-3	74.3	-10	-13	18,653
	8	66.3	-2	74.4	-12	-14	19,930
	12	57.8	-3	76.4	- 3	- 6	19,938
2	3	55.7	-4	70.8	-21	-25	18,141
	8	55.0	-4	73.0	-18	-22	19,922
	12	54.7	-4	74.2	-13	-17	19,927
3	3	58.6	-3	73.0	-14	-17	18,254
	8	58.0	-3	75.3	- 1	- 4	19,940
	12	55.1	-4	77.8	+ 4	0	19,944

* Taken with respect to 77°F

** Obtained from Equation (F-2)

TABLE F-4

SENSIBLE ENTHALPY OF PRODUCTS/NET ENTHALPY OF REACTION

Configuration	Condition	Station	Average Gas Temperature (°F)	Sensible Enthalpy of Products (Btu/lbmC_3H_8)	Net Enthalpy of Reaction* (Btu/lbmC_3H_8)
1	3	1	1363	5808	12,845
		2	1201	5020	13,633
		3	976	3949	14,704
		4	792	3100	15,553
		5	658	2496	16,157
	8	1	1480	8368	11,562
		2	1333	7418	12,512
		3	1152	6271	13,659
		4	940	4962	14,968
		5	828	4284	15,646
	12	1	1560	8994	10,944
		2	1459	8329	11,609
		3	1269	7092	12,846
		4	1074	5855	14,083
		5	977	5247	14,691
2	3	1	1424	6011	12,130
		2	1205	4957	13,184
		3	991	3955	14,186
		4	811	3136	15,005
		5	710	2687	15,454
	8	1	1500	8181	11,741
		2	1299	6935	12,987
		3	1108	5774	14,148
		4	954	4859	15,063
		5	859	4304	15,618
	12	1	1572	8706	11,221
		2	1397	7600	12,327
		3	1211	6448	13,479
		4	1058	5520	14,407
		5	964	4944	14,983
3	3	1	1413	5977	12,277
		2	1192	4912	13,342
		3	978	3909	14,345
		4	822	3197	15,057
		5	716	2723	15,531
	8	1	1474	8060	11,880
		2	1280	6852	13,088
		3	1092	5708	14,232
		4	937	4783	15,157
		5	826	4133	15,807
	12	1	1543	8512	11,432
		2	1384	7510	12,434
		3	1190	6313	13,631
		4	1037	5388	14,556
		5	931	4757	15,187

* Obtained from Equation (F-3)

approximation essentially assumes that the heat flux for the top 6-inch portion of the fifth cooling-water section is approximately that of the portion between Stations 4 and 5. Figure 24 shows that this is a reasonable assumption.

The results of this calculation procedure is tabulated below:

TABLE F-5

NET ENTHALPY OF REACTION AT THE EXIT

Configuration	Condition	Sensible Enthalpy of Products at Exit (Btu/lbm C_3H_8)	Net Enthalpy of Reaction at Exit (Btu/lbm C_3H_8)
1	3	2194	16,459
	8	3945	15,985
	12	4943	14,995
2	3	2462	15,679
	8	4027	15,896
	12	4656	15,271
3	3	2486	15,768
	8	3803	16,132
	12	4442	15,503

APPENDIX G

CONFIGURATION FACTOR CALCULATIONS

External Factors

There are two external configuration factor calculations required: factors from the copper base plate to each furnace column section, and factors from the square annulus formed by the area of the vortex chamber top plate less the copper base plate to each furnace column section. The geometry is shown in Figure G-1 where one-eighth of the copper base plate is shown as area A_1 and one-eighth of the vortex chamber top plate as area A_2; each section of furnace column is shown by letters A through E (thus section 1 is designated A, 2 as B, etc.). This figure has been taken from a report by Tripp, Hwang, and Crank [441]. In this reference a procedure is presented that permits the calculation of configuration factors from a cylinder to a perpendicular right triangle positioned at its base. In order to determine the needed factor for the square annulus, a series of calculations must be performed: the configuration factors must be found from the furnace column to the smaller triangle (A_1 on Figure G-1) which represents the copper base plate, then the factors from the furnace column to the larger triangle (A_2) need to be found, and finally by means of configuration factor algebra the factor between the furnace column and the square annulus can be found. Once this factor is known, further use of configuration algebra can readily yield the inverse of this factor. Similarly, the factors from the copper base plate to the furnace column sections may also be found.

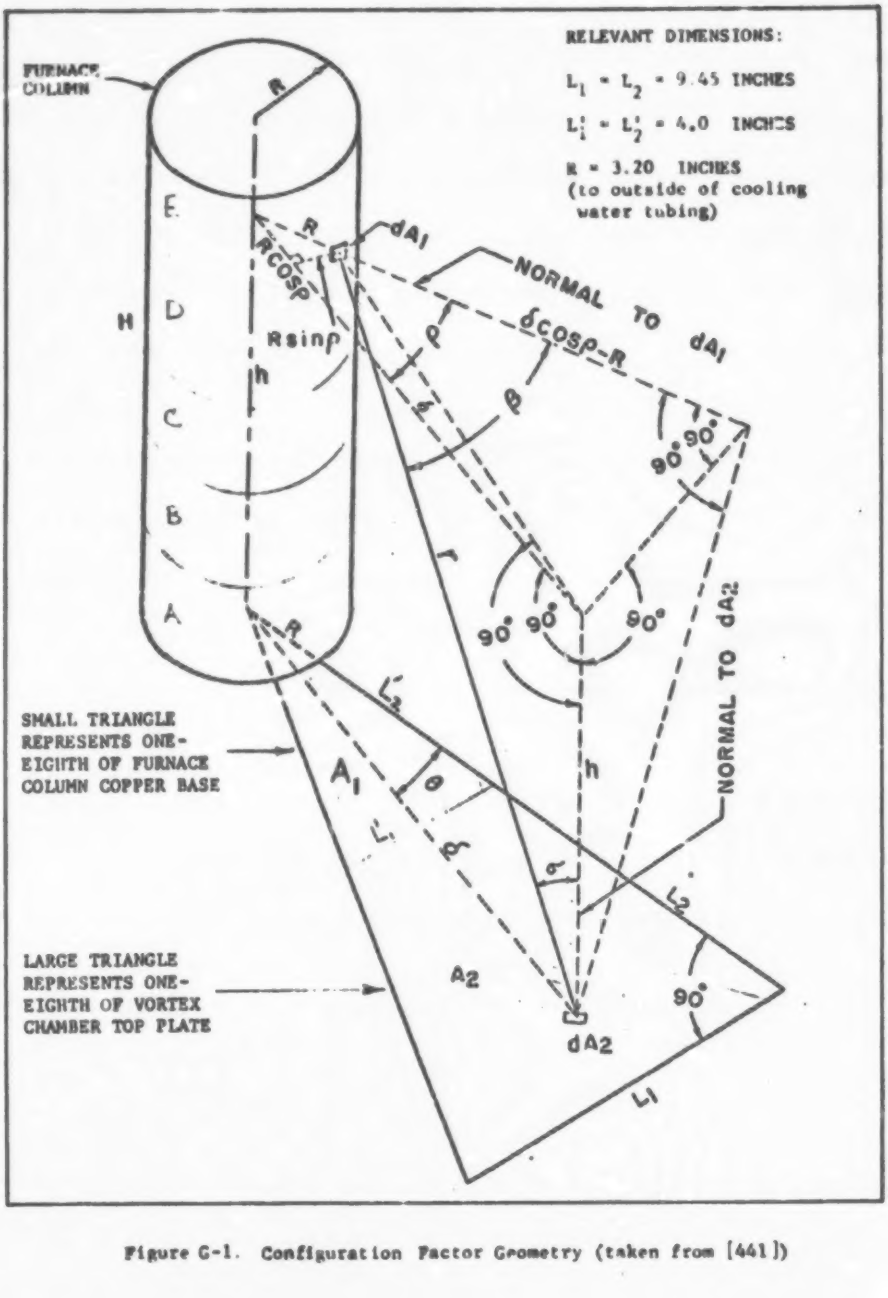
RELEVANT DIMENSIONS:
$L_1 = L_2 = 9.45$ INCHES
$L_1' = L_2' = 4.0$ INCHES
R = 3.20 INCHES
(to outside of cooling water tubing)
FURNACE COLUMN
R
E
D
C
B
A
H
h
R
dA_1
R COS ρ
R sin ρ
NORMAL TO dA_1
δ cos ρ − R
ρ
δ
β
r
90°
90°
90°
90°
90°
90°
90°
NORMAL TO dA_2
R
L_2'
SMALL TRIANGLE REPRESENTS ONE-EIGHTH OF FURNACE COLUMN COPPER BASE
A_1
θ
L_1'
δ
σ
h
L_2
LARGE TRIANGLE REPRESENTS ONE-EIGHTH OF VORTEX CHAMBER TOP PLATE
A_2
dA_2
90°
L_1

Figure G-1. Configuration Factor Geometry (taken from [441])

The report by Trip provided a series of graphs for readily determining these factors based upon the known values of H, R, L_1, and L_2 (defined in Figure G-1). Unfortunately, the ranges of these variables presented in their graphs does not include the physical dimensions of this furnace column/vortex chamber; since the authors were concerned with modeling people on floors, they used short cylinders on large plates whereas the geometry here is one of a relatively long cylinder standing on a small plate. As a result it was necessary to numerically integrate their equation for the configuration factor. The equation used is given in Figure G-2 which is page 19 of their report [441].

The numerical integration was performed using a Three-Eights Simpson's Rule on a CDC 6000 computer. The results of this program are given in Table G-1 for the configuration factor for furnace column heights of from one to five sections to each of the triangles (one representing the copper base plate and the other the vortex chamber top plate).

To convert these results so that the factor from the square annulus to the various furnace column section can be found, it is first necessary to perform the following subtraction:

$$\begin{aligned} F_{(A-E)\rightarrow(2-1)} &= F_{(A-E)\rightarrow(2)} - F_{(A-E)\rightarrow(1)} \qquad \text{(G-1)} \\ &= 0.00524 - 0.00103 \\ &= 0.00421 \end{aligned}$$

which follows from configuration factor algebra where F represents the configuration factor, with the subscripts (A-E) representing the total furnace column area of all five sections (i.e. section A to section E),

Radiation Shape Factor Between a Finite Cylinder and a Plane Surface

Case I: The finite cylinder is perpendicular to a right triangle.

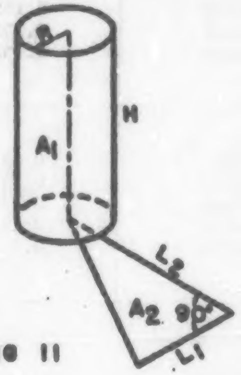

FIG 11

Shape factors for this case, in which one base of the cylinder lies in the same plane as the triangle, and the center line of the cylinder is normal to the triangle and passes through the apex of one of the acute angles of the triangle, Fig. 11, were obtained by integrating, partially, Equation (2) to the form

$$F_{12} = \frac{1}{2\pi^2 W}\left\{\int_1^{\sqrt{B^2+C^2}} \tan^{-1}\frac{B}{C}\left[\tan^{-1}\sqrt{\frac{\alpha+1}{\alpha-1}}\right.\right.$$

$$\left. - \frac{W^2+(\alpha+1)(\alpha-1)}{\sqrt{(W^2+(\alpha+1)^2)(W^2+(\alpha-1)^2)}}\tan^{-1}\sqrt{\frac{(\alpha-1)(W^2+(\alpha+1)^2)}{(\alpha+1)(W^2+(\alpha-1)^2)}}\right]\alpha\, d\alpha$$

$$\left. - \int_C^{\sqrt{B^2+C^2}}\left[\tan^{-1}\sqrt{\frac{\alpha+1}{\alpha-1}} - \frac{W^2+(\alpha+1)(\alpha-1)}{\sqrt{(W^2+(\alpha+1)^2)(W^2+(\alpha-1)^2)}}\tan^{-1}\sqrt{\frac{(\alpha-1)(W^2+(\alpha+1)^2)}{(\alpha+1)(W^2+(\alpha-1)^2)}}\right]\sec^{-1}\frac{\alpha}{C}\,\alpha\, d\alpha\right\} \tag{7}$$

where $B = L_1/R$, $C = L_2/R$, $W = H/R$, $\alpha = \delta/R$.

Equation (7) was integrated by the authors to a further extent (see Appendix III); however, for purposes of computation, through the use of the IBM 650 Computer, it was decided to use Equation (7) to obtain the numerical values of the shape factors. These values are presented in Figs. 5a to 5e, using the parameters $U = H/L_1$ and $V = H/L_2$ instead of $B = L_1/R$ and $C = L_2/R$.

Figure G-2. Configuration Factor Equation (page 19 of [441])

TABLE G-1

NUMERICAL INTEGRATION RESULTS FOR CONFIGURATION FACTOR

TRIANGLE*	CYLINDER*	CONFIGURATION FACTOR FROM CYLINDER TO TRIANGLE	CONFIGURATION FACTOR FROM TRIANGLE TO CYLINDER
1	A	0.00511	0.154
	A+B	0.00257	0.155
	A+B+C	0.00172	0.155
	A+B+C+D	0.00129	0.155
	A+B+C+D+E	0.00103	0.155
2	A	0.0232	0.125
	A+B	0.0127	0.137
	A+B+C	0.00864	0.139
	A+B+C+D	0.00653	0.140
	A+B+C+D+E	0.00524	0.141

*See Figure G-1 for definition of these areas.

TABLE G-2

CONFIGURATION FACTOR FROM VORTEX CHAMBER TO EACH FURNACE COLUMN SECTION

	Cylinder Sections*				
	A-E	A-D	A-C	A-B	A
From Cylinder to Area 2-1*	0.00421	0.00524	0.00692	0.0101	0.0181
From Area 2-1* to Cylinder	0.138	0.137	0.136	0.132	0.119

	Cylinder Sections*				
	E	D	C	B	A
From Area 2-1* to each Cylinder Section	0.001	0.001	0.004	0.013	0.119

*See Figure G-1 for definition of these areas subscript 1 representing triangle A_1, and subscript 2 triangle A_2 all defined in Figure G-1. Similar calculations are required to find the configuration factor for sections A through D to the area formed by subtracting A_1 from A_2. To convert these five factors so that they represent the energy fraction leaving the top plate and striking the appropriate furnace column section requires use of the reciprocity relation as follows:

$$
\begin{aligned}
F_{(2-1)\rightarrow(A-E)} &= F_{(A-E)\rightarrow(2-1)} \left[S_{(A-E)} / S_{(2-1)}\right] \qquad \text{(G-2)} \\
&= 0.00421 \ (8.38/0.256) \\
&= 0.138
\end{aligned}
$$

where $S_{(A-E)}$ represents the area of furnace column sections A through E and $S_{(2-1)}$ represents the area of the trapezoid formed by subtracting A_1 from A_2. A summary of this calculation procedure is given in Table G-2.

The configuration factors from the copper base plate to each furnace column section can be found directly from Table G-1 by simple subtraction. Since the factor to areas A plus B is 0.155 and that to A only is 0.154, the factor to B only must be 0.001. Likewise it can be seen that to three decimal places the factor to each of the remaining furnace column sections is zero.

The configuration factors from the vortex chamber bottom plate can be found somewhat more directly. A schematic of this internal radiation path is presented in Figure G-3.

The factor from the vortex chamber cavity to the bottom section is very difficult to calculate due to the fact that the bottom portion of the furnace column walls can "see around the corner".

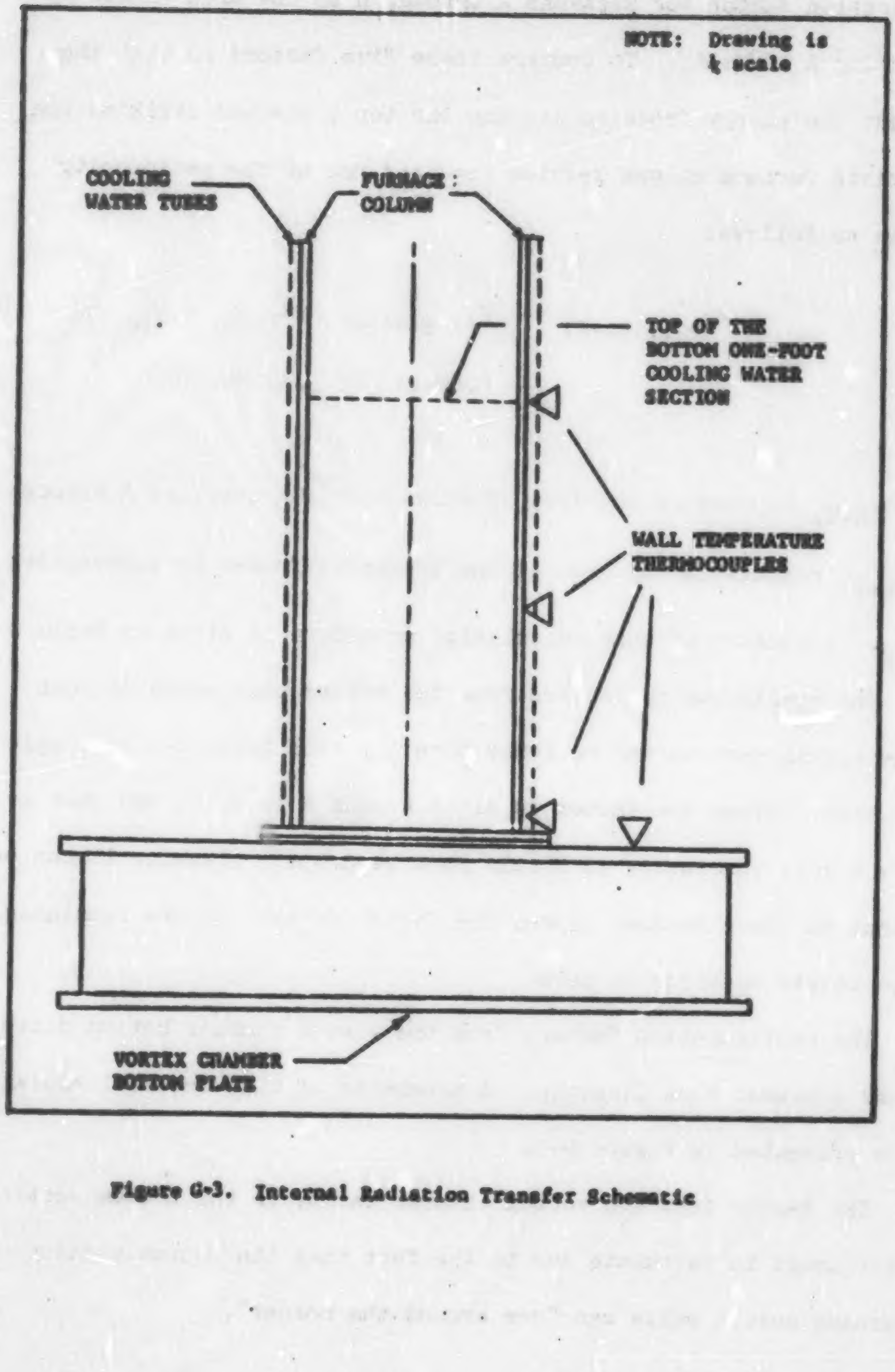
NOTE: Drawing is ¼ scale
COOLING WATER TUBES
FURNACE COLUMN
TOP OF THE BOTTOM ONE-FOOT COOLING WATER SECTION
WALL TEMPERATURE THERMOCOUPLES
VORTEX CHAMBER BOTTOM PLATE

Figure G-3. Internal Radiation Transfer Schematic

The cavity, therefore, resembles (to a degree) a black body radiator. Since the vortex-wall emissivity has been estimated to be 0.80, it appears to be a reasonable estimate to account for this enhanced configuration factor to the bottom one-foot section of furnace column by taking the effective emissivity to be 0.95. The radiating area is the furnace column area which is 0.1810 square feet.

The configuration factor from section to section can now be calculated using equations presented by Siegel and Howell ([422], page 787):

$$F_{1\rightarrow 2} = \tfrac{1}{2}\left[X - \sqrt{X^2 - 4\,(R_2/R_1)^2}\right] \qquad \text{(G-3)}$$

where

$$X = 1 + (1 + R_2^2)/R_1^2 \qquad \text{(G-4)}$$

and where R_1 is defined as the ratio of r_1/H and R_2 as r_2/H where r_1 is the radius of the top disk, r_2 the bottom disk, and H the separation distance. For the configuration under investigation here r_1 and r_2 are equal and are 2.88 inches, H is the height of each furnace column section which is 12 inches. By substituting these values in the above equations yields a configuration factor of 0.05179 from the disk at the bottom of the furnace column to the disk separating furnace column section 1 from 2; thus the factor from the bottom disk to the furnace column wall of section 1 is 0.94821.

Continuing in a similar manner results in configuration factors from the bottom disk to sections 2 through 5 as follows: 0.0491, 0.00254, 0.00013, and 0.00000.

APPENDIX H

NUSSELT NUMBER CALCULATIONS

Mean Nusselt Number

The mean Nusselt number has been defined in Chapter IV by Equation (14) in terms of the mean convection conductance given in Table 31, the furnace column diameter, and the thermal conductivity evaluated at the average furnace column gas temperature (found in Table 14).

The thermal conductivity will be evaluated as a function of temperature using Maxwell's curve [401] which he found to be relatively independent of the degree of excess air and thus only a function of temperature. A graph of the conductivity versus gas temperature is given as Figure H-1.

The calculation of mean Nusselt number is given in Table H-1.

Local Nusselt Number

The local Nusselt number may be found in an analogous calculation to that performed for the mean Nusselt number above. The local value of convection conductance is used (given in Table 31) and the thermal conductivity relation given in Figure H-1 is evaluated at the local average gas temperature (from Table 14).

The results of this calculation is given in Table H-2.

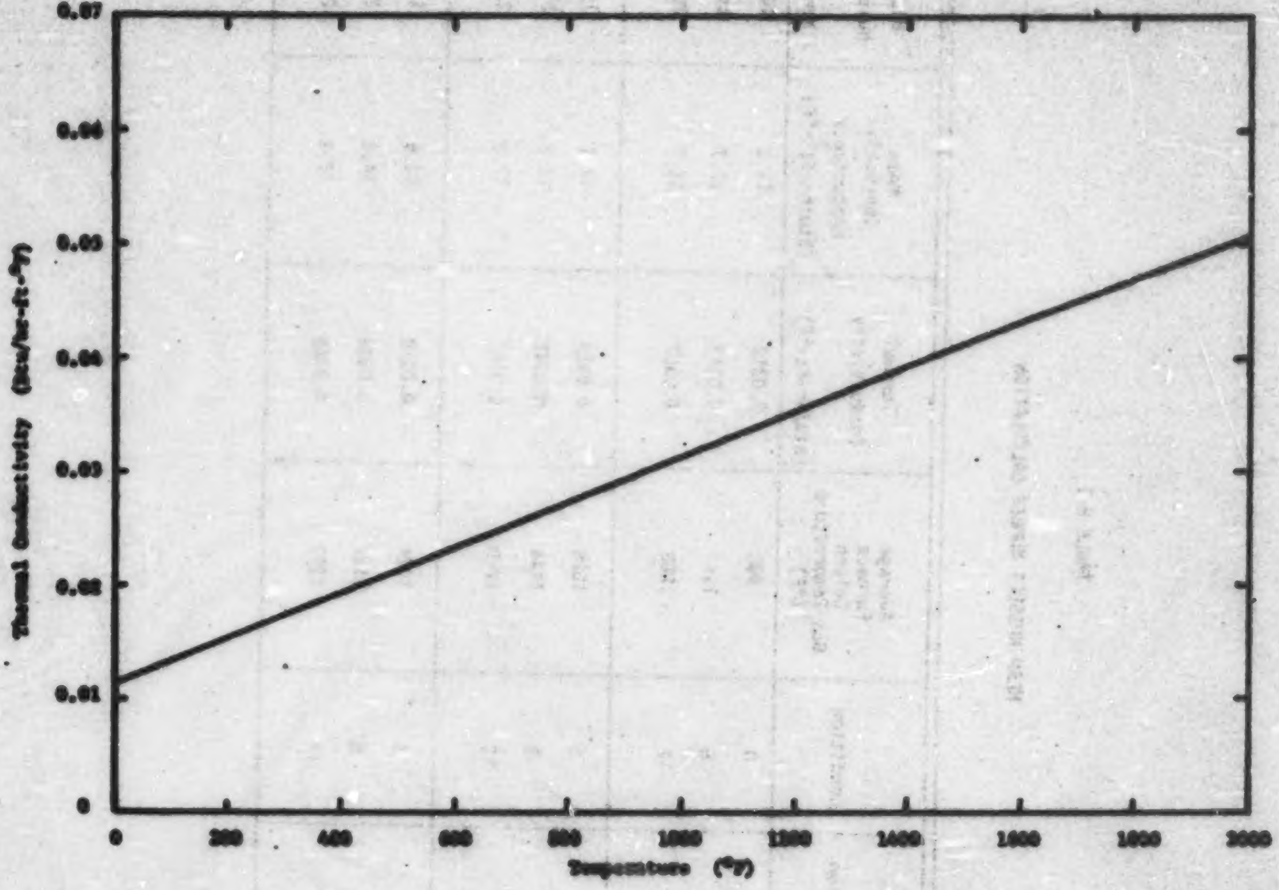

Figure B-1. Thermal Conductivity of Flue Gas

TABLE H-1

MEAN NUSSELT NUMBER CALCULATION

Exit Configuration	Condition	Average Furnace Column Gas Temperature (°F)	Thermal Conductivity (Btu/hr-ft-°F)	Mean Convection Conductance (Btu/hr-ft^2-°F)	Mean Nusselt Number
1	3	988	0.0312	11.0	169
	8	1147	0.0343	13.7	192
	12	1268	0.0367	15.7	205
2	3	1028	0.0319	12.7	191
	8	1144	0.0342	15.2	213
	12	1240	0.0362	17.3	229
3	3	1024	0.0318	12.6	190
	8	1122	0.0338	14.8	210
	12	1217	0.0358	17.2	231

TABLE H-2
LENGTH NUSSELT NUMBER CALCULATION

Configuration	Condition	Furnace Column Section	L/D	Average Gas Temperature (°F)	Thermal Conductivity (Btu/hr-ft-°F)	Axial Nusselt Number	Length Nusselt Number
1	3	1	2.08	1363	0.0386	153	318
		2	4.17	1201	0.0354	148	617
		3	6.25	976	0.0308	156	975
		4	8.33	792	0.0272	163	1360
		5	10.42	658	0.0245	210	2190
	8	1	2.08	1480	0.0409	221	460
		2	4.17	1333	0.0381	156	651
		3	6.25	1162	0.0344	151	944
		4	8.33	940	0.0302	175	1460
		5	10.42	828	0.0278	223	2320
	12	1	2.08	1560	0.0424	241	501
		2	4.17	1469	0.0406	181	755
		3	6.25	1269	0.0367	184	1150
		4	8.33	1074	0.0328	173	1440
		5	10.42	977	0.0309	205	2140
2	3	1	2.08	1424	0.0398	181	376
		2	4.17	1206	0.0354	173	721
		3	6.25	991	0.0312	178	1113
		4	8.33	811	0.0276	183	1520
		5	10.42	710	0.0255	222	2310
	8	1	2.08	1500	0.0412	238	495
		2	4.17	1299	0.0373	205	856
		3	6.25	1108	0.0335	176	1100
		4	8.33	964	0.0304	178	1480
		5	10.42	869	0.0286	217	2260
	12	1	2.08	1572	0.0427	256	532
		2	4.17	1397	0.0393	233	972
		3	6.25	1211	0.0356	192	1200
		4	8.33	1058	0.0325	189	1570
		5	10.42	964	0.0307	230	2400
3	3	1	2.08	1413	0.0396	177	368
		2	4.17	1192	0.0353	179	746
		3	6.25	978	0.0309	180	1125
		4	8.33	822	0.0278	178	1480
		5	10.42	716	0.0256	214	2230
	8	1	2.08	1474	0.0407	244	508
		2	4.17	1288	0.0369	181	758
		3	6.25	1082	0.0332	175	1094
		4	8.33	937	0.0301	180	1500
		5	10.42	826	0.0278	230	2400
	12	1	2.08	1543	0.0422	262	545
		2	4.17	1384	0.0391	219	913
		3	6.25	1190	0.0352	196	1225
		4	8.33	1037	0.0321	192	1600
		5	10.42	931	0.0299	239	2490

APPENDIX I

STANTON NUMBER CALCULATIONS

The Stanton number has been defined in Chapter IV by Equations (21) and (48) in terms of the free-stream velocity W. The calculation of the free-stream velocity has been presented in Table 35 for the 9 combinations of Configuration/Condition.

The fluid properties are evaluated at the film temperature, defined as the mean of the average gas temperature (Table 14) and the gas temperature at the wall (Tables 11-13), in accordance with the usual procedure. The density is calculated by means of the perfect gas law for the assumption of atmospheric pressure throughout the vortex chamber using the gas constants calculated in Table 32. The specific heat at constant pressure is evaluated from air property tables (Reference [439] page 565) for the film temperature.

Colburn j-Factor

The Colburn j-Factor is defined as the product of the Stanton number and the Prandtl number raised to the two-thirds power. The Prandtl number is evaluated at the film temperature using air property tables [439].

The results of this calculation are given in Table I-1. The density used in the calculation was taken from Table D-6. The film temperature at which the specific heat and Prandtl number were evaluated is also given in Table D-6.

TABLE I-1

CALCULATION OF COLBURN j-FACTOR

Configuration	Condition	Furnace Column Section	Convection Conductance (Btu/lbm-ft^2-°F)	Specific Heat (Btu/lbm°F)	Stanton Number x 10^3	Colburn j-Factor x 10^3
1	3	1	11.3	0.255	5.56	4.31
		2	10.8	0.253	5.05	3.92
		3	10.0	0.249	4.23	3.28
		4	9.24	0.246	3.53	2.73
		5	10.7	0.245	3.79	2.94
	8	1	17.3	0.258	5.75	4.47
		2	12.3	0.256	3.97	3.08
		3	10.8	0.253	3.18	2.47
		4	11.0	0.249	2.97	2.30
		5	12.9	0.248	3.30	2.55
	12	1	19.6	0.259	6.00	4.67
		2	16.2	0.259	4.61	3.59
		3	14.1	0.256	4.06	3.16
		4	11.8	0.251	2.98	2.31
		5.	13.2	0.249	3.20	2.47
2	3	1	13.8	0.257	7.15	5.56
		2	12.7	0.253	6.03	4.67
		3	11.6	0.249	5.03	3.89
		4	10.5	0.247	4.15	3.21
		5	11.8	0.245	4.44	3.44
	8	1	18.7	0.258	6.56	5.10
		2	15.8	0.256	5.25	4.08
		3	12.3	0.251	3.66	2.83
		4	11.3	0.249	3.13	2.42
		5	12.9	0.247	3.43	2.65
	12	1	21.0	0.260	6.72	5.23
		2	19.0	0.259	5.91	4.60
		3	14.2	0.254	4.00	3.10
		4	12.8	0.251	3.34	2.58
		5	14.7	0.249	3.68	2.85
3	3	1	13.4	0.257	6.85	5.32
		2	13.1	0.253	6.16	4.77
		3	11.6	0.249	4.96	3.84
		4	10.3	0.247	4.05	3.14
		5	11.4	0.245	4.26	3.30
	8	1	19.0	0.258	6.53	5.08
		2	13.8	0.254	4.40	3.41
		3	12.1	0.251	3.55	2.75
		4	11.3	0.249	3.08	2.38
		5	13.3	0.247	3.45	2.67
	12	1	21.1	0.259	6.68	5.20
		2	17.7	0.258	5.49	4.27
		3	14.4	0.253	4.03	3.13
		4	12.8	0.250	3.30	2.56
		5	14.9	0.249	3.66	2.83

Modified Colburn j-Factor

The modified Colburn j-Factor is defined by using the Stanton number obtained from Equation (48). The calculation procedure is identical to that for the usual Colburn j-Factor with the exception that a calculation is required for the enthalpy potential instead of the specific heat.

The enthalpy potential has been defined in Equation (49) in terms of the net enthalpy of combustion (given in Table F-3) and the sensibly enthalpies of the reactants (evaluated at the average gas temperature) and the products (evaluated at the wall gas temperature).

The calculation of the enthalpy potential together with the result for the modified Colburn j-Factor is given in Table I-2.

TABLE I-2

CALCULATION OF MODIFIED COLBURN j-FACTOR

Configuration	Condition	Furnace Column Section	Enthalpy Potential (Btu/lbm products)	Modified Colburn Factor x 10^{+4}
1.	3	1	1484.7	1.17
		2	1433.7	9.28
		3	1380.2	6.37
		4	1341.4	4.45
		5	1301.3	3.97
	8	1	1268.2	15.3
		2	1224.1	9.54
		3	1179.3	6.69
		4	1126.3	5.15
		5	1097.0	5.02
	12	1	1276.1	16.7
		2	1227.6	11.6
		3	1167.3	8.63
		4	1155.3	6.03
		5	1131.7	5.96
2	3	1	1477.6	15.7
		2	1432.6	11.4
		3	1363.1	7.99
		4	1334.7	5.43
		5	1308.8	5.01
	8	1	1307.7	17.0
		2	1240.1	11.5
		3	1216.3	7.36
		4	1178.6	5.54
		5	1153.8	5.44
	12	1	1315.4	18.1
		2	1242.9	13.5
		3	1220.3	8.48
		4	1190.7	6.42
		5	1166.6	6.46
3	3	1	1485.3	15.0
		2	1427.2	11.4
		3	1376.7	7.67
		4	1340.4	5.35
		5	1313.2	4.85
	8	1	1296.3	16.7
		2	1251.9	10.0
		3	1207.8	7.05
		4	1170.0	5.38
		5	1140.0	5.27
	12	1	1310.5	17.7
		2	1242.9	12.4
		3	1216.5	8.37
		4	1188.9	6.24
		5	1160.9	6.22

APPENDIX J

LEAST-SQUARES CURVE-FIT CALCULATION

The calculation of a least-squares curve-fit to data is performed in accordance with the procedure outline in Reference [427].

The equation for the Colburn j-Factor can be written in terms of the free-stream Reynolds number and two constants to be determined from the data:

$$St_x \, Pr^{2/3} = a \, Re_x^{\,b} \tag{J-1}$$

The constants a and b can be determined from N data points by summing each ith data point as follows:

$$\ln a = \frac{K_1 K_2 - K_3 K_4}{N K_2 - (K_4)^2} \tag{J-2}$$

$$b = \frac{N K_3 - K_1 K_4}{N K_2 - (K_4)^2} \tag{J-3}$$

where

$$K_1 = \sum_i \ln (St_x \, Pr^{2/3}) \tag{J-4}$$

$$K_2 = \sum_i \ln^2 (Re_x) \tag{J-5}$$

$$K_3 = \sum_i \ln (St_x \, Pr^{2/3}) \ln(Re_x) \tag{J-6}$$

$$K_4 = \sum_i \ln (Re_x) \tag{J-7}$$

Performing the above calculations upon the free-stream Reynolds number values tabulated in Table D-6 ($N = 45$) results in the following:

$$K_2 = 9559$$

$$K_4 = 654.4$$

Similarly using the values given in Table I-1 results in:

$$K_1 = -255.7$$

$$K_3 = -3729$$

Substituting these values into Equations (J-2) and (J-3) results in the following correlation for all Stations/Configurations/Conditions of the Colburn j-Factor given in Table I-1:

$$St_x \, Pr^{2/3} = 0.117 \, Re_x^{-0.241} \tag{J-8}$$

Using the same procedure to find the least-squares fit for the modified Colburn j-Factor first for Stations 1 and 2 only and then for Stations 2, 3, and 4 only for all Configurations and Conditions results in the following:

For Stations 1 + 2 ($N = 18$)

$$K_1 = -119.2$$

$$K_2 = 3284$$

$$K_3 = -1611$$

$$K_4 = 242.9$$

$$(St_x \, Pr^{2/3})_{1-2} = 0.0683 \, Re_x^{-0.290} \tag{J-9}$$

For Stations 2 + 3 + 4 $(N = 27)$

$K_1 = -193.4$

$K_2 = 5861$

$K_3 = -2852$

$K_4 = 397.6$

$$(St_x \, Pr^{2/3})_{2-4} = 3.39 \, Re_x^{-0.570} \qquad \text{(J-10)}$$

For all Stations/Configurations/Conditions for the modified Colburn j-Factor using Equations (J-1) through (J-7) results in the following:

For Stations 1 + 2 + 3 + 4 + 5 $(N = 45)$

$K_1 = -319.3$

$K_2 = 9559$

$K_3 = -4662$

$K_4 = 654.4$

$$(St_x \, Pr^{2/3})_{1-5} = 0.488 \, Re_x^{-0.439} \qquad \text{(J-11)}$$

REFERENCES

1. Patterson, W. D. "Progress in Satisfying Environmental Requirements," presented at the American Power Conference, Chicago, Illinois, 29 April - 1 May 1974.

2. Hollander, H. I. and Cunningham, N. F. "Beneficiated Solid Waste Cubettes as Salvage Fuel for Steam Generation," *Proceedings of the 1972 National Incinerator Conference*. ASME, New York (1972):75-86.

3. Williams, R. H. "When the Well Runs Dry," *Environment* 14, No. 5 (June 1972):20.

4. Hauser, L. G. and Wright W. L. "An Assessment of Oil Gasification Processes for Electric Utility Power Generation," presented at the American Power Conference, Chicago, Illinois, 29 April - 1 May 1974.

5. Black, R. J.; Muckich, A. J.; Klee, A. J.; Hickman, H. L.; and Vaughan, R. D. *The National Solid Wastes Survey--An Interim Report*. United States Environmental Protection Agency, 1968.

6. Cohen, L. J. and Fernandes, J. H. "The Heat Value of Refuse," *Mechanical Engineering* 90, No. 9 (September 1968):47-51.

7. Regan, J. W. "Generating Steam from Prepared Refuse," *Proceedings of the 1970 National Incinerator Conference*. ASME, New York (1970):216-223.

8. Stabenow, G. "Results of the Stack Emission Tests of the New Chicago Northwest Incinerator," *Journal of Engineering for Power, Transactions of the ASME Series A* 95, No. 3 (July 1973): 137-141.

9. Niessen, W. R. and Chansky, S. H. "The Nature of Refuse," *Proceedings of the 1970 National Incinerator Conference*. ASME, New York (1970):1-24

10. "Refuse Power," *Resource Recovery* (January/February/March 1974): 6-9.

11. Murray, D. L.; Hartz, K. E.; and Carlson, R. G. "The Economics and Technology of Refuse as an Energy Source," presented at the American Power Conference, Chicago, Illinois, 29 April - 1 May 1974.

12. Finney, C. S. and Garrett, D. E. "The Flash Pyrolysis of Solid Wastes," presented at the Sixty-Sixth Annual Meeting of the AIChE, Philadelphia, Pennsylvania, 11-15 November 1973.

13. "Waste: A Materials Reservoir," *Mechanical Engineering* 96, No. 3 (March 1974):31.

14. Train, R. address to the Edison Electric Institute/Environmental Protection Agency Seminar, Washington, D. C., 3 December 1973.

15. Engdahl, R. B. "Incineration of Wastes," presented at the North American Fuel Technology Conference, Ottawa, Canada, 31 May 1970.

16. "Garbage In: Fuel Out," *Mechanical Engineering* 96, No. 3 (March 1974):81.

17. De Marco, J.; Keller, D. J.; Lechman, J.; and Newton, J. L. *Incinerator Guidelines--1969*. U. S. Department of Health, Education, and Welfare, Washington, D. C., 1969.

18. Engdahl, R. B. "Process By-Products and Wastes as Fuels," *Pyrodynamics* 2, Nos. 2 and 3 (March 1965):165-176.

19. Hescheles, C. A. "Burning All Industrial Wastes in a Central Facility," presented at the ASME Plant Engineering and Maintenance Division Conference, paper no. 68-PEM-10, Kansas City, Missouri, 29 April 1968.

20. Fernandes, J. H. and Shenk, R. C. "Solid Waste Fuel Burning in Industry," presented at the American Power Conference, Chicago, Illinois, 29 April - 1 May 1974.

21. *Resource Recovery from Municipal Solid Waste*. Lexington Books, Lexington, Massachusetts, 1974.

22. Bailie, R. C. and Alpert, S. B. "Use of Fluidised Beds for Conversion of Municipal Refuse to Fuel Gas," presented at the Sixty-Sixth Annual Meeting of the AIChE, Philadelphia, Pennsylvania, 11-15 November 1973.

23. Carlson, R. G. "Economics and Technology of Urban Refuse as an Energy Source," presented at the American Power Conference, Chicago, Illinois, 29 April - 1 May 1974.

24. Hering, R. and Greeley, S. A *Collection and Disposal of Municipal Refuse*. McGraw-Hill, New York, 1921.

25. Eberhardt, H. "European Practice in Refuse and Sewage Sludge Disposal by Incineration," *Proceedings of the 1966 National Incinerator Conference*. ASME, New York (1966):124-143.

26. Rogus, C. A. "An Appraisal of Refuse Incineration in Western Europe," *Proceedings of the 1966 National Incinerator Conference*. ASME, New York (1966):114-123.

27. Stephenson, J. W. and Cafiero, A. S. "Municipal Incinerator Design Practices and Trends," *Proceedings of the 1966 National Incinerator Conference*. ASME, New York (1966): 1-38.

28. Achinger, W. C. and Daniels, L. E. "An Evaluation of Seven Incinerators," *Proceedings of the 1970 National Incinerator Conference*. ASME, New York (1970):32-64.

29. Zinn, R. E.; La Mantia, C. R.; and Niessen, W. R. "Total Incineration," *Proceedings of the 1970 National Incinerator Conference*. ASME, New York (1970):116-127.

30. Benforado, D. M.; Pauletta, C. E.; and Hazzard, N. D. "Economics of Heat Recovery in Direct-Flame Fume Incineration," *Air Engineering* 9, No. 3 (March 1967):29-32.

31. Hartz, K. E. "Shredding Speeds Solid Waste Reduction," *Allis-Chalmers Engineering Review* 38, No. 2 (1973):4-7.

32. Stabenow, G. "Survey of European Experience with High Pressure Boiler Operation Burning Wastes and Fuel," *Proceedings of the 1966 National Incinerator Conference*. ASME, New York (1966):144-160.

33. Frankel, J. I. "Incineration of Process Wastes," presented at the ASME Winter Annual Meeting and Energy Systems Exposition, paper no. 68-WA/INC-1, New York, 1-5 December 1968.

34. Krause, H. H.; Vaughan, D. A.; and Miller, P. D. "Corrosion and Deposits from Combustion of Solid Wastes," *Journal of Engineering for Power, Transactions of the ASME Series A* 95 No. 1 (January 1973):45-52.

35. Corey, R. C., ed. *Principles and Practices of Incineration*. Wiley-Interscience, New York, 1969.

36. Essenhigh, R. H. "Incineration--A Practical and Scientific Approach," *Environmental Science and Technology* 2, No. 7 (July 1968):524-534.

37. *Municipal Refuse Disposal*. Committee on Refuse Disposal, American Public Works Association, Public Service Administration, 1961.

38. Ziel, P. H. *Apartment House Incinerators*. Building Research Advisory Board Technical Study for the Federal Housing Administration, National Academy of Sciences, National Research Council, publication no. 1280, 1965.

39. Starkman, E. S., ed. Combustion-Generated Air Pollution. Plenum Press, New York, 1971.

40. Stern, A. C., ed. Air Pollution. 2nd ed. Academic Press, New York, 1968.

41. Gilpin, A. Control of Air Pollution. Butterworths, London, 1963.

42. Thring, M. W., ed. Air Pollution. Butterworths, London, 1957.

43. Magill, P. L.; Holden, F. R.; and Ackley, C., ed. Air Pollution Handbook. McGraw-Hill, New York, 1956.

44. Stabenow, G. "Performance and Design Data for Large European Refuse Incinerators with Heat Recovery," Proceedings of the 1968 National Incinerator Conference. ASME, New York (1968): 278-286.

45. Cohan, L. J. and Fernandes, J. H. "Potential Energy Conversion Aspects of Refuse," presented at the ASME Winter Annual Meeting, paper no. 67-WA/PID-6, Pittsburgh, Pennsylvania, 12-17 November 1967.

46. Shequine, E. R. "Steam Generation from Incineration," Proceedings of the 1964 National Incinerator Conference. ASME, New York (1964):90-94.

47. Stirrup, F. Public Cleansing: Refuse Disposal. Pergamon Press, London, 1965.

48. Hansen, E. G. and Rousseau, H. "An Engineering Approach to the Waste Disposal Crisis," Combustion 41, No. 9 (March 1970): 8-13.

49. Tous, J. "Refuse Incineration with Heat Recovery in the Paris Region," Revue Generale de Thermique 12 (October 1973): 1045-1032.

50. Pope, P. D. and Turner, G. H. "Design of the First Large United Kingdom Power Producing Refuse Disposal Plant," Journal of Engineering for Power, Transactions of the ASME Series A 92, No. 3 (July 1970):239-251.

51. Singer, J. G. "Planning for Refuse Firing in Utility Steam Generators," 1974 Generation Planbook. McGraw-Hill, New York (1974):77-79.

52. Wisely, F. E.; Sutterfield, G. W.; and Klumb, D. L. "St. Loius Power Plant to Burn City Re[illegible]," Journal of the Power Division, Proceedings of the ASCE 97, No. 1 (January 1971):56-59.

53. Fife, J. A. "Design of the Northwest Incinerator for the City of Chicago," *Proceedings of the 1970 National Incinerator Conference*. ASME, New York (1970):249-260.

54. "Northwest Incinerator Plant is the Largest Complex of its Kind in the Western Hemisphere," *Solid Waste Management/Resource Recovery Journal* (May 1971):74, 150, 152.

55. Herrmann, W.; Stevens, W. A.; and Ramspeck, E. A. "1700 MW-Dickerson Plant Design Includes Refuse and Sewage Sludge Firing," presented at the American Power Conference, Chicago, Illinois, 29 April - 1 May 1974.

56. "Nashville Turns Garbage to Fuel," *Dallas Times Herald*, 10 May 1974, Sec. A, p. 16.

57. Vander Molen, R. H. "Energy from Municipal Refuse Through Fluidized Combustion: the CPU-400 Pilot Plant," presented at the Sixty-Sixth Annual Meeting of the AIChE, Philadelphia, Pennsylvania, 11-15 November 1973.

58. O'Conner, J. J. "Conservation Goal Met by Pollution Free Incineration, Heat Recovery," *Power* 119, No. 4 (April 1974): 62-63.

59. Mockridge, E. H. "Utilization of Package Boilers for the Combustion of Waste Fuels," presented at the American Power Conference, Chicago, Illinois, 29 April - 1 May 1974.

60. Swithenbank, J. "2000 Years More Oil," *Journal of Fluids Engineering, Transactions of the ASME Series I* 96, No. 1 (March 1974):2.

61. Rayleigh, O. M. "On the Dynamics of Revolving Fluids," 93 *Proceedings of the Royal Society of London Series A* (1917):148-154.

62. Proudman, J. "On the Motion of Solids in Liquids Possessing Vorticity," *Proceedings of the Royal Society of London* 92A (1916):408-424.

63. Taylor, G. I. "Experiments with Rotating Fluids," *Proceedings of the Royal Society of London* 100A (1921):114-121.

64. von Karman, T. "Uber Laminare und Turbulente Reibeing," *Zeitschrift Angew. Math. Mech.* 1 (August 1921):233-252.

65. Lamb, H. *Hydrodynamics.* Cambridge Press, Cambridge, Great Britain, 1924.

66. Goldstein, S., ed. *Modern Developments in Fluid Mechanics*. Clarendon Press, Oxford, Great Britain, 1938.

67. Truesdell, C. *Kinematics of Vorticity*. Indiana Unversity Press, Bloomington, Indiana, 1954.

68. Batchellor, G. K. *Fluid Dynamics*. Cambridge Press, Cambridge, Great Britain, 1967.

69. Owczarek, J. A. *Introduction to Fluid Dynamics*. International Textbook Company, Scranton, Pennsylvania, 1968.

70. Greenspan, H. P. *Theory of Rotating Flows*. Cambridge Press, Cambrdige, Great Britain, 1968.

71. Murthy, S. N. B. *Survey of Some Aspect of Swirling Flows*. Aerospace Research Laboratories Report ARL-71-0244, November 1971.

72. Soehngen, E. E., private communication 26 June 1974.

73. Bergles, A. E. "Survey and Evaluation of Techniques to Augment Convective Heat and Mass Transfer," *Progress in Heat and Mass Transfer*. Vol. 1, edited by U. Gridgull and E. Hahne, Pergamon Press, London, Great Britain (1969):331-424.

74. Bergles, A. E. "Techniques to Augment Heat Transfer," *Handbook of Heat Transfer*. Edited by W. M. Rohsenow and J. P. Hartnett, McGraw-Hill, New York, New York (1973):10-1 to 10-32.

75. Kreith, F. "Convection Heat Transfer in Rotating Systems," *Advances in Heat Transfer*. Vol. 5, edited by T. F. Irvine, Jr. and J. P. Hartnett, Academic Press, New York, New York (1968): 129-253.

76. Eckert, E. R. G. and Irvine, T. J., Jr. , ed. *Progress in Heat and Mass Transfer*. Vol. 3, Pergamon Press, London, Great Britain, 1971.

77. Gartshore, I. S. *Recent Work in Swirling Incompressible Flow*. National Research Council of Canada Aero. Report LR-343, 1962.

78. Gartshore, I. S. *Some Numerical Solutions for the Viscous Core of an Irrotational Vortex*. National Research Council of Canada Aero. Report LR-378, 1963.

79. Hall, M. G. "The Structure of Concentrated Vortex Cores," *Progress in Aeronautical Sciences*. Vol. 7, edited by D. Kuchemann, Pergamon Press, London, Great Britain (1966): 53-110.

80. Kuchemann, D. "Report on the I.U.T.A.M. Symposium on Concentrated Vortex Motion in Fluids," *Journal of Fluid Mechanics* 21, Part 1 (January 1965):1-20.

81. Riley, N. "Flows with Concentrated Vorticity: A Report on EUROMECH 41," Journal of Fluid Mechanics 62, Part 1 (8 January 1974):33-39.

82. Morton, R. B. "Geophysical Vortices," Progress in Aeronautical Sciences, Vol. 7, edited by D. Kuchemann, Pergamon Press, London, Great Britain (1966):145-194.

83. Howard, L. N. "Fundamentals of the Theory of Rotating Fluids," Journal of Applied Mechanics, Transactions of the ASME, Series E 30, No. 4 (December 1963):481-485.

84. Lighthill, M. J. "Dynamics of Rotating Fluids; A Survey," Journal of Fluid Mechanics 26, Part 2 (October 1966):411-431.

85. Carrier, G. F. "Phenomena in Rotating Flows," Proceedings of the Eleventh Congress on Applied Mechanics. Springer, Berlin, Germany, 1966.

86. Emmons, H. W. and Ying , S. "The Fire Whirl," Eleventh Symposium (International) on Combustion. The Combustion Institute, Pittsburgh, Pennsylvania (1967):475-488.

87. Lees, S. and Garris, C. A. "Formation of Multiple Fire Whirls," Twelfth Symposium (International) on Combustion. The Combustion Institute, Pittsburgh, Pennsylvania (1969):265-273.

88. Kuchemann, D., ed. Progress in Aeronautical Sciences. Vol. 7, Pergamon Press, London, Great Britain, 1966.

89. Baldwin, B. S.; Chigier, N. A.; and Sheaffer, Y. S. Decay of Far Flow Field in Trailing Vortices. NASA Technical Note TN-D-7568, February 1974.

90. Donaldson, C. D.; Bilanin, A. J.; and Crow, S. C. "Vortex Wakes of Large Aircraft," AIAA Professional Study Series Short Course, Palo Alto, California, 15-16 June 1974.

91. Lyttleton, R. A. The Stability of Rotating Masses. Cambridge Press, Cambridge, Great Britain, 1953.

92. Chandrasekhar, S. Hydrodynamic and Hydromagnetic Stability. Clarendon Press, Oxford, Great Britain, 1961.

93. Harvey, J. K. "Some Observations of the Vortex Breakdown Phenomenon," Journal of Fluid Mechanics 14, Part 4 (1962): 585-592.

94. Maxworthy, T. "On the Structure of Concentrated Columnar Vortices," Astronautica Acta 17, Nos. 4 and 5 (October 1972):363-374.

95. Orloff, K. L. and Bossel, H.H. *Laser Doppler Velocity Measurements of Swirling Flows with Upstream Influence*. NASA Contractor Report CR-2284, July 1973.

96. Hall, M. G. "Vortex Breakdown," *Annual Review of Fluid Mechanics*. Vol. 4, Annual Reviews Inc., Palo Alto, California (1972):195-217.

97. Hall, M. G. "A New Approach to Vortex Breakdown," *Proceedings of the 1967 Heat Transfer and Fluid Mechanics Institute*. Stanford University Press, Stanford, California (1967): 319-340.

98. Ludwieg, H. "Experimentelle Nachprufung der Stabilitatsthierien mit Schraubenlinien Formings Stromlinien," *Zeitschrift fur Flugwissenschaften* 12 (1964):304-309.

99. Benjamin, T. B. "Theory of Vortex Breakdown Phenomenon," *Journal of Fluid Mechanics* 14, Part 4 (1962):593-629.

100. Benjamin, T. B. "Some Developments in the Theory of Vortex Breakdown," *Journal of Fluid Mechanics* 28, Part 1 (12 April 1967):65-84.

101. Benjamin, T. B. "Upstream Influence," *Journal of Fluid Mechanics* 40, Part 1 (14 January 1970):49-79.

102. Bossel, H. H. "Vortex Breakdown Flowfield," *The Physics of Fluids* 12, No. 3 (March 1969):498-508.

103. Bossel, H. H. *Vortex Equations: Singularities, Numerical Solution, and Axi-Symmetric Vortex Breakdown*. NASA Contractor Report CR-2090, 1972.

104. Bossel, H. H. "Swirling Flows in Streamtubes of Variable Cross-Section," *AIAA Journal* 11, No. 8 (August 1973):1161-1165.

105. Lewellen, W. S. *A Review of Confined Vortex Flows*. NASA Contractor Report CR-1772, July 1971.

106. Chanaud, R. "Observation of Oscillatory Motion in Certain Swirling Flows," *Journal of Fluid Mechanics* 21, Part 1 (January 1965):111-127.

107. Cassidy, J. J. and Falvey, H. T. "Observations of Unsteady Flow Arising After Vortex Breakdown," *Journal of Fluid Mechanics* 41, Part 4 (15 May 1970):727-736.

108. Wotring, G. H. *Atomizing Oil Burner*. U. S. Patent 2,300,190, 1940.

109. Nolan, E. J. and Kishner, W. R. "An Atomized Spray Vortex Incinerator for Burning Dilute Sludge," *Proceedings of the 1972 National Incinerator Conference*. ASME, New York, New York (1972):281-289.

110. Berman, K. :Note on Compressible Flow through a Vortex Swirl Cup," *Journal of Applied Mechanics, Transactions of the ASME Series E* 40, No. 2 (June 1973):619-620.

111. Ullrich, H. "Stromungsvorgange in Drallbrennern mit Regelbaren Drall und bei Rotationssymmetrischen Freistrahlen," *Forschungsberichte auf dem Gebiete Ingenieur Wesens* 26, No. 1 (1960):19-28.

112. Rose, W. G. "A Swirling Round Turbulent Jet," *Journal of Applied Mechanics, Transactions of the ASME Series E* 29, No. 4 (December 1962):615-625.

113. Gore, R. W. and Ranz, W. E. "Back Flows in Rotating Fluids Moving Axially Through Expanding Cross Sections," *AIChE Journal* 10, No. 1 (January 1964):83-88.

114. Chigier, N. A. and Beer, J. M. "Velocity and Static Pressure Distributions in Swirling Air Jets Issuing from Annular and Divergent Nozzles," *Journal of Basic Engineering, Transactions of the ASME Series D* 86, No. 4 (December 1964):788-796.

115. Chigier, N. A. and Chervinsky, A. "Experimental Investigation of Swirling Vortex Motion in Jets," *Journal of Applied Mechanics, Transactions of the ASME Series E* 89, No. 2 (June 1967):443-451.

116. Loitsyanskii, L.G. "The Propagation of a Twisted Jet in an Unbounded Space Filled with the Same Fluid," *Prikladnaya Matematika i Mekhanika* 17 (1953):3-16.

117. Gortler, H. "Decay of Swirl in an Axially Symmetric Jet Far from the Orifice," *Revista Matematica Hispano Americanas* 14, Nos. 4 and 5 (1954):143-178.

118. Steiger, M. H. and Bloom, M. H. "Axially Symmetric Laminar Free Mixing with Swirl," *Proceedings of the 1961 Heat Transfer and Fluid Mechanics Institute*. Stanford University Press, Stanford, California, 1961.

119. Steiger, M. H. and Bloom, M. H. "Axially Symmetric Laminar Free Mixing with Large Swirl," *Journal of Heat Transfer, Transactions of the ASME Series C* 84, No. 4 (November 1962):370-374.

120. Shao-Lin, L. "Axisymmetric Turbulent Swirling Jet," *Journal of Applied Mechanics, Transactions of the ASME Series E* 87, No. 2 (June 1965):258-262.

121. Chigier, N. A. and Chervinsky, A. "Experimental and Theoretical Study of Turbulent Swirling Jets Issuing from a Round Orifice," *Israel Journal of Technology* 4, Nos. 1 and 2 (February 1966): 44-54.

122. Fejer, A. A.; Hermann, W. G.; and Torda, T. P. *Factors that Enhance Jet Mixing*. Aerospace Research Laboratories Report ARL 69-0175, 1969.

123. Pratte, B. D. and Keffer, J. R. "The Swirling Turbulent Jet," *Journal of Basic Engineering, Transactions of the ASME Series D* 94, No. 4 (December 1972):739-748.

124. Lilley, D. G. and Chigier, N. A. "Nonisotropic Turbulent Stress Distribution in Swirling Flows from Mean Value Distributions," *International Journal of Heat and Mass Transfer* 14, No. 4 (April 1971):573-585.

125. Lilley, D. G. "Prediction of Inert Turbulent Swirl Flows," *AIAA Journal* 11, No. 7 (July 1973):955-960.

126. Hottel, H. C. and Person, R. A. "Heterogeneous Combustion of Gases in a Vortex System," *Fourth Symposium (International) on Combustion*. Williams and Wilkins, Baltimore, Maryland (1953):781-788.

127. Pistor, R. "Industriegasbrenner," *Chemie-Ingenieur-Technik* 26, No. 4 (April 1954):206-220.

128. Albright, L. F. and Alexander, L. G. "Stable Cyclonic Flames of Natural Gas and Air," *Jet Propulsion* 26, No. 10 (October 1956):876-873.

129. Albright, L. F. and Alexander, L. G. "Flame Stabilization in Gases Flowing Cyclonically: Flow Characteristics," *Sixth Symposium (International) on Combustion*. Reinhold, New York, New York (1957):464-472.

130. Kenny, W. F. and Albright, L. F. "Energy Release in Flames Stabilized by Cyclonic Flow," *Industrial and Engineering Chemistry* 51, No. 2 (February 1959):227-228.

131. Drake, P. F. and Hubbard, E. H. "Effect of Swirl on Completeness of Combustion," *Journal of the Institute of Fuel, London* 36, No. 272 (September 1963):389-390.

132. Kerr, N. M. and Fraser, D. "Swirl. Part I: Effect of Axisymmetrical Turbulent Jets," *Journal of the Institute of Fuel, London* 38, No. 299 (December 1965):519-526.

133. Kerr, N. M. "Swirl. Part II: Effect on Flame Performance and the Modeling of Swirling Flames," *Journal of the Institute of Fuel, London* 38, No. 299 (December 1965):527-538.

134. Chigier, N. A. and Chervinsky, A. "Aerodynamic Study of Turbulent Burning Free Jets with Swirl," *Eleventh Symposium (International) on Combustion*. The Combustion Institute, Pittsburgh, Pennsylvania (1967):489-499.

135. Chervinsky, A. "Turbulent Swirling Jet Diffusion Flames," *AIAA Journal* 7, No. 10 (October 1969):1877-1883.

136. Beer, J. M.; Chigier, N. A.; Davies, T. W.; and Bassindale, K. "Laminarization of Turbulent Flames in Rotating Environments," *Combustion and Flame* 16, No. 1 (February 1971):39-45.

137. Syred, N.; Chigier, N. A.; and Beer, J. M. "Flame Stabilization in Recirculation Zones of Jets with Swirl," *Thirteenth Symposium (International) on Combustion*. The Combustion Institute, Pittsburgh, Pennsylvania (1971):617-624.

138. Beer, J. M. and Chigier, N. A. *Combustion Aerodynamics*. Wiley and Sons, New York, New York, 1972.

139. Syred, N. and Beer, J. M. "The Damping of Precessing Vortex Cores by Combustion in Swirl Generators," *Astronautica Acta* 17, Nos. 4 and 5 (October 1972):783-801.

140. Chigier, N. A. "Gasdynamics of Swirling Flow in Combustion Systems," *Astronautica Acta* 17, Nos. 4 and 5 (October 1972): 387-395.

141. James, H. and Green, F. D. "Laser-Dopler Velocity Measurements in Laminar Diffusion Flames," *Journal of Physics D: Applied Physics* 4, No. 5 (May 1971):738-740.

142. Parker, K. H. and Guillen, O. "Local Measurements in a Turbulent Flame by Hot-Wire Anemometry," *Thirteenth Symposium (International) on Combustion*. The Combustion Institute, Pittsburgh, Pennsylvania (1971):667.

143. Durst, F.; Melling, A.; and Whitelaw, J. H. "The Application of Optical Anemometry to Measurement in Combustion Systems," *Combustion and Flame* 18, No. 2 (April 1972):197-202.

144. Rubel, A. *Some Effects of Swirl on Turbulent Mixing and Combustion*. NASA Contractor Report CR-1956, 1972.

145. Rubler, A. *Swirling Jet Turbulent Mixing and Combustion Calculations*. NASA Contractor Report CR-2231, March 1973.

146. Lilley, D. G. and Chigier, N. A. "Nonisotropic Exchange Coefficients in Turbulent Swirling Flames from Mean Value Distributions," *Combustion and Flame* 16, No. 2 (April 1971): 177-189.

147. Lilley, D. G. and Chigier, N. A. "An Inverse Procedure for Turbulent Swirling Boundary Layer Combustion Flow," *Journal of Computational Physics* 9, No. 2 (April 1972): 237-253.

148. Lilley, D. G. "Turbulent Swirling Flame Prediction," *AIAA Journal* 12, No. 2(February 1974):219-223.

149. Lilley, D. G. "Swirl Flow Modeling for Combustors," presented at the AIAA Seventh Fluid and Plasma Dynamics Conference, Palo Alto, California, 17-19 June 1974.

150. Hacker, D. S. "A Simplified Mixing Length Model of Flame Stability in Swirling Combustion," *AIAA Journal* 12, No. 1 (January 1974):65-71.

151. Dergarabedian, P. "The Behavior of Vortex Motion in an Emptying Container," *Proceedings of the 1960 Heat Transfer and Fluid Mechanics Institute*. Stanford University Press, Stanford, California (1960):47-61.

152. Sibulkin, M. "A Note on the Bathtub Vortex," *Journal of Fluid Mechanics* 14, Part 1 (September 1962):21-24.

153. Einstein, H. A. and Li, H. "Steady Vortex Flows in a Real Fluid," *1951 Heat Transfer and Fluid Mechanics Institute*. Stanford University Press, Stanford, California (1951): 33-44.

154. Donaldson, C. D. and Sullivan, R. D. "Behavior of Solutions of the Navier-Stokes Equations for a Complete Class of Three-Dimensional Viscous Vortices," *Proceedings of the 1960 Heat Transfer and Fluid Mechanics Institute*. Stanford University Press, Stanford, California (1960):16-30.

155. Donaldson, C. D. and Sullivan, R. D. *Examination of the Solutions of the Navier-Stokes Equations for a Class of Three-Dimensional Vortices*. Aeronautical Research Associates of Princeton Inc., AFOSR TN 60-1227, October, 1960.

156. Donaldson, C. D. and Snedeker, R. S. *Experimental Investigation of the Structure of Vortices in Simple Cylidrical Vortex Chambers*, Aeronautical Research Associates of Princeton Inc. Report No. 47, 1962.

157. Lewellen, W. S. "A Solution for Three-Dimensional Flows with Strong Circulation," *Journal of Fluid Mechanics* 14, Part 3 (November 1962):420-432.

158. Rosenzweig, M. L.; Lewellen, W. S.; and Ross, D. H. "Confined Vortex Flows with Boundary-Layer Interaction," *AIAA Journal* 2, No. 12 (December 1964):2127-2134.

159. Rott, N. and Lewellen, W. S. "Boundary Layers in Rotating Flows," *Progress in Aeronautical Sciences*. Vol. 7, edited by D. Kuchemann, Pergamon Press, London, Great Britain (1966):111-144.

160. Serrin, J. "The Swirling Vortex," *Philosophical Transactions of the Royal Society of London Series A, Mathematical and Physical Sciences* 271, No. 1214 (27 January 1972):325-360.

161. Chi, S. W. and Glowacki, W. J. "Applicability of Mixing Length Theory to Turbulent Boundary Layers Beneath Intense Vortices," *Journal of Applied Mechanics, Transactions of the ASME Series E* 41, No. 1 (March 1974):15-19.

162. Hoffman, J. A. "Similarity Solutions for the Interaction of a Potential Vortex with Free Stream Sink Flow and a Stationary Surface," *Journal of Fluids Engineering, Transactions of the ASME Series I* 96, No. 1 (March 1974):49-54.

163. Smithson, I. K. "Some Pressure Characteristics of Confined Vortex Flow," *Journal of the Institute of Fuel* 45, No. 373 (March 1972):147-153.

164. Talbot, L. "Laminar Swirling Pipe Flow," *Journal of Applied Mechanics* 21, No. 1 (March 1954):1-7.

165. Laufer, J. *The Structure of Turbulence in Fully Developed Pipe Flow*. NACA Report No. 1174, 1954.

166. Thompson, J. F., Jr. *The Structure of Free and Confined Turbulent Vortices*. Mississippi State University Aerophysics Department Research Note No. 44, 1963.

167. Musolf, A. O. *An Experimental Investigation of the Decay of a Turbulent Swirl Flow in a Pipe*. Thesis, University of Colorado, 1963.

168. Kreith, F. and Sonju, O. K. "The Decay of a Turbulent Swirl in a Pipe," *Journal of Fluid Mechanics* 22, Part 2 (June 1965):257-271.

169. Youssef, T. E. A. "Some Investigations on Rotating Flow with a Recirculation Core in Straight Pipes," ASME paper no. 66-WA-FE-36, 1966.

170. Lavin, Z. and Fejer, A. A. *Investigation of Swirling Flow in Ducts*. Aerospace Research Laboratories Report ARL 66-0083, May 1966.

171. Baker, D. W. *Decay of Swirling Turbulent Flow of Incompressible Fluids in Long Pipes*. Ph.D. Thesis, University of Maryland, 1961.

172. Wolf, L., Jr.; Lavan, Z.; and Fejer, A. A. "Measurement of the Decay of Swirl in Turbulent Flows," *AIAA Journal* 7, No. 5 (May 1969):971-973.

173. Rochino, A. and Lavan, Z. "Analytical Investigations of Incompressible Turbulent Swirling Flow in Stationary Ducts," *Journal of Applied Mechanics, Transactions of the ASME Series E* 36, No. 2 (June 1969):151-158.

174. Yajnik, K. S. and Subbaiah, M. V. "Experiments on Swirling Turbulent Flows. Part 1. Similarity in Swirling Flows," *Journal of Fluid Mechanics* 60, Part 4 (9 October 1973): 665-687.

175. Love, W. J. "Prediction of Pressure Drop in Straight Vortex Tubes," *AIAA Journal* 12, No. 7 (July 1974):959-965.

176. Filippov, G. V. and Shakhov, V. G. "The Turbulent Boundary Layer in the Initial Segment of Axisymmetric Channels when Flow Swirling Occurs at the Inlet," *Journal of Engineering Physics* 17, No. 1 (1972):855-860.

177. Gostinets, Yu. A. and Zaitsev, V. M. "Kinematic Similarity of a Turbulent Swirled Flow in a Pipe," *Journal of Engineering Physics* 20, No. 3 (1 September 1973):311-314.

178. Liane, R. and Ivanov, Iu. "Development of Swirling Flow in a Cylindrical Chamber with a Diaphragm-Free Inlet Section," *Eesti NSV Teaduste Akadeemia, Toimetised, Fuusika-Matemaatika* 19, No. 4 (1970):456-462.

179. Veske, D. R. and Sturov, G. E. "Experimental Investigations of Turbulent Swirl Flow in a Cylindrical Tube," *Akademiia Nauk SSSR, Sibirskoe, Otdelenie, Izvestiia, Seriia Tekhnicheskikh Nauk* (October 1972):3-7.

180. Murtse, Kh. "Decay of Swirl in a Flow Through a Circular Section Pipe," *Eesti NSV Teaduste Akadeemia Toimetised Fuusika-Matemaatika* 22, No. 1 (1973):77-82.

181. Gambill, W. R. and Greene, N. D. "Boiling Burnout with Water in Vortex Flow," *Chemical Engineering Progress* 54 No. 10 (October 1958):68-76.

182. Greene, N. D. and Gambill, W. R. *A Preliminary Investigation of Air Film Heat Transfer Coefficients for Free and Forced Vortex Flows within Tubes*. Oak Ridge National Laboratory Report ORNL 58-5-67, May 1958.

183. Blum, H. A. and Oliver, L. R. "Heat Transfer in a Decaying Vortex System," ASME paper No. 66-WA/HT-62, 1966.

184. Andrade, Y. and Erfurth, K. "An Experimental Investigation of a Vortex-Stabilized Long Alternating Current Arc Discharge," *Proceedings of the First Plasma Arc Seminar of the Thermo-Mechanics Research Laboratory*. Aerospace Research Laboratories, Wright-Patterson AFB (September 1963):100-144.

185. [illegible], U. Y. *Effects of Vortex Chamber Flow by Varying the Chamber Length and Convective Heat Transfer in a Vortex Tube Flow from a Centrally Located Cylinder*. M.S. Thesis, Air Force Institute of Technology, August 1960.

186. Moore, G. D., Jr. *An Experimental and Analytical Study of Vortex Flow*. M.S. Thesis, Air Force Institute of Technology, August 1959.

187. Holman, J. P. and Moore, G. D. "An Experimental Study of Vortex Chamber Flow," *Journal of Basic Engineering, Transactions of the ASME Series D* 83, No. 4 (December 1961): [illegible]-637.

188. McKelvey, R. *Heat Transfer from a Heated Cylinder in a Vortex Type Flow*. M.S. Thesis, Air Force Institute of Technology, August 1960.

189. Kelsey, T. L. *Evaluation of a Cylindrical Probe to Measure Flow Properties in a Vortex Tube*. M.S. Thesis, Air Force Institute of Technology, August 1961.

190. Loesley, D. J. *Heat Transfer from a Centrally Located Source in a Vortex Flow*. M.S. Thesis, Air Force Institute of Technology, August 1961.

191. Talcott, R. C. *Experimental Investigation of the Heat Transfer from a Coaxial Heat Source to a Confined Straight Axial or Vortex Flow*. M.S. Thesis, Air Force Institute of Technology, March 1965.

192. Palasek, E. J. *Experimental Study of Vortex Flow in a Cylinder*. M.S. Thesis, Air Force Institute of Technology, March 1966.

193. Murthy, S. N. B. and Soehngen, E. E. *Nonisothermal Swirling Flows in Ducts, Part I*. Aerospace Research Laboratories ARL 70-0151, August 1970.

194. Murthy, S. N. B. and Soehngen, E. E. *Nonisothermal Swirling Flows in Ducts, Part II*. Aerospace Research Laboratories unpublished manuscript on loan from E. E. Soehngen.

195. Alimov, R. Z. "Flow Friction and Heat and Mass Transfer in a Swirled Flow," *Inzhenerno-Fizicheskii Zhurnal* 10, No. 4 (April 1966):437-445, *Journal of Engineering Physics* (1966): 251-257.

196. Migay, V. K. and Golubev, L. K. "Friction and Heat Transfer in Turbulent Swirl Flow with a Variable Swirl Generator in a Pipe," *Heat Transfer-Soviet Research* 2, No. 3 (May 1970): 68-73.

197. Bol'shakov, A. G. and Ryabykh, V. G. "Study of Fluid Dynamics of a Heat Exchanger with Swirled Gas and Liquid Flows," *Heat Transfer-Soviet Research* 3, No. 2 (March-April 1971): 104-109.

198. Koval'nogov, A. F. and Shchukin, V. K. "Heat Transfer and Hydraulic Resistance in Tubes with Bladed Swirls," *Inzhenerno-Fizicheskii Zhurnal* 14, No. 2 (February 1968):239-247, *Journal of Engineering Physics* (1972):121-126.

199. Koval'nogov, A. F. and Goldobeev, V. I. "Analogy Factor in a Tube with Local Twisting of the Flow by Swirl Vanes," *Kazanskii Aviatsionnyi Institut, Trudy, Seriia Aviatsionnye Dvigateli* No. 133 (1971):37-41.

200. Sudarev, A. V. "Heat Transfer and Drag of a Turbulent Swirling Air Stream in the Entrance Section of an Annular Channel," *Inzhenerno-Fizicheskii Zhurnal* 15, No. 5 (November 1968): 827-831, *Journal of Engineering Physics* (1972):1049-1052.

201. Borisenko, K. F.; Nechitailo, K. R.; Safonov, V. A.; and Yakovlev, A. I. "Hydraulic Resistance and Heat Transfer in an Annular Channel with Rotating Flow," *Inzhenerno-Fizicheskii Zhurnal* 21, No. 1 (July 1971):38, *Journal of Engineering Physics* (15 November 1973):838-840.

202. Bukhman, M. A. and Ustimenko, B. P. "A Study of Aerodynamics and Heat Transfer of Swirled Flows Developing in an Constrained Space," *Heat Transfer-Soviet Research* 5, No. 4 (July-August 1973):123-127.

203. Shchukin, V. K.; Koval'nogov, A. F.; and Kolkunov, V. S. "Study of Local Heat Transfer Coefficients in a Tube in the Case of a Local Flow Swirling by Swirl Vanes," *Inzhenerno-Fizicheskii Zhurnal* 23, No. 3 (September 1972): 430-434.

204. Kharitonov, V. P. "The Effect of Liquid Flow Swirl on the Intensification of Convection Heat Transfer in a Circular Tube," *Inzhenerno-Fizicheskii Zhurnal* 16, No. 2 (February 1969):225, *Journal of Engineering Physics* (1972):141-146.

205. Ghil, M. and Solan, A. "Heat Transfer through a Rankine Vortex," *Journal of Heat Transfer, Transactions of the ASME Series C* 95, No. 1 (February 1973):137-139.

206. Ranque, G. J. "Experiences Sur la Dentente Giratoire Avec Productions Simultanees d'un Echappement d'Air Froid," *Bull Bi-Mensuel de la Societe Francaise de Physique* (June 1933):1125.

207. Ranque, G. J. *Method and Apparatus for Obtaining from a Fluid* [illegible] U. S. Patent 1,952,281, 27 March 1934.

208. Hilsch, R. "The Use of the Expansion of Gases in a Centrifugal Field as a Cooling Process," *Review of Scientific Instruments* 18, No. 2 (1947):108-113.

209. Milton, R. M. "Maxwellian Demon at Work." *Industrial and Engineering Chemistry, Industrial Edition* 38, No. 5 (May 1946):5A.

210. Fulton, C. D. "Ranque's Tube," *Refrigerating Engineering, Journal of the ASRE* 58, No. 5 (May 1950):473-479.

211. Curley, W. and McGree, R. "Bibliography of Vortex Tube," *Refrigerating Engineering, Journal of the ASRE* 59, No. 2 (February 1951):191-193.

212. Westley, R. *Vortex Tube Performance Data Sheets.* College of Aeronautics, Cranfield University, Note No. 67, 1957.

213. Eckert, E. R. G. and Hartnett, J. P. "Measurements of the Energy Separation in a High Velocity Vortex Type Flow," *Proceedings of the Fourth Midwestern Conference on Fluid Mechanics,* Purdue University Engineering Experiment Station Research Series No. 128, Lafayette, Indiana (1955):65-92.

214. Eckert, E. R. G. and Hartnett, J. P. "Experimental Study of the Velocity and Temperature Distributions in a High Velocity Vortex Type Flow," *Proceedings of the Heat Transfer and Fluid Mechanics Institute,* [illegible] (1955):135-150.

215. Hartnett, J. P. and Eckert, E. R. G. "Experimental Study of the Velocity and Temperature Distribution in a High Velocity Vortex Type Flow," *Transactions of the ASME* 79, No. 5 (May 1957):751-757.

216. Keyes, J. J., Jr. "An Experimental Study of Gas Dynamics in High Velocity Vortex Flow," *Proceedings of the 1960 Heat Transfer and Fluid Mechanics Institute.* Stanford University Press, Stanford, California (1960):31-46.

217. Schowalter, W. R. and Johnstone, H. F. "Characteristics of the Mean Flow Patterns and Structure of Turbulence in Spiral Gas Streams," *AIChE Journal* 6, No. 4 (December 1960):648-655.

218. Savino, J. M. and Ragsdale, R. G. "Some Temperature and Pressure Measurements in Confined Vortex Flows," *Journal of Heat Transfer, Transactions of the ASME Series C* 83, No. 1 (February 1961):33-38.

219. Kassner, R. and Knoernschild, E. *Friction Laws and Energy Transfer in Circular Flow*. Wright-Patterson Air Force Base Technical Report No. F-TR-2198-ND, March 1948.

220. Deissler, R. G. and Perlmutter, M. "Analysis of the Flow and Energy Separation in a Turbulent Vortex," *International Journal of Heat and Mass Transfer* 1, Nos. 2 and 3 (August 1960):173.

221. Deissler, R. G. and Perlmutter, M. "An Analysis of the Energy Separation in Laminar and Turbulent Compressible Vortex Flows," *1958 Heat Transfer and Fluid Mechanics Institute*. Stanford Press, Stanford, California (1958):40-53.

222. Lay, J. E. "An Experimental and Analytical Study of the Vortex-Flow Temperature Separation by Super Position of Spiral and Axial Flows," *Journal of Heat Transfer, Transactions of the ASME Series C* 81, No. 3 (August 1959): 202-212.

223. Lay, J. E. "An Experimental and Analytical Study of the Vortex-Flow Temperature Separation by Super Position of Spiral and Axial Flows," *Journal of Heat Transfer, Transactions of the ASME Series C* 81, No. 3 (August 1959): 213-222.

224. Sibulkin, M. "Unsteady, Viscous, Circular Flow I. The Line Impulse of Angular Momentum," *Journal of Fluid Mechanics* 11, Part 2 (September 1961):291-308.

225. Sibulkin, M. "Unsteady, Viscous, Circular Flow II. The Cylinder of Finite Radius," *Journal of Fluid Mechanics* 12, Part 1 (August 1962):148-158.

226. Sibulkin, M. "Unsteady, Viscous, Circular Flow III. Application to the Ranque-Hilsch Vortex Tube," *Journal of Fluid Mechanics* 12, Part 2 (September 1962):269-293.

227. Linderstrom-Lang, C. U. "The Three-Dimensional Distributions of Tangential Velocity and Total-Temperature in Vortex Tubes," *Journal of Fluid Mechanics* 45, Part 1 (15 January 1971): 161-187.

228. Reynolds, A. J. "A Note on Vortex-Tube Flows," *Journal of Fluid Mechanics* 14, Part 1 (September 1962):18-20.

229. Timm, G. K. *Survey of Experimental Velocity Distributions in Vortex Flows with Bibliography*. Boeing Scientific Research Laboratories Document D1-82-0687, November 1967.

230. Gulyaev, A. I. "Investigation of Conical Vortex Tube," *Inzhenerno-Fizicheskii Zhurnal* 10, No. 3 (March 1966):326, *Journal of Engineering Physics* (1969):193-195.

231. Martynov, A. V. and Brodyanskii, V. M. "Investigation of the Parameters of a Vortex Flow Inside a Ranque-Hilsch Tube," *Inzhenerno-Fizicheskii Zhurnal* 12, No. 5 (May 1967):639, *Journal of Engineering Physics* (1971):345-348.

232. Westley, R. *A Bibliography and Survey of the Vortex Tube*. The College of Aeronautics, Cranfield University, Note No. 9, 1954.

233. Dobratz, B. M. *Vortex Tubes, A Bibliography*. University of California Lawrence Radiation Laboratory Report UCRL-7829, 1964.

234. Ter Linden, A. J. "Investigations into Cyclone Dust Collection," *Proceedings of the Institution of Mechanical Engineers* 160 ([illegible]):[illegible].

235. Iinoya, K. "Study on the Cyclone," *Faculty of Engineering, Nagoya University* 5, No. 2 (1953):131.

236. Davies, C. N. "The Separation of Airborne Dust and Particles," *Proceedings of the Institution of Mechanical Engineers* 166, No. 5 ([illegible]):[illegible]-213.

237. Smith, J. L., Jr. "An Analysis of the Vortex in the Cyclone Separator," *Journal of Basic Engineering, Transactions of the ASME Series D* 84, No. 4 (December 1962):609-618.

238. Smith, J. L., Jr. "An Experimental Study of the Vortex in the Cyclone Separator," *Journal of Basic Engineering, Transactions of the ASME Series D* 84, No. 4 (December 1962):[illegible].

239. Fiorino, T. D. and Poplawski, R. *Experimental Optimization of the Reverse-Flow Swirl Chamber*. Aerospace Research Laboratories Report ARL 65-68, April 1965.

240. Poplawski, R. and Pinchak, A. C. *Aerodynamic Performance of Reversed Flow Vortex Chambers*. Aerospace Research Laboratories Report ARL 65-219. October 1965.

241. Uspenskii, V. A.; Solov'ev, V. I.; and Gur'eva, V. S. "Studying Velocity Fields in a Cyclone Separator," *Fluid Mechanics-Soviet Research* 1, No. 1 (January-February 1972):128-135.

242. Rietema, K. and Verver, C. G. *Cyclones in Industry*. Elsevier Publishing Company, 1961.

243. Bradley, D. *The Hydrocyclone*. Pergamon Press, 1965.

244. Thoma, D. *Fluid Lines*. U. S. Patent 1,839,616, June 1928.

245. Hain, K. "An Investigation of the Thoma Counterflow Brake," *Transactions of the Hydraulic Institute*, Munich Technical Institute, Bulletin No. 3, 1929.

246. Mayer, E. A. and Taplin, L. B. "Vortex Devices," *Fluidics*. Fluid Amplifier Associates, Boston, Massachusetts (1965): 185-200.

247. Lawley, T. J. *Vortex Fluid Amplifier—An Experimental Study of Flow Characteristics and Internal Flow Field*. Ph.D. Dissertation, Southern Methodist University, July 1970.

248. Lee, J. F., Jr. *An Experimental and Analytical Study of Receiver Characteristics of Vented and Non-Vented Vortex Fluid Amplifiers*. Ph.D. Dissertation, Southern Methodist University, April 1970.

249. "Vortex Techniques Stir up Flowmetering," *Process Engineering* (May 1974):69-70.

250. Schoenherr, O. "Die Fabrikation des Luft Stickstoff Salpeters Elektrotechn 22," *Elektrotechnische Zeitschrift* 30 (1909):365.

251. Grey, J. "A Gaseous-Core Nuclear Rocket Utilizing Hydrodynamic Containment of Fissionable Material," American Rocket Society Paper No. ARS 848-59, June 1959.

252. Kerrebrock, J. L. "Diffusion in Neutral and Ionized Gases with Extreme Pressure Gradients," *1959 Heat Transfer and Fluid Mechanics Institute*. Stanford University Press, Stanford, California (1959):193-206.

253. Kerrebrock, J. L. and Meghreblian, R. V. "Vortex Containment for the Gaseous Fission Rocket," *Journal of the Aerospace Sciences* 28, No. 9 (September 1961):710-724.

254. Lewellen, W. S. "Magnetohydrodynamically Driven Vortices," *Proceedings of the 1960 Heat Transfer and Fluid Mechanics Institute*. Stanford University Press, Stanford, California (1960):1-13.

255. Ragsdale, R. G. *NASA Research on the Hydrodynamics of the Gaseous Vortex Reactor*. NASA Technical Note TN D-288, September 1960.

256. Kendall, J. M., Jr. *Experimental Study of a Compressible Viscous Vortex*. Jet Propulsion Laboratory Technical Report No. 32-290, 5 June 1962.

257. Farris, G. J.; Kidd, G. L., Jr.; Lick, D. W.; and Textor, R. E. "A Theoretical and Experimental Study of Confined Vortex Flow," *Journal of Applied Mechanics, Transactions of the ASME Series E* 36, No. 4 (December 1969):687-692.

258. Swithenbank, J. and Chigier, N. A. "Vortex Mixing for Supersonic Combustion," *Twelfth Symposium (International) on Combustion*. The Combustion Institute, Pittsburgh, Pennsylvania (1969):1153-1162.

259. Murthy, S. N. B. *Containment Problems in Electrical and Nuclear Propulsion*. Aerospace Research Laboratories Report ARL 71-0126, August 1971.

260. Guderley, K. G. and Tabak, D. *On the Determination of Optimum Supersonic Thrust Nozzles of a Given Length for a Flow with Swirl, Theoretical Part*. Aerospace Research Laboratories Report ARL 66-0013, January 1966.

261. Guderley, K. G. and Breiter, M. C. *Approximation of Swirl Flows in the Vicinity of the Throat of a Laval Nozzle*. Aerospace Research Laboratories Report ARL 70-0009, January 1970.

262. Kugerley, K. G. and Breiter, M. C. *On the Determination of Optimum Thrust Nozzle of a Given Length for a Flow with Swirl, Numerical Results*. Aerospace Research Laboratories Report ARL 70-0161, September 1970.

263. Boerner, C. J.; Sparrow, E. M.; and Scott, C. J. "Compressible Flow Through Convergent-Divergent Nozzles," *Warme-und Stoffubertragung* 5, No. 2 (1972):101-115.

264. So, K. L. "Vortex Phenomena in a Conical Diffuser," *AIAA Journal* 5, No. 6 (June 1967):1072-1078.

265. Chow, C. Y. "Swirling Flow in Tubes of Non-Uniform Cross-Sections," *Journal of Fluid Mechanics* 38, Part 4 (6 October 1969):843-854.

266. Baumeister, T., ed. *Standard Handbook for Mechanical Engineers*. 7th ed., McGraw-Hill, New York, New York, 1967.

267. "Cyclone Furnace," *McGraw-Hill Encyclopedia of Science and Technology*. Vol. 3, McGraw-Hill, New York, New York (1971): 690-691.

268. *Steam/Its Generation and Use.* 38th ed., The Babcock and Wilcox Company, New York, New York, 1972.

269. Hurley, T. F. "Some Factors Affecting the Design of a Small Combustion Chamber of Pulverized Fuel," *The Institute of Fuel Journal* 6 (April 1931):243-254.

270. Vroom, R. C. *Pulverized Fuel Burner*. U. S. Patent 2,325,442, 27 July 1943.

271. Parmele, B. J. *Cyclone Burner*. U. S. Patent 2,476,507, 1946.

272. Grunert, A. E.; Skog, L.; and Wilcoxson, L. S. "The Horizontal Cyclone Burner," *Transactions of the ASME* 69, No.6 (August 1947):613-634.

273. Gilg, F. X. "The Cyclone Furnace--Latest Thing in Coal Burning," *Power Generation* 54, No. 4 (April 1950): 64-70.

274. Schroeder, H. C. and Strasser, R. J. "Station Design Experience with Cyclone-Fired Steam Generators," *Transactions of the ASME* 74, No. 5 (May 1952):573-578.

275. Katsnel'son, B. D. and Bogdanov, L. A. "Aerodynamic Characteristics of a Vertical Cyclone Furnace with Top Gas Outlet," *Thermal Engineering* 17, No. 4 (1970):82-86.

276. Smith, M. L. and Stinson, K. W. *Fuels and Combustion*. McGraw-Hill, New York, New York, 1952.

277. Garner, F. H. and Cheetham, H. A. "The Flow Pattern of Gas Turbine Combustion," *The Journal of the Institute of Petroleum* 37, No. 333 (September 1951):554-566.

278. Stone, V. L. and Wade, I. I. "Operating Experience with Cyclone-Fired Steam Generators," *Mechanical Engineering* 74, No. 5 (May 1952):359-368.

279. Dumontet, P. and Tissandier, G. "Pilot Study of Swirling Flow Burners Intended for Pulverized Coal Boiler Furnaces," *Revue Generale Thermique* 11, No. 130 (October 1972):921-931.

280. Seidl, H. "The Development and Practice of Cyclone Firing in Germany," *Proceedings of the Joint Conference on Combustion of the Institution of Mechanical Engineers and the ASME 1955*. The Institution of Mechanical Engineers (1955):92-102.

281. Kalishevskii, L. L. and Ganchev, B. G. "Flow Pattern of Cyclone Process During Combustion of a Solid Fuel," *Thermal Engineering* 14, No. 2 (August 1967):70-74.

282. Basina, I. P. and Tugay, O. I. "Motion of Burning Coal Particles in Swirling Flow," *Heat Transfer-Soviet Research* 1, No. 3 (May 1969):202-211.

283. Ryzhakov, A. V.; Zhukov, I. T.; and Morozov, I. N. "Realization of an Analytical Model of Heat Exchange Between the Flame and the Surfaces of a Vortex Burner on a Digital Computer," *Thermal Engineering* 20, No. 1 (January 1973):41-45.

284. Marshak, Y. L.; Zhukov, I. T.; Verbovetskii, I. K.; Andryushkin, V. M.: Mandzyuk, A. P.; and Cherkasov, I. I. "Vortex Burners with Increased Hub-Tip Ratio to Improve Combustion Efficiency of Anthracite Fines," *Thermal Engineering* 20, No. 2 (February 1973):44-48.

285. Mills, R. G. and Berman, L. G. "Operating Experience in the Suspension Burning of Waste Materials in Cyclone Incinerators," *Proceedings of the 1972 National Incinerator Conference*, ASME, New York, New York (1972):195-200.

286. Niedzwiecki, R. W. and Jones, R. E. *Combustion Stability of Single-Can Combustor Modules Using ASTM-A1 Liquid Fuel*. NASA Technical Note TN D-5436, October 1969.

287. Niedzwiecki, R. W. and Jones, R. E. "Pollution Measurements of a Swirl-Can Combustor," *AIAA Journal* 12, No. 6 (June 1974):844-849.

288. Osgerby, I. T. "Literature Review of Turbine Combustor Modelling and Emissions," *AIAA Journal* 12, No. 6 (June 1974):743-754.

289. Salisbury, J. K., ed. *Kent's Mechanical Engineer's Handbook, Power Volume*. 12th ed., John Wiley and Sons, New York, New York (1950):pages 2-35 to 2-37.

290. "Furnace, Steam Generating," *McGraw-Hill Encyclopedia of Science and Technology*. Vol. 5, McGraw-Hill, New York, New York (1971):606-607.

291 Corey, R. C.; Spano, L. A.; Schwartz, C. H.; and Perry, H. "Experimental Study of Effects of Tangential Overfire Air on the Incineration of Combustible Wastes," *Air Repair* 3, No. 2 (November 1953):109-116.

292. Corey, R. C. and Schwartz, C. H. "Combustion of Low-Ash, High-Volatile Solids with Tangential Overfire Air," *University of Sheffield Fuel Society Journal* 8 (1957):5-13.

293. Corey, R. C.; Orning, A. A.; Schwartz, C. H.; and Pfeiffer, J. J. "A Progress Report on the Experimental Studies of Incineration by the U.S. Bureau of Mines," paper presented at the Symposium on Developments in Incinerator Design sponsored by New York University, New York, 23 May 1957.

294. Weintraub, M.; Orning, A. A.; and Schwertz, C. H. Experimental Studies of Incineration in a Cylindrical Combustion Chamber. U. S. Bureau of Mines Report RI 6908, 1967.

295. Schwartz, C. H.; Orning, A. A.; Snedden, R. B.; Demeter, J. J.; and Bienstock, D. "Development of a Vortex Incinerator with Continuous Feed," Proceedings of the 1972 National Incinerator Conference, ASME, New York, New York (1972):145-154.

296. Dorfman, L. A. Hydrodynamic Resistance and the Heat Loss of Rotating Solids. Translated by N. Kemmer, Oliver and Boyd, Edinburgh, Great Britain, 1963.

297. Dorfman, L. A. "Heat and Mass Transfer Near Rotating Surfaces," Inzhenerno-Fizicheskii Zhurnal 22, No. 2 (February 1972):350,. Journal of Engineering Physics (April 1974):247-257.

298. Cham, T. S. and Head, M. R. "Turbulent Boundary Layer Flow on a Rotating Disc," Journal of Fluid Mechanics 37, Part 1 (1969):129-147.

299. Cham, T. S. and Head, M. R. "The Turbulent Boundary Layer on a Rotating Cylinder in an Axial Stream," Journal of Fluid Mechanics 42, Part 1 (1970):1-15.

300. Cham, T. S. and Head, M. R. "The Turbulent Boundary Layer on a Rotating Nose-Body," Aeronautical Quarterly 22, Part 4 (November 1971):389-402.

301. Chin, D-T "Turbulent Flow and Mass Transfer on a Rotating Hemispherical Electrode," AIChE Journal 20, No. 2 (March 1974):245.

302. Koosinlin, M. R. and Lockwood, F. C. "The Prediction of Axisymmetric Turbulent Swirling Boundary Layers," AIAA Journal 12, No. 4 (April 1974):547-554.

303. Johnson, T. R. and Joubert, P. N. "The Influence of Vortex Generators on the Drag and Heat Transfer from a Cylinder Normal to an Air-Stream," Journal of Heat Transfer, Transactions of the ASME Series C 91, No. 1 (February 1969):91-99.

304. Eisele, E. H.; Leidenfrost, W.; and Muthuanayagam, A. E. "Studies of Heat Transfer from Rotating Heat Exchangers," Progress in Heat and Mass Transfer. Vol. 2, Pergamon Press, London, Great Britain (1969):483-499.

305. Eastop, T. D. "The Influence of Rotation on the Heat Transfer from a Sphere to an Air Stream," *International Journal of Heat and Mass Transfer* 16, No. 10 (October 1973):1954-1957.

306. Kooslin, M. L.; Launder, B. E.; and Sharma, B. I. *Prediction of Momentum, Heat, and Mass Transfer in Swirling Turbulent Boundary Layers*. NASA Accession No. N74-13976, 1973.

307. Koosinlin, M. L.; Launder, B. E.; and Sharma, B. I. "Prediction of Momentum, Heat, and Mass Transfer in Swirling Turbulent Boundary Layers," *Journal of Heat Transfer, Transactions of the ASME Series C* 96, No. 2 (May 1974):204-209.

308. Launder, B. E.; Koosinlin, M. L.; and Sharma, B. I. "Prediction of Momentum, Heat, and Mass Transfer in Swirling, Turbulent Boundary Layers," paper presented at the AIAA/ASME Thermophysics and Heat Transfer Conference, Boston, Massachusetts, 15-17 July 1974.

309. Bien, F. and Penner, S. S. "The Velocity Profiles in Steady and Unsteady Rotating Flows for a Finite Cylindrical Geometry," *The Physics of Fluids* 13, No. 7 (July 1970):1665-1671.

310. Carrier, G. F. "Swirling Flow Boundary Layers," *Journal of Fluid Mechanics* 49, Part 1 (13 September 1971):133-144.

311. Wagner, R. E. and Velkoff, H. R. "Measurements of Secondary Flows in a Rotating Duct," *Journal of Engineering for Power, Transactions of the ASME Series A* 94, No. 4 (October 1972):261-270.

312. Bakke, E.; Kreider, J. F.; and Kreith, F. "Turbulent Source Flow Between Parallel Stationary and Co-Rotating Disks," *Journal of Fluid Mechanics* 58, Part 2 (17 April 1973): 209-231.

313. Moore, J. "A Wake and an Eddy in a Rotating Radial Flow Passage, Part 1," *Journal of Engineering for Power, Transactions of the ASME Series A* 95, No. 3 (July 1973): 205-212.

314. Moore, J. "A Wake and an Eddy in a Rotating Radial Flow Passage, Part 2," *Journal of Engineering for Power, Transactions of the ASME Series A* 95, No. 3 (July 1973): 213-219.

315. Huppert, H. E. and Stern, M. E. "The Effect of Side Walls on Homogeneous Rotating Flow over Two-Dimensional Obstacles," *Journal of Fluid Mechanics* 62, Part 3 (11 February 1974): 417-436.

316. Benton, E. R. and Clark, A., Jr. "Spin Up," *Annual Review of Fluid Mechanics,* Vol. 6, Annual Reviews Inc., Palo Alto, California (1974):257-280.

317. Miyaski, H. "Combined Free and Forced Convective Heat Transfer in Rotating Curved Rectangular Tubes," *Journal of Heat Transfer, Transactions of the ASME Series C* 95, No. 1 (February 1973):64-71.

318. Kapinos, V. M. *Heat Transfer of a Disk Rotating in a Casing*. NASA Technical Report TT F-15199, 1973.

319. Yu, J. P.; Sparrow, E. M.; and Eckert, E. R. G. "Experiments on a Shrouded, Parallel Disk System with Rotation and Coolant Throughflow," *International Journal of Heat and Mass Transfer* 16, No. 2 (February 1973):311-328.

320. Sparrow, E. M.; Shamsundar, N.; and Eckert, E. R. G. "Heat Transfer in Rotating Cylindrical Enclosures with Axial Inflow and Outflow of Coolant," *Journal of Engineering for Power, Transactions of the ASME Series A* 95, No. 3 (July 1973): 278-280.

321. Hammond, W. E. "Summary--Selected References on Gas Turbines, Regenerative Cycles, Rotary Regenerators, and Associated Heat Exchange and Pressure Drop Information," *Journal of Heat Transfer, Transactions of the ASME Series C* 81, No. 1 (February 1959):75-78.

322. Bjorklund, I. S. and Kays, W. M. "Heat Transfer Between Concentric Rotating Cylinders," *Journal of Heat Transfer, Transactions of the ASME Series C* 81, No. 3 (August 1959): 175-186.

323. Haas, F. C. and Nissan, A. H. "The Effects of Onset of Taylor Vortices on Heat Transfer," *International Developments in Heat Transfer Part III*. ASME, New York, New York (1961): 643-651.

324. Zmeykov, V. N.; Ustimendo, B. P.; and Yakokev, A. T. "The Hydrodynamics and Heat Transfer of a Circular Turbulent Flow in a Annulus Formed by Two Simultaneous Rotating Cylinders," *Heat Transfer-Soviet Research* 2, No. 6 (November 1970):87-95.

325. Sharman, R. D.; Catton, I.; and Ayyaswamy, P. "Convective Heat Transfer Between Concentric Rotating Cylinders," *Heat Transfer: Fundamentals and Industrial Applications*. AIChE Symposium Series 69, No. 131 (1973):118-125.

326. Scott, C. J. *Turbulent Annular Swirl Flows*. University of Minnesota Report No. HTL-110, July 1973.

327. Kuo, C. Y.; Iida, H. T.; Taylor, J. H.; and Kreith, F. "Heat Transfer in Flow Through Rotating Ducts," *Journal of Heat Transfer, Transactions of the ASME Series C* 82, No. 2 (May 1960):139-151.

328. Pattenden, R. F. and Richards, A. D. "Tests on a Rotating Tube Heat Exchanger Having Controlled Fluid Flow," *International Developments in Heat Transfer Part V*. ASME, New York, New York (1961):903-911.

329. Pattenden, R. F. "Heat Transfer from a Rotating Tube with Control Fluid Flow," *Journal of Mechanical Engineering Science*, 6, No. 2 (June 1964):144-149.

330. Briggs, D. C. *Heat Transfer in Rotating Turbulent Pipe Flow*. Technical Report No. 45, Department of Mechanical Engineering Stanford University, Stanford, California, 1959.

331. Cannon, J. N. and Kays, W. M. "Heat Transfer to a Fluid Flowing Inside a Pipe Rotating About its Longitudinal Axis," *Journal of Heat Transfer, Transactions of the ASME Series C* 91, No. 1 (February 1969):135-139.

332. Busnik, V. M.; Geller, Z. I.; and Pimenov, A. K. "Heat Transfer in the Initial Segment of a Rotating Tube in the Case of Turbulent Gas Flow," *Inzhenerno-Fizicheskii Zhurnal* 16, No. 4 (April 1969):507, *Journal of Engineering Physics* (1972):400-403.

333. Busnik, V. M.; Artemov, G. A.; Bandura, V. N.; and Fedorovskii, A. M. "Experimental Investigation of Heat Exchange Between a Turbulent Airflow and a Short Rotating Cylindrical Tube," *Inzhenerno-Fizicheskii Zhurnal* 15, No. 5 (November 1968): 832, *Journal of Engineering Physics* (1972):1053-1055.

334. Busnik, V. M.; Geller, Z. I.; Pimenov, A. K.; Fedorovskii, A. M. "Investigation of Heat Transfer in the Initial Section of a Rotating Cylindrical Tube to a Turbulent Air Flow," *Teploenergetika* 16, No. 4 (1969):53-56, *Thermal Engineering* (October 1969):77-80.

335. Gortler, H. "Uber eine Dreidimensionale Instabilitat Laminarer Grenzschichten an Konkaven Wanden," *Nachr. Ges. Wiss. Gottingen, Math.-Phys. Kl.* 2 (1940):1.

336. Gortler, H. *On the Three Dimensional Instability of Laminar Boundary Layers on Concave Walls*. NACA Technical Report TM 1375, 1954.

337. Gortler, H. "Uber eine Analogie Zwischen den Instabilitaten Laminarer Grenzschichtstromungen an Konkaven Wanden und an Erwarmten Wanden," *Ingenieur-Archive* 28 (1959):71-78.

338. Tani, I. "Production of Longitudinal Vortices in the Boundary Layer Along a Concave Wall," *Journal of Geophysical Research* 67, No. 8 (July 1962):3075-3080.

339. Kreith, F. *Preliminary Investigation of Influence of Heating Surface Curvature on Heat Transfer Coefficient*. Jet Propulsion Laboratory Progress Report No. 4-115, California Institute of Technology, 25 August 1945.

340. Kreith, F. "Heat Transfer in Curved Channels," *Proceedings of the Heat Transfer and Fluid Mechanics Institute*. Vol. 6, 1953, Swets and Zeitinger, Amsterdam (1971):111-122.

341. Kreith, F. "The Influence of Curvature on Heat Transfer to Incompressible Fluids," *Transactions of the ASME* 77 (1955):1247-1256.

342. Eskinazi, S. and Yeh, H. "An Investigation on Fully Developed Turbulent Flows in a Curved Channel," *Journal of Aeronautical Sciences* 23 (1956):23-35.

343. Kestin, J. and Wood, R. T. "Enhancement of Stagnation-Line Heat Transfer by Turbulence," *Progress in Heat and Mass Transfer*. Vol. 2, Pergamon Press, London, Great Britain, 1969.

344. Schultz-Grunow, F. and Breuer, W. "Laminar Boundary Layers on Cambered Walls," *Basic Developments in Fluid Mechanics*. Vol. 1, Academic Press, New York, New York (1965):377-436.

345. Persen, L. N. *A Simplified Approach to the Influence of Gortler-Type Vortices on the Heat Transfer from a Wall*. Aerospace Research Laboratories Report ARL 65-88, 1965.

346. Persen, L. N. *Preliminary Analytical Explorations of Heat Transfer from Boundary Layers Containing Streamwise Vorticity*. Aerospace Research Laboratories Report ARL 67-0280, 1967.

347. Persen, L. N. *Investigation of Streamwise Vortex Systems Generated in Certain Classes of Curved Flow, Part I*. Aerospace Research Laboratories Report ARL 68-0134, 1968.

348. Persen, L. N. *Investigation of Streamwise Vortex Systems Generated in Certain Classes of Curved Flow, Part II*. Aerospace Research Laboratories Report ARL 68-0133, 1968.

349. Persen, L. N. "Streamwise Directed Vortices and Cross-Hatched Surfaces of Re-Entry Vehicles," *Journal of Spacecraft and Rockets* 7, No. 1 (January 1970):108-110.

350. Persen, L. N. *Investigation of Streamwise Vortex Systems in Curved Flow.* Aerospace Research Laboratories Report ARL 70-0137, 1970.

351. Persen, L. N. "On the Concept of Local Instability of Curved Flow," *Zeitschrift fur Flugwissenschaften* 19, No. 3 (March 1971):116-119.

352. Ellis, L. B. and Joubert, P. N. "Turbulent Shear Flow in a Curved Duct," *Journal of Fluid Mechanics* 62, Part 1 (8 January 1974):65-84.

353. Shchukin, V. K. and Filin, V. A. "Convective Heat Transfer in Short Curved Channels," *Inshenerno-Fizcheskii Zhurnal* 12, No. 2 (February 1967):169, *Journal of Engineering Physics* (1970):78-82.

354. Bradshaw, P. *Effects of Streamline Curvature on Turbulence*. AGARDograph No. 169, NASA Langley, August 1973.

355. Grindley, J. H. and Gibson, A. H. "On the Frictional Resistance to the Flow of Air Through a Pipe," *Proceedings of the Royal Society of London, Series A* 80 (1908):114-139.

356. Eustice, J. "Flow of Water in Curved Pipes," *Proceedings of the Royal Society of London, Series A* 84 (1910):107-118.

357. Eustice, J. "Experiments on Stream-Line Motion in Curved Pipes," *Proceedings of the Royal Society of London, Series A* 85 (1911):119-131.

358. Jeschke, D. "Heat Transfer and Pressure Loss in Coiled Pipes," *Ergaenzungsheft Zeitshrift Verein Deutscher Ingenieure* 69 (1925):24-28.

359. Dean, W. R. "Note on the Motion of Fluid in a Curved Pipe," *The London, Edinburgh, and Dublin Philosophical Magazine and Journal of Science* 4, No. 20 (1927):208-223.

360. Dean, W. R. "The Stream Line Motion of Fluid in a Curved Pipe," *The London, Edinburgh, and Dublin Philosophical Magazine and Journal of Science* 5, No. 30 (1928):673-695.

361. White, C. M. "Streamline Flow Through Curved Pipes," *Proceedings of the Royal Society of London, Series A* 123 (1929): 645-663.

362. White, C. M. "Fluid Friction and Its Relation to Heat Transfer," *Transactions of the Institution of Chemical Engineers* 10 (1932):66-80.

363. McAdams, W. H. *Heat Transmission.* 3rd ed., McGraw-Hill, New York, New York (1954):228.

364. Ito, H. "Friction Factors for Turbulent Flow in Curved Pipes," *Journal of Basic Engineering, Transactions of the ASME Series D* 81, No. 2 (June 1959):123-134.

365. Seban, R. A. and McLaughlin, E. F. "Heat Transfer in Tube Coils with Laminar and Turbulent Flow," *International Journal of Heat and Mass Transfer* 6, No. 5 (May 1963): 387-395.

366. Rogers, G. F. C. and Mayhew, Y. R. "Heat Transfer and Pressure Loss in Helically Coiled Tubes with Turbulent Flow," *International Journal of Heat and Mass Transfer* 7, No. 11 (November 1964):1207-1216.

367. Mori, Y. and Nakayama, W. "Study on Forced Convective Heat Transfer in Curved Pipes," *International Journal of Heat and Mass Transfer* 10 (1967):681-695.

368. Kalb, C. E. and Seader, J. D. "Heat and Mass Transfer Phenomena for Viscous Flow in Curved Circular Tubes," *International Journal of Heat and Mass Transfer* 15, No. 4 (April 1972): 801-817.

369. Kalb, C. E. and Seader, J. D. "Fully Developed Viscous Flow Heat Transfer in Curved Circular Tubes with Uniform Wall Temperature," *AIChE Journal* 20, No. 2 (March 1974):340.

370. Patankar, S. V.; Pratap, V. S.; and Spalding, D. B. "Prediction of Laminar Flow and Heat Transfer in Helically Coiled Pipes," *Journal of Fluid Mechanics* 16, Part 3 (11 February 1974): 539-551.

371. Malkin, Y. E. "Investigating a Spiral Heat Exchanger under Conditions of Heat Transfer by Radiation and Convection," *Teploenergetika* 18, No. 9 (1971), *Thermal Engineering* (1971):119-123.

372. Babii, V. I.; Pervyshev, B. A.; Lokshina, V. A.; and Verbovetskii, E. K. "Investigation of a Heater Heating Pulverized Anthracite Fines to a High Temperature," *Teploenergetika* 20, No. 4 (1973):39-41, *Thermal Engineering* (1973):56-58.

373. Royds, R. *Heat Transmission by Radiation, Conduction, and Convection*. 1st ed., Constable and Comp Ltd., London, Great Britain (1921):190-201.

374. Colburn, A. P. and King, W. J. "Heat Transfer and Pressure Drop in Empty, Baffled, and Packed Tubes," *Industrial and Engineering Chemistry* 23 (1931):910-923.

375. Siegel, L. G. "The Effect of Turbulence Promoters on Heat Transfer Coefficients for Water Flowing in Horizontal Tubes," *Heating, Piping, and Air Conditioning* 18, No. 6 (1946):111-114.

376. Evans, S. I. and Sarjant, R. J. "Heat Transfer and Turbulence in Gases Flowing Inside Tubes," *Journal of the Institute of Fuel* 24 (1951):216-227.

377. Koch, R. "Druckverlust eind Waermeuebergang bei Verwirbelter Stroemung," *Forschhft. Ver. dt. Ing. Series B* 24 (1958): 1-24.

378. Judd, R. L., Canadian General Electric Company Ltd., private communication to W. R. Gambill cited in 381 , 27 October 1959.

379. Kreith, F. and Margolis, D. "Heat Transfer in Swirling Turbulent Flow," *1958 Heat Transfer and Fluid Mechanics Institute*. Stanford University Press, Stanford, California (1958):126-134.

380. Kreith, F. and Margolis, D. "Heat Transfer and Friction in Turbulent Vortex Flow," *Applied Scientific Research Section A* 8 (1959):457-473.

381. Gambill, W. R. and Bundy R. D. *An Evaluation of the Present Status of Swirl Flow Heat Transfer*. Oak Ridge National Laboratory Report ORNL 61-4-61, 1961 (also ASME paper no. 62-HT-42).

382. Greene, N. D., Convair Aircraft Company, private communication to W. R. Gambill cited in 381 , May 1960.

383. Gambill, W. R.; Bundy, R. D.; and Wansbrough, R. W. "Heat Transfer Burnout and Pressure Drop for Water in a Swirl Flow through Tubes with Internal Twisted Tapes," *Chemical Engineering Progress Symposium Series* 57, No. 32 (1961): 127-137.

384. Ibragimov, M. H.; Nomofelov, E. V.; and Subbotin, V. I. "Heat Transfer and Hydraulic Resistance with Swirl Type Motion of Liquid in Pipes," *Teploenergetika* 8, No. 7 (July 1961):57-60.

385. Smithberg, E. and Landis, F. "Friction and Forced Convection Heat Transfer Characteristics in Tubes with Twisted Tape Swirl Generators," *Journal of Heat Transfer, Transactions of the ASME Series C* 86, No. 1 (February 1964):39-49.

386. Gambill, W. R. and Bundy, R. D. "High-Flux Heat Transfer Characteristics of Pure Ethylene Glycol in Axial and Swirl Flow," *AIChE Journal* 9, No. 1 (January 1963):55-59.

387. Seymour, E. V. "A Note on the Improvement in Performance Obtainable from Fitting Twisted-Tape Turbulence-Promoters to Tubular Heat Exchangers," *Transactions of the Institution of Chemical Engineers* 41 (1963):159-162.

388. Lopina, R. F. and Bergles, A. E. "Heat Transfer and Pressure Drop in Tape Generated Swirl Flow of Single Phase Water," *Journal of Heat Transfer, Transactions of the ASME Series C* 91, No. 3 (August 1969):434-442.

389. Thorsen, R. S. and Landis, F. "Friction and Heat Transfer Characteristics in Turbulent Swirl Flow Subjected to Large Traverse Temperature Gradients," *Journal of Heat Transfer, Transactions of the ASME Series C* 90, No. 1 (February 1968): 87-98.

390. Poppendiek, H. F. and Gambill, W. R. "Helical Forced-Flow Heat Transfer and Fluid Dynamics in Single and Two-Phase Systems," *Proceedings of the Third International Conference on the Peaceful Uses of Atomic Energy* 8, United Nations, New York, New York (1965):274-282.

391. Lopina, R. F. and Bergles, A. E. "Subcooled Boiling of Water in Tape-Generated Swirl Flow," *Journal of Heat Transfer, Transactions of the ASME Series C* 95, No. 2 (May 1973): 281-283.

392. Bergles, A. E.; Lee, R. A.; and Mikic, B. B. "Heat Transfer in Rough Tubes with Tape-Generated Swirl-Flow," *Journal of Heat Transfer, Transactions of the ASME Series C* 91, No. 3 (August 1969):443-445.

393. Gutstein, M. U.; Converse, G. L.; and Peterson, J. R. *Theoretical Analysis and Measurement of Single Phase Pressure Losses and Heat Transfer for Helical Flow in a Tube*. NASA Technical Note TN D-6097, 1970.

394. Seban, R. A. and Hunsbedt, A. "Friction and Heat Transfer in the Swirl Flow of Water in an Annulus," *International Journal of Heat and Mass Transfer* 16, No. 2 (February 1973):303-310.

395. Klaczak, A. "Heat Transfer in Tubes with Spiral and Helical Turbulators," *Journal of Heat Transfer, Transactions of the ASME Series C* 95, No. 4 (November 1973):557-559.

396. Megerlin, F. E.; Murphy, R. W.; and Bergles, A. E. "Augmentation of Heat Transfer in Tubes by the Use of Mesh and Brush Inserts," *Journal of Heat Transfer, Transactions of the ASME Series C* 96, No. 2 (May 1974):145-151.

397. Klepper, O. H. "Heat Transfer Performance of Short Twisted Tapes," *Heat Transfer: Fundamentals and Industrial Applications.* AIChE Symposium Series 69, No. 131 (1973):87-93.

398. *Specifications for Incinerator Testing at Federal Facilities*. U.S. Department of Health, Education, and Welfare, October 1967.

399. *Addendum to Specifications for Incinerator Testing at Federal Facilities*. U.S. Department of Health, Education, and Welfare, 6 December 1967.

400. Kays, W. M. *Convective Heat and Mass Transfer*. McGraw-Hill, New York, New York, 1966.

401. Maxwell, J. B. *Data Book on Hydrocarbons*. Van Nostrand, Princeton, New Jersey, 1950.

402. *Instructions for Operation of Burrell Flue Gas Analyzers*. Burrell Technical Supply Co., Pittsburgh, Pennsylvania.

403. Wark, K. *Thermodynamics*. 2nd. ed., McGraw-Hill, New York, New York, 1966.

404. *JANAF Thermochemical Tables*. The Thermal Research Laboratory, Dow Chemical Company, Midland, Michigan, August 1965.

405. *JANAF Thermochemical Tables Addendum*. The Thermal Research Laboratory, Dow Chemical Company, Midland, Michigan, August 1966.

406. Kent, R. T., ed. *Kent's Mechanical Engineers' Handbook, Power*. 11th ed., Wiley, New York, New York, 1936.

407. Hudson, J. E. "Heat Transmission in Boilers," *The Engineer (of London)* 70 (26 December 1890):449-525.

408. Broido, B. N. "Radiation in Boiler Furnaces," *Transactions of the ASME* 47 (1925):1123-1147.

409. Orrok, G. A. "Discussion of Broido's 'Radiation in Boiler Furnaces'" *Transactions of the ASME* 47 (1925):1148-1155.

410. Wohlenberg, W. J. and Morrow, D. G. "Radiation in the Pulverized-Fuel Furnace," Transactions of the ASME 47 (1925):127.

411. Wholenberg, W. J. and Lindseth, E. L. "The Influence of Radiation in Coal-Fired Furnaces on Boiler Surface Requirements and a Simplified Method for its Calculation," *Transactions of the ASME* 48 (1926):849.

412. Wohlenberg, W. J. and Mulliken, H. E. "Review of Methods of Computing Heat Absorption in Boiler Furnaces," *Transactions of the ASME* 57 (1935):331.

413. Hurvich, A. M. "Analogy of Heat Transfer Phenomena in Boiler Houses," *Acad. des Sci. URSS* 1-2 (1943):23.

414. [illegible], F. G. "Heat Transfer in Boiler Fireboxes," Bull. Acad. Sci. USSR Tech. Sci. Sect. (March 1950):367-373.

415. [illegible], H.; [illegible], G. P.; Myers, J. W.; Corey, R. C.; and Good, R. C. "Evaluation of Factors Affecting Heat Transfer in Furnaces," Transactions of the ASME 70 (November 1948): 1741-1746.

416. Holman, J. P. Heat Transfer. 3rd ed., McGraw-Hill, New York, New York, 1972.

417. Myers, J. W. and Corey, R. C. "Furnace Heat Absorption in Pulverized-Coal-Fired Steam Generator, Willow Island Station," Transactions of the ASME 73 (May 1951):419-431.

418. Yagi, S. and Iino, H. "Radiation from Soot Particles in Luminous Flames," Eighth Symposium (International) on Combustion. The Combustion Institute (1962):288-293.

419. Beer, J. M. and Howarth, C. R. "Radiation from Flames in Furnaces," Twelfth Symposium (International) on Combustion. The Combustion Institute, Pittsburgh, Pennsylvania (1969): 1205-1217.

420. Brovkin, L. A. and Burlakova, T. G. "Zonal Calculation of Radiant Heat Transfer in Industrial Furnaces," Heat Transfer-Soviet Research 4, No. 3 (May-June 1972):108-114.

421. Edwards, D. K. and Balakrishnan, A. "Thermal Radiation by Combustion Gases," International Journal of Heat and Mass Transfer 16, No. 1 (January 1973):25-40.

422. Siegel, R. and Howell, J. R. Thermal Radiation Heat Transfer. McGraw-Hill, New York, New York, 1972.

423. Gas Engineers Handbook. American Gas Association, Inc., New York, New York, 19[illegible].

424. Viskanta, R. "Radiation Transfer and Interaction of Convection with Radiation Heat Transfer," Advances in Heat Transfer. Vol. 3, Academic Press, New York, New York (1966):176-252.

425. Machen, N. A. and Hartnett, J. P. "Radiation-Convection Interaction for Flow over a Flat Plate Compared to Flows in the Region of a Two-Dimensional and Axisymmetric Stagnation Point," Progress in Heat and Mass Transfer. Vol. 4, Pergamon Press, London, Great Britain, 1971.

426. Bratis, J. C. and Novotny, J. L. "Radiation-Convection Interaction in the Boundary Layer Regime of an Enclosure," International Journal of Heat and Mass Transfer 17, No. 1 (January 1974): 23-36.

427. Young, H. D. *Statistical Treatment of Experimental Data*. McGraw-Hill, New York, New York, 1962.

428. Bartz, D. R. "Turbulent Boundary-Layer Heat Transfer from Rapidly Accelerating Flow of Rocket Combustion Gases and of Heated Air," *Advances in Heat Transfer Vol. 2.* Academic Press, New York, New York (1965):2-109.

429. Chung, P. M. "Chemically Reacting Nonequilibrium Boundary Layers," *Advances in Heat Transfer Vol. 2.* Academic Press, New York New York (1965):110-271.

430. Chung, P. M. "Heat Transfer in Chemically Reacting Gases," *Advanced Heat Transfer*. University of Illinois Press, Urbana, Illinois (1969):319-338.

431. Conolly, R. "Study of Convective Heat Transfer from Flames," *International Journal of Heat and Mass Transfer* 15, No. 11 (November 1972):2155-2172.

432. Emmons, H. W. "Heat Transfer in Fire," *Journal of Heat Transfer, Transactions of the ASME Series C* 95, No. 2 (May 1973):145-151.

433. *Model 8686 and 8686-2 Precision Millivolt Potentiometer Operating Instructions*. Leeds and Northrup Company, North Wales, Pennsylvania.

434. *Chek-A-Log/TBB-1, Thermocouple Buying Book*. Honeywell Industrial Division, Fort Washington, Pennsylvania, October 1971.

435. *Buyer's Guide . . . Rotameters*. Catalog 10A1000-70, Fischer and Porter Company, Warminster, Pennsylvania, June 1970.

436. *Variable Area Flowmeter Handbook. Volume II. Rotameter Calculation*. Catalog 10A1022, Fischer and Porter Company, Warminster, Pennsylvania, November 1969.

437. *Orifice Meter Constants*. Handbook E-2, American Meter Company, Inc., Albany, New York, 1936.

438. *Operating Instructions/Model 1655 Electronic Programmable Display Calculator*. Monroe, The Calculator Company, A Division of Litton Industries, 1970.

439. Chapman, A. J. *Heat Transfer*. 2nd ed., Macmillan, New York, New York, 1967.

440. *ARI Thermocouples/High Accuracy Gas Temperature Measurements*. Catalog 7.0, American Standard Aero Research Instrument Dept. Franklin Park, Illinois, April 1967.

441. Tripp, W.; Hwang, C.; and Crank, R. E. *Radiation Shape Factors for Plane Surfaces and Spheres, Circles, or Cylinders*. Special Report 16, Kansas State University Bulletin 46, No. 4 (1962).